



# Superelectrophilic Activation in Ga(III)- and Ca(II)-Catalyzed Reactions

Shengwen Yang

## ► To cite this version:

Shengwen Yang. Superelectrophilic Activation in Ga(III)- and Ca(II)-Catalyzed Reactions. Organic chemistry. Université Paris-Saclay, 2021. English. NNT: 2021UPASF039 . tel-03436501

HAL Id: tel-03436501

<https://tel.archives-ouvertes.fr/tel-03436501>

Submitted on 19 Nov 2021

**HAL** is a multi-disciplinary open access archive for the deposit and dissemination of scientific research documents, whether they are published or not. The documents may come from teaching and research institutions in France or abroad, or from public or private research centers.

L'archive ouverte pluridisciplinaire **HAL**, est destinée au dépôt et à la diffusion de documents scientifiques de niveau recherche, publiés ou non, émanant des établissements d'enseignement et de recherche français ou étrangers, des laboratoires publics ou privés.

## Superelectrophilic Activation in Ga(III)- and Ca(II)-Catalyzed Reactions

*Rôle des superélectrophiles dans des réactions  
catalysées par le gallium(III) ou le calcium(II)*

### Thèse de doctorat de l'université Paris-Saclay

École doctorale n°571, sciences chimiques : molécules, matériaux,  
instrumentation et biosystèmes (2MIB)

Spécialité de doctorat : Chimie

Unité de recherche : Université Paris-Saclay, CNRS, Institut de chimie moléculaire et

des matériaux d'Orsay, 91405, Orsay, France

Référent : Faculté des sciences d'Orsay

**Thèse présentée et soutenue à Paris-Saclay,  
le 22/10/2021, par**

**Shengwen YANG**

#### Composition du Jury

##### **Guillaume VINCENT**

Directeur de Recherches CNRS, Université Paris-Saclay

Président

##### **Etienne DERAT**

Maître de Conférences (HDR), Sorbonne Université

Rapporteur et Examinateur

##### **Gilles FRISON**

Directeur de Recherches CNRS (HDR), Sorbonne Université

Rapporteur et Examinateur

##### **Isabelle CHATAIGNER**

Professeure, Université Rouen Normandie

Examinateuse

#### Direction de la thèse

##### **Vincent GANDON**

Professeur, Université Paris-Saclay

Directeur de thèse



# Table of Contents

<b>Acknowledgements .....</b>	1
<b>List of Abbreviations .....</b>	5
<b>General Introduction.....</b>	7
<b>Chapter 1. Mechanisms Involved in Selected Lewis Acid-Mediated Organic Reactions.....</b>	13
1.1. The Friedel-Crafts Alkylation: More Complex than It Looks .....	15
1.1.1. Bridged Homodimers, Heterodimers and Superelectrophiles .....	16
1.1.2. Concerted Reactions .....	25
1.1.3. The Role of the Catalyst Beyond the Generation of the Electrophile .....	30
1.2. Skeletal Reorganization of Enynes: What Makes A Good $\pi$ -Lewis Acid? .....	31
1.2.1. Introduction .....	31
1.2.2. Late Transition Metal-Catalyzed Skeletal Reorganization of Enynes .....	36
1.2.3. Main Group Metal-Catalyzed Skeletal Reorganization of Enynes.....	42
1.3. Coupling of Alcohols with Vinylboronic Acids: A Lewis Acid at the Rescue of Another?.....	44
1.3.1. Introduction .....	44
1.3.2. The Nature of $\text{Ca}(\text{NTf}_2)_2$ and $\text{Ca}(\text{NTf}_2)(\text{PF}_6)$ .....	46
1.3.3. Mechanistic Hypotheses .....	49
1.4. Conclusions.....	54
<b>Chapter 2. Superelectrophilic Gallium(III) Homodimers in Gallium Chloride-Mediated Methylation of Benzene: A Theoretical Study .....</b>	55
2.1. Abstract.....	57
2.2. Introduction.....	57
2.3. Computational Methods.....	60
2.4. Results and Discussion .....	61
2.5. Conclusions.....	67
2.6. References.....	67
<b>Chapter 3. Alkynophilicity of Group 13 <math>\text{MX}_3</math> Salts: A Theoretical Study .....</b>	71
3.1. Abstract.....	73

3.2. Introduction.....	73
3.3. Computational Methods.....	78
3.4. Results and Discussion .....	78
3.4.1. Superelectrophilic vs “Standard” Activation.....	78
3.4.2. $\sigma$ - vs $\pi$ -Lewis Acidity .....	91
3.4.3. Deactivation Pathways?.....	92
3.4.4. Origin of the Alkynophilicity .....	95
3.5. Conclusions.....	97
3.6. References.....	98
<b>Chapter 4. DFT Analysis into the Calcium(II)-Catalyzed Coupling of Alcohols with Vinylboronic Acids: Cooperativity of Two Different Lewis Acids and Counterion Effects .....</b>	<b>107</b>
4.1. Abstract.....	109
4.2. Introduction.....	109
4.3. Computational Methods.....	112
4.4. Results and Discussion .....	113
4.4.1. Mechanism of the Calcium(II)-Catalyzed Alkenylation of Allylbenzyl Alcohol <b>1a</b> with ( <i>E</i> )-Styrylboronic Acid <b>2a</b> .....	113
4.4.2. Mechanism of the Calcium(II)-Catalyzed Alkenylation of 3-Hydroxyisoindolinone <b>1a'</b> with ( <i>E</i> )-Styrylboronic Acid <b>2a</b> .....	120
4.5. Conclusions.....	125
4.6. References.....	126
<b>General Conclusion.....</b>	<b>131</b>
<b>Publications List.....</b>	<b>133</b>
<b>Supplementary Information .....</b>	<b>135</b>
Supplementary Information of Chapter 2 .....	137
Supplementary Information of Chapter 3 .....	143
Supplementary Information of Chapter 4 .....	167
<b>French Summary .....</b>	<b>177</b>

## Acknowledgements

My doctoral work could be carried out smoothly in France. I would like to thank the China Scholarship Council (CSC) for their support for my study and life, as well as Université Paris-Saclay (CNRS UMR 8182) and Ecole Polytechnique (CNRS UMR 9168, Institut Polytechnique de Paris) for providing me a perfect environment to conduct scientific research.

Unconsciously, I have spent three years in France and will soon be welcoming my doctoral thesis defense. Three years is so long that I have been able to make many lovely and warm-hearted friends in France. Three years is also so short that I still want to do more meaningful projects with my supervisor Prof. Vincent Gandon. No matter in terms of study or life, the past three years in France have left me so many great memories. Here, I would like to take this opportunity to thank the people who helped and supported me.

Firstly, I would like to thank Dr. Christophe Bour, who was the key person for me to get the doctoral position. At the end of 2017, I saw an advertisement for Christophe's doctoral position in organic chemistry when I accidentally browsed the web. Because I just started looking for a doctoral position and wanted to develop in organic synthesis, I didn't hesitate to send my resume to Christophe, even though my graduate major is physical chemistry. Not surprisingly, I did not pass the interview without experience in organic synthesis. Fortunately, Christophe introduced my background in physical organic chemistry to Prof. Vincent Gandon. A few days later, Christophe offered me another doctoral project, which is my supervisor Vincent's project. Therefore, I would like to sincerely thank Christophe, because of him I got this unexpected offer.

Secondly, I would like to express my greatest gratitude to my supervisor, Prof. Vincent Gandon, who helped me the most during my doctoral career. Before praising my supervisor, I want to tell an interesting story. When I told my Chinese colleague Jiaxin

that I had received the scholarship from CSC, he went to tell my future supervisor. The interesting thing is that my supervisor couldn't remember at all that he recruited me as a doctoral student. At that moment, he might be thinking: Who is this guy? Every time my colleague talked to me about this story, we all laughed loudly. In fact, Vincent is a very careful and patient person at work and I can feel he loves chemistry. Every time I have a question to ask him in his office, he can explain it to me in detail. Even if he is not in the office sometimes, he will discuss with me according to our appointment, and he has never missed one. He once told me, "You can ask me anything you want to learn and I will teach you everything I know." These words have stuck with me to this day. I have been deeply influenced by his abundant academic knowledge and unique personality. I am very grateful that he taught me a lot in chemistry, especially for setting me a good example. Therefore, I am very grateful to my supervisor Prof. Vincent Gandon.

Next, I would like to sincerely thank Dr. Etienne Derat (Sorbonne Université), Dr. Gilles Frison (Sorbonne Université), Prof. Isabelle Chataigner (Université Rouen Normandie) and Dr. Guillaume Vincent (Université Paris-Saclay) for being the jury members of my thesis defense and reviewing my work.

And, I would also like to thank my colleagues who work together with me at ECM: Emilie Kolodziej, Dr. Emmanuelle Schulz, Prof. Giang Vo-Thanh, Dr. David Lebœuf, Dr. Aurelien Alix, Dr. Martial Toffano, Dr. Mohamed Mellah, Dr. Richard Gil, Dr. Sophie Bezzanine, Dr. Chloée Bournaud, Dr. Jérôme Hannedouche, Dr. Sakna Bazzi, Dr. Solène Miaskiewicz, Dr. Stephane Wittmann, Mariam Abd El Sater, Julie Kong, Sandra Abifayssal, Louis Chassillan, Dr. Guillaume Force, Dr. Alexandre Djurovic, Sophie Rodrigues, Dr. Nicolas Grimblat, Dr. Quentin Gaignard-Gaillard, Adrien Stadler, Charlie Lacroix, Charlotte David, Djamila Azrou, Dr. Erigene Bakangura, etc, and also Chinese colleagues: Dr. Chenxiao Qi, Dr. Zhilong Li, Dr. Xu Han, Dr. Shengdong Wang, Dr. Yuchao Yuan, Dr. Zhiwei Jiang, Jiaxin Tian, Yan Chen, Dr. Dongliang Wang, Donghuang Chen, Liangjian Hu, Hailong Zhang, Wenhua Lin, Xiangmeng Chen. In

addition, I would also like to thank my Chinese friends outside ECM: Prof. Juan Li, Xuefeng He, Cong Wang, Fulin Liu, Yi Yu, Shiyuan Feng, Shengying Zhao, Weixian Wang, Peng Pan, Sunbing Huang, Dayi Liu, Chanjuan Zhang, Qi Zhang, Weipeng Zeng and others.

Last but not least, I would like to sincerely thank my family: my mom, dad, sisters, and brothers. I am so lucky to live in a loving family. I am grateful to my parents for raising us and supporting us to receive a good education. I would also like to thank my girlfriend Qiuyin Zhu for encouraging and supporting me during my doctoral career. Thank you and love you all.



# List of Abbreviations

$\text{\AA}$	<i>Ångström</i>	<i>nBu</i>	<i>n-Butyl</i>
Ar	<i>Aryl</i>	NCIs	<i>Noncovalent interactions analysis</i>
CHD	<i>Cyclohexadiene</i>	NPA	<i>Natural population analysis</i>
DCE	<i>1,2-dichloroethane</i>	$\text{NTf}_2$	<i>Bis(trifluoromethane)sulfonimide</i>
DFT	<i>Density functional theory</i>	OTf	<i>Trifluoromethanesulfonate</i>
ECP	<i>Effective core potential</i>	PCM	<i>Polarizable continuum model</i>
Et	<i>Ethyl</i>	PES	<i>Potential energy surface</i>
FMO	<i>Frontier molecular orbital</i>	Ph	<i>Phenyl</i>
HOMO	<i>Highest occupied molecular orbital</i>	RDS	<i>Rate-determining step</i>
HFIP	<i>Hexafluoroisopropanol</i>	S <sub>E</sub> Ar	<i>Electrophilic aromatic substitution</i>
IBO	<i>Intrinsic bond orbital</i>	SMD	<i>Solvation model (“D” stands for density)</i>
iPr	<i>Isopropyl</i>	S <sub>N</sub> 1	<i>Nucleophilic substitution (“I” stands for the RDS is unimolecular)</i>
IRC	<i>Intrinsic reaction coordinate</i>	S <sub>N</sub> 2	<i>Nucleophilic substitution (“2” stands for the RDS is a two reacting species)</i>
LUMO	<i>Lowest unoccupied molecular orbital</i>	TS	<i>Transition state</i>
Me	<i>Methyl</i>	$\Delta G$	<i>Gibbs free energy variation</i>
NBO	<i>Natural bond orbital</i>	S <sub>Ni</sub>	<i>Substitution nucleophilic intramolecular</i>



## General Introduction

Main-group metal catalysis is an effective strategy to achieve novel reactivity and selectivity in various synthetic organic reactions, especially in carbon-carbon bond forming reactions. With more than a hundred years of efforts, this field is now an essential aspect of modern synthetic organic chemistry and has a wide range of applications in medicinal chemistry, agrochemistry, materials, and natural products. Among them, gallium and calcium complexes as Lewis acidic catalysts have been well recognized for their high reactivity towards the activation of benzenes, enynes, hydroxyl groups, etc.

The development of Lewis acidic catalytic reactions often relies on a thorough understanding of the catalyst model, reaction mechanism, reactivity, selectivity and factors controlling the rate. Ancillary ligands and counterions, exemplified by  $\text{NTf}_2^-$  or  $\text{PF}_6^-$ , largely contribute to delicately control the reactivity and selectivity of main-group metal catalyzed processes, such as the calcium(II)-catalyzed coupling of alcohols with vinylboronic acids. This is because the modifications of the ligand structure can often lead to a significant impact on steric and electronic properties, and consequently on the reaction outcomes. However, it remains challenging to thoroughly understand catalyst models only from pure chemical intuition, given the complexity of ligand effects, as multiple factors (electron withdrawing ability, steric bulkiness, solubility, etc.) may all contribute to a Lewis acid catalyzed reaction. Experimental studies of reaction mechanisms and ligand effects are also often challenging due to the difficulty to characterize the short-living reactive organometallic intermediates.

Computational analysis has been widely applied to almost all types of Lewis acid-catalyzed carbon-carbon forming reactions to predict the most favorable reaction pathway, to understand the effects of ligands and substituents, and to provide plausible rationales to design new catalysts. Although reaction mechanisms of most Lewis acid catalyzed reactions, as exemplified by the classical  $\text{GaCl}_3$ -mediated Friedel-Crafts

alkylation of benzene, are well accepted, some mechanistic details like the role of superelectrophilic homodimers and the existence of textbook intermediates such as Wheland-type  $\sigma$ -complexes remains unclear. In the last few decades, density functional theory (DFT) calculations have developed into an important tool for studying the mechanism of Lewis acid catalyzed reactions. The generally accepted procedure to explore the reaction mechanism involves optimization of reaction substrates and calculation of the energies of intermediates and transition states along a plausible reaction coordinate to construct an energy profile. Conventionally, the proposed reaction mechanism is constructed by well-defined elementary steps containing various competing chemo-, regio-, and enantio-isomeric reaction pathways. The rate- and selectivity-determining steps can be determined by comparing computed Gibbs free energies of each competing pathways. The identified key intermediates and transition states are then further analyzed to provide chemically meaningful interpretation of ligand-controlled reactivity and selectivity in complicated reaction systems and to build predictive models for well-reasoned catalyst design.

In this doctoral thesis, I present computational studies on the gallium(III)-catalyzed methylation of benzene (Chapter 2), the gallium(III)-catalyzed skeletal reorganization of enynes (Chapter 3) and the calcium(II)-catalyzed coupling reactions (Chapter 4). The overall objectives of my studies include investigation of reaction mechanisms, analysis of ligand effects and construction of predictive models.

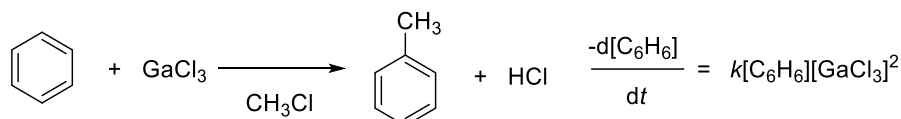
***Excerpt from Chapter 2. Superelectrophilic Gallium(III) Homodimers in Gallium Chloride-Mediated Methylation of Benzene: A Theoretical Study***

Although the Friedel-Crafts reaction has been discovered more than a 140 years ago, its reaction mechanism is still a matter of debate. DeHaan, Brown and others have performed a great number of kinetic studies in this field. They reported that the rate law of the  $\text{GaCl}_3$ -catalyzed methylation of benzene is  $-\frac{d[\text{C}_6\text{H}_6]}{dt} = k[\text{C}_6\text{H}_6][\text{GaCl}_3]^2$ . Regarding the second order of  $\text{GaCl}_3$ , the topic of debate is about the precise role of the

catalyst in this reaction: is it a simple electrophile? does it assist the deprotonation? does it activate the substrate through unsuspected forms (*superelectrophilic homodimer*, ion pair or dual activation)? These are the kind of questions we have tried to address using computational techniques.

A second topic of debate is about the stepwise or concerted nature of the Friedel-Crafts reaction. Is this a stepwise process through a Wheland-type  $\sigma$ -complex as shown in any textbook? or it is a concerted reaction? This is one of the topics that keeps being discussed and to which we have tried to make a contribution.

All of the above issues are good reasons to use DFT calculations to further clarify the specific reaction mechanisms.

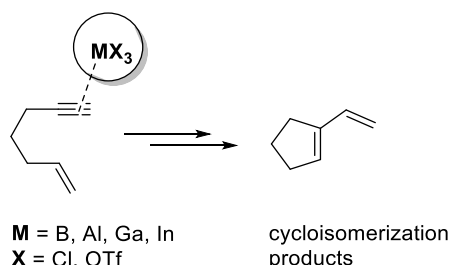


1. Real nature of the active species?
2. A stepwise process via Wheland-type  $\sigma$ -complex or a concerted reaction?

### *Excerpt from Chapter 3. Alkynophilicity of Group 13 MX<sub>3</sub> Salts: A Theoretical Study*

The cycloisomerization of 1,*n*-enyne is a well-established strategy to rapidly increase the molecular complexity from simple substrates and provide useful synthons. As early as 2002, Chatani et al. reported the GaCl<sub>3</sub>-catalyzed skeletal reorganization of enynes to 1-vinylcycloalkenes. The reaction mechanism that has been proposed when GaCl<sub>3</sub> is used as catalyst is actually not much different from the one that has been well-established with Au(I) complexes. However, for alkynophilicity, the typical features of late-transition metal gold(I) complex cannot be used to explain the properties of the main-group metal derived GaCl<sub>3</sub> salt. This raises the question of what makes a simple species such as GaCl<sub>3</sub> a good alkynophilic  $\pi$ -Lewis acid in comparison to late-transition-metal complexes such as LAu(I)<sup>+</sup> species, or even compared to BCl<sub>3</sub>, AlCl<sub>3</sub>,

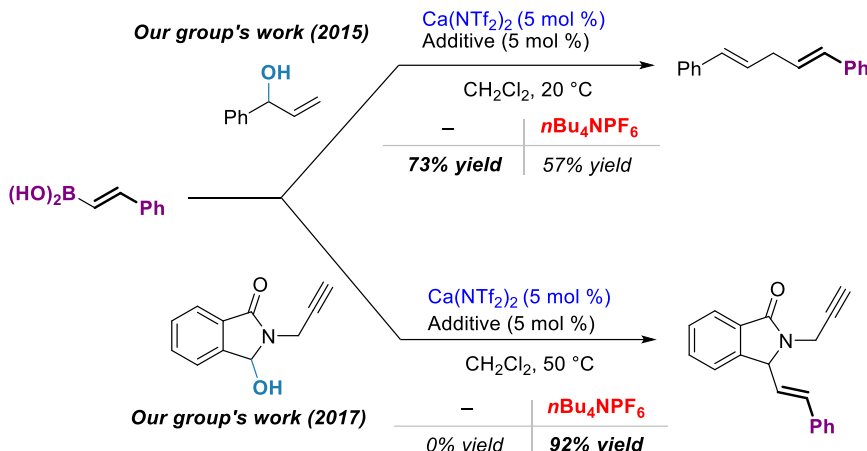
or  $\text{Ga}(\text{OTf})_3$  which do not work as catalysts for enyne cycloisomerization? In addition, the possible role of *superelectrophilic associations* also needs further theoretical study.



1. What makes  $\text{GaCl}_3$  a good alkynophilic  $\pi$ -Lewis acid among  $\text{MX}_3$  salts?
2. Why  $\text{BCl}_3$ ,  $\text{AlCl}_3$  or  $\text{Ga}(\text{OTf})_3$  do not work as catalysts for enyne cycloisomerization?
3. Any possible role of superelectrophilic associations in  $\text{GaCl}_3$ -catalyzed skeletal reorganization of enynes?

### ***Excerpt from Chapter 4. DFT Analysis into the Calcium(II)-Catalyzed Coupling of Alcohols with Vinylboronic Acids: Cooperativity of Two Different Lewis Acids and Counterion Effects***

Our group has developed the calcium-catalyzed coupling of alcohols with vinylboronic acids in 2015 and 2017, respectively. Allyl-, benzyl- and propargyl alcohols, as well as N,O-acetals were evaluated as reaction substrates. In the calcium-catalyzed alkylation reaction with allyl alcohol as the substrate, the yield decreases in the presence of the  $n\text{Bu}_4\text{NPF}_6$  ammonium salt. On the other hand, no product was observed when N,O-acetals were used as substrates in the absence of this additive. In order to deeply understand the mechanism of these two reactions and the features controlling the reactivity, we have studied four possible reaction pathways: **a.** The metal activates the hydroxyl group of the substrate. **b.** The boronic acid activates the hydroxyl group. **c.** The calcium and the boron Lewis acid synergistically activate the hydroxyl group. **d.** The calcium salt activates the boronic acid, which in turn activates the hydroxyl group (*superelectrophilic activation*). Based on the above reaction pathways, we have carried out theoretical calculations to get a better insight into a mechanism involving two different main group metals, both likely acting as Lewis acids, and sometimes an ammonium salt as activator.



Before describing these selected studies, an overview of the mechanisms typically involved in related Lewis acid mediated organic transformations will be presented (Chapter 1).

The computations described in Chapters 2-4 have been carried out on the Hopper High Performance Computer of the Ecole Polytechnique. It has 708 cores of the DELL E6220 (2,0 GHz Intel® Xeon® E5-2650 v2) series. A typical run uses 16 cores and 32 gb of RAM. I also used the HPC resources of CINES under the allocation 2020-A0070810977 made by GENCI. I have access to the OCCIGEN cluster, which is equiped with 2,6 GHz Intel® Xeon® Haswell et Broadwell processors (total of 85824 cores). A typical calculation uses 24 cores and 48 gb of RAM.

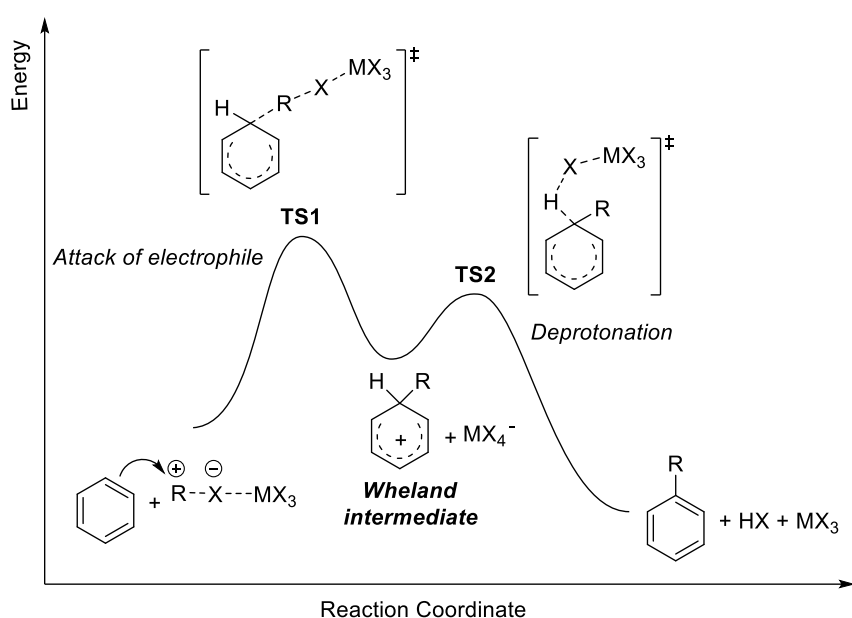


## **Chapter 1. Mechanisms Involved in Selected Lewis Acid-Mediated Organic Reactions**



## 1.1. The Friedel-Crafts Alkylation: More Complex than It Looks

In 1877, Friedel and Crafts reported the alkylation and acylation of aromatic compounds.<sup>1</sup> The classical mechanistic interpretations of such electrophilic aromatic substitutions mainly involve two steps (**Scheme 1.1**): **a.** The electrophile R is attacked by the electron-rich benzene, causing benzene to lose its aromaticity to form a Wheland intermediate (also referred to as  $\sigma$ -complex). **b.** Deprotonation occurs from the Wheland intermediate to give an aromatic alkylation (or acylation) product.



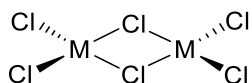
**Scheme 1.1.** The classical mechanism of the Friedel-Crafts reaction.

As discussed above, this classical view eludes several features regarding the exact nature of the active species and the possibility of having the two events within a single transition state rather than two.

1 (a) Friedel, C.; Crafts, J. M. Sur Une Nouvelle Méthode Générale de Synthèse d'Hydrocarbures, d'Acétones, etc. *Compt. Rend.* **1877**, *84*, 1392–1395. (b) Friedel, C.; Crafts, J. M. Sur Une Nouvelle Méthode Générale de Synthèse d'Hydrocarbures, d'Acétones, etc. *Compt. Rend.* **1877**, *84*, 1450–1454.

### 1.1.1. Bridged Homodimers, Heterodimers and Superelectrophiles

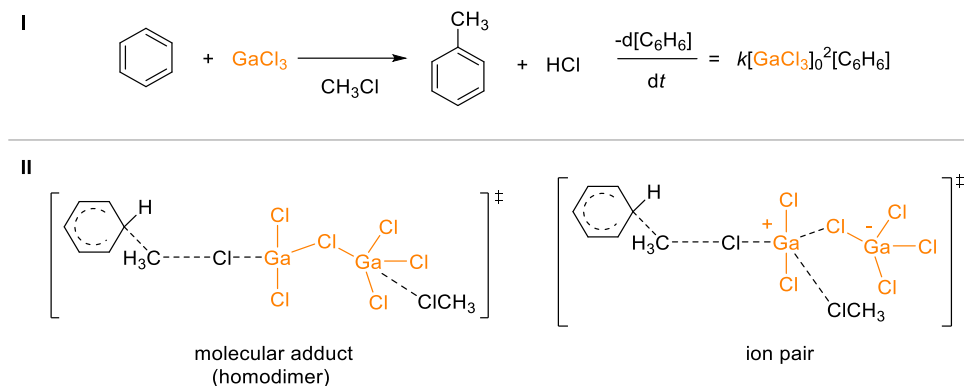
$\text{MX}_3$  salts of the group 13 metals or of the transition metal series such as  $\text{AlCl}_3$ ,  $\text{GaCl}_3$ ,  $\text{FeCl}_3$ , etc, are typical catalysts of the Friedel-Crafts alkylation or acylation.  $\text{AlCl}_3$  and  $\text{GaCl}_3$  exist as  $\text{M}_2\text{Cl}_6$  homodimers in the solid state and in weakly coordinating solvent (**Scheme 1.2**). This point will be developed in Chapter 2. While this feature has been usually ignored in theoretical studies on “ $\text{MX}_3$ ”-catalyzed reactions, a scrutiny of the old literature reveals that it cannot be put aside.



**Scheme 1.2.**  $\text{M}_2\text{Cl}_6$  homodimers of “ $\text{MCl}_3$ ”.

Herbert C. Brown is a recognized figure in the kinetic study of Friedel-Crafts reaction. In one of his multiple 1950-1960 reports about this reaction,<sup>2</sup> the observation of the second-order rate dependence of  $\text{GaCl}_3$  in the methylation of benzene in excess methyl chloride suggested an activation mode based on homodimers of general formula  $\text{Ga}_2\text{Cl}_6$  (**Scheme 1.3, I**), but their nature, molecular adduct or ion pair, could not be established. Thus, they proposed two transition state models, namely the activation by the  $\text{Ga}_2\text{Cl}_6$  molecular adduct and the activation by the  $\text{GaCl}_2^+\text{GaCl}_4^-$  ion pair (**Scheme 1.3, II**). In each case, additional coordination by  $\text{MeCl}$ , present in large excess, was suggested.

<sup>2</sup> DeHaan, F. P.; Brown, H. C. Kinetics of the Gallium Chloride Catalyzed Methylation of Benzene in Excess Methyl Chloride. *J. Am. Chem. Soc.* **1969**, *91*, 4844–4850.



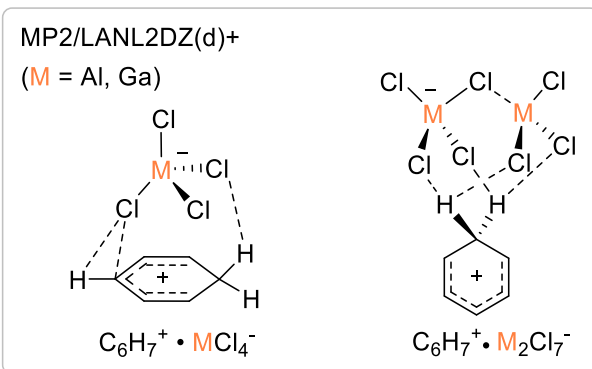
**Scheme 1.3.** Possible transition states for the second-order  $\text{GaCl}_3$ -mediated methylation of benzene in excess methyl chloride proposed by DeHaan and Brown.

Although the proposed transition states can well explain why  $\text{GaCl}_3$  follows a second-order rate law, the preferred activation model requires further research and this relatively unexplored field has aroused our interest (see Chapter 2). The importance of dimeric forms of Al and Ga trichlorides in electrophilic aromatic substitution reactions has only been partially studied. Suvorov et al. studied the monomeric and dimeric forms of metal halides in the protonation of arenes by HCl through theoretical calculations in 2004 and 2005. The calculation results show that for both metals Al and Ga, the formation of  $\text{C}_6\text{H}_7^+\cdot\text{M}_2\text{Cl}_7^-$  ion pairs (dimeric form) is more favorable than  $\text{C}_6\text{H}_7^+\cdot\text{MCl}_4^-$  (monomeric form) in electrophilic aromatic substitution reactions (**Scheme 1.4**).<sup>3,4</sup>

3 Volkov, A. N.; Timoshkin, A. Y.; Suvorov, A. V. On the Importance of Dimeric Forms of Al and Ga Trichlorides in the Electrophilic Aromatic Substitution Reactions: An Ab Initio Study. *Int. J. Quantum Chem.* **2004**, *100*, 412–418.

4 Volkov, A. N.; Timoshkin, A. Y.; Suvorov, A. V. Pathways of Electrophilic Aromatic Substitution Reactions Catalyzed by Group 13 Trihalides: An Ab Initio Study. *Int. J. Quantum Chem.* **2005**, *104*, 256–260.

**Suvorov et al. (2004, 2005)**



**Scheme 1.4.** The formation of  $\text{C}_6\text{H}_7^+ \cdot \text{M}_2\text{Cl}_7^-$  ion pairs and  $\text{C}_6\text{H}_7^+ \cdot \text{MCl}_4^-$  (M = Al, Ga).

Although the theoretical studies suggest that homodimers of metal halides can participate in electrophilic aromatic substitutions,<sup>5, 6, 7, 8</sup> there remains a lack of experiments validating the fact that dimers may be active catalysts and dominate the reaction. There is yet an experimental validation that homodimers are the active species in another category of reactions: the carbonyl-olefin metathesis. In 2019, Schindler and co-workers reported the experimental and theoretical study of Fe(III) homodimers as Lewis acid *superelectrophiles* catalyzing the carbonyl-olefin metathesis of aliphatic ketones (**Scheme 1.6**).<sup>9</sup>

5 Yamabe, S.; Yamazaki, S. A Remarkable Difference in the Deprotonation Steps of the Friedel-Crafts Acylation and Alkylation Reactions. *J. Phys. Org. Chem.* **2009**, 22, 1094–1103.

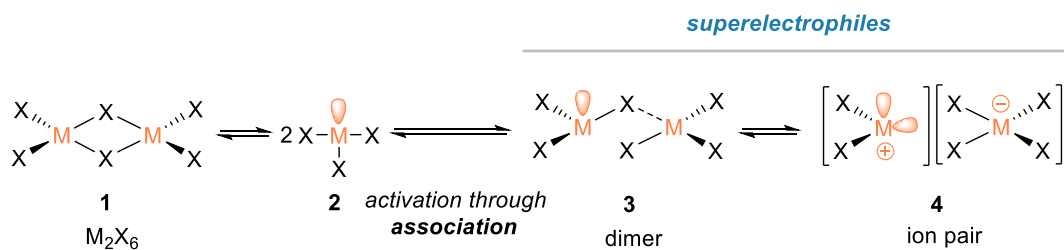
6 Melissen, S. T. A. G.; Tognetti, V.; Dupas, G.; Jouanneau, J.; Lê, G.; Joubert, L. A DFT Study of the  $\text{Al}_2\text{Cl}_6$ -Catalyzed Friedel-Crafts Acylation of Phenyl Aromatic Compounds. *J. Mol. Model.* **2013**, 19, 4947–4958.

7 Šakić, D.; Vrček, V. Prereactive Complexes in Chlorination of Benzene, Triazine, and Tetrazine: A Quantum Chemical Study. *J. Phys. Chem. A* **2012**, 116, 1298–1306.

8 Michelet, B.; Thiery, G.; Bour, C.; Gandon, V. On the Non-Innocent Behavior of Substrate Backbone Esters in Metal-Catalyzed Carbocyclizations and Friedel-Crafts Reactions of Enynes and Arenynes. *J. Org. Chem.* **2015**, 80, 10925–10938.

9 Albright, H.; Riehl, P. S.; McAtee, C. C.; Reid, J. P.; Ludwig, J. R.; Karp, L. A.; Zimmerman, P. M.;

As early as the 1960s, “superelectrophiles” were described as “highly desirable” stronger Lewis acids that can be generated by the inherent tendency of Lewis acids to associate.<sup>2,9,10</sup> As shown in **Scheme 1.5**, singly bridged dimers **3** can be obtained by the combination of two individual Lewis acids **2**, but, unlike the doubly bridged dimers of type **1**, they retain an open coordination site. The electron-withdrawing ability of the coordinated MX<sub>3</sub> unit should potentialize the “Lewis acidity” of this vacant orbital. Ultimately, the polarization induced by this coordinated MX<sub>3</sub> unit could lead to the abstraction of the X atom forming ion pairs **4** with high activity. Both singly bridged dimers **3** and ion pairs **4** belong to the family of superelectrophiles as defined by Olah.<sup>11</sup>



**Scheme 1.5.** Postulated activation mode: “superelectrophiles”.

The carbonyl-olefin metathesis is a type of metathesis reaction, that is, through the cleavage and regeneration of carbon-carbon and carbon-oxygen double bonds, the olefin and carbonyl moieties are redistributed (**Scheme 1.6, I**).<sup>12</sup> Mechanistic studies have revealed the involvement of superelectrophilic species in such Lewis acid catalyzed transformations. Although the experimental results show that complex **B**

---

Sigman, M. S.; Schindler, C. S. Catalytic Carbonyl-Olefin Metathesis of Aliphatic Ketones: Iron(III) Homo-Dimers as Lewis Acidic Superelectrophiles. *J. Am. Chem. Soc.* **2019**, *141*, 1690–1700.

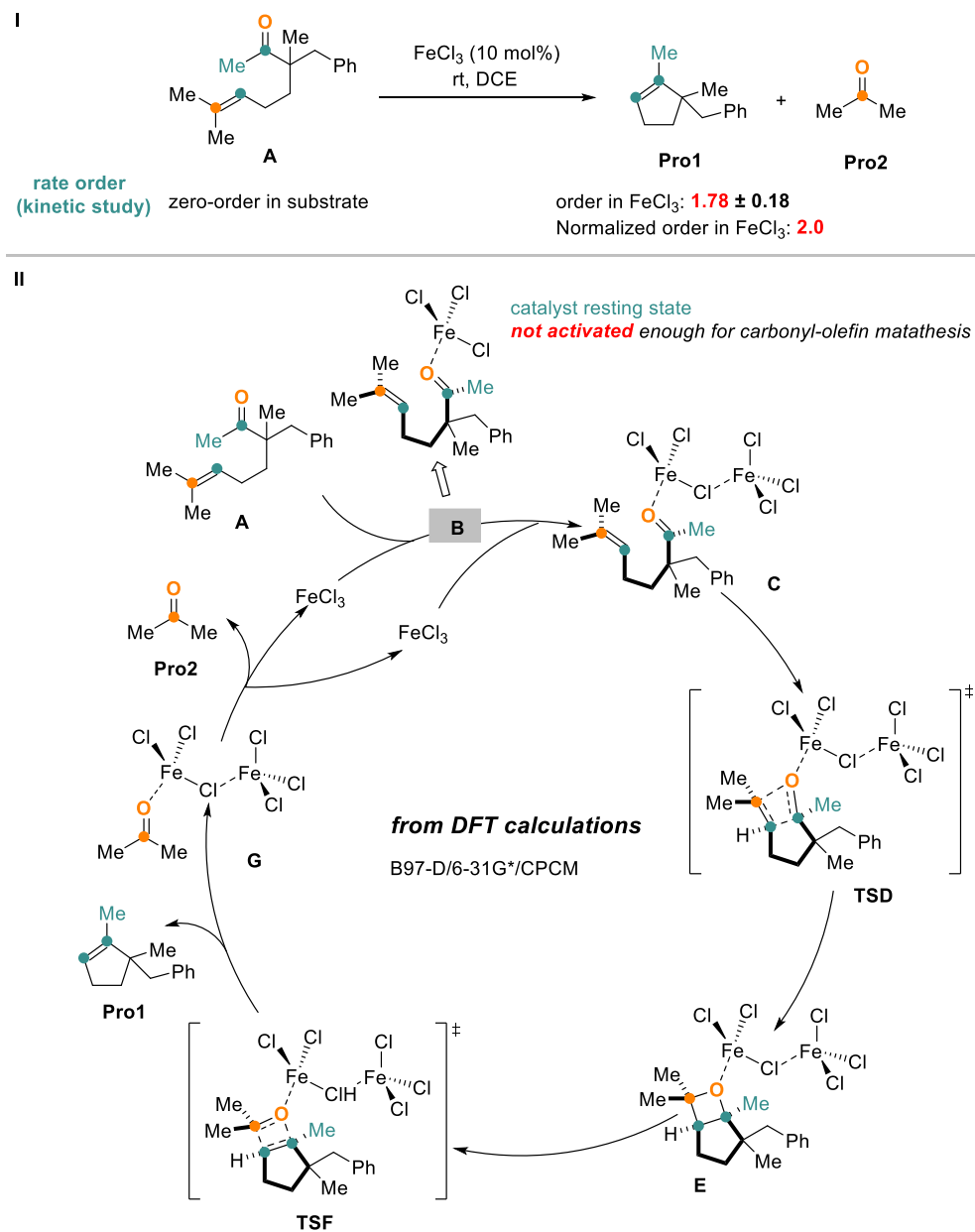
10 Negishi E. Principle of activation of electrophiles by electrophiles through dimeric association-two are better than one. *Chem. - Eur. J.* **1999**, *5*, 411–420.

11 (a) Olah, G. A. Superelectrophiles *Angew. Chem., Int. Ed. Engl.* **1993**, *32*, 767–788. (b) Olah, G. A.; Klumpp, D. A. *Superelectrophiles and Their Chemistry*; Wiley-VCH Verlag GmbH & Co. KGaA, 2007.

12 Becker, M. R.; Watson, R. B.; Schindler, C. S. Beyond olefins: new metathesis directions for synthesis. *Chem. Soc. Rev.*, **2018**, *47*, 7867–7881.

formed by the coordination of a single  $\text{FeCl}_3$  molecule with aliphatic ketones is a catalyst resting state, a single  $\text{FeCl}_3$  is not strong enough to activate the substrate and trigger a carbonyl-olefin metathesis reaction (**Scheme 1.6, II**). However, by increasing the catalyst loading, that is, from 5 mol%  $\text{FeCl}_3$  to 10 mol%  $\text{FeCl}_3$ , the amount of desired carbonyl-olefin metathesis product **Pro1** can be significantly increased. Therefore, it is particularly important to clarify the model of activated catalyst. The authors conducted a kinetic study on the carbonyl-olefin metathesis of aliphatic ketones which revealed a zero-order dependence in substrate and second-order kinetics in  $\text{FeCl}_3$  (nomalized order in  $\text{FeCl}_3$ : 2.0), implying that a different mode of Lewis acid activation is operative for the carbonyl-olefin metathesis of aliphatic ketones. According to previous literature and kinetic studies, they believe that the activated catalyst is a single-bridge dimer or an ion pair. In order to further clarify the structure of the active catalyst, infrared spectroscopy was used to relate Lewis acid-carbonyl activation to Lewis acid strength based on change in absorption frequency. When the ketone **A** is treated with an equimolar amount of  $\text{FeCl}_3$ , a new signal with an absorption frequency of  $1642\text{ cm}^{-1}$  was observed, which is consistent with the complex **B** formed by the coordination of a single  $\text{FeCl}_3$  to **A**. The addition of the second equivalent of  $\text{FeCl}_3$  resulted in the third signal, the absorption frequency of which was lowered to  $1615\text{ cm}^{-1}$ , indicating that stronger Lewis acid increased the carbonyl activation of **A**. Since both the single bridged  $\text{FeCl}_3$  dimer and the corresponding ion pair can reduce the carbonyl absorption frequencies, which is consistent with the results of IR calculations, the existence of the single bridged  $\text{FeCl}_3$  dimer or the corresponding ion pair was proved. In a second step, Raman spectroscopy was used to verify the presence of  $\text{FeCl}_4^-$  signals, so as to check whether there is an ion pair  $[\text{FeCl}_2]^+[\text{FeCl}_4]^-$  or not. Experiments based on Raman spectroscopy show that when  $\text{FeCl}_3$  was added to aliphatic ketone **A** in dichloroethane (DCE),  $\text{FeCl}_4^- (330\text{ cm}^{-1})$  was not formed, which indicates that the ion pair  $[\text{FeCl}_2]^+[\text{FeCl}_4]^-$  does not exist. In summary, the superelectrophile homo-dimer  $\text{Fe}_2\text{Cl}_6$  is the active catalyst for this reaction. Based on the above studies and on the support of DFT computations, a reaction mechanism involving  $\text{Fe}_2\text{Cl}_6$  as the Lewis acid

superelectrophile was finally proposed (**Scheme 1.6, II**).



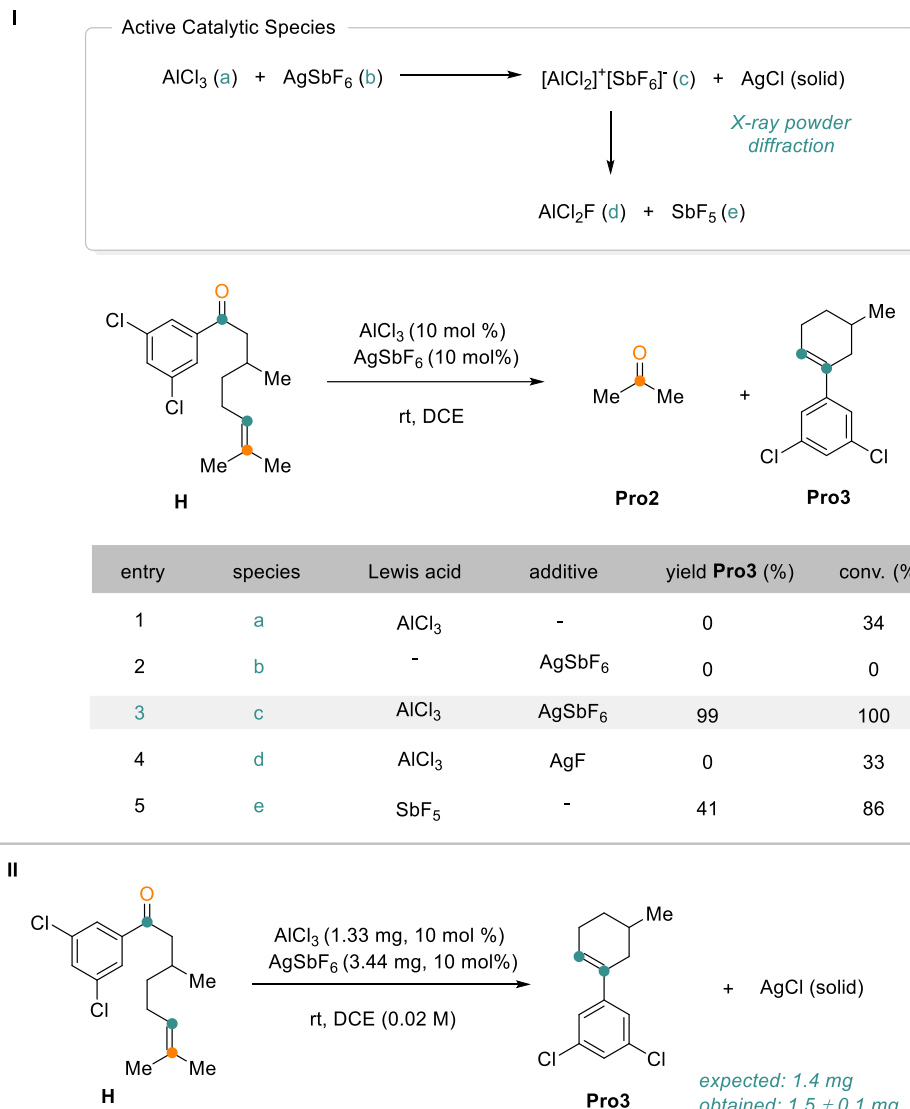
**Scheme 1.6.** Mechanistic hypothesis of  $\text{Fe}_2\text{Cl}_6$ -catalyzed carbonyl-olefin metathesis of aliphatic ketones.

The involvement of the  $[\text{AlCl}_2]^+[\text{SbF}_6]^-$  ion pair as a superelectrophile in the  $\text{AlCl}_3/\text{AgSbF}_6$ -catalyzed carbonyl-olefin metathesis towards medium-sized rings was also reported by Schindler and co-workers (**Scheme 1.7**).<sup>13</sup> There may be five Lewis

13 Davis, A. J.; Watson, R. B.; Nasrallah, D. J.; Gomez-Lopez, J. L.; Schindler, C. S. Superelectrophilic

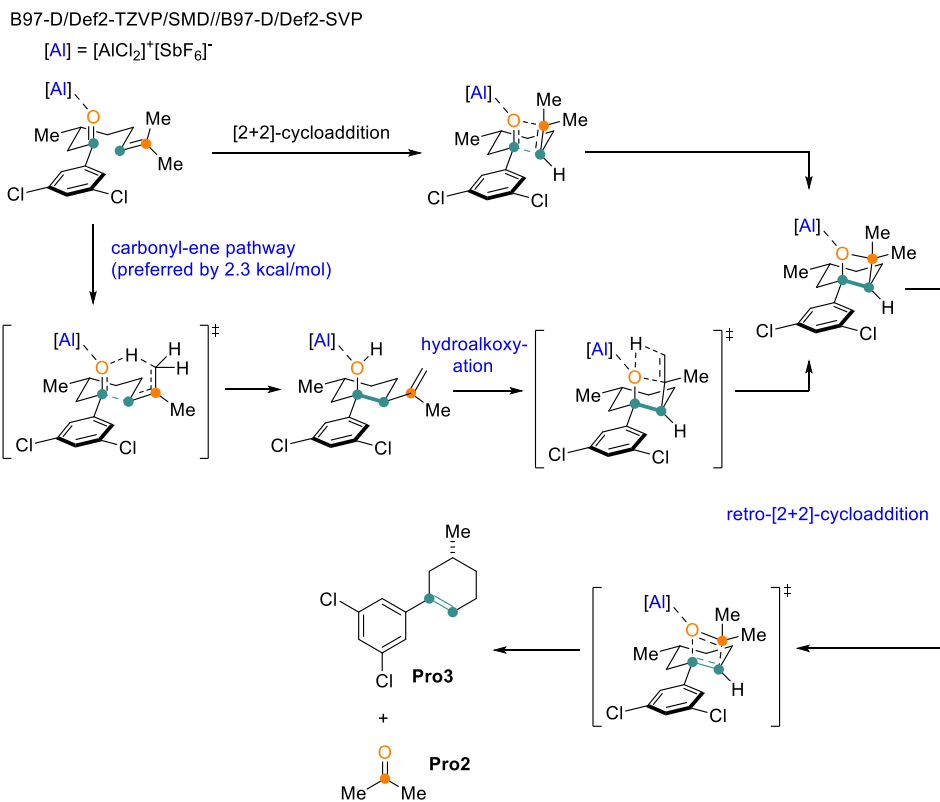
acidic species:  $\text{AlCl}_3$  (a),  $\text{AgSbF}_6$  (b), the heterobimetallic ion pair  $[\text{AlCl}_2]^+[\text{SbF}_6]^-$  (c), or  $\text{AlCl}_2\text{F}$  (d) and  $\text{SbF}_5$  (e) formed from the ion pair (**Scheme 1.1.7, I**). Therefore, it is necessary to confirm which Lewis acid is the active catalyst. Experiments show that the conversion of aryl ketone **H** with a catalytic amount of  $\text{AlCl}_3$  does not produce the desired metathesis product **Pro3** (**entry 1**). Similarly, a catalytic amount of  $\text{AgSbF}_6$  cannot promote the carbonyl-olefin metathesis reaction (**entry 2**). In contrast, the optimal reaction conditions using  $\text{AlCl}_3$  (10 mol%) and  $\text{AgSbF}_6$  (10 mol%) provided the desired product **Pro3** in 99% yield (**entry 3**). In addition, the formation of a white solid was observed, which was identified as  $\text{AgCl}$  by X-ray powder diffraction. Similarly, the use of  $\text{AlCl}_3$  (10 mol%) and  $\text{AgF}$  (10 mol%) did also lead to the formation of  $\text{AgCl}$ , indicating that  $\text{AlCl}_2\text{F}$  is formed under these conditions. However, no formation of the desired metathesis product was observed (**entry 4**). Lastly, when  $\text{SbF}_5$  (10 mol%) was used for the reaction, although the desired metathesis product **Pro3** was observed, the yield was reduced by 41% (**entry 5**).

Additionally, they could quantitatively and qualitatively support the formation of  $\text{AgCl}$  during the conversion process (**Scheme 1.7, II**). The weight of  $\text{AgCl}$  recovered was found to be consistent with the calculated weight of  $\text{AgCl}$  (expected: 1.4 mg, obtained: 1.5 mg). Overall, these results indicate that  $[\text{AlCl}_2]^+[\text{SbF}_6]^-$  is the catalytically active species under the optimal conditions for carbonyl-olefin ring-closing metathesis towards medium sized rings.



**Scheme 1.7.** (I) Investigation of possible catalytic species. (II) Formation of AgCl under the optimized conditions for catalytic carbonyl-olefin metathesis with AlCl<sub>3</sub> and AgSbF<sub>6</sub>.

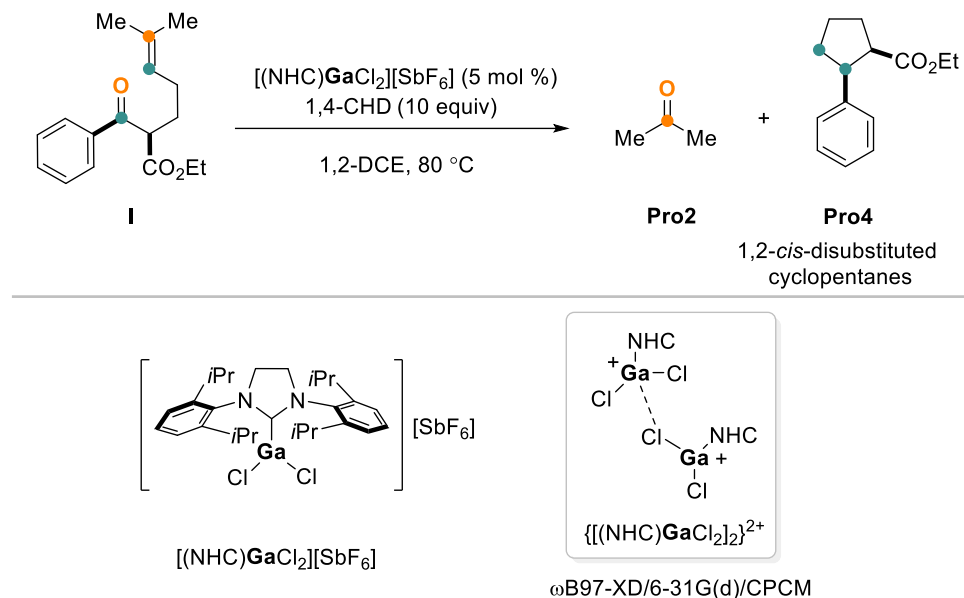
The calculated mechanism using the superelectrophilic [AlCl<sub>2</sub>]<sup>+</sup>[SbF<sub>6</sub>]<sup>-</sup> heterobimetallic ion pair as the active catalyst is shown in **Scheme 1.8**.



**Scheme 1.8.** Mechanism of superelectrophilic Al(III)-ion pairs catalyzed carbonyl-olefin metathesis supported by DFT computations.

In 2019, our group reported an experimental and theoretical study on gallium(III)-catalyzed tandem carbonyl-olefin metathesis/transfer hydrogenation.<sup>14</sup> The calculated results show that superelectrophilic homodimers of type  $\{[(\text{NHC})\text{GaCl}](\mu\text{-Cl})[\text{GaCl}_2(\text{NHC})_2]\}^{2+}$  are more active catalyst than the corresponding monomer  $[(\text{NHC})\text{GaCl}_2]^+$  (**Scheme 1.9**).

<sup>14</sup> Djurovic, A.; Vayer, M.; Li, Z.; Guillot, R.; Baltaze, J.-P.; Gandon, V.; Bour, C. Synthesis of Medium-Sized Carbocycles by Gallium-Catalyzed Tandem Carbonyl-Olefin Metathesis/Transfer Hydrogenation. *Org. Lett.* **2019**, *21*, 8132–8137.



**Scheme 1.9.** Superelectrophilic  $\{[(\text{NHC})\text{GaCl}_2]_2\}^{2+}$ -catalyzed carbonyl-olefin metathesis and transfer hydrogenation (CHD = cyclohexadiene).

In this context, the involvement of superelectrophilic species can also be envisaged in Friedel-Crafts or other reactions. We have kept this point in mind during our studies shown in Chapters 2-4.

### 1.1.2. Concerted Reactions

There is another feature of Friedel-Crafts reaction that caught our attention. Whether the Wheland-type  $\sigma$ -complex is involved in the electrophilic aromatic substitution mechanism has been a recent hot topic of discussion. In fact, the classical interpretations of electrophilic aromatic substitution mechanisms via Wheland-type  $\sigma$ -complex have been refuted several times, both in the presence or absence of a catalyst. Contrary to traditional interpretations, no  $\sigma$ -complex intermediate was found along the direct substitution reaction pathway. We have listed some representative computed mechanism examples with  $\text{SO}_3$ ,  $\text{Br}_2$ ,  $\text{Cl}_2$  and alkynes as electrophiles in which concerted reactions have been proposed.

### 1.1.2.1. SO<sub>3</sub> as electrophile

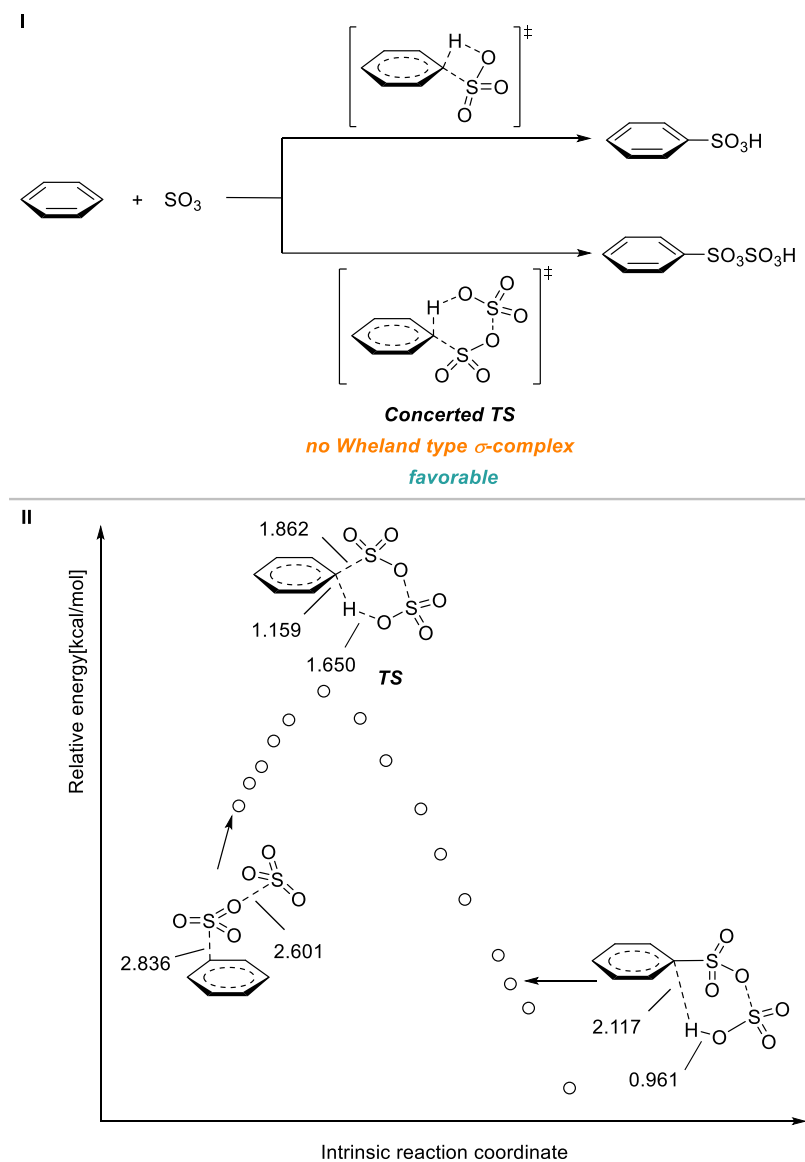
The computational study of the electrophilic aromatic sulfonation with SO<sub>3</sub> has been reported by Schleyer and co-workers (**Scheme 1.10**).<sup>15</sup> Such a reaction requires no catalyst. The potential energy surfaces of a single SO<sub>3</sub> and two SO<sub>3</sub> molecules as electrophiles have been calculated. The computational results show that the electrophilic aromatic substitution mechanism with a single SO<sub>3</sub> molecule is concerted in the gas phase or in non-complexing solvents (such as CCl<sub>4</sub> or CFCl<sub>3</sub>), rather than involving a  $\sigma$ -complex. However, the activation energy is high, while the activation energy using two SO<sub>3</sub> molecules is 12–20 kcal/mol lower, which is consistent with the experimental kinetics (second-order in SO<sub>3</sub>). The IRC analysis showed that the expected  $\sigma$ -complex is not a stationary point and so there is a direct collapse to the product. Thus, the mechanism of electrophilic aromatic sulfonation with two SO<sub>3</sub> molecules was also found concerted.

It is worth noting that in solvents with higher polarity (complexing solvents), such as CH<sub>3</sub>NO<sub>2</sub>, Wheland-type  $\sigma$ -intermediates could be optimized. Although the reaction has to overcome the association energy of the complexing solvent, it is consistent with the experimental kinetics, that is, in CH<sub>3</sub>NO<sub>2</sub>, the reaction of two SO<sub>3</sub> molecules is still more favorable than the reaction of a single SO<sub>3</sub> molecule.

---

<sup>15</sup> Koleva, G.; Galabov, B.; Kong, J.; Schaefer, H. F., III; Schleyer, P. v. R. Electrophilic Aromatic Sulfonation with SO<sub>3</sub>: Concerted or Classic SEAr Mechanism? *J. Am. Chem. Soc.* **2011**, *133*, 19094–19101.

Schleyer et al. (2011)  
 gas phase or non-complexing solvents  
 M06-2X/6-311+G(2d,2p)/IEPCM



**Scheme 1.10.** (I) Mechanism of electrophilic aromatic sulfonation with a single  $\text{SO}_3$  and two  $\text{SO}_3$  molecules in non-complexing media. (II) IRC plot for the sulfonation of benzene with two  $\text{SO}_3$  molecules in simulated  $\text{CFCl}_3$  solution computed at the M06-2X/6-311+G(2d,2p) level.

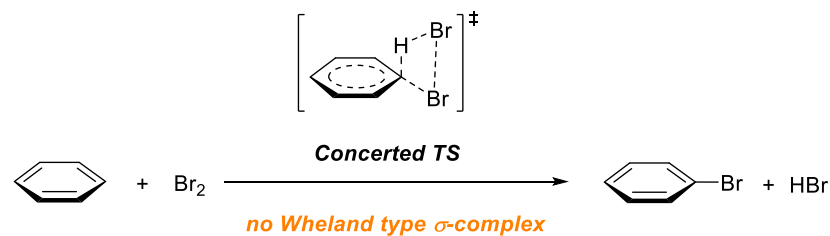
### 1.1.2.2. $\text{Br}_2$ as electrophile

Schleyer and co-workers also reported the mechanism of the functionalization of arenes

by  $\text{Br}_2$  without a catalyst.<sup>16</sup> The focus of this article was to compare the mechanism of the addition-elimination and the concerted substitution by  $\text{Br}_2$  of benzene and other arenes. Although substitution products may be formed more rapidly via stepwise addition-elimination pathways than by concerted substitution pathways, the computational results clearly show that the substitution reaction in the gas phase or the nonpolar solvent  $\text{CCl}_4$  is a concerted process and does not involve a Wheland type intermediate (**Scheme 1.11**). This again refutes the classic explanation of electrophilic aromatic substitution reaction, which involves Wheland type  $\sigma$ -complex.

**Schleyer et al. (2011)**  
**gas phase or non-complexing solvents**

B2-PLYP/6-311+G(2d,2p)/IEFPCM//B3LYP-D3/6-311+G(2d,2p)



**Scheme 1.11.** Mechanism of electrophilic aromatic bromination with a single  $\text{Br}_2$  molecule in nonpolar media.

### 1.1.2.3. $\text{Cl}_2$ as electrophile

In this theoretical investigation, Schleyer and co-workers reported the mechanism of arene chlorination in the nonpolar solvent  $\text{CCl}_4$  (**Scheme 1.12**).<sup>17</sup> It not only evaluated two competing mechanisms, namely addition-elimination and direct substitution, but also the effect of  $\text{HCl}$  as catalyst on the mechanism. The Gibbs free energies show that the barriers of addition-elimination and direct substitution mechanisms are very close

16 Kong, J.; Galabov, B.; Koleva, G.; Zou, J.-J.; Schaefer, H. F., III; Schleyer, P. v. R. The Inherent Competition between Addition and Substitution Reactions of  $\text{Br}_2$  with Benzene and Arenes. *Angew. Chem., Int. Ed.* **2011**, *50*, 6809–6813.

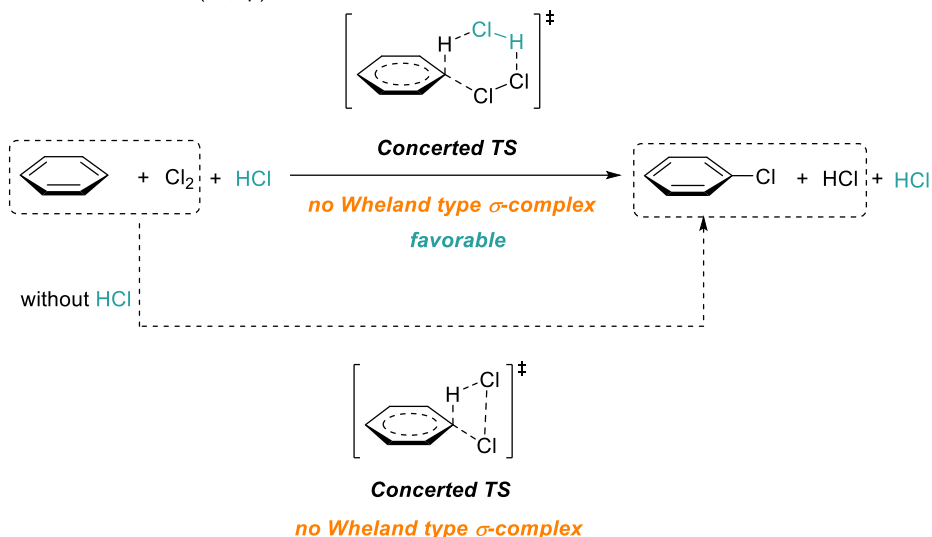
17 Galabov, B.; Koleva, G.; Kong, J.; Schaefer, H. F., III; Schleyer, P. v. R. Addition-Elimination versus Direct Substitution Mechanisms for Arene Chlorination. *Eur. J. Org. Chem.* **2014**, *2014*, 6918–6924.

(the latter being slightly higher than the former), and the catalyst HCl can greatly reduce the energy barriers of the two mechanisms. In the presence or absence of catalyst (HCl), the Wheland type  $\sigma$ -complex was not observed in the direct substitution mechanism, which means a concerted process. This was also supported by Vrček and co-worker.<sup>7</sup>

**Schleyer et al (2014)**

**gas phase or non-complexing solvents**

B3LYP-D3/6-311+G(2d,2p)/IEFPCM



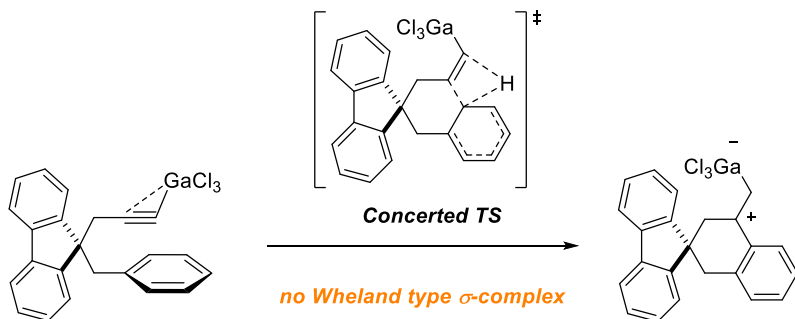
**Scheme 1.12.** Mechanism of electrophilic aromatic chlorination with  $\text{Cl}_2$  in the presence (or absence) of HCl.

#### 1.1.2.4. Alkynes as electrophiles

In addition to  $\text{SO}_3$ ,  $\text{Br}_2$  and  $\text{Cl}_2$ , alkynes have also been reported as potent electrophiles. In 2015, our group reported the mechanism of Ga(III)-catalyzed hydroarylation of arenynes in 1,2-dichloroethane (DCE) as the solvent.<sup>8</sup> In this mechanism, the calculated results show that the hydroarylation proceeds via a concerted mechanism, and no Wheland-type intermediate was obtained (**Scheme 1.13**).

***Our group's work (2015)***

M06-2X/6-311+G(d,p)/CPCM



**Scheme 1.13.** Mechanism of the  $\text{GaCl}_3$ -catalyzed intramolecular hydroarylation of alkynes.

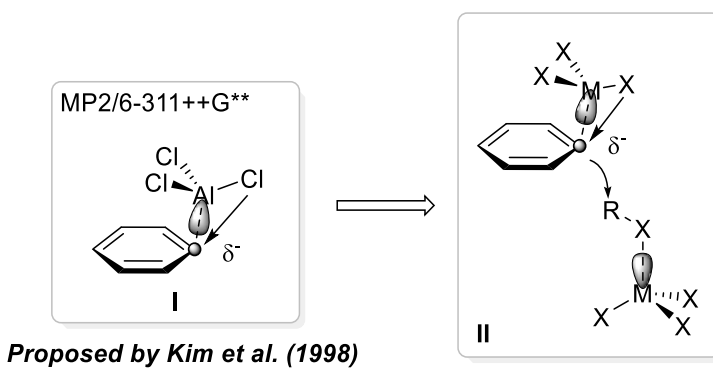
Based on the above examples, it seems that the Friedel-Crafts reaction has no causal relationship with the type of electrophile or the presence or absence of catalyst, but it could be related to the polarity of the solvent. When the solvent has a low polarity and a low complexing ability, the Wheland-type  $\sigma$ -complex might not be a stable intermediate and collapses during IRCS.

### 1.1.3. The Role of the Catalyst Beyond the Generation of the Electrophile

As we know, the role of catalysts in the electrophilic aromatic substitution mechanism is not only the generation of the electrophile, but also to assist the deprotonation. In addition, Kim and co-workers proposed a third role that is the activation of the aromatic nucleophile, which seems counterintuitive.<sup>18</sup> Their theoretical pieces of evidence suggest that the Lewis acid  $\text{AlCl}_3$  and the aromatic substrate  $\text{C}_6\text{H}_6$  can form the remarkably stable adduct  $\text{AlCl}_3 \cdot \text{C}_6\text{H}_6$  (**Scheme 1.14, I**). Although such a combination will lose the nodal plane of benzene, the loss of aromaticity can be prevented by back-

<sup>18</sup> Tarakeshwar, P.; Lee, J. Y.; Kim, K. S. Role of Lewis Acid( $\text{AlCl}_3$ )-Aromatic Ring Interactions in Friedel-Craft's Reaction: An Ab Initio Study. *J. Phys. Chem. A* **1998**, *102*, 2253–2255.

donation from Cl 3p orbital to the benzene highest occupied molecular orbital (HOMO). Therefore, Kim et al. provide us with a new idea to explore (**Scheme 1.14, II**). In this view, the benzene nucleophile is activated by coordination. This should decrease its electron density and therefore its nucleophilicity, however, the Cl back-donation enhances the negative charge of the carbon bound to Al, which supposedly increases its nucleophilicity.



**Scheme 1.14.** Unexpected role of the Lewis acid ( $\text{AlCl}_3$ ) in the electrophilic aromatic substitution of benzene.

## 1.2. Skeletal Reorganization of Enynes: What Makes A Good $\pi$ -Lewis Acid?

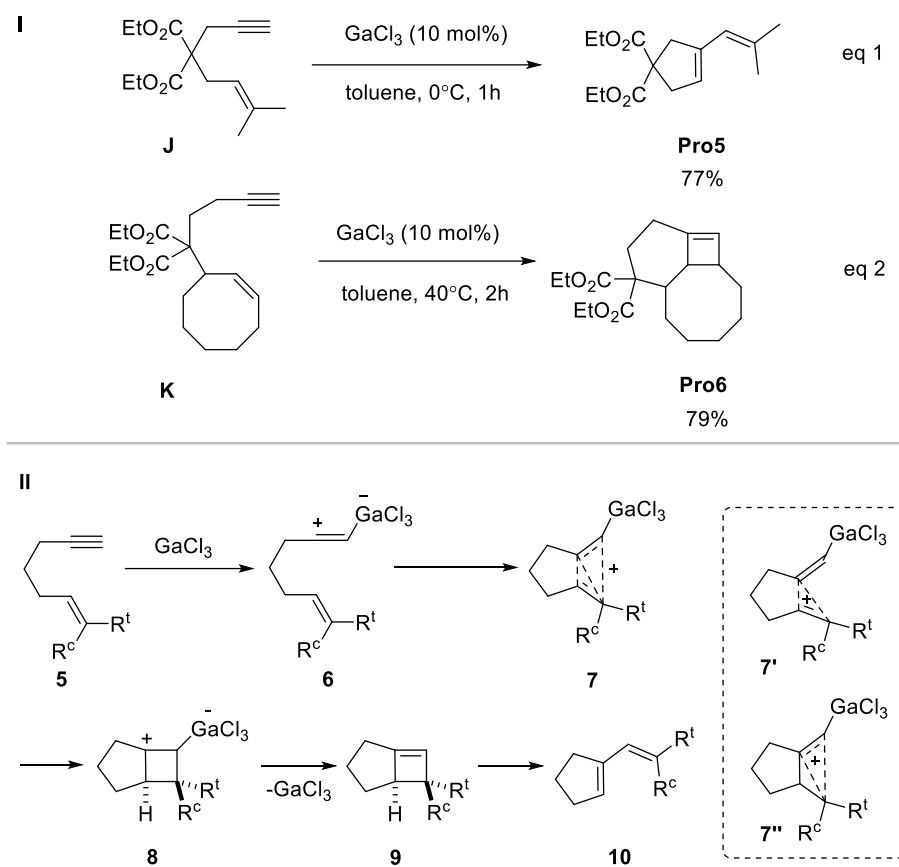
### 1.2.1. Introduction

Since the metal-catalyzed cycloisomerization of  $1,n$ -enynes is a well-established strategy to selectively produce a wide range of carbo- and heterocyclic products, it is perfectly suited for the synthesis of natural products, pharmaceuticals, agrochemicals

or materials.<sup>19,20</sup> However, all catalysts suitable for skeletal reorganization reported

- 
- 19 (a) Diver, S. T.; Giessert, A. J. Enyne Metathesis (Enyne Bond Reorganization). *Chem. Rev.* **2004**, *104*, 1317–1382. (b) Nicolaou, K. C.; Bulger, P. G.; Sarlah, D. Metathesis Reactions in Total Synthesis. *Angew. Chem., Int. Ed.* **2005**, *44*, 4490–4527. (c) Zhang, L.; Sun, J.; Kozmin, S. A. Gold and Platinum Catalysis of Enyne Cycloisomerization. *Adv. Synth. Catal.* **2006**, *348*, 2271–2296. (d) Mori, M. Synthesis of Natural Products and Related Compounds using Enyne Metathesis. *Adv. Synth. Catal.* **2007**, *349*, 121–135. (e) Mori, M.; Kitamura, T. Ene-Yne and Alkyne Metathesis. In Comprehensive Organometallic Chemistry III, Mingos, D. M. P.; Crabtree, R. H., Eds.; 2007; Vol. 11, pp 271–310. (f) Mori, M. Recent Progress on Enyne Metathesis: Its Application to Syntheses of Natural Products and Related Compounds. *Materials* **2010**, *3*, 2087–2140. (g) Echavarren, A. M.; Jiménez-Núñez, E. Complexity via Gold-Catalyzed Molecular Gymnastics. *Top. Catal.* **2010**, *53*, 924–930. (h) Dragutan, I.; Dragutan, V.; Demonceau, A.; Delaude, L. Enabling Access to Diverse Bioactive Molecules Through Enyne Metathesis Concepts. *Curr. Org. Chem.* **2013**, *17*, 2678–2720. (i) Michelet, V. Noble Metal-Catalyzed Enyne Cycloisomerizations and Related Reactions. In Comprehensive Organic Synthesis, 2nd ed.; Knochel, P.; Knochel, P.; Molander, G. A., Eds.; Elsevier: 2014; Vol. 5, pp 1483–1536. (j) Dorel, R.; Echavarren, A. M. Gold(I)-Catalyzed Activation of Alkynes for the Construction of Molecular Complexity. *Chem. Rev.* **2015**, *115*, 9028–9072. (k) Echavarren, A. M.; Muratore, M. E.; López-Carrillo, V.; Escribano-Cuesta, A.; Huguet, N.; Obradors, C. Gold-Catalyzed Cyclizations of Alkynes with Alkenes and Arenes. *Org. React.* **2017**, *92*, 1–288. (l) Hu, Y.; Bai, M.; Yang, Y.; Zhou, Q. Metal-Catalyzed Enyne Cycloisomerization in Natural Product Total Synthesis. *Org. Chem. Front.* **2017**, *4*, 2256–2275.
- 20 (a) Trost, B. M.; Krische, M. J. Transition Metal Catalyzed Cycloisomerizations. *Synlett* **1998**, *1998*, 1–16. (b) Aubert, C.; Buisine, O.; Malacria, M. The Behavior of 1,*n*-Enynes in the Presence of Transition Metals. *Chem. Rev.* **2002**, *102*, 813–834. (c) Lloyd-Jones, G. C. Mechanistic Aspects of Transition Metal Catalysed 1,6-Diene and 1,6-Enyne Cycloisomerisation Reactions. *Org. Biomol. Chem.* **2003**, *1*, 215–236. (d) Echavarren, A. M.; Nevado, C. Non-stabilized transition metal carbenes as intermediates in intramolecular reactions of alkynes with alkenes. *Chem. Soc. Rev.* **2004**, *33*, 431–436. (e) Bruneau, C. Electrophilic Activation and Cycloisomerization of Enynes: A New Route to Functional Cyclopropanes. *Angew. Chem., Int. Ed.* **2005**, *44*, 2328–2334. (f) Nieto-Oberhuberr, C.; López, S.; Jiménez-Núñez, E.; Echavarren, A. M. The Mechanistic Puzzle of Transition-Metal-Catalyzed Skeletal Rearrangements of Enynes. *Chem. - Eur. J.* **2006**, *12*, 5916–5923. (g) Zhang, L.; Sun, J.; Kozmin, S. A. Gold and Platinum Catalysis of Enyne Cycloisomerization. *Adv. Synth. Catal.* **2006**, *348*, 2271–2296. (h) Michelet, V.; Toullec, P. Y.; Genêt, J.-P. Cycloisomerization of 1,*n*-Enynes: Challenging Metal-Catalyzed Rearrangements and Mechanistic Insights. *Angew. Chem., Int. Ed.* **2008**, *47*, 4268–4315. (i) Jiménez-Núñez, E.; Echavarren, A. M. Gold-Catalyzed Cycloisomerizations of Enynes: A Mechanistic Perspective. *Chem. Rev.* **2008**, *108*, 3326–3350. (j) Lee, S. I.; Chatani, N. Catalytic Skeletal Reorganization of Enynes Through Electrophilic Activation of Alkynes: Double Cleavage of C–C Double and Triple Bonds. *Chem. Commun.* **2009**, *371–384*. (k) Toullec, P. Y.; Michelet, V. Cycloisomerization of 1,*n*-Enynes Via Carbophilic Activation. In Topics in Current Chemistry, Soriano,

before 2002 involved late-transition-metal complexes, especially gold and platinum. In 2002, Chatani and co-workers reported that a main-group-metal complex (i.e.  $\text{GaCl}_3$ ) catalyzes the skeletal reorganization of enynes to 1-vinylcycloalkenes, as shown in **Scheme 1.17** (eq 1).<sup>21</sup>



**Scheme 1.17. (I)**  $\text{GaCl}_3$ -catalyzed skeletal reorganization of enynes; **(II)** Proposed reaction mechanism.

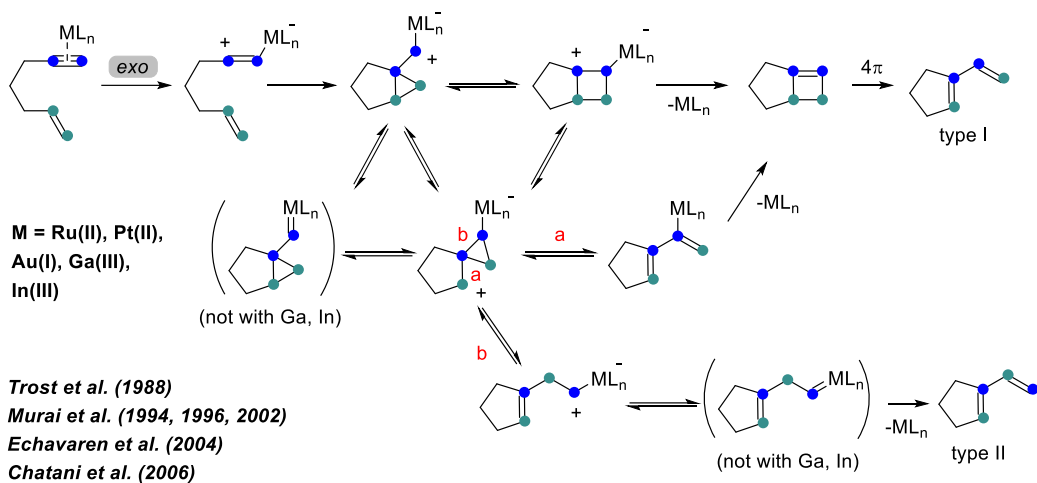
We have selected two representative reactions from this article (**Scheme 1.17, I**): eq 1: The reaction of 1,6-enyne **J** with a catalytic amount of  $\text{GaCl}_3$  in toluene at  $0^\circ\text{C}$  was completed within 1 h and 1-vinylcyclopentene **Pro5** was obtained with a yield of 77%.

E.; Marco-Contelles, J., Eds.; Springer: Berlin, Heidelberg, 2011; Vol. 302, pp 31–80. (l) Marinetti, A.; Jullien, H.; Voituriez, A. Enantioselective, transition metal catalyzed cycloisomerisations. *Chem. Soc. Rev.* **2012**, *41*, 4884–4908.

21 Chatani, N.; Inoue, H.; Kotsuma, T.; Murai, S. Skeletal Reorganization of Enynes to 1-Vinylcycloalkenes Catalyzed by  $\text{GaCl}_3$ . *J. Am. Chem. Soc.* **2002**, *124*, 10294–10295.

eq 2: Using 1,7-enyne **K** as substrate, the tricyclic compound **Pro6** containing a cyclobutene ring was obtained with a yield of 79% after 2 h at 40 °C. This reaction indicates that cyclobutene may be involved in the skeletal reorganization of enynes, which is a very important information for understanding the reaction mechanism. Chatani et al. proposed the following mechanism (**Scheme 1.17, II**): First, the enyne **5** forms a vinyl carbocation **6** when the alkyne moiety is coordinated with GaCl<sub>3</sub>. The nucleophilic attack of the alkene moiety generates the nonclassical carbocation **7** or other isomers (**7'** or **7''**). The latter is then transformed into the  $\eta^1$ -cyclobutene complex **8**. The elimination of GaCl<sub>3</sub> leads to strained cyclobutene **9**. Finally, cyclobutene **9** undergoes  $4\pi$  ring opening to provide 1-vinylcyclopentene **10**, which is obtained in a stereospecific manner.

The skeletal reorganization of enynes is often considered to be the territory of late-transition metals, especially gold and platinum. One of the reason apart from the softness of such metals, which makes them ready to activate soft functionalities such as alkynes, is the ease by which transition metals form carbenoid intermediates by  $\pi$  back-donation. Since back-donation is not possible with gallium or other main group metals, it seems relevant to study the mechanism of GaCl<sub>3</sub>-catalyzed skeletal reorganization of enynes to rationalize why the same result can be obtained nonetheless. The general mechanism of metal-catalyzed skeletal reorganization of 1,6-enynes is shown in **Scheme 1.18**. One common cycloisomerization pathway is the skeletal reorganization of 1,6-enyne towards 1-vinylcyclopentenes. Specific examples will be discussed later.



**Scheme 1.18.** General mechanism of the metal-catalyzed skeletal reorganization of 1,6-enynes.

The alkynophilicity of gold(I) complexes has been confirmed to be related to the relativistic effects and the ability of the soft polarizable gold atom to stabilize nonclassical carbocations by back-donation,<sup>22,23</sup> but these typical features of late-transition metals are not suitable to explain the alkynophilicity of main-group-based species. Therefore, compared with the late transition metal complexes  $LAu(I)^+$ , and even compared with  $BCl_3$ ,  $AlCl_3$ , or  $Ga(OTf)_3$  that cannot be used as catalysts for enyne cycloisomerization, what makes  $GaCl_3$  or  $InCl_3$  becoming a good alkynophilic  $\pi$ -Lewis acid is an issue we need to address. Whether there is specific activation of the substrate, such as superelectrophilic activation, is also our focus (see Chapter 3).

22 Fürstner, A.; Davies, P. W. Catalytic Carbophilic Activation: Catalysis by Platinum and Gold  $\pi$  Acids. *Angew. Chem., Int. Ed.* **2007**, *46*, 3410–3449.

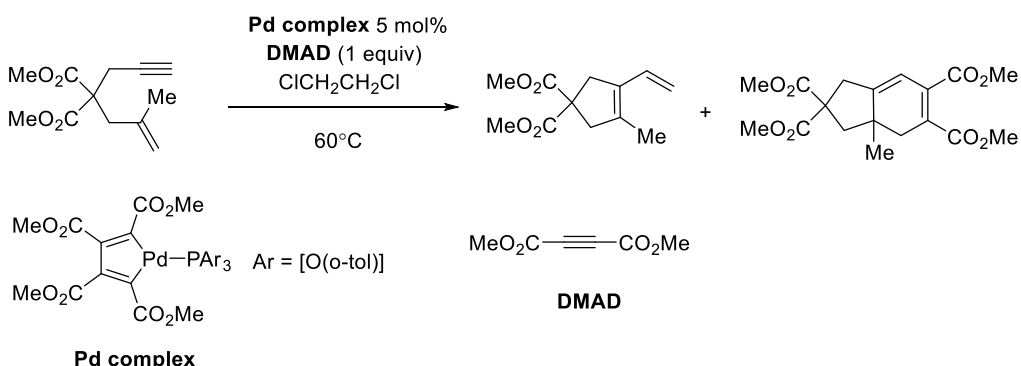
23 Gorin, D. J.; Toste, F. D. Relativistic Effects in Homogeneous Gold Catalysis. *Nature* **2007**, *446*, 395–403.

## 1.2.2. Late Transition Metal-Catalyzed Skeletal Reorganization of Enynes

### 1.2.2.1. Ru(II)-catalyzed skeletal reorganization of enynes

The first example of a transition metal complex triggering the skeletal reorganization of enynes was reported by Trost et al. in 1988.<sup>24</sup> They reported that Pd(II) complexes (pallacyclopentadiene and tris(*o*-tolyl) phosphite) catalyzed the skeletal reorganization of 1,6-enynes into 1-vinylcyclopentenes (**Scheme 1.19**).

*Trost et al. (1988)*

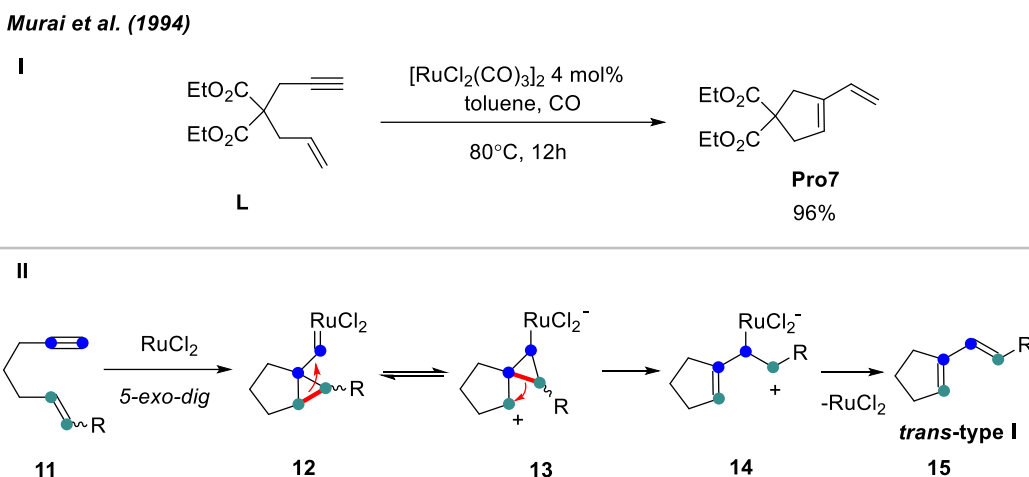


**Scheme 1.19.** First example of transition metal complex catalyzed skeletal reorganization of enynes.

Although the Pd(II)-catalyzed reaction reported by Trost et al. is very attractive, it appears highly selective only when the substrate has a terminal olefinic moiety. This limitation reduces the utility of this novel skeletal reorganization reaction. The first example of the Ru(II)-catalyzed skeletal reorganization of 1,6-enynes to 1-vinylcyclopentenes with high chemical yield and high selectivity was reported by

24 (a) Trost, B. M.; Tanoury, G. J. An Unusual Mechanism of a Palladium-Catalyzed Intramolecular Carbametalation. A Novel Palladium-Catalyzed Rearrangement *J. Am. Chem. Soc.*, **1988**, *110*, 1636-1638; (b) Trost, B. M.; Tour, J. M. Intramolecular carbametalations. A [2 + 2 + 2] cycloaddition as evidence for a palladacyclopentene intermediate *J. Am. Chem. Soc.*, **1987**, *109*, 4753-4755.

Murai et al. in 1994 (**Scheme 1.20**).<sup>25</sup>



**Scheme 1.20.** Ru(II)-catalyzed skeletal reorganization of 1,6-enynes.

Through experimental investigation, they found that the reaction of substrate **L** (1 mmol) and  $[\text{RuCl}_2(\text{CO})_3]_2$  (0.04 mmol) in toluene (5 mL) at  $80^\circ\text{C}$  under an atmosphere of CO was completed within 12 h to give product **Pro7** with a yield of 96% (**Scheme 1.20, I**). The possible mechanism they proposed is shown in **Scheme 1.20, II**.<sup>20j,25</sup> The metal carbene intermediate **12** is generated via *5-exo-dig* cyclization by the electrophilic of the alkyne moiety by Ru(II). Intermediate **13** can be obtained by cleavage of the carbon-carbon bond of **12**. Subsequently, the second carbon-carbon bond cleavage affords **14**, and finally, the catalyst is eliminated to give the thermodynamically stable *trans* 1-vinyl cyclopentenes **15**.

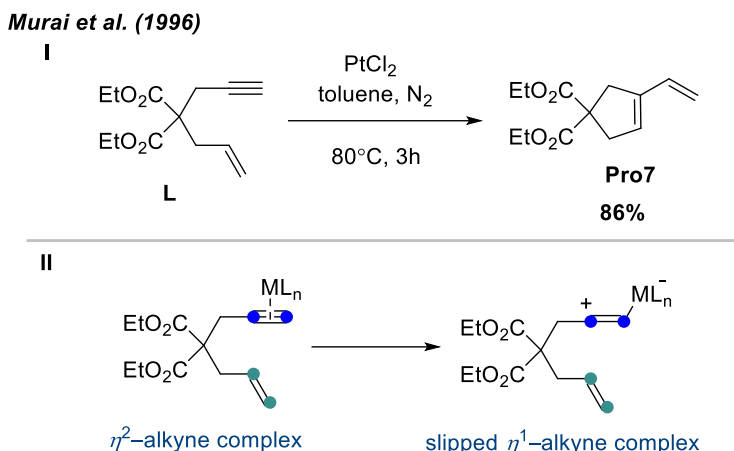
### 1.2.2.2. Pt(II)-catalyzed skeletal reorganization of enynes

It is well-known that a variety of transition metals can coordinate alkynes through their  $\pi$  system.<sup>26</sup> Pioneering studies of Murai et al. have shown that  $\text{PtCl}_2$  is a versatile

<sup>25</sup> N. Chatani, N.; Morimoto, T.; Muto, T.; Murai, S. Highly Selective Skeletal Reorganization of 1,6- and 1,7-Enynes to 1-Vinylcycloalkenes Catalyzed by  $[\text{RuCl}_2(\text{CO})_3]_2$ . *J. Am. Chem. Soc.*, **1994**, *116*, 6049–6050.

<sup>26</sup> Collman, J. P.; Hegedus, L. S.; Norton, J. R.; Finke, R. G. *Principles and Applications of*

catalyst for the skeletal rearrangements of enynes.<sup>27</sup> As shown in **Scheme 1.21**, part I, treatment of 1,6-enyne **L** with 4 mol% PtCl<sub>2</sub> in toluene at 80 °C under nitrogen for 3 h resulted in its skeletal reorganization to give 1-vinylcyclopentenes **Pro7** with a yield of 86%. The reaction is believed to involve a slipped  $\eta^1$ -alkyne complex rather than a  $\eta^2$ -alkyne complex (**Scheme 1.21**, II).<sup>28</sup>



**Scheme 1.21.** Pt(II)-catalyzed skeletal reorganization of 1,6-enynes.

### 1.2.2.3. Au(I)-catalyzed skeletal reorganization of enynes

In 2004, Echavarren et al. reported the gold(I)-catalyzed cycloisomerization of enynes (**Scheme 1.22**, I) and proposed a mechanism (**Scheme 1.22**, II).<sup>29,30</sup> The coordination

---

*Organotransition Metal Chemistry*; University Science Books: Mill Valley, CA, 1987.

27 Chatani, N.; Furukawa, N.; Sakurai, H.; Murai, S. PtCl<sub>2</sub>-Catalyzed Conversion of 1,6- and 1,7-Enynes to 1-Vinylcycloalkenes. Anomalous Bond Connection in Skeletal Reorganization of Enynes. *Organometallics* **1996**, *15*, 901–903.

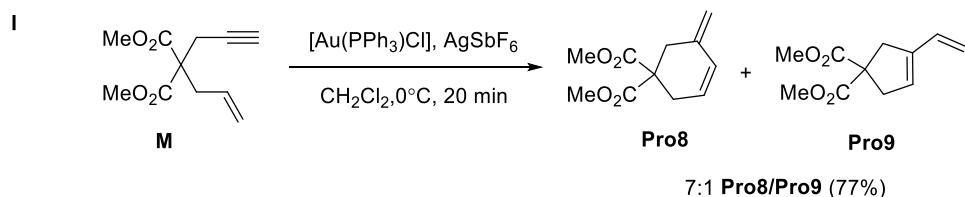
28 (a) Enda, J.; Kuwajima, I. A Lewis acid mediated rearrangement of 1-(trimethylsilyl)prop-2-ynyl trimethylsilyl ethers to 2-trimethylsilyl enones *J. Chem. Soc., Chem. Commun.* **1984**, 1589–1589. (b) Pilette, D.; Moreau, S.; Le Bozec, H.; Dixneuf, P. H.; Corrigan, J. F.; Carty, A. J. Novel behaviour of dialkylamino-substituted propargylic alcohols in reactions with arene ruthenium(II) complexes *J. Chem. Soc., Chem. Commun.* **1994**, 409–410.

29 Nieto-Oberhuber, C.; Muñoz, M. P.; Buñuel, E.; Nevado, C.; Cárdenas, D. J.; Echavarren, A. M. Cationic Gold(I) Complexes: Highly Alkynophilic Catalysts for the *exo*- and *endo*-Cyclization of Enynes. *Angew. Chem., Int. Ed.* **2004**, *43*, 2402–2406.

30 (a) Lloyd-Jones, G. C. Mechanistic aspects of transition metal catalysed 1,6-diene and 1,6-enyne

of the metal catalyst with the alkyne forms a ( $\eta^2$ -alkyne)-metal complex **16**, which subsequently forms the metal cyclopropyl carbene complex **17** (via *5-exo-dig* cyclization) or **22** (via *6-endo-dig* cyclization). The skeletal rearrangement of enynes can be carried out through intermediate **17** (or resonance structure **17'**) to form conjugated dienes **18** (via bond **a** cleavage) and **19** (via bond **b** cleavage). Alternatively, when a nucleophile of type R'OH (alcohols or water) is present, R'OH will attack **17** to give alkoxy- or hydroxycyclization products **20** and **21**. When Z = O or NTs in the substrate, the product **23** derived from intermediate **22** is found in the product, and this process is produced by the shift of the  $\beta$ -hydrogen ( $M = \text{PtCl}_2^{31}$ ,  $\text{PtCl}_4^{32}$ ). In addition, the resonance structure **22'** of metal cyclopropyl carbene complex **22** can lead to **24**. Since  $[\text{Au}(\text{PPh}_3)]^+$  cannot coordinate with alkenes and alkynes simultaneously,<sup>33</sup> Alder-ene cycloisomerization cannot compete, and the cyclization can only be carried out through **16**-type complexes.

**Echavarren et al. (2004)**

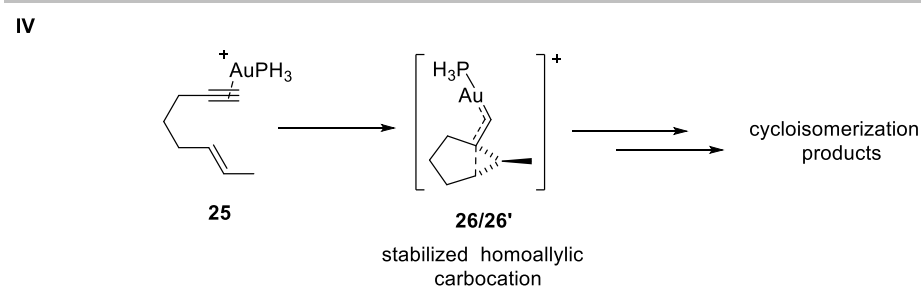
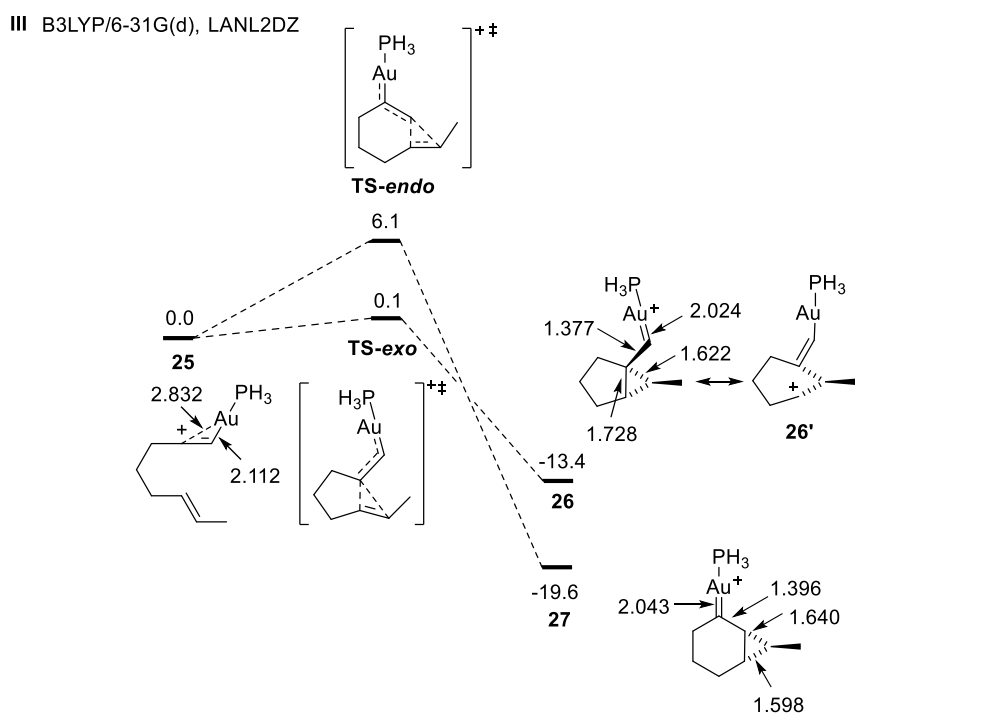
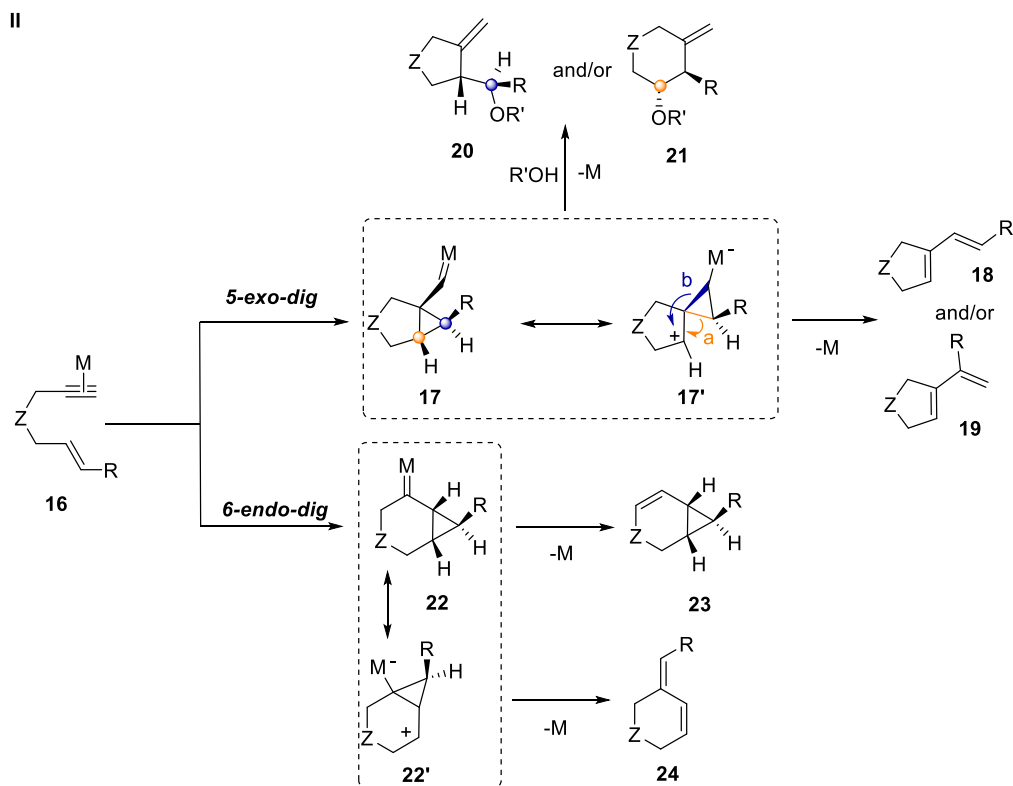


cycloisomerisation reactions *Org. Biomol. Chem.* **2003**, *1*, 215–236; (b) Aubert, C.; Buisine, O.; Malacria, M. The behavior of 1, *n*-enyne in the presence of transition metals. *Chem. Rev.* **2002**, *102*, 813–834.

31 Fürstner, A.; Szillat, H.; Stelzer, F. Novel Rearrangements of Enynes Catalyzed by  $\text{PtCl}_2$ . *J. Am. Chem. Soc.* **2000**, *122*, 6785–6786.

32 (a) Blum, J.; Berr-Kraft, H.; Badrieh, Y. A Novel  $\text{PtCl}_4$ -Catalyzed Cyclorearrangement of Allyl Propynyl Ethers to 3-Oxabicyclo[4.1.0]heptenes *J. Org. Chem.* **1995**, *60*, 5567–5569.

33 (a) Hoffmann, R. Building bridges between inorganic and organic chemistry (Nobel Lecture) *Angew. Chem. Int. Ed. Engl.* **1982**, *21*, 711–724; (b) Hall, K. P.; Mingos, D. M. P. *Prog. Inorg. Chem.* **1984**, *32*, 237–325.



**Scheme 1.22.** (I) Gold(I) complex catalyzed cycloisomerization of enynes. (II)

Proposed mechanism for the skeletal reorganization of enynes. (III) Reaction coordinates for the cyclization of (*E*)-6-octen-1-yne with  $[\text{AuPH}_3]^+$ . (IV)  
Alkynophilicity of  $[\text{Au}(\text{PH}_3)]^+$ .

Next, they used  $[\text{Au}(\text{PH}_3)]^+$  as the active catalyst and (*E*)-6-octene-1-yne as a model substrate to perform DFT calculations (Scheme 1.22, III). The calculation results show that when  $[\text{Au}(\text{PH}_3)]^+$  is coordinated to the C-C triple bond of (*E*)-6-octene-1-yne, a highly polarized ( $\eta^1$ -alkyne)-gold complex **25** is formed, which shows obvious electron deficiency at C2. Complex **25** can easily react with intramolecular alkene through *exo*-cyclization. The activation energy of this process is very small and only 0.1 kcal/mol (TS-*exo*) is needed to obtain intermediate **26**. The C-C bond of cyclopropane conjugated with carbene in complex **26** has a particularly long bond length (1.728 Å). Therefore, this complex **26** can also be similar to the resonance structure **26'** (a gold(I)-stabilized homoallylic carbocation). The concept of alkynophilicity was first proposed, that is, to evaluate the ability of a Lewis acid to promote the skeletal rearrangement (or alkoxy cyclization) of enynes through highly polarized ( $\eta^1$ -alkynes)-metal complexes, thereby producing stable homoallylic carbocations (Scheme 1.22, IV). The activation energy of the *6-endo-dig* process to produce the carbene is 6.1 kcal/mol (TS-*endo*), which is 6 kcal/mol higher than the activation energy of the *5-exo-dig* process. Therefore, for (*E*)-6-octene-1-yne related substrates, the *exo*-cyclization reaction should be favored with gold(I) catalysts.

For comparison, they used  $[\text{Pt}(\text{H}_2\text{O})\text{Cl}_2]$  as the catalyst. The calculation results show that the activation energy of the *5-exo-dig* process and the *6-endo-dig* process are 10.3 and 11.2 kcal/mol, respectively. This is consistent with the conclusion that the gold(I) complex is more active.

### 1.2.3. Main Group Metal-Catalyzed Skeletal Reorganization of Enynes

#### 1.2.3.1. Ga(III)- and In(III)-catalyzed skeletal reorganization of enynes.

A number of reports indicate that  $\text{GaCl}_3$  is a good activator of alkynes.<sup>34,35</sup> The aforementioned  $\text{GaCl}_3$ -catalyzed skeletal reorganization of enynes also supports this view.<sup>21</sup> Similarly,  $\text{InCl}_3$  also has been reported to have a high affinity toward acetylenic bonds.<sup>36</sup> In 2006, Chatani et al. reported that  $\text{InCl}_3$  catalyzes the skeletal reorganization of enynes (**Scheme 1.23**).<sup>37</sup> Experimental results showed that when the 1,6-enyne L

34 (a) Yamaguchi, M.; Nishimura, Y. Trichlorogallium and trialkylgalliums in organic synthesis *Chem. Commun.*, **2008**, 35–48; (b) Arisawa, M.; Miyagawa, C.; Yoshimura, S.; Kido, Y.; Yamaguchi, M.  $\text{GaCl}_3$ -Promoted Ethenylation of Thioester Silyl Enolate and Dienolate with Silylethyne *Chem. Lett.*, **2001**, 1080–1081; (c) Asao, N.; Asano, T.; Ohishi, T.; Yamamoto, Y. Chelation Control through the Coordination of Lewis Acids to an Acetylenic  $\pi$ -Bond *J. Am. Chem. Soc.*, **2000**, *122*, 4817–4818; (d) Kobayashi, K.; Arisawa, M.; Yamaguchi, M.  $\text{GaCl}_3$ -Catalyzed Ortho-Ethynylation of Phenols *J. Am. Chem. Soc.*, **2002**, *124*, 8528–8529; (e) Viswanathan, G. S.; Wang, M.; Li, C.-J. A Highly Regioselective Synthesis of Polysubstituted Naphthalene Derivatives through Gallium Trichloride Catalyzed Alkyne–Aldehyde Coupling *Angew. Chem., Int. Ed.*, **2002**, *114*, 2242–2245.

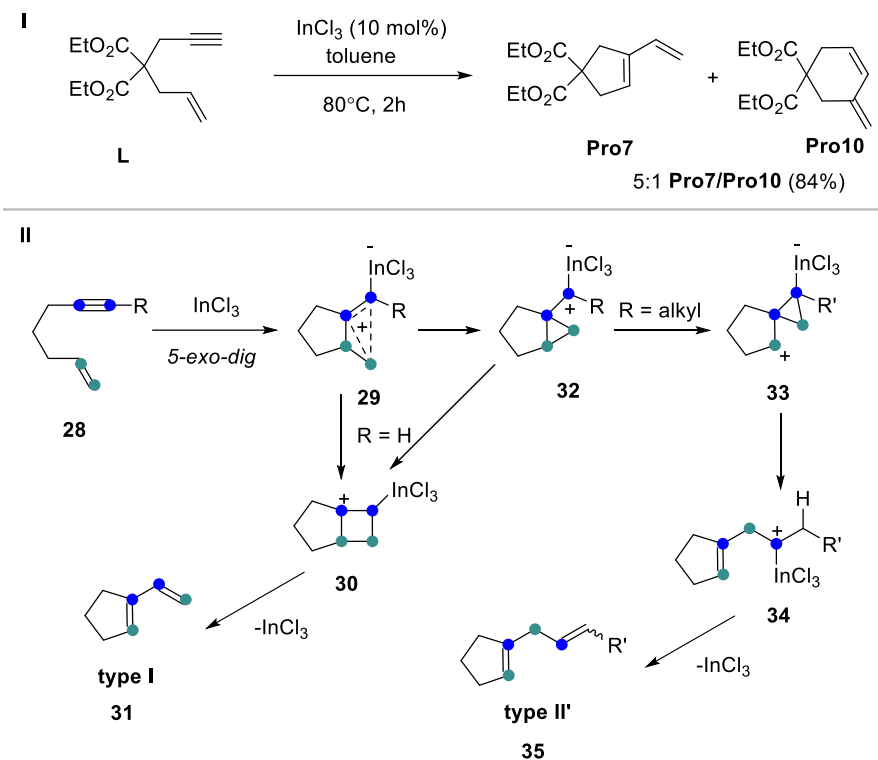
35 (a) Tobisu, M.; Oshita, M.; Yoshioka, S.; Kitajima A.; Chatani, N.  $\text{GaCl}_3$ -catalyzed reactions utilizing isocyanides as a Cl source *Pure Appl. Chem.*, **2006**, *78*, 275–280; (b) Chatani, N.; Oshita, M.; Tobisu, M.; Ishii, Y.; Murai, S. A  $\text{GaCl}_3$ -catalyzed [4+1] cycloaddition of  $\alpha,\beta$ -unsaturated carbonyl compounds and isocyanides leading to unsaturated  $\gamma$ -lactone derivatives *J. Am. Chem. Soc.*, **2003**, *125*, 7812–7813; (c) Oshita, M.; Tobisu, M.; Yamashita K.; Chatani, N. A Catalytic [4 + 1] Cycloaddition of  $\alpha$ ,  $\beta$ -Unsaturated Carbonyl Compounds with Isocyanides *J. Am. Chem. Soc.*, **2005**, *127*, 761–766; (d) Yoshioka, S.; Oshita, M.; Tobisu, M.; Chatani, N.  $\text{GaCl}_3$ -Catalyzed Insertion of Isocyanides into a C–O Bond in Cyclic Ketals and Acetals *Org. Lett.*, **2005**, *7*, 3697–3699.

36 (a) Nakamura, M.; Endo, K.; Nakamura, E. Indium-Catalyzed Addition of Active Methylene Compounds to 1-Alkynes *J. Am. Chem. Soc.* **2003**, *125*, 13002–13003. (b) Tsuchimoto, T.; Hatanaka, K.; Shirakawa, E.; Kawakami, Y. Indium triflate-catalysed double addition of heterocyclic arenes to alkynes *Chem. Commun.* **2003**, 2454–2455.

37 Miyanohana, Y.; Chatani, N. Skeletal Reorganization of Enynes Catalyzed by  $\text{InCl}_3$  *Org. Lett.*, **2006**, *8*, 2155–2158.

was treated with  $\text{PtCl}_2$  (10 mol%) in toluene at 80 °C for 2 h, the skeletal reorganization took place to give 1-vinylcyclopentene **Pro7** and the six-membered cycloisomerization product **Pro10** with a yield of 86% (**Scheme 1.23, I**).

*Chatani et al. (2006)*



**Scheme 1.23.**  $\text{In(III)}$ -catalyzed skeletal reorganization of 1,6-enynes.

The possible mechanism of  $\text{InCl}_3$ -catalyzed skeletal reorganization of enynes (type **I** and type **II'**) is shown in **Scheme 1.23, II**. The electrophilic interaction of  $\text{InCl}_3$  with alkyne moiety gives nonclassical carbocation **29**, followed by the formation of cyclobutane ring **30** (when  $\text{R} = \text{H}$ ). From **29** to **30**, the stereochemical retention of the terminal olefinic carbon is consistent with the stereospecificity observed. Next, **30** undergoes electrocyclic ring-opening to give type **I** product (**31**). When  $\text{R}$  is an alkyl group, the cation can be stabilized by  $\text{R}$  group resulting in **32** from **29**. Then, **32** is transformed into **33**, which undergoes ring-opening to obtain type **II'** product (**35**).

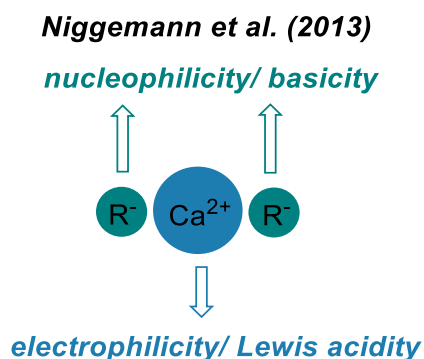
In conclusion, we can say once again that even if similar mechanisms have been

proposed for late transition metals and main-group metals, the alkynophilicity of main-group metal complexes remains unclear. The properties of transition metals such as gold that are linked to its relativistic effects cannot be invoked, nor back-donation that is effective with Pd or Ru, and yet simple salts such as  $\text{GaCl}_3$  or  $\text{InCl}_3$  are excellent  $\pi$ -Lewis acids. Our work shown in Chapter 3 aims at clarifying this issue.

## 1.3. Coupling of Alcohols with Vinylboronic Acids: A Lewis Acid at the Rescue of Another?

### 1.3.1. Introduction

The reactivity of calcium(II) compounds can be roughly understood from their two moieties: **a**. As a member of alkali metal compounds, it is highly ionic character due to its low electronegativity. Therefore, calcium endows its counterion with high nucleophilicity and strong basicity. **b**. The calcium center itself is similar to the metal center of a typical Group 3 compound with Lewis acidity ( $\text{Sc}$ ,  $\text{Y}$ ,  $\text{Ln}$ ).<sup>38</sup>



**Scheme 1.24.** Reactivity of calcium compounds.

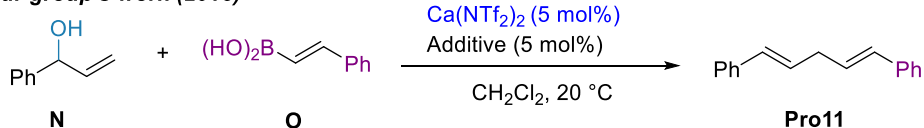
We have developed a calcium-catalyzed coupling reaction of alcohols and vinylboronic

38 Begouin, J.-M.; Niggemann, M. Calcium-Based Lewis Acid Catalysts. *Chem. Eur. J.* **2013**, *19*, 8030–8041.

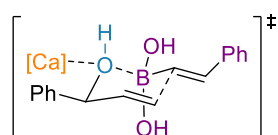
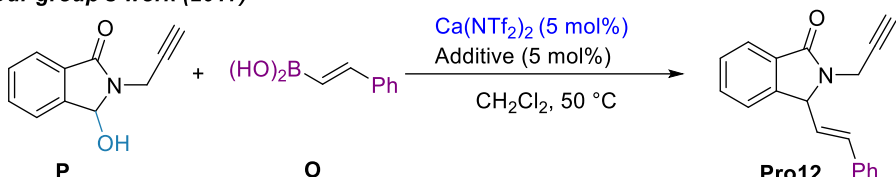
acids in 2015 and 2017 respectively (**Scheme 1.25**).<sup>39,40</sup> This alkenylation reaction is effective for allyl, benzyl and propargyl alcohols (**Scheme 1.25, I**) and N,O-acetals (**Scheme 1.25, II**). As shown in **Scheme 1.25**, the positive effect of ammonium salt with N,O-acetal **P** was obvious, that is, a better yield was obtained in the absence of allyl alcohol **N**. On the contrary, in the presence of allyl alcohol **N**, the same additive (*n*Bu<sub>4</sub>NPF<sub>6</sub>) did not give a better yield. The fact that different catalytic systems (Ca(NTf<sub>2</sub>)<sub>2</sub> and Ca(NTf<sub>2</sub>)(PF<sub>6</sub>), see below) lead to different yields has attracted our attention. Besides, the proposed mechanism of the calcium-catalyzed alkenylation reaction of allylbenzyl alcohol **N** and (*E*)-styrylboronic acid **O** reported by our group does not suggest a S<sub>N</sub>1 reaction, but rather a S<sub>N</sub>2' process. Furthermore, the mechanism by which calcium catalyzes the alkenylation reaction of *N*-acyliminium **P** and vinylboronic acid **O** is not yet clear. In our original proposal, both Ca and B are bond to the same oxygen of the alcohol substrate. While both are Lewis acids, other association might also be considered, such as the coordination of Ca to the oxygen of the B(OH)<sub>2</sub> moiety. In such case, this would result in a heterobimetallic superelectrophile. Thus, a thorough analysis of the species present in solution, including the counterion, which play an obvious role here, will be presented.

39 Lebœuf, D.; Presset, M.; Michelet, B.; Bour, C.; Bezzanine-Lafollée, S.; Gandon, V. Ca(II)-Catalyzed Alkenylation of Alcohols with Vinylboronic Acids. *Chem. Eur. J.* **2015**, *21*, 11001–11005.

40 Qi, C.; Gandon, V.; Lebœuf, D. Calcium(II)-Catalyzed Alkenylation of N-Acyliminiums and Related Ions with Vinylboronic Acids. *Adv. Synth. Catal.* **2017**, *359*, 2671–2675.

**I Our group's work (2015)**

Entry	Additive	Yield of Pro11 (%)
1	-	73
2	<i>n</i> Bu <sub>4</sub> NPF <sub>6</sub>	57

**Proposed transition state****II Our group's work (2017)**

Entry	Additive	Yield of Pro12 (%)
3	-	0
4	<i>n</i> Bu <sub>4</sub> NPF <sub>6</sub>	92

**Scheme 1.25.** Calcium-catalyzed alkenylation of alcohols.**1.3.2. The Nature of Ca(NTf<sub>2</sub>)<sub>2</sub> and Ca(NTf<sub>2</sub>)(PF<sub>6</sub>)****1.3.2.1. The structure of Ca(NTf<sub>2</sub>)<sub>2</sub>·4H<sub>2</sub>O**

DesMarteau and co-workers reported the structure of Ca(NTf<sub>2</sub>)<sub>2</sub>·4H<sub>2</sub>O in 2005.<sup>41</sup> CYLview plot shows that calcium ion is not bound to the nitrogen atom of the NTf<sub>2</sub><sup>-</sup> counterion, but to the oxygen atom of the SO<sub>2</sub>CF<sub>3</sub> moiety, and the CF<sub>3</sub> group adopts the *cis* configuration (**Figure 1.26**). The relationship between metallic calcium and its counterion (i.e. calcium ion is coordinated to oxygen atoms) is in sharp contrast with

<sup>41</sup> Xue, L.; DesMarteau, D. D.; Pennington, W. T. Synthesis and Structures of Alkaline Earth Metal Salts of bis[(Trifluoromethyl)-sulfonyl]imide. *Solid State Sci.* **2005**, 7, 311–318.

soft transition metals that are usually coordinated with the nitrogen atom of the  $\text{NTf}_2^-$  anion, which reveals the strong oxophilicity of calcium. Therefore,  $\text{Ca}(\text{NTf}_2)_2$  is not a very strong Lewis acid because the counterions are strongly coordinated and occupy four coordination sites of the metal.

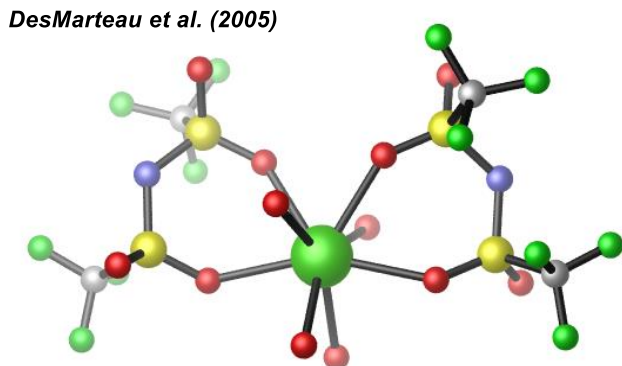


**Figure 1.26.** CYLview plot of  $\text{Ca}(\text{NTf}_2)_2 \cdot 4\text{H}_2\text{O}$  based on experimental crystal structure.

### 1.3.2.2. The formation of $\text{Ca}(\text{NTf}_2)(\text{PF}_6)$

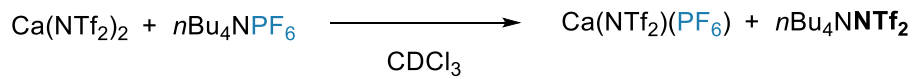
In 2011, Niggemann and co-workers performed  $^{19}\text{F}$  NMR spectroscopy on the formation of  $\text{Ca}(\text{NTf}_2)(\text{PF}_6)$  by anion exchange (**Scheme 1.27**).<sup>42</sup> As they expected, the  $^{19}\text{F}$  NMR spectrum of the additive  $n\text{Bu}_4\text{NPF}_6$  alone has a doublet of the  $\text{PF}_6^-$  anion centered at 72.6 ppm ( $J_{PF} = 767$  Hz), which is consistent with the corresponding  $^{31}\text{P}$  NMR spectrum (not shown in their paper and SI). The  $^{31}\text{P}$  NMR and  $^{19}\text{F}$  NMR spectra of the 1:1 mixture of  $\text{Ca}(\text{NTf}_2)_2$  and  $n\text{Bu}_4\text{NPF}_6$  did not show any of the above  $\text{PF}_6^-$  signals. The  $^{31}\text{P}$  NMR spectrum has no signal (not shown again), while the  $^{19}\text{F}$  NMR spectrum shows a new singlet at 79.10 ppm, which corresponds very accurately to the signal of the  $\text{CF}_3$  moiety of  $n\text{Bu}_4\text{NNTf}_2$ . Therefore, based on the above spectral observation, the 1:1 mixture of  $\text{Ca}(\text{NTf}_2)_2$  and  $n\text{Bu}_4\text{NPF}_6$  has formed  $\text{Ca}(\text{NTf}_2)(\text{PF}_6)$ .

<sup>42</sup> Haubenreisser, S.; Niggemann, M. Calcium-Catalyzed Direct Amination of  $\pi$ -Activated Alcohols. *Adv. Synth. Catal.* **2011**, 353, 469–474.

through anion exchange. The driving force might be the higher solubility of  $\text{Ca(NTf}_2\text{)}(\text{PF}_6)$  compared to  $\text{Ca(NTf}_2)_2$ .

**Niggemann et al. (2011)**

**$^{19}\text{F}$  NMR-spectroscopic analysis**

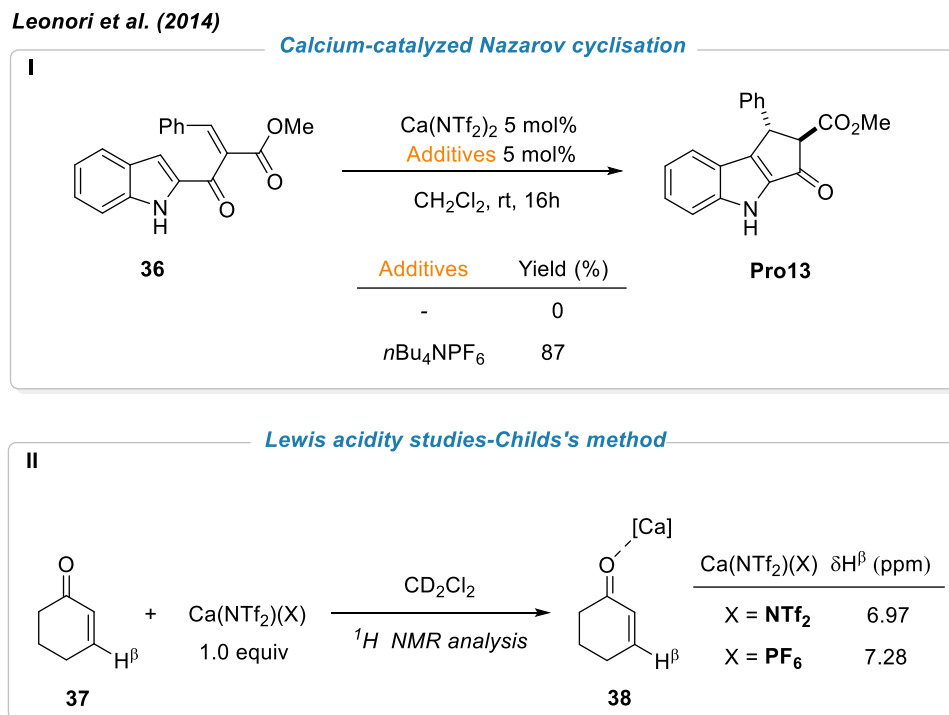


**Scheme 1.27.**  $^{19}\text{F}$  NMR-spectroscopic analysis of the formation of  $\text{Ca(NTf}_2)(\text{PF}_6)$  via anion exchange.

### 1.3.2.3. Lewis acidity of $\text{Ca(NTf}_2)_2$ and $\text{Ca(NTf}_2)(\text{PF}_6)$

In order to better understand the difference between the Lewis acidity of  $\text{Ca(NTf}_2)_2$  and  $\text{Ca(NTf}_2)(\text{PF}_6)$ , Leonori et al. made some efforts in 2014 (**Scheme 1.28**).<sup>43</sup> They reported a calcium-catalyzed Nazarov cyclization. Through controlled experiments, they found that using solely  $\text{Ca(NTf}_2)_2$  as a catalyst did not provide any product, while adding the additive  $n\text{Bu}_4\text{NPF}_6$  gave the desired cyclization product, and the yield was as high as 87% (**Scheme 1.28, I**).

43 Davies, J.; Leonori, D. The First Calcium-Catalysed Nazarov Cyclisation. *Chem. Commun.* **2014**, 50, 15171–15174.



**Scheme 1.28.** (I) Calcium-catalyzed Nazarov cyclization; (II) Lewis acidity studies based on Childs's method.

Leonori et al. believe that the difference in Lewis acidity between  $\text{Ca}(\text{NTf}_2)_2$  and  $\text{Ca}(\text{NTf}_2)(\text{PF}_6)$  may explain the observed reactivity trend. Thus, they evaluated the Lewis acidity by measuring the variation of the chemical shifts of  $\text{H}^\beta$  when the  $\text{C}=\text{O}$  group is combined with calcium-complex based on the Childs's method.<sup>44</sup> As shown in **Scheme 1.28, II** the addition of  $\text{Ca}(\text{NTf}_2)(\text{PF}_6)$  to **37** resulted in the largest change in the chemical shift of  $\text{H}^\beta$  compared to the  $\text{Ca}(\text{NTf}_2)_2$  complex. The trend reflects the catalytic activity observed in Nazarov cyclization:  $\text{Ca}(\text{NTf}_2)(\text{PF}_6) > \text{Ca}(\text{NTf}_2)_2$ .

### 1.3.3. Mechanistic Hypotheses

After understanding the nature of Lewis acid catalysts  $\text{Ca}(\text{NTf}_2)_2$  and  $\text{Ca}(\text{NTf}_2)(\text{PF}_6)$ ,

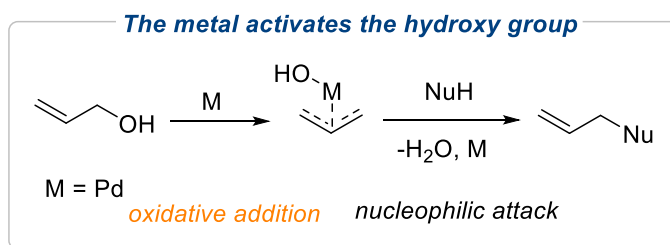
<sup>44</sup> Childs, R. F.; Mulholland, D. L.; Nixon, A. The Lewis acid complexes of  $\alpha, \beta$ -unsaturated carbonyl and nitrile compounds. A nuclear magnetic resonance study. *Canadian Journal of Chemistry*, **1982**. *60*, 801–808.

we will next discuss the reaction mechanism of the calcium-catalyzed alkenylation. Through literature search, we found that most of the data on the cross-coupling of allyl alcohols and vinylboronic acids are related to palladium catalysis. Therefore, we have classified the possible calcium-catalyzed alkenylation reaction mechanisms on the basis of palladium and calcium catalysts. There are mainly the following four types.

### 1.3.3.1. The metal activates the hydroxy group

As shown in **Scheme 1.29**, Bandini and co-workers reported on the catalytic enantioselective allylations with allylic alcohols in a short review in 2012.<sup>45</sup> First, the transition metal palladium activates the hydroxy group of allyl alcohol, then the transition metal species will oxidatively insert into the C-OH bond to form a  $\pi$ -allylpalladium intermediate. Finally, the nucleophile NuH undergoes a nucleophilic attack, and the allylation product is released and accompanied by the regeneration of the catalyst.

*Bandini et al. (2012)*



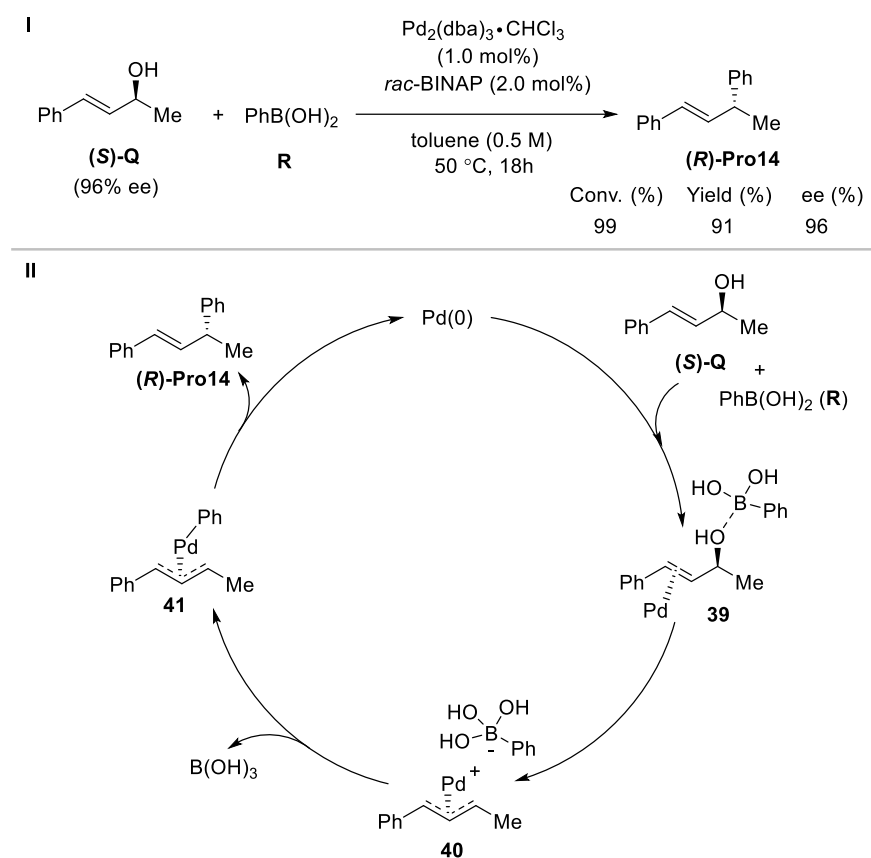
**Scheme 1.29.** Mechanism of transition metal-catalyzed nucleophilic allylation reaction.

### 1.3.3.2. The boronic acid activates the hydroxy group

In 2013, Zhang et al. reported the stereospecific allyl-aryl coupling reaction of allylic

45 Bandini, M.; Cera, G.; Chiarucci, M. Catalytic Enantioselective Alkylation with Allylic Alcohols. *Synthesis* **2012**, 504–512.

alcohols and aryl boronic acids catalyzed by palladium.<sup>46</sup> The experimental results show that in the presence of  $\text{Pd}_2(\text{dba})_3 \cdot \text{CHCl}_3$  (1.0 mol%) Pd source, racemic BINAP (2.0 mol%) ligand and toluene as solvent, the enantionenriched allylic alcohol (*S*)-**Q** (96% ee) and phenylboronic acid (**R**) reacted at 50 °C for 18 h, the yield of coupling product (*R*)-**Pro14** was 91% with complete enantiospecificity (from 96% *ee* to 96% *ee*) (**Scheme 1.30, I**).



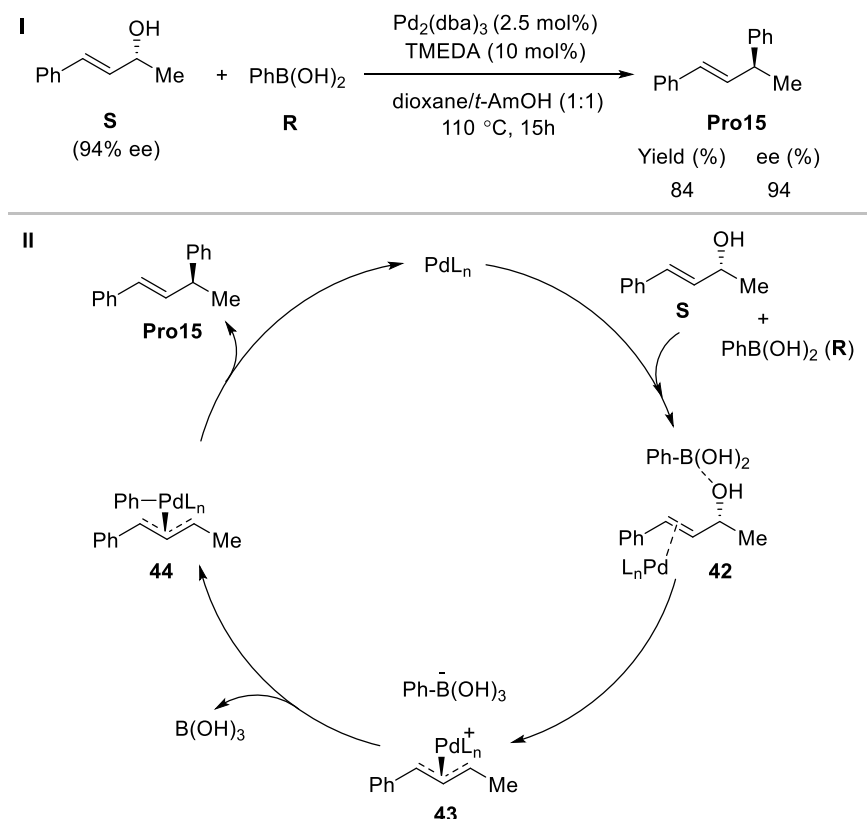
**Scheme 1.30.** Plausible reaction pathway for the cross-coupling of allylic alcohol with arylboronic acid (*rac*-BINAP = racemic-2,2'-Bis(diphenylphosphino)-1,1'-binaphthyl).

As shown in **Scheme 1.30, II**, they proposed a plausible mechanism. First, the hydroxy group of allylic alcohol (*S*)-**Q** is activated by phenylboronic acid **R** to give intermediate

46 Ye, J.; Zhao, J.; Xu, J.; Mao, Y.; Zhang, Y. J. Pd-Catalyzed Stereospecific Allyl–Aryl Coupling of Allylic Alcohols with Arylboronic Acids. *Chem. Commun.* **2013**, 49, 9761–9763.

**39**, and then  $\pi$ -allylpalladium intermediate **40** is formed by the oxidative addition of the Pd-complex into the activated chiral (*S*)-**Q** from the back side stereospecifically. Subsequently, the  $\pi$ -allylpalladium intermediate **40** undergoes the transmetalation to form allylaryl palladium **41**, followed by reductive elimination on the side with less steric hindrance, and finally provides an allyl-aryl coupling product (*R*)-**Pro14** with excellent stereospecificity.

Tian and co-workers also did a palladium-catalyzed coupling reaction of enantioenriched allylic alcohols and boronic acids (**Scheme 1.31**).<sup>47</sup> Although the optimal reaction conditions and the configurations of allylic alcohol and product are different, the proposed reaction mechanism is similar. The first step of the mechanism is also the activation of the hydroxy group of the allylic alcohol by phenylboronic acid to give intermediate **42**.

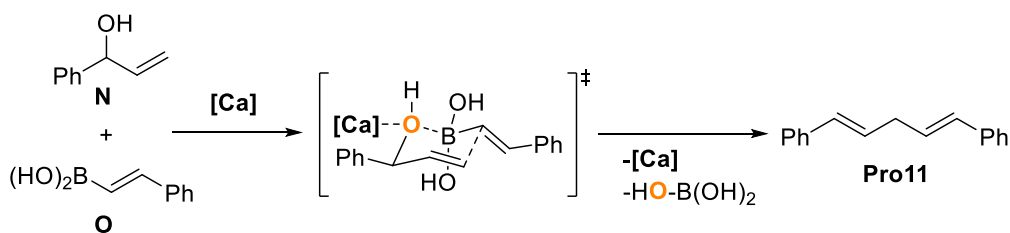


<sup>47</sup> Wu, H.-B.; Ma, X.-T.; Tian, S.-K. Palladium-catalyzed stereospecific cross -coupling of enantioenriched allylic alcohols with boronic acids. *Chem. Commun.*, **2014**, *50*, 219–221.

**Scheme 1.31.** Proposed catalytic cycle (TMEDA = Tetramethylethylenediamine).

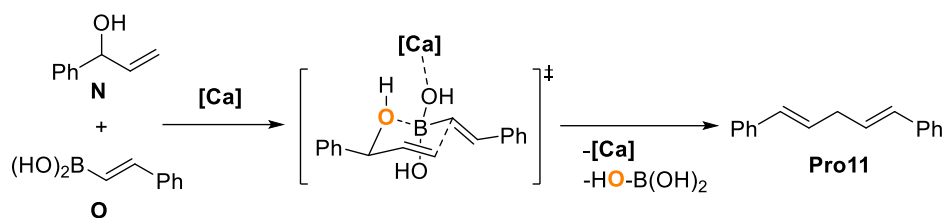
### 1.3.3.3. Calcium and boronic acid synergistically activates the hydroxy group

Considering that the hydroxyl groups can be individually activated by boric acid and metal catalysts as mentioned above, it may also be activated synergistically by the boronic acid and the metal catalyst. For example, the possible transition state proposed by our group in Ca(II)-catalyzed alkenylation of allylbenzyl alcohol **N** with (*E*)-styrylboronic acid **O** (**Scheme 1.32**).<sup>39</sup> The hydroxy group of **N** may be activated synergistically by calcium and boron.

**Scheme 1.32.** Originally proposed transition state in the Ca(II)-catalyzed alkenylation of allylbenzyl alcohol **N** with (*E*)-styrylboronic acid **O**.

### 1.3.3.4. Other hypotheses: superelectrophilic activation?

As mentioned above, one can also assume other associations such as the coordination of calcium to the boron oxygens (**Scheme 1.33**). This coordination would strengthen the Lewis acidity of the boron center and form a heterobimetallic superelectrophile. The concerted or stepwise nature of the mechanism, the role of the counterion and the differences observed between simple allyl alcohols and N,O-acetals were also objectives of our study (Chapter 4).



**Scheme 1.33.** Other possible transition state in the Ca(II)-catalyzed alkenylation of allylbenzyl alcohol **N** with (E)-styrylboronic acid **O**.

## 1.4. Conclusions

The above literature survey has pointed out some lack of knowledge regarding the mechanisms of important main group metal-catalyzed reactions. Further development of such transformations may suffer from these grey areas and we set out to shed light on these. As shown above, many surprises can be anticipated from theoretical studies on such reactions.

In this manuscript, I have chosen to focus on main group metal-catalyzed transformations in which superelectrophilic activation may play a role. I have been involved in more projects that are not detailed here (see publications list). The following Chapters 2-4 are selected publications. Their numbering and references are independent from each other.

# **Chapter 2. Superelectrophilic Gallium(III) Homodimers in Gallium Chloride-Mediated Methylation of Benzene: A Theoretical Study**

Shengwen Yang, Christophe Bour, and Vincent Gandon

Publication Date: February 13, 2020

*ACS Catal.* 2020, 10, 5, 3027–3033

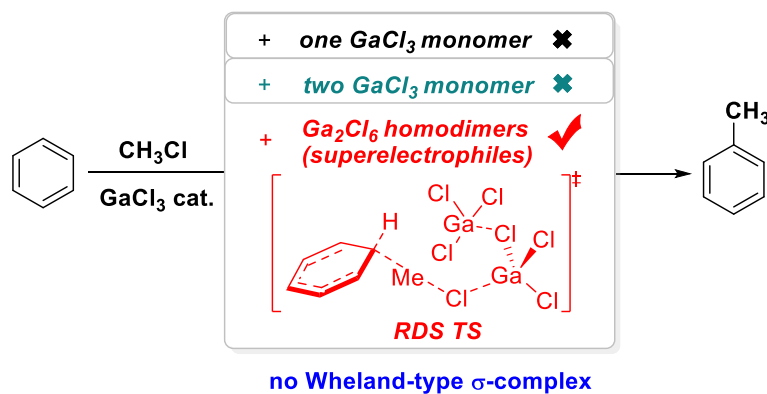
<https://doi.org/10.1021/acscatal.9b05509>

Copyright © 2020 American Chemical Society



## 2.1. Abstract

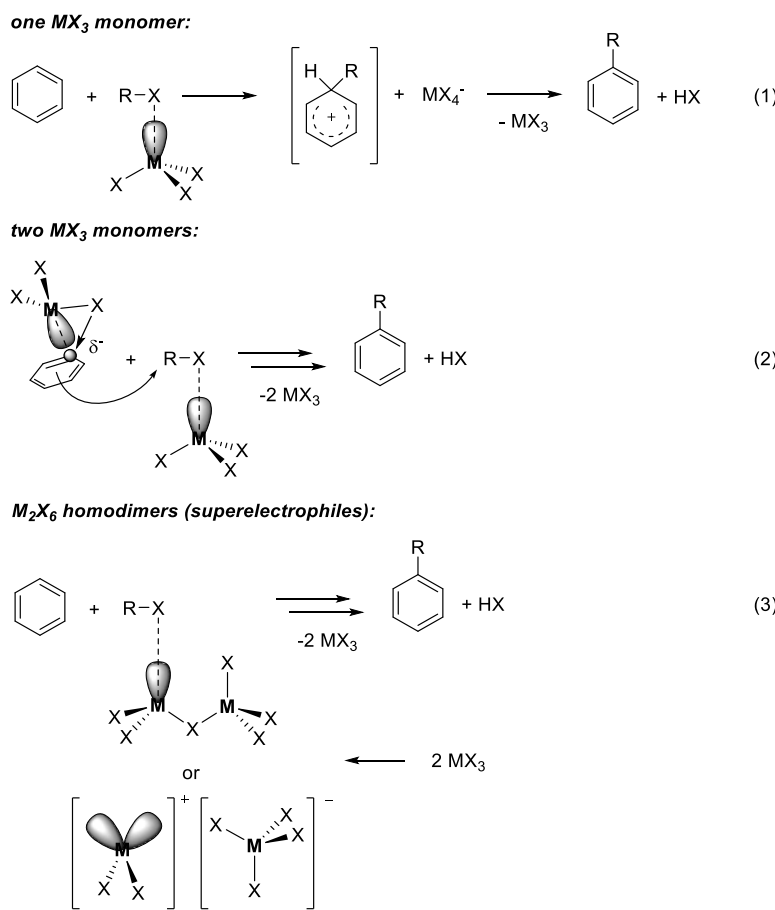
The  $\text{GaCl}_3$ -mediated Friedel-Crafts alkylation of benzene by methyl chloride has been studied by means of density functional theory computations at the M062X/6-311+G(2d,2p) level of theory. The role of superelectrophilic  $\text{Ga}_2\text{Cl}_6$  homodimers has been confirmed and explained. The results are consistent with the observation of second-order rate dependence in  $\text{GaCl}_3$ -mediated Friedel–Crafts alkylations. This work also reveals that, even in a typical Friedel–Crafts alkylation, no Wheland-type  $\sigma$ -complex can be modeled, suggesting a concerted electrophilic aromatic substitution. Also refuted is the possibility of activation of the arene nucleophile by the Lewis acid.



## 2.2. Introduction

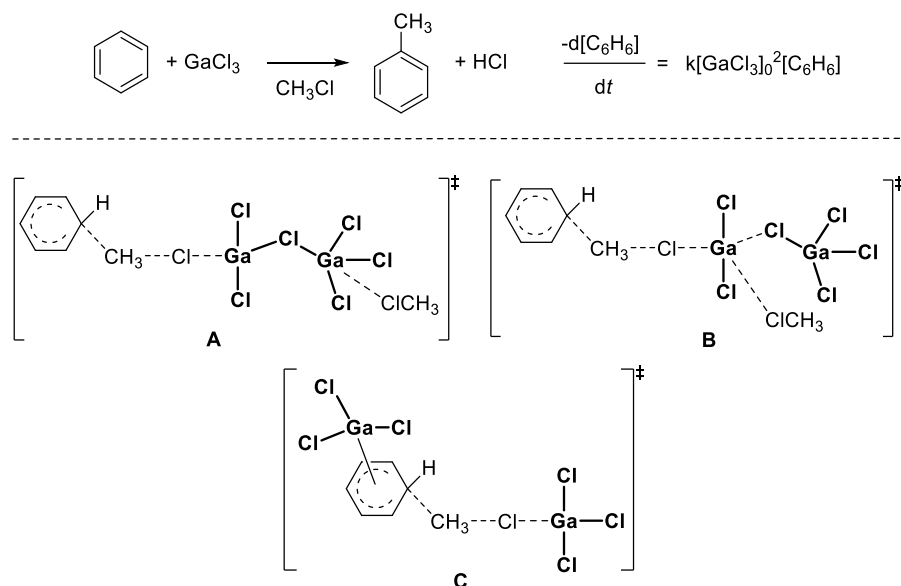
Although widely used since its discovery more than 140 years ago,<sup>1,2</sup> the Friedel–Crafts reaction remains a topic of mechanistic debate, substantiated by computational studies. First, the classical interpretations of electrophilic aromatic substitution mechanisms depicting a Wheland-type  $\sigma$ -complex have been refuted several times, even in the presence of a catalyst (**Scheme 2.1**, eq 1), with electrophiles such as  $\text{SO}_3$ ,<sup>3</sup>  $\text{Br}_2$ ,<sup>4</sup>  $\text{Cl}_2$ ,<sup>5</sup> or alkynes,<sup>6</sup> in favor of a concerted mechanism. Second, the role of the catalyst, not only for the generation of the electrophile and the deprotonation step, but also as activator of the aromatic nucleophile, has been proposed.<sup>7</sup> Kim et al. reported that the remarkable stability of the  $\text{AlCl}_3 \cdot \text{C}_6\text{H}_6$  complex, despite the loss of the benzene nodal plane, is due to a back-donation of charge from the Cl 3p orbital to the benzene highest

occupied molecular orbital (HOMO), which prevents the loss of aromaticity (see **Scheme 2.1**, eq 2). This strong interaction between AlCl<sub>3</sub> and benzene renders the C atom of benzene closest to the Al atom supposedly highly nucleophilic. Thus, these authors concluded that, in addition to the generation of the electrophile, the Lewis acid also has an important role in the activation of the aromatic substrate. Third, still related to the number of MX<sub>3</sub> molecules involved, the importance of dimeric forms of AlCl<sub>3</sub> and GaCl<sub>3</sub> in electrophilic aromatic substitutions has been revealed.<sup>8</sup> This aspect is taking on a new dimension nowadays, as more and more pieces of evidence are being provided that homodimers of metal halides can act as superelectrophiles in homogeneous catalysis and trigger new reactions.<sup>9</sup> Although considered as uncommon and underexplored, compared to heterobimetallic superelectrophiles comprising two different metals, it is now better accepted that MX<sub>3</sub> (or L·MX<sub>3</sub>) monomers can also associate in situ to generate Lewis acidic superelectrophiles that are either M<sub>2</sub>X<sub>6</sub> molecular adducts or MX<sub>2</sub><sup>+</sup>MX<sub>4</sub><sup>-</sup> ion pairs (see **Scheme 2.1**, eq 3).<sup>10,11</sup> The superelectrophilicity of the molecular adducts can be explained by the formation of a singly bridged dimers of type X<sub>2</sub>M( $\mu$ -X)MX<sub>3</sub>, in which one metal center remains unsaturated and more deprived of electrons than the corresponding monomer. This adduct can be ionized to MX<sub>2</sub><sup>+</sup>MX<sub>4</sub><sup>-</sup>, in which the MX<sub>2</sub><sup>+</sup> moiety is even more electron-deficient and potentially highly active.



**Scheme 2.1.** Possible mechanisms in  $\text{MX}_3$ -mediated Friedel-Crafts alkylation.

While it is difficult to trace the first indication that homodimers can be involved in Friedel–Crafts alkylations, a kinetic study by DeHaan and Brown is considered to be a cornerstone:<sup>12</sup> The observation of second-order rate dependence in  $\text{GaCl}_3$ -mediated methylation of benzene (or hexadeuteriobenzene) in excess methyl chloride suggests an activation mode based on Lewis acid superelectrophiles, but their nature (molecular adduct or ion pair) could not be established (see **Scheme 2.2**).<sup>9a</sup> Two transition states were proposed: **A**, which accounts for an activation by the  $\text{Ga}_2\text{Cl}_6$  molecular adduct, and **B**, which accounts for the  $\text{GaCl}_2^+\text{GaCl}_4^-$  activation mode. Following Kim's proposal<sup>7</sup> of a dual activation of the electrophile and of the nucleophile, one could add hypothesis **C**, which would also correspond to the methylation rate law.



**Scheme 2.2.** Possible transition states for the second-order  $\text{GaCl}_3$ -mediated methylation of benzene by methyl chloride<sup>a</sup> (<sup>a</sup>**A**, homodimer; <sup>12</sup> **B**, ion pair;<sup>12</sup> and **C**, dual activation.<sup>7</sup>).

Our interest for gallium-catalyzed reactions,<sup>9b,13</sup> the recent increase of studies highlighting the role of superelectrophilic homodimers,<sup>9</sup> and the pivotal position occupied by Brown's kinetic study in this field encouraged us to study the gallium-mediated methylation of benzene computationally.

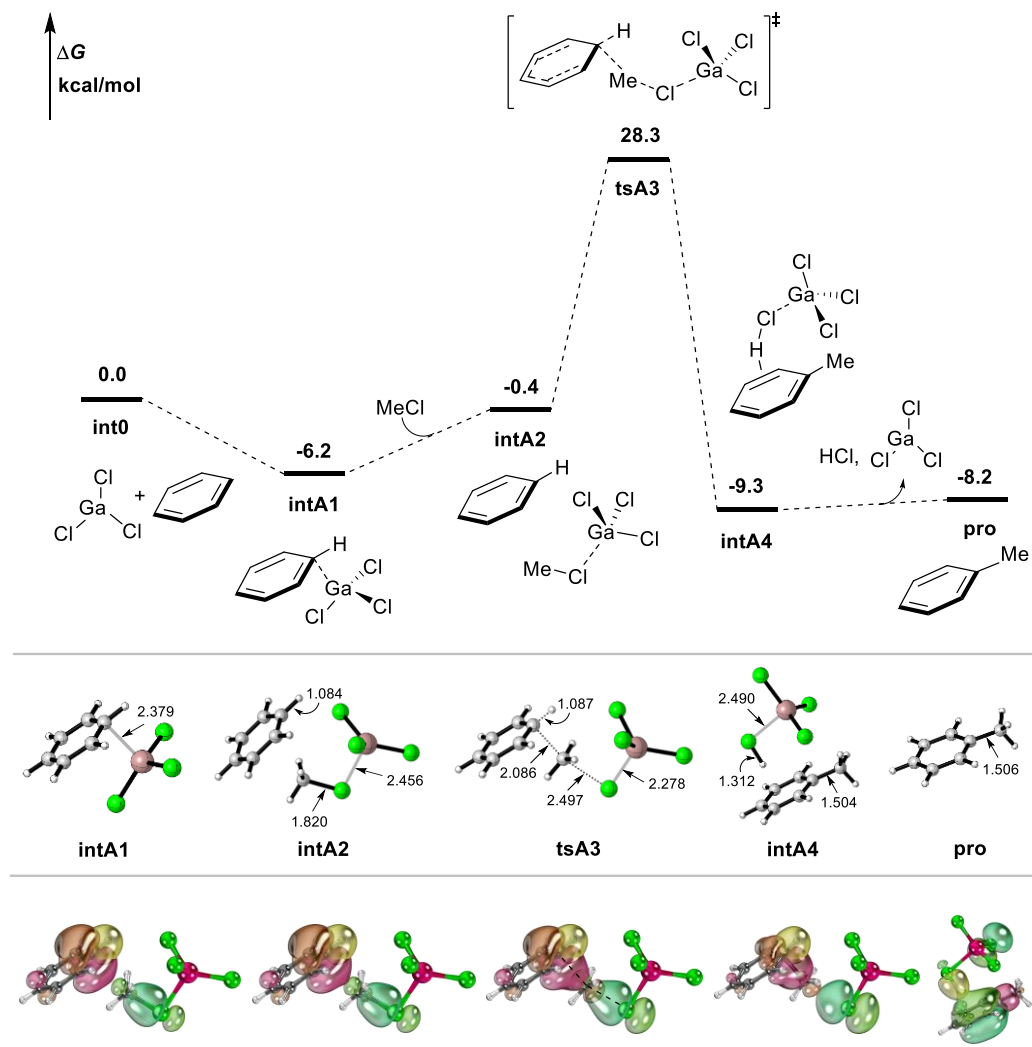
## 2.3. Computational Methods

All calculations were performed with the Gaussian 09 software package.<sup>14</sup> Density functional theory (DFT) calculations using the M06-2X functional<sup>15</sup> were performed to locate the stationary points (minima or transition states). The 6-311+G(2d,2p) basis set<sup>16,17</sup> was applied to all elements. This level of theory proved reliable to reveal the concerted or classic nature of S<sub>E</sub>Ar mechanisms.<sup>3</sup> Harmonic vibrational frequency calculations were performed at the same level of theory for the geometry optimizations to confirm the nature (transition state or an energy minimum) of each stationary point. The connectivity on the potential energy surface (PES) of the transition states was

confirmed by intrinsic reaction coordinate (IRC) calculations.<sup>18,19</sup> The values presented are  $\Delta G_{298}$  (kcal/mol). The three-dimensional images of the optimized structures were prepared using CYLview.<sup>20</sup> Intrinsic bond orbital (IBO) analyses were performed with Iboview software from the optimized geometries with the default method (PBE0/def2-TZVP) to generate Kohn–Sham wave functions.<sup>21,22</sup> The IBO method allows quantitative interpretation of bonding in an intuitive way, by visualization of electronic structure changes (electron flow) along the reaction paths.

## 2.4. Results and Discussion

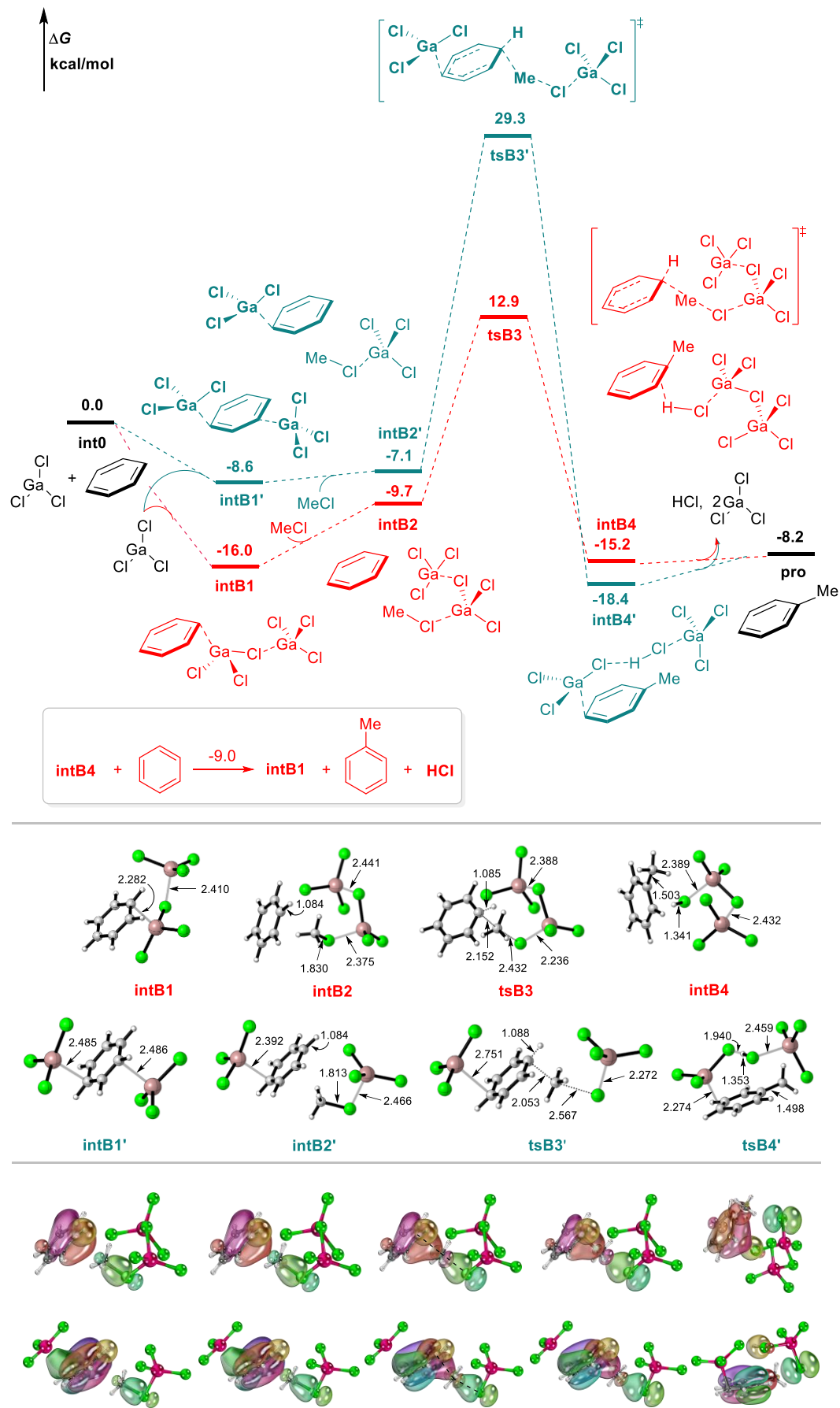
We started our investigations by studying the methylation of benzene mediated by a single  $\text{GaCl}_3$  molecule (see **Scheme 2.3**). The coordination of  $\text{GaCl}_3$  to benzene provides the  $\eta^1$ -complex **intA1**, lying 6.2 kcal/mol below the reactants **int0**. Ligand exchange by methyl chloride raised the free energy to −0.4 kcal/mol while forming **intA2**. The latter could be connected to the methylbenzene adduct **intA4** via the transition state **tsA3**. This step requires a high free energy of activation of 28.7 kcal/mol, i.e., 28.3 kcal/mol from **int0** or 34.5 kcal/mol from **intA1**. Complex **intA4** is actually an adduct of methylbenzene and  $\text{HCl}\cdot\text{GaCl}_3$  exhibiting an interaction between the HCl proton and the  $\pi$ -cloud of the aromatic ring. The IRC analysis did not lead directly to this product, but optimization of its last point systematically collapsed to **intA4** as the chlorine ligands play the role of base and catch the proton. Thus, no Wheland-type  $\sigma$ -complex could be found, as it is an unstable high-order point on the PES. Therefore, the methylation seems to be a concerted process. Elimination of HCl and  $\text{GaCl}_3$  finally leads to the final product lying at −8.2 kcal/mol.



**Scheme 2.3.** Free-energy profile of the  $\text{GaCl}_3$ -mediated methylation of benzene, selected geometries (Distances given in Å) and IBO pathway from **intA2** to **intA4**.

Our next move was to investigate the methylation of benzene in the presence of two  $\text{GaCl}_3$  molecules (see **Scheme 2.4**). Coordination of  $\text{GaCl}_3$  to benzene led either to the  $\eta^1\text{-}\text{Ga}_2\text{Cl}_6$  complex **intB1** or to the bis- $\eta^1$ -sandwich complex **intB1'**. The former is more stable by 7.4 kcal/mol. Addition of methyl chloride gave the corresponding adducts **intB2** and **intB2'**, with a thermodynamic preference for the  $\text{Ga}_2\text{Cl}_6$  complex of 2.6 kcal/mol. The alkylation transition state from **intB2'** culminates at 29.3 kcal/mol, which is slightly higher than the value found with only one  $\text{GaCl}_3$  molecule. Of note, it was not possible to use the benzene carbon coordinated to  $\text{GaCl}_3$  to make the attack to methyl chloride, but only the one in the para position. All this refutes the hypothesis of

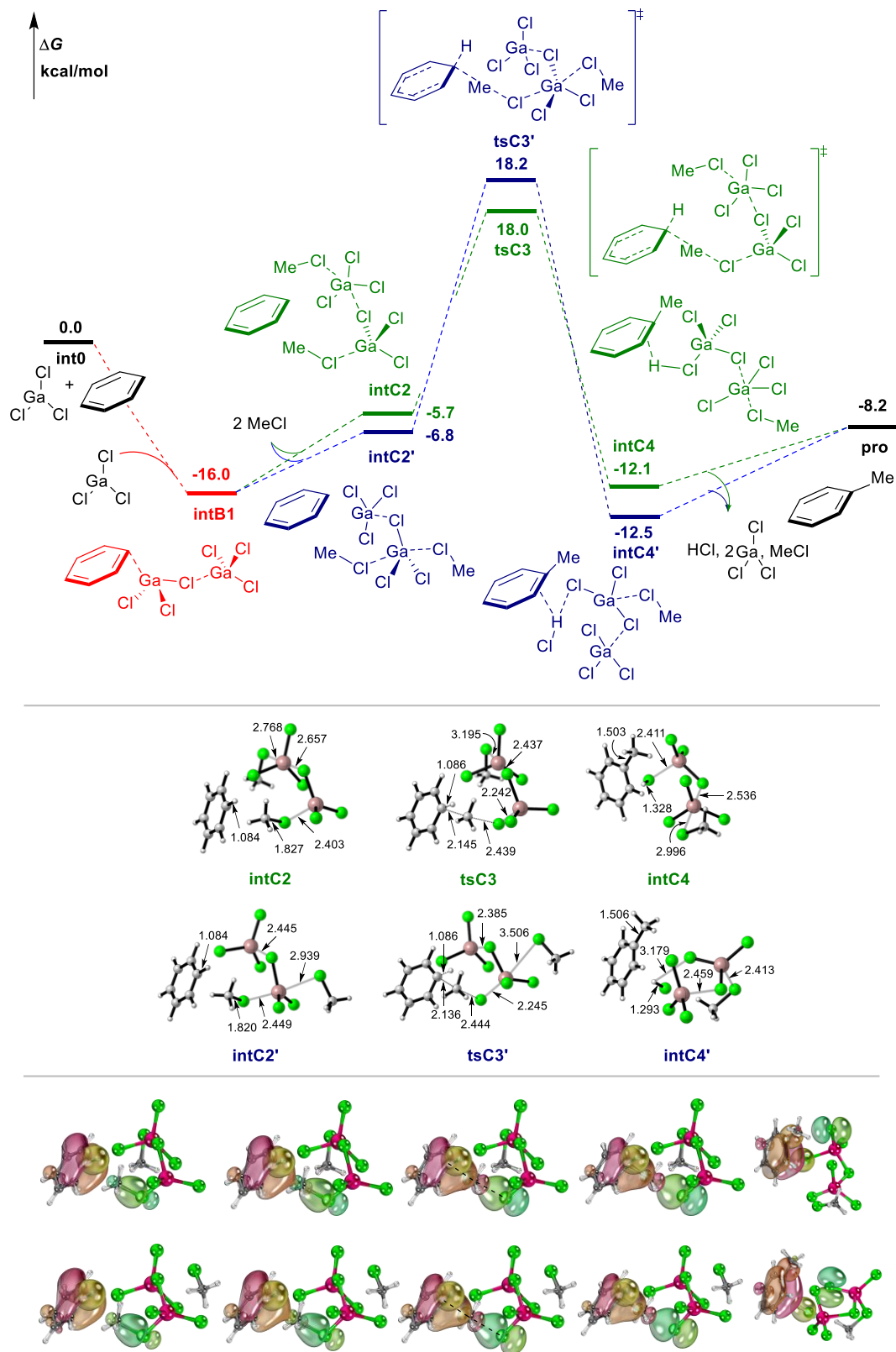
nucleophilic activation by the Lewis acid discussed in the **Introduction (Scheme 2.1, eq 2)**. On the other hand, the alkylation transition state from **intB2** was located much lower on the PES, at only 12.9 kcal/mol. This hypothesis also does not involve a Wheland-type  $\sigma$ -complex for the same reasons as those given previously. It is in perfect agreement with the experimentally established kinetic results,<sup>12</sup> which show a first-order kinetics, with respect to the aromatic reactant, and second-order kinetics for the  $\text{GaCl}_3$  catalyst. The fact that the rate-limiting step does not involve the breakdown of the Wheland-type  $\sigma$ -complex is also in harmony with DeHaan and Brown's experimental results. Indeed, the methylation of  $\text{C}_6\text{D}_6$  was found to proceed at essentially the same rate as benzene.<sup>12</sup> Dissociation of the final complex **intB4** into methylbenzene,  $\text{HCl}$ , and two  $\text{GaCl}_3$  units is endergonic by 7.0 kcal/mol, which makes the overall process exergonic by 8.2 kcal/mol. However, it is more interesting to look at the free energy associated with the regeneration of **intB1** from **intB4**, which is actually  $-9.0$  kcal/mol. Thus, the formation of  $\text{HCl}$  is not an issue, which is consistent with the fact that this reaction, like many Friedel–Crafts alkylation, does not require a base.



**Scheme 2.4.** Free-energy profiles of the  $\text{Ga}_2\text{Cl}_6$ -mediated methylation of benzene, selected geometries (Distances in Å) and IBO pathways from **intB2** to **intB4** (Top) and from **intB2'** to **intB4'** (Bottom), respectively.

$\text{Ga}_2\text{Cl}_6$  is a solution in noncoordinating solvents and remains a dimer.<sup>23</sup> It could be dissociated in  $\text{MeCl}$  or form highly valent species. Following Brown's hypothesis to involve methyl chloride in the transition states, we then added an additional  $\text{MeCl}$  molecule in the system (see **Scheme 2.5**). It led to either **intC2**, pertaining to the molecular adduct activation, or **intC2'**, related to the ion-pair activation. However, both are significantly less stable than **intB1** and the corresponding alkylation transition state lie higher in free energy than the one that does not display an additional  $\text{MeCl}$  molecule, i.e., **tsB3** in **Scheme 2.4** at 12.9 kcal/mol, which corresponds to the best of all computed pathways. It is noticeable that, even if the species **intC2** and **intC2'** were operative, the two pathways cannot be differentiated, since the corresponding alkylation transition states are virtually at the same energy on the PES (18.0 vs 18.2 kcal/mol). Again, the alkylations were found concerted.

IBO analysis shows no significant differences between the computed mechanisms. The C–Cl  $\text{sp}^3$  orbital is used to create a C–C bond with a  $\pi$ -extended p orbital of a benzene carbon. The deprotonation of the  $\sigma$ -complex along the reaction coordinates is ensured by a Cl p orbital interacting with the C–H  $\text{sp}^3$  orbital. The  $\text{sp}^3$  orbital of the released  $\text{HCl}$  then slightly overlaps with the benzene  $\pi$ -orbital.



**Scheme 2.5.** Free-energy profiles of the Ga<sub>2</sub>Cl<sub>6</sub>-mediated methylation of benzene, selected geometries (Distances in Å) and IBO pathways from **intB2** to **intB4** (Top) and from **intB2'** to **intB4'** (Bottom), respectively.

## 2.5. Conclusions

This theoretical study of the  $\text{GaCl}_3$ -mediated methylation of benzene by methyl chloride shows that the  $\text{Ga}_2\text{Cl}_6$  molecular adduct is much more active than discrete  $\text{GaCl}_3$  molecules. It behaves as a superelectrophile in this Friedel–Crafts reaction and rationalizes the rate law reported by DeHaan and Brown. The other lessons of this study are that (i) the intervention of an additional  $\text{MeCl}$  molecule is not necessary, the best option being that displayed in red in **Scheme 2.4**; (ii) the activation of the nucleophile by the Lewis acid is not a viable option, and (iii) once again, we have dealt with a Friedel–Crafts reaction, which, although typical, does not seem to involve a Wheland-type  $\sigma$ -complex. Beyond the Friedel–Crafts alkylation, these findings are likely to pertain to many catalytic processes involving Lewis acids of the main group or transition-metal series that can form homodimers ( $\text{BX}_3$ ,  $\text{AlX}_3$ ,  $\text{GaX}_3$ ,  $\text{FeX}_3$ , etc.)<sup>24</sup> and should encourage people to reconsider the related mechanisms.

## 2.6. References

- 1 (a) Friedel, C.; Crafts, J. M. Sur Une Nouvelle Méthode Générale de Synthèse d'Hydrocarbures, d'Acétones, etc. *Compt. Rend.* **1877**, *84*, 1392–1395. (b) Friedel, C.; Crafts, J. M. Sur Une Nouvelle Méthode Générale de Synthèse d'Hydrocarbures, d'Acétones, etc. *Compt. Rend.* **1877**, *84*, 1450–1454.
- 2 Rueping, M.; Nachtsheim, B. J. A Review of New Developments in the Friedel-Crafts Alkylation-From Green Chemistry to Asymmetric Catalysis. *Beilstein J. Org. Chem.* **2010**, *6*, DOI: 10.3762/bjoc.6.6.
- 3 Koleva, G.; Galabov, B.; Kong, J.; Schaefer, H. F., III; Schleyer, P. v. R. Electrophilic Aromatic Sulfonation with  $\text{SO}_3$ : Concerted or Classic SEAr Mechanism? *J. Am. Chem. Soc.* **2011**, *133*, 19094–19101.
- 4 Galabov, B.; Koleva, G.; Kong, J.; Schaefer, H. F., III; Schleyer, P. v. R. Addition Elimination versus Direct Substitution Mechanisms for Arene Chlorination. *Eur. J. Org. Chem.* **2014**, *2014*, 6918–6924.
- 5 (a) Kong, J.; Galabov, B.; Koleva, G.; Zou, J.-J.; Schaefer, H. F., III; Schleyer, P. v. R. The Inherent

- Competition between Addition and Substitution Reactions of Br<sub>2</sub> with Benzene and Arenes. *Angew. Chem., Int. Ed.* **2011**, *50*, 6809–6813. (b) Šakić, D.; Vrček, V. Prereactive Complexes in Chlorination of Benzene, Triazine, and Tetrazine: A Quantum Chemical Study. *J. Phys. Chem. A* **2012**, *116*, 1298–1306.
- 6 Michelet, B.; Thiery, G.; Bour, C.; Gandon, V. On the Non-Innocent Behavior of Substrate Backbone Esters in Metal-Catalyzed Carbocyclizations and Friedel-Crafts Reactions of Enynes and Arenynes. *J. Org. Chem.* **2015**, *80*, 10925–10938.
- 7 Tarakeshwar, P.; Lee, J. Y.; Kim, K. S. Role of Lewis Acid(AlCl<sub>3</sub>)-Aromatic Ring Interactions in Friedel-Craft's Reaction: An Ab Initio Study. *J. Phys. Chem. A* **1998**, *102*, 2253–2255.
- 8 (a) Volkov, A. N.; Timoshkin, A. Y.; Suvorov, A. V. On the Importance of Dimeric Forms of Al and Ga Trichlorides in the Electrophilic Aromatic Substitution Reactions: An Ab Initio Study. *Int. J. Quantum Chem.* **2004**, *100*, 412–418. (b) Volkov, A. N.; Timoshkin, A. Y.; Suvorov, A. V. Pathways of Electrophilic Aromatic Substitution Reactions Catalyzed by Group 13 Trihalides: An Ab Initio Study. *Int. J. Quantum Chem.* **2005**, *104*, 256–260. (c) Yamabe, S.; Yamazaki, S. A Remarkable Difference in the Deprotonation Steps of the Friedel-Crafts Acylation and Alkylation Reactions. *J. Phys. Org. Chem.* **2009**, *22*, 1094–1103. (d) Melissen, S. T. A. G.; Tognetti, V.; Dupas, G.; Jouanneau, J.; Lê, G.; Joubert, L. A DFT Study of the Al<sub>2</sub>Cl<sub>6</sub>-Catalyzed Friedel-Crafts Acylation of Phenyl Aromatic Compounds. *J. Mol. Model.* **2013**, *19*, 4947–4958.
- 9 (a) Albright, H.; Riehl, P. S.; McAtee, C. C.; Reid, J. P.; Ludwig, J. R.; Karp, L. A.; Zimmerman, P. M.; Sigman, M. S.; Schindler, C. S. Catalytic Carbonyl-Olefin Metathesis of Aliphatic Ketones: Iron(III) Homo-Dimers as Lewis Acidic Superelectrophiles. *J. Am. Chem. Soc.* **2019**, *141*, 1690–1700. (b) Djurovic, A.; Vayer, M.; Li, Z.; Guillot, R.; Baltaze, J.-P.; Gandon, V.; Bour, C. Synthesis of Medium-Sized Carbocycles by Gallium-Catalyzed Tandem Carbonyl-Olefin Metathesis/Transfer Hydrogenation. *Org. Lett.* **2019**, *21*, 8132–8137. (c) Davis, A. J.; Watson, R. B.; Nasrallah, D. J.; Gomez-Lopez, J. L.; Schindler, C. S. Superelectrophilic Aluminium (III)-Ion Pairs Promote a Distinct Reaction Path for Carbonyl-Olefin Ring-Closing Metathesis. *Nat. Catal.* **2020**, *3*, 787–796.
- 10 (a) Olah, G. A. Superelectrophiles. *Angew. Chem., Int. Ed. Engl.* **1993**, *32*, 767–788. (b) Olah, G. A.; Klumpp, D. A. *Superelectrophiles and Their Chemistry*; Wiley–VCH Verlag GmbH & Co. KGaA, 2007. (c) Negishi, E. Principle of Activation of Electrophiles by Electrophiles through Dimeric Association-Two Are Better than One. *Chem. - Eur. J.* **1999**, *5*, 411–420.
- 11 El-Hellani, A.; Monot, J.; Guillot, R.; Bour, C.; Gandon, V. Molecular versus Ionic Structures in

- Adducts of  $\text{GaX}_3$  with Monodentate Carbon-Based Ligands. *Inorg. Chem.* **2013**, *52*, 506–514.
- 12 DeHaan, F. P.; Brown, H. C. Kinetics of the Gallium Chloride Catalyzed Methylation of Benzene in Excess Methyl Chloride. *J. Am. Chem. Soc.* **1969**, *91*, 4844–4850.
- 13 (a) Li, H.-J.; Guillot, R.; Gandon, V. A Gallium-Catalyzed Cycloisomerization/Friedel-Crafts Tandem. *J. Org. Chem.* **2010**, *75*, 8435–8449. (b) Tang, S.; Monot, J.; El-Hellani, A.; Michelet, B.; Guillot, R.; Bour, C.; Gandon, V. Cationic Gallium(III) Halide Complexes: a New Generation of p-Lewis Acids. *Chem. - Eur. J.* **2012**, *18*, 10239–10243. (c) Michelet, B.; Bour, C.; Gandon, V. Gallium-Assisted Transfer Hydrogenation of Alkenes. *Chem. - Eur. J.* **2014**, *20*, 14488–14492. (d) Michelet, B.; Tang, S.; Thiery, G.; Monot, J.; Li, H.; Guillot, R.; Bour, C.; Gandon, V. Catalytic Applications of  $[\text{IPr}\cdot\text{GaX}_2][\text{SbF}_6]$  and Related Species. *Org. Chem. Front.* **2016**, *3*, 1603–1613. (e) Li, Z.; Thiery, G.; Lichtenthaler, M. R.; Guillot, R.; Krossing, I.; Gandon, V.; Bour, C. Catalytic Use of Low-Valent Cationic Gallium(I) Complexes as –Acids. *Adv. Synth. Catal.* **2018**, *360*, 544–549. (f) Pareek, M.; Bour, C.; Gandon, V. Gallium-Catalyzed Scriabine Reaction. *Org. Lett.* **2018**, *20*, 6957–6960.
- 14 Frisch, M. J.; Trucks, G. W.; Schlegel, H. B.; Scuseria, G. E.; Robb, M. A.; Cheeseman, J. R.; Scalmani, G.; Barone, V.; Mennucci, B.; Petersson, G. A.; Nakatsuji, H.; Caricato, M.; Li, X.; Hratchian, H. P.; Izmaylov, A. F.; Bloino, J.; Zheng, G.; Sonnenberg, J. L.; Hada, M.; Ehara, M.; Toyota, K.; Fukuda, R.; Hasegawa, J.; Ishida, M.; Nakajima, T.; Honda, Y.; Kitao, O.; Nakai, H.; Vreven, T.; Montgomery, J. A., Jr.; Peralta, J. E.; Ogliaro, F.; Bearpark, M.; Heyd, J. J.; Brothers, E.; Kudin, K. N.; Staroverov, V. N.; Kobayashi, R.; Normand, J.; Raghavachari, K.; Rendell, A.; Burant, J. C.; Iyengar, S. S.; Tomasi, J.; Cossi, M.; Rega, N.; Millam, J. M.; Klene, M.; Knox, J. E.; Cross, J. B.; Bakken, V.; Adamo, C.; Jaramillo, J.; Gomperts, R.; Stratmann, R. E.; Yazyev, O.; Austin, A. J.; Cammi, R.; Pomelli, C.; Ochterski, J. W.; Martin, R. L.; Morokuma, K.; Zakrzewski, V. G.; Voth, G. A.; Salvador, P.; Dannenberg, J. J.; Dapprich, S.; Daniels, A. D.; Farkas, O.; Foresman, J. B.; Ortiz, J. V.; Cioslowski, J.; Fox, D. J. *Gaussian 09*, Revision D.01; Gaussian, Inc.: Wallingford, CT, 2009.
- 15 Zhao, Y.; Truhlar, D. G. The M06 Suite of Density Functionals for Main Group Thermochemistry, Thermochemical Kinetics, Non-covalent Interactions, Excited States, and Transition Elements. *Theor. Chem. Acc.* **2008**, *120*, 215–241.
- 16 Curtiss, L. A.; McGrath, M. P.; Blaudeau, J. P.; Davis, N. E.; Binning, R. C., Jr.; Radom, L. Extension

- of Gaussian-2 Theory to Molecules Containing Third-Row Atoms Ga-Kr. *J. Chem. Phys.* **1995**, *103*, 6104–6113.
- 17 Clark, T.; Chandrasekhar, J.; Spitznagel, G. W.; Schleyer, P. v. R. Efficient Diffuse Function-Augmented Basis Sets for Anion Calculations. III. The 3-21+G Basis Set for First-Row Elements, Li-F. *J. Comput. Chem.* **1983**, *4*, 294–301.
- 18 Fukui, K. Formulation of the Reaction Coordinate. *J. Phys. Chem.* **1970**, *74*, 4161–4163.
- 19 Fukui, K. The Path of Chemical Reactions - the IRC Approach. *Acc. Chem. Res.* **1981**, *14*, 363–368.
- 20 Legault, C. Y. *CYLview*, Version 1.0b; Universitéde Sherbrooke, 2009 (available via the Internet at: <http://www.cylview.org>).
- 21 (a) Knizia, G. Intrinsic Atomic Orbitals: an Unbiased Bridge Between Quantum Theory and Chemical Concepts. *J. Chem. Theory Comput.* **2013**, *9*, 4834–4843. (b) Knizia, G.; Klein, J. E. M. N. Electron Flow in Reaction Mechanisms. Revealed from First Principles. *Angew. Chem., Int. Ed.* **2015**, *54*, 5518–5522. (c) *IboView*, v20150427; available via the Internet at: <http://www.iboview.org/>.
- 22 For a recent example and a detailed description of the IBO method, see: Bertus, P. From Dialkyltitanium Species to Titanacyclo-propanes: An Ab Initio Study. *Organometallics* **2019**, *38*, 4171–4182.
- 23 Černý, Z.; Macháček, J.; Fusek, J.; Čásenský, B.; Kříž, O.; Tuck, D. G. Multinuclear NMR studies of mixtures of aluminium and gallium trihalides in benzene. *J. Chem. Soc., Dalton Trans.* **2001**, 2698–2703.
- 24 For other developments of GaCl<sub>3</sub>-catalyzed reactions, see inter alia: (a) Wang, X.; Makha, M.; Chen, S.-W.; Zheng, H.; Li, Y. GaCl<sub>3</sub>-Catalyzed C-H Cyanation of Indoles with N-Cyanosuccinimide. *J. Org. Chem.* **2019**, *84*, 6199–6206. (b) Albright, H.; Vonesh, H. L.; Becker, M. R.; Alexander, B. W.; Ludwig, J. R.; Wiscons, R. A.; Schindler, C. S. GaCl<sub>3</sub>-Catalyzed Ring-Opening Carbonyl-Olefin Metathesis. *Org. Lett.* **2018**, *20*, 4954–4958.

# **Chapter 3. Alkynophilicity of Group 13 MX<sub>3</sub> Salts: A Theoretical Study**

Shengwen Yang, Aurélien Alix, Christophe Bour, and Vincent Gandon

Publication Date: March 26, 2021

*Inorg. Chem.* 2021, 60, 8, 5507–5522

<https://doi.org/10.1021/acs.inorgchem.0c03302>

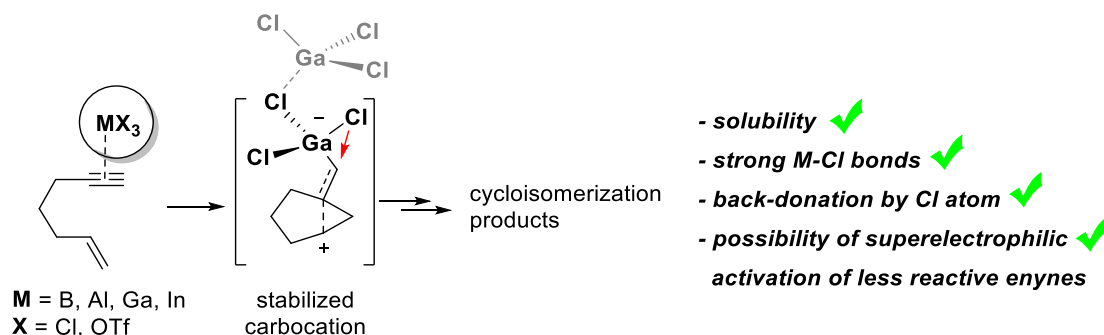
Copyright © 2021 American Chemical Society



### 3.1. Abstract

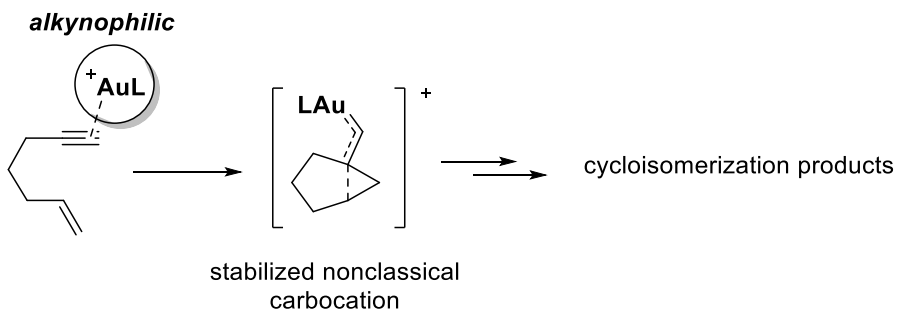
The concept of alkynophilicity is revisited with group 13 MX<sub>3</sub> metal salts (M = In, Ga, Al, B; X = Cl, OTf) using M06-2X/6-31+G(d,p) calculations. This study aims at answering why some of these salts show reactivity toward enynes that is similar to that observed with late-transition-metal complexes, notably Au(I) species, and why some of them are inactive. For this purpose, the mechanism of the skeletal reorganization of 1,6-enynes into 1-vinylcyclopentenes has been computed, including monomeric (“standard”) and dimeric (superelectrophilic) activation. Those results are confronted with deactivation pathways based on the dissociation of the M–X bond. The role of the X ligand in the stabilization of the intermediate nonclassical carbocation is revealed, and the whole features required to make a good  $\pi$ -Lewis acid are discussed.

**what makes GaCl<sub>3</sub> a good alkynophilic  $\pi$ -Lewis acid among MX<sub>3</sub> salts?**



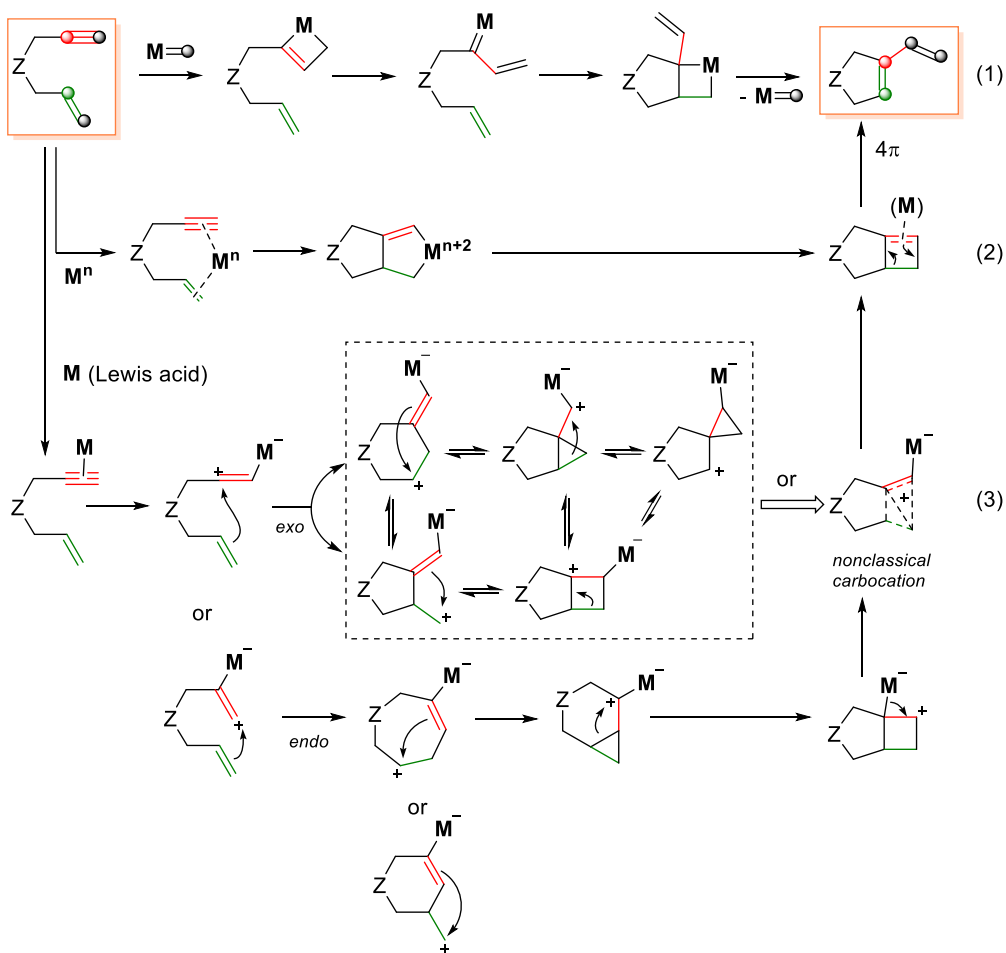
### 3.2. Introduction

Alkynophilicity is a term that was coined in 2004 by Echavarren in the field of homogeneous gold catalysis to qualify Lewis acids able to promote the skeletal rearrangement (or alkoxy-cyclization) of enynes through highly polarized ( $\eta^1$ -alkyne)-gold(I) complexes leading to gold(I)-stabilized homoallylic (nonclassical) carbocations (Scheme 3.1).<sup>1</sup>



**Scheme 3.1.** Alkynophilicity of LAu(I)<sup>+</sup> complexes in the cycloisomerization of enynes.

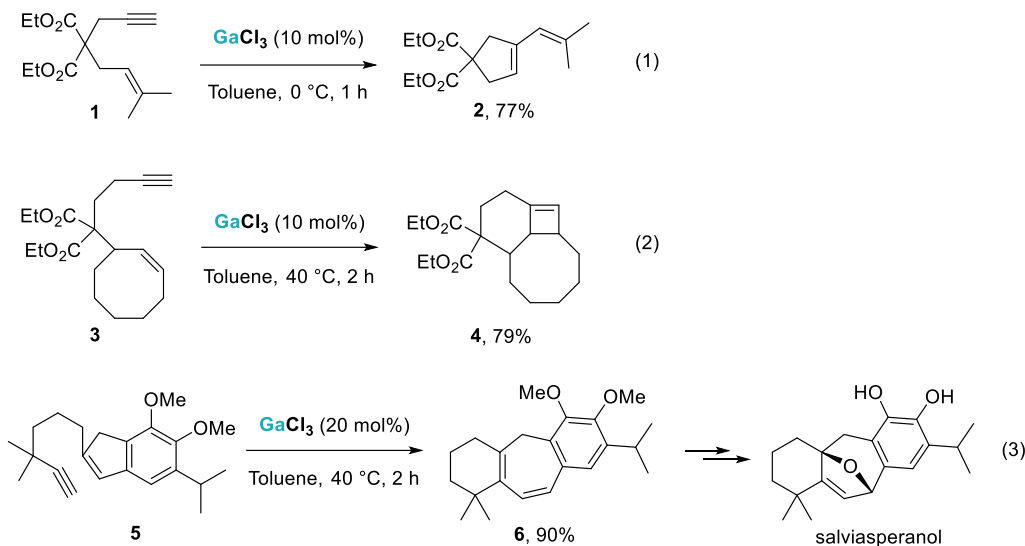
Since then, the interpretation of this term has been extended to any kind of Lewis or Brønsted acid promoting any kind of nucleophilic addition to a simple alkyne, even if not catalytic.<sup>2</sup> The skeletal reorganization of 1,*n*-enynes yet remains a specific area among cycloisomerization reactions, and it requires specific catalysts. As a general rule, the cycloisomerization of 1,*n*-enynes is a well-established strategy to rapidly increase the molecular complexity from simple substrates and provide useful synthons. Under metal catalysis, this transformation can lead to a wide range of carbo- and heterocyclic products in a selective manner and is therefore perfectly suited for the diversity-oriented synthesis of complex molecular architectures that are present in natural products, pharmaceuticals, agrochemicals, or materials.<sup>3</sup> One common cycloisomerization pathway is the 1,6-enyne metathesis, which leads to cyclic 1,3-dienes (1-vinylcyclopentenes, **Scheme 3.2**). It can be catalyzed by metal carbene complexes typically used for olefin metathesis (e.g., Grubbs-type catalysts, metallacyclobutene pathway, eq 1), by oxidizable transition-metal complexes (metallacyclopentene pathway, eq 2) or by transition- or main-group-based Lewis acids (outer sphere activation, eq 3).<sup>3,4</sup> The mechanistic scenario is more complex in the latter case, as it involves many possible intermediates, some of them being either discrete energy minima in equilibrium, or resonance structures of a nonclassical carbocation.<sup>5</sup> A common feature in eqs 2 and 3 is the formation of a fused cyclobutene intermediate,<sup>6</sup> which undergoes 4π conrotatory ring opening to give the final product (catalyzed by the Lewis acid or not).



**Scheme 3.2.** General mechanistic pathways of the metal-catalyzed 1,6-enyne metathesis.

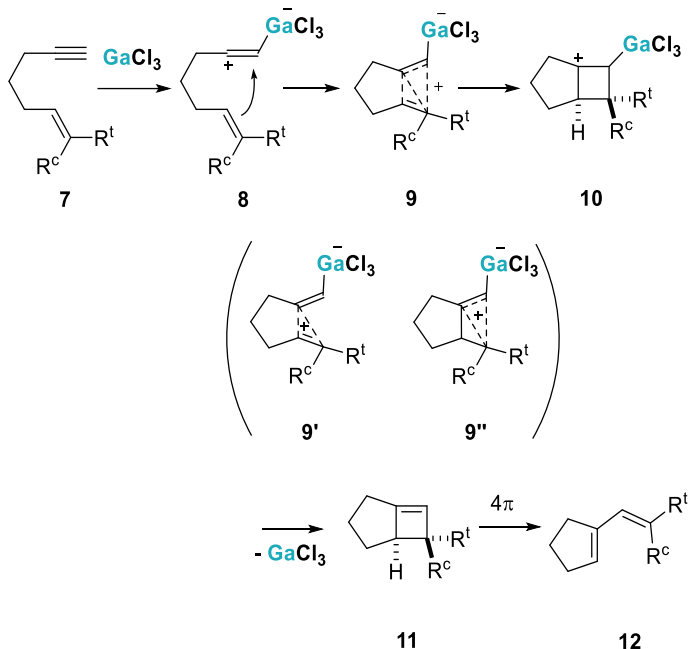
The precise pathway with Lewis acids depends on many factors such as the nature of the metal (including its oxidation state), ligands, counterions, solvent, etc. In any case, it starts with the activation of the alkyne moiety, which gains a vinyl carbocation character, triggering an *exo*- or *endo*-nucleophilic attack of the alkene. While this chemistry is often regarded as the territory of late-transition-metal-based Lewis acid catalysis, especially gold and platinum, main-group-metal complexes, mostly gallium(III) and indium(III) halides,<sup>7</sup> have also been used to promote skeletal reorganization of enynes,<sup>8</sup> including enyne metathesis.<sup>9</sup> Chatani et al. reported in 2002 the first examples of GaCl<sub>3</sub>-catalyzed enyne metathesis, as shown in **Scheme 3.3**, eq 1.<sup>9a</sup> A cyclobutene could also be isolated when formed from a large cycloalkene (eq 2), which is consistent with early observations reported by Trost et al., who pointed the

likely intermediacy of cyclobutenes in the formation of 1-vinylcycloalkenes when using Pd(II) Lewis acids.<sup>10</sup> With medium-size cycloalkenes, the normal metathesis product is obtained, i.e., an endocyclic 1,3-diene (eq 3).<sup>9a,9b</sup> This reaction was exploited for the synthesis of various natural products, such as salviasperanol by Sarpong et al.<sup>11</sup>



**Scheme 3.3.** Gallium-catalyzed cycloisomerization of enynes.

The mechanism of the GaCl<sub>3</sub>-catalyzed enyne metathesis postulated by Chatani et al. is shown in **Scheme 3.4**.<sup>9a</sup> Enyne **7** first forms the vinyl carbocation **8** upon coordination of the alkyne moiety to GaCl<sub>3</sub>. Nucleophilic attack of the alkene part generates the nonclassical carbocation **9** or other isomers (**9'** or **9''**). The latter is then transformed into the  $\eta^1$ -cyclobutene complex **10**. Elimination of GaCl<sub>3</sub> leads to the strained cyclobutene **11**, which undergoes conrotatory  $4\pi$  ring opening to provide 1-vinylcyclopentene **12**. The product is obtained in a stereospecific manner, the cis- and trans-substituent R<sup>c</sup> and R<sup>t</sup> being found with the indicated stereochemical relationships.



**Scheme 3.4.** Mechanism proposed by Chatani et al. for the  $\text{GaCl}_3$ -catalyzed enyne metathesis<sup>9a</sup>.

As such, the proposed mechanism with  $\text{GaCl}_3$  does not differ much from the one postulated with late-transition-metal-based Lewis acid catalysts, notably gold(I) complexes.<sup>1,12</sup> While the alkynophilicity (or enynophilicity) of Au(I) complexes has been related to relativistic effects and to the ability of the soft polarizable gold atom to stabilize the intermediate nonclassical carbocation by back-donation,<sup>5b,13</sup> these typical features of late-transition metals cannot be used to explain the alkynophilicity of main-group-based species. This raises the question of what makes  $\text{GaCl}_3$  and  $\text{InCl}_3$  good alkynophilic  $\pi$ -Lewis acids in comparison to late-transition-metal complexes such as  $\text{LAu(I)}^+$  species, or even compared to  $\text{BCl}_3$ ,  $\text{AlCl}_3$ , or  $\text{Ga(OTf)}_3$  which do not work as catalysts for enyne cycloisomerization. Is it simply a matter of hardness or softness of the Lewis acid?<sup>14</sup> Is there any specific activation of the substrate (superelectrophilic activation?) or specific stabilization of the nonclassical carbocation? Can an analogy be made between relativistic contraction of the 6s orbital of gold<sup>13</sup> and the d-block contraction of gallium?<sup>15</sup> This theoretical study aims at answering these questions and demystifies some stereotypes about the alkynophilicity of Lewis acids.

### 3.3. Computational Methods

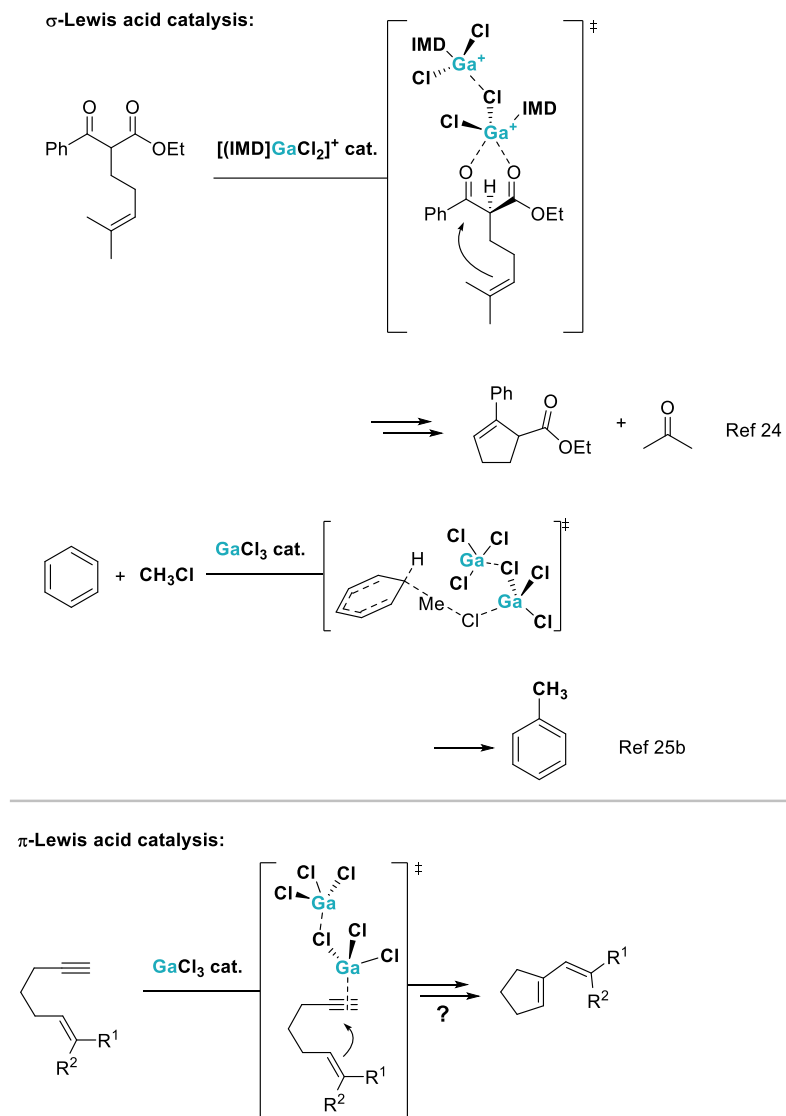
All of the density functional theory (DFT) calculations were performed with the Gaussian 09 set of programs.<sup>16</sup> The M06-2X<sup>17</sup> functional was used for the geometry optimization in the gas phase with the 6-31+G(d,p) basis set<sup>18</sup> for all elements, except Au and In for which the LANL2DZ(ECP) basis set was employed.<sup>19</sup> Harmonic vibrational frequency calculations were performed for all of the stationary points to determine whether they are local minima or transition structures and to derive the thermochemical corrections at 273.15 K for the enthalpies and free energies. The same functional and basis set were used to calculate the single-point energies in toluene from the gas-phase stationary points with the CPCM model.<sup>20</sup> The discussed energies are Gibbs free energies ( $\Delta G_{273}$ , kcal/mol). The connectivity of all transition states has been verified by the intrinsic reaction coordinate (IRC) analysis.<sup>21</sup> NPA<sup>22</sup> charges were computed with the NBO program implemented in Gaussian (version 3.1).

## 3.4. Results and Discussion

### 3.4.1. Superelectrophilic vs “Standard” Activation

In addition to being powerful  $\pi$ -activators, neutral and cationic gallium(III) and gallium(I) species are well-known  $\sigma$ -activators of C–O or C–halide bonds.<sup>7a,23</sup> Recent studies of the mechanism of the carbonyl-olefin metathesis reaction (C–O bond activation),<sup>24</sup> or of the gallium-catalyzed Friedel–Crafts alkylation (C–halide bond activation)<sup>25</sup> have revealed that gallium(III) homodimers such as  $[(LGaCl_2)_2]^{2+}$  or  $Ga_2Cl_6$  are much more active  $\sigma$ -Lewis acids than the corresponding monomers  $[(LGaCl)_2]^+$  or  $GaCl_3$  (**Scheme 3.5**). These findings are in line with the inspiring work of Schindler and co-workers, who demonstrated that iron(III) homodimers are involved in the carbonyl-olefin metathesis of aliphatic ketones.<sup>26</sup> Such reactions echo Negishi’s principle of activation of electrophiles by electrophiles<sup>27</sup> and were linked by Schindler et al. to Olah’s concept of superelectrophiles.<sup>28</sup> Previous computational studies on

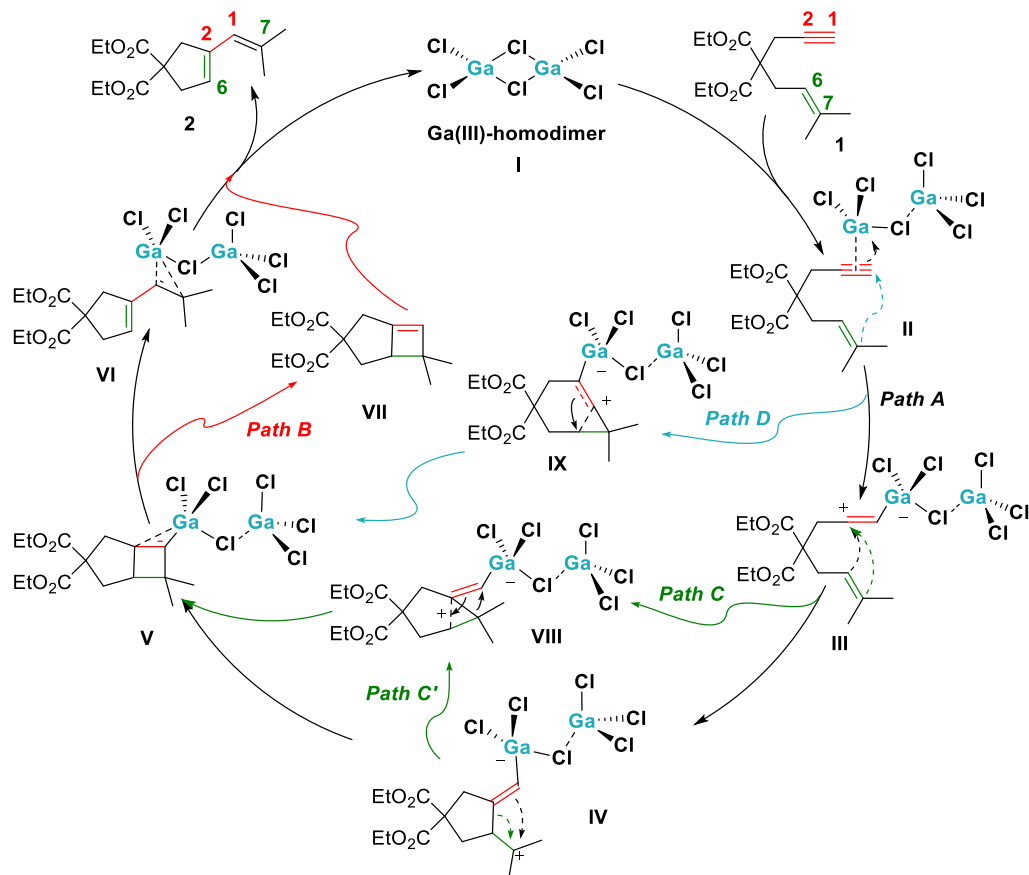
GaCl<sub>3</sub>-catalyzed cycloisomerization of enynes,<sup>8e,f,29</sup> allenynes,<sup>30</sup> or arenynes<sup>31</sup> have focused on monomeric activation.<sup>32</sup> The objective of this part is to check whether superelectrophilic gallium(III) homodimers could also be involved in the activation of a  $\pi$ -system, using the well-studied 1,6-enyne scaffold as a prototype.



**Scheme 3.5.** Gallium(III) homodimers in  $\sigma$ - and  $\pi$ -Lewis acid catalysis (IMD = 1,3-dimethylimidazol-2-ylidene).

As a model substrate, we chose enyne **1** shown in **Scheme 3.3** in the **Introduction** section and in **Scheme 3.6** below. Considering the body of the mechanistic studies available now (see the **Introduction** section), we envisaged more options than the sole

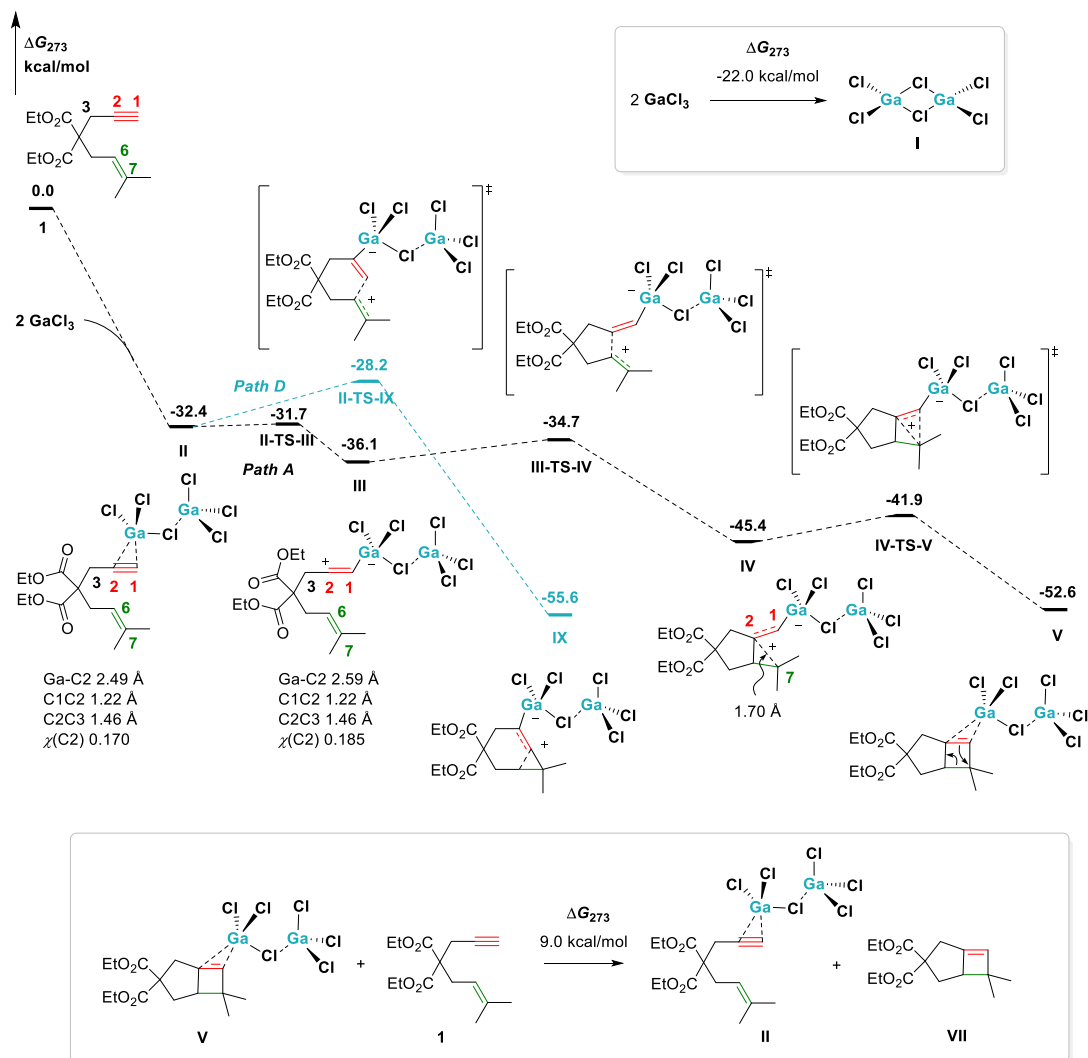
2002 Chatani's proposal.<sup>9a</sup> Four pathways for superelectrophilic Ga(III)-homodimer-catalyzed skeletal reorganization of enyne **1** have been considered, all starting from the Ga<sub>2</sub>Cl<sub>6</sub> homodimer **I** and its coordination to the C≡C bond of enyne **1** to give the gallium-alkyne complex **II**. In path A (black), complex **II** reveals its vinyl carbocation character depicted as **III** and undergoes nucleophilic attack of the alkene moiety at C2 to give the tertiary carbocation **IV**. The cyclobutene complex **V** is then obtained after C1–C7 bond formation. 4π Ring opening then takes place in the presence of the gallium cluster to give **VI** and then the final product **2** after demetallation, which regenerates catalyst **I**. Alternatively, the demetallation may precede the 4π ring opening, the free cyclobutene **VII** becoming an intermediate (path B). The six-membered ring vinyl gallium complex **VIII** is also a possible intermediate toward **V**. It can be accessed from **III** (path C) or from **IV** (path C'). Finally, 7-*endo*-dig cyclization forming the C1–C7 bond may also be considered from **II**, leading to complex **IX**, which could undergo ring contraction to the cyclobutene complex **V** (path D).



**Scheme 3.6.** Possible reaction pathways for Ga(III)-homodimer-catalyzed skeletal reorganization of enyne **1** to form 1-vinylcycloalkene **2**.

Following the above proposal, calculations were performed to reveal the mechanism of the Ga(III)-homodimer-catalyzed skeletal reorganization of 1,6-enyne **1**. Enyne **1** and two molecules of GaCl<sub>3</sub> were chosen as the reference system for the free energy profile (**Scheme 3.7**). These two discrete molecules of GaCl<sub>3</sub> were used instead of the Ga<sub>2</sub>Cl<sub>6</sub> dimer **I** to allow direct comparison with a single GaCl<sub>3</sub> catalyst molecule (**Scheme 3.10**). The computed free energy of the formation of **I** from 2 GaCl<sub>3</sub> is -22.0 kcal/mol (see upper box in **Scheme 3.7**). The experimental value is -21.0 kcal/mol,<sup>33</sup> which validates the chosen level of theory. Optimized geometries of some key transition structures and intermediates are presented in **Figure 3.1**. Coordination of 1,6-enyne **1** to the gallium center generates intermediate **II**, which is exergonic by 32.4 kcal/mol. From Ga<sub>2</sub>Cl<sub>6</sub>, a correction of 22.0 kcal/mol must be applied, i.e., -10.4 kcal/mol instead of -32.4 kcal/mol, meaning that Cl/alkyne ligand exchange is favorable. Depending on the ester orientation, a more stable isomer **III** was found (-36.1 kcal/mol). Both **II** and **III** have geometrical features that are close to what is expected for a vinyl carbocation (C1C2 1.22 Å; C2C3 1.46 Å),<sup>34</sup> but the longer GaC2 distance in **III** (2.59 vs 2.49 Å) and the higher charge at C2 (0.185 vs 0.170) advocate such a depiction for this species. The two isomers are connected by a low-lying transition state corresponding to the rotation of one ester function (**II-TS-III**). Bringing the alkene closer to the vinyl carbocation promotes the formation of the C2–C6 bond. The energy barrier for this step is only 1.4 kcal/mol (**III-TS-IV**). The resulting complex **IV** is more stable than **III** by 9.3 kcal/mol. With its long C2C7 distance of 1.70 Å, its structure corresponds to a resonance hybrid between an  $\alpha$ -cyclopropyl carbocation and a homoallyl carbocation. Contrarily to the proposed intermediate **9** in **Scheme 3.4**, there is no interaction between C1 and C7 at this stage (C1C7 2.62 Å), so the species is actually closer to **9'**. The formation of the cyclobutene complex **V** is achieved through **IV-TS-V**, which lies only 3.5 kcal/mol above **IV**. This step is exergonic by 7.2 kcal/mol. In **V**, the gallium atom coordinated to the double bond is significantly shifted toward the *gem*-dimethyl group (GaC1 2.26

Å; GaC2 2.47 Å). Ligand exchange between **V** and **1** to give back **II** and liberate **VII** has a reasonable free energy cost of 9.0 kcal/mol (lower box).



**Scheme 3.7.** Free energy profile of the  $(\text{GaCl}_3)_2$ -catalyzed skeletal reorganization of 1,6-ene **1**: Part 1.

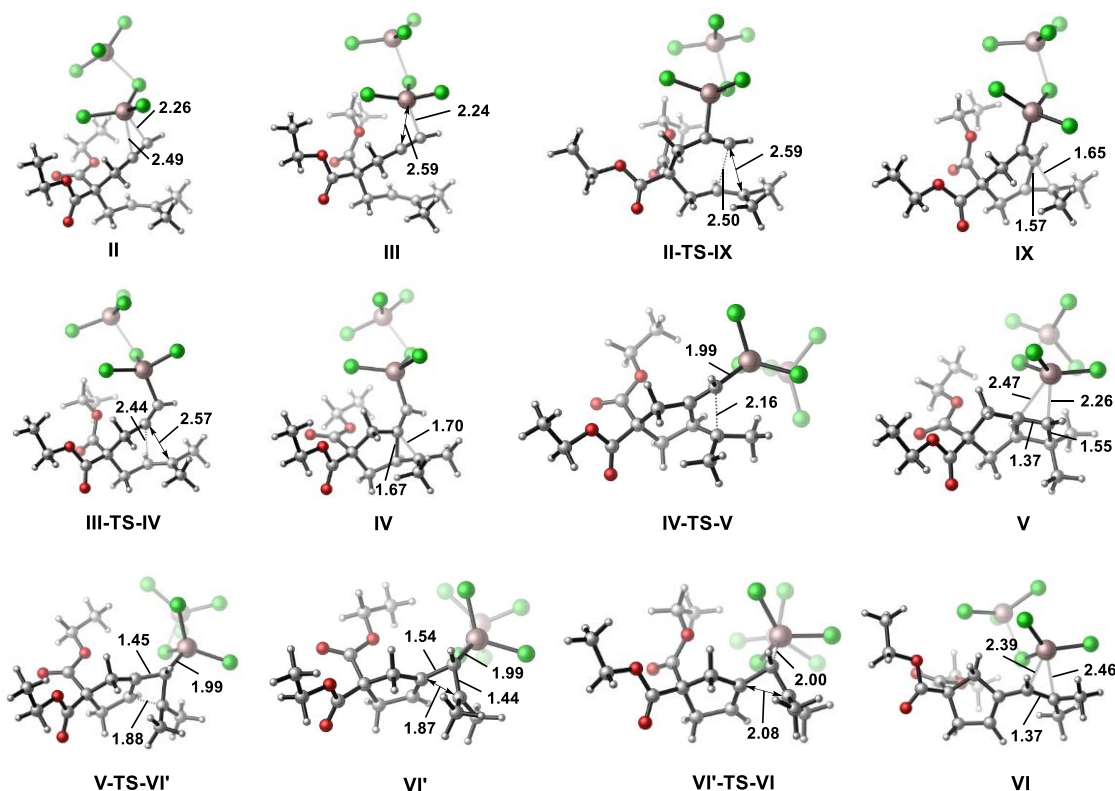
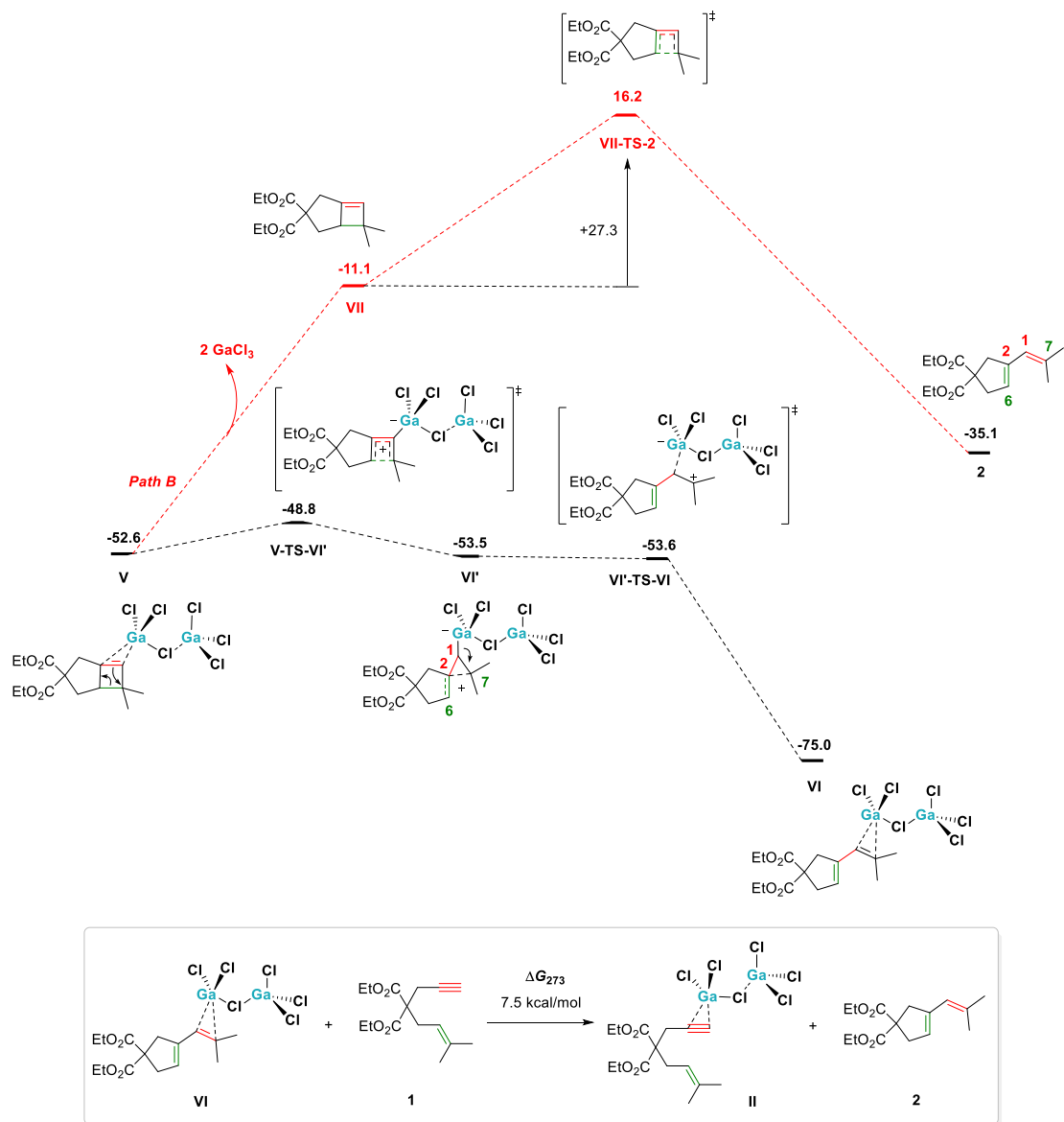


**Figure 3.1.** Selected calculated geometries of transition structures and intermediates shown in **Schemes 3.7** and **3.8** (distances in Å).

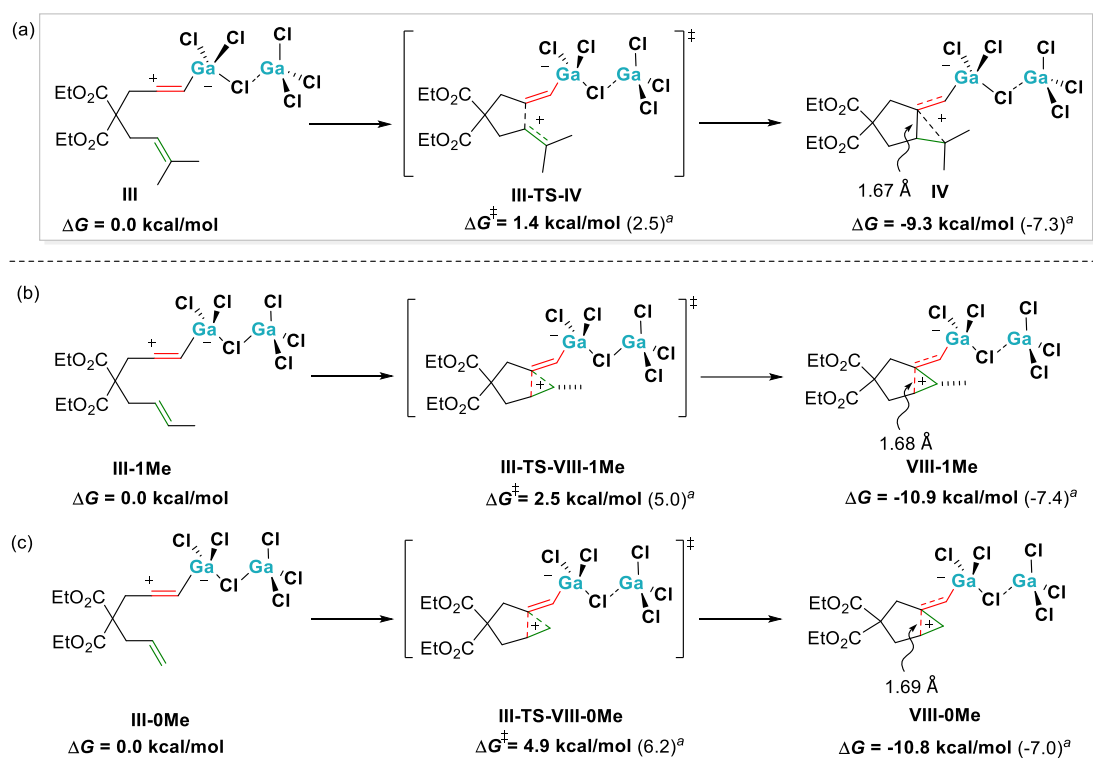
Ring opening is achieved through another low-lying transition state providing **VI'**, in which the positive charge is delocalized between C7 and C6 (C2C7 1.87 Å) (**Scheme 3.8**). The energy barrier for this step, which releases 0.9 kcal/mol free energy, is 3.8 kcal/mol. Elongation of the C2–C7 bond is barrierless and provides the final complex **VI** with a gain of 21.5 kcal/mol. In **VI**, the gallium center is shifted toward C1 (GaC7 2.46 Å; GaC1 2.39 Å). Ligand exchange between **VI** and **1** to give back **II** and furnish **2** is endergonic by 7.5 kcal/mol only (see lower box). According to Chatani's proposal (**Scheme 3.4**), the catalyst is removed from complex **V** to form the free cyclobutene **VII** (Path B). The latter is more stable than **1** by 11.1 kcal/mol. The 4π ring-opening transition state between **VII** and **2** culminates at 16.2 kcal/mol, i.e., a barrier of 27.3 kcal/mol. Thus, even though the ligand exchange between **V** and **1** to give back **II** and provide **VII** has a reasonable free energy cost of 9.0 kcal/mol (see lower box in **Scheme 3.7**), the Lewis acid-assisted ring opening appears much more favorable.



**Scheme 3.8.** Free energy profile of the Ga<sub>2</sub>Cl<sub>6</sub>-catalyzed skeletal reorganization of 1,6-ene 1: Part 2.

An alternative pathway corresponding to the 7-*endo*-dig cyclization discussed above (**Scheme 3.7**, path D) was also envisaged (blue part). This was achieved through **II-TS-IX**, lying 4.2 kcal/mol above **II**. This step is strongly exergonic by 23.2 kcal/mol. Since the energy barrier is higher than those found in path A, path D was not further considered. Overall, the selectivity-determining transition state is **III-TS-IV** in **Scheme 3.7**.

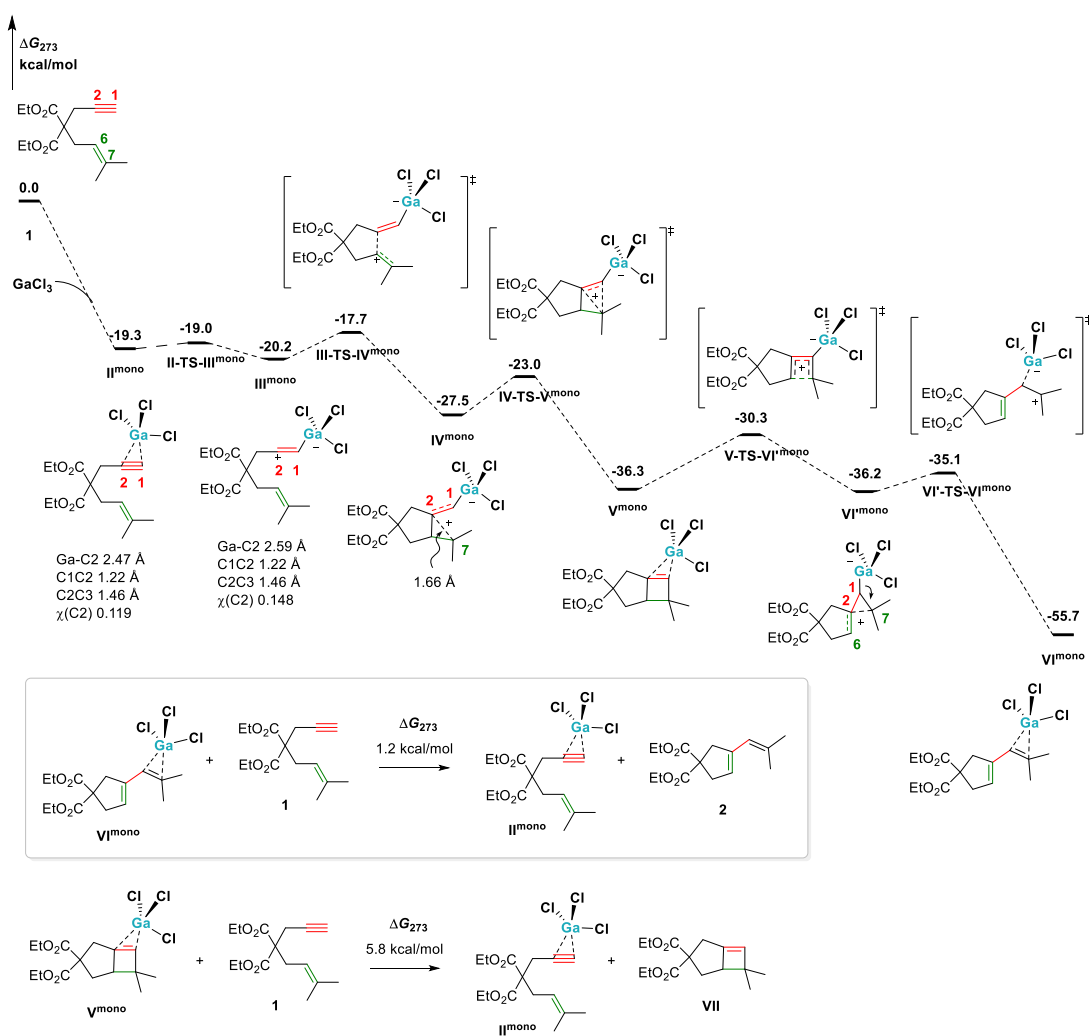
As mentioned above (**Scheme 3.6**), **III** and **IV** could possibly evolve to intermediate **VIII** (paths C and C'). However, no such complex could be optimized. Yu's group reported that the monomeric GaCl<sub>3</sub> can form such complexes without substituents at the terminal alkene carbon.<sup>8e</sup> Therefore, we calculated an annulation transition state with a monosubstituted and an unsubstituted terminal alkene carbon (**Scheme 3.9**). In such cases, the formation of type **VIII** compound became indeed possible with Ga<sub>2</sub>Cl<sub>6</sub> as shown below, or with GaCl<sub>3</sub> (not shown). Thus, there is a continuum between type **IV** and type **VIII** complexes, which depends on the ability of the substitution pattern to stabilize the positive charge at position 6 or 7.



**Scheme 3.9.** Formation of type **VIII** products with two or one methyl group, or no substituent at C7<sup>a</sup> (<sup>a</sup>The values in parentheses were obtained with one GaCl<sub>3</sub> unit instead of the (GaCl<sub>3</sub>)<sub>2</sub> dimer.).

After having studied the superelectrophilic activation, we turned our attention to the standard one. The free energy profile with a single molecule of GaCl<sub>3</sub> as a catalyst is shown in **Scheme 3.10**. All intermediates and transition states lie approximately 15

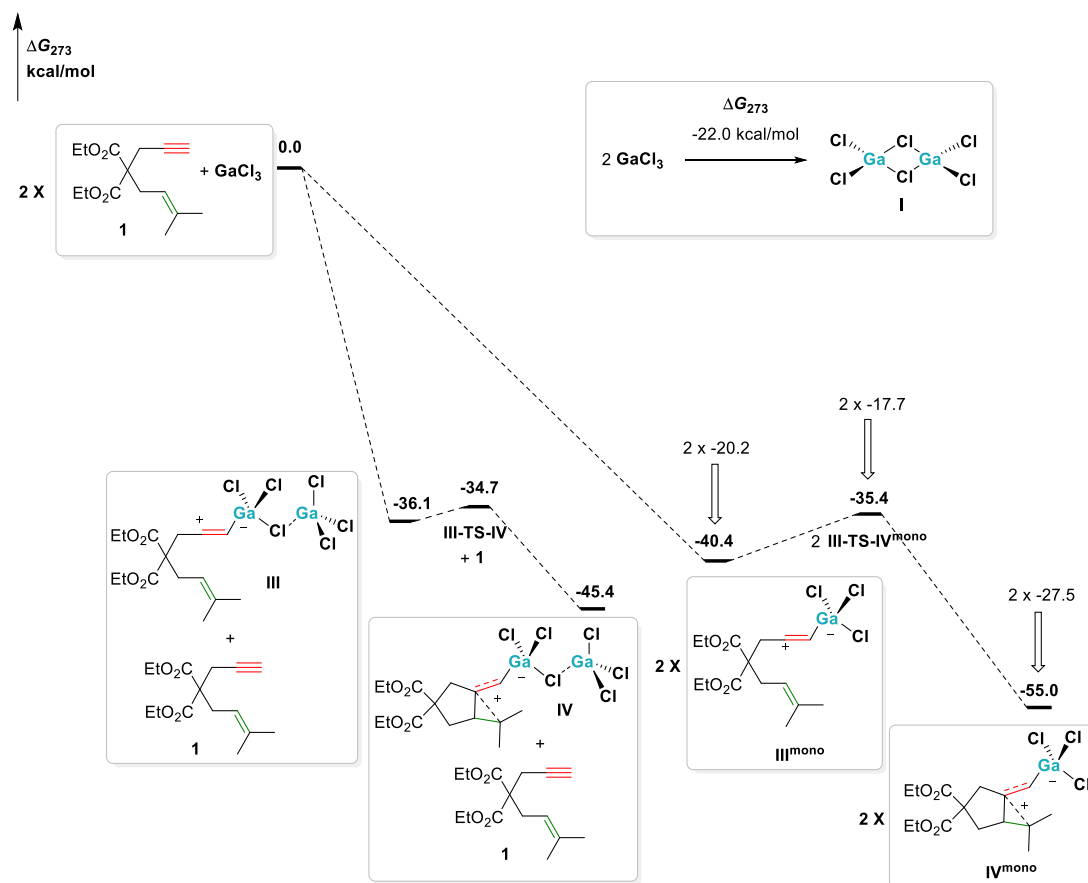
kcal/mol above those computed with Ga<sub>2</sub>Cl<sub>6</sub>. The transition state **III-TS-IV<sup>mono</sup>** corresponds to the RDS. The related free energy barrier is 2.5 vs 1.4 kcal/mol in the two-gallium series. A notable difference in the structures is a shorter C2-C7 distance in **IV<sup>mono</sup>** (1.66 vs 1.70 Å), which can be attributed to an electron-richer character of the C1–C2 bond with only one GaCl<sub>3</sub>, making it more able to delocalize electrons to C7. In addition, the final complex **VI<sup>mono</sup>** converges as an  $\eta^2$  rather than a slipped  $\eta^1$  species (GaC7 2.48 Å; GaC1 2.42 Å).



**Scheme 3.10.** Free energy profile of the GaCl<sub>3</sub>-catalyzed skeletal reorganization of 1,6-alkyne **1**.

Isomer **III<sup>mono</sup>**, which has a higher  $\eta^1$  character than **II<sup>mono</sup>**, is more stable than **II<sup>mono</sup>** by 0.9 kcal/mol. This is much less than in the two-gallium series, for which this

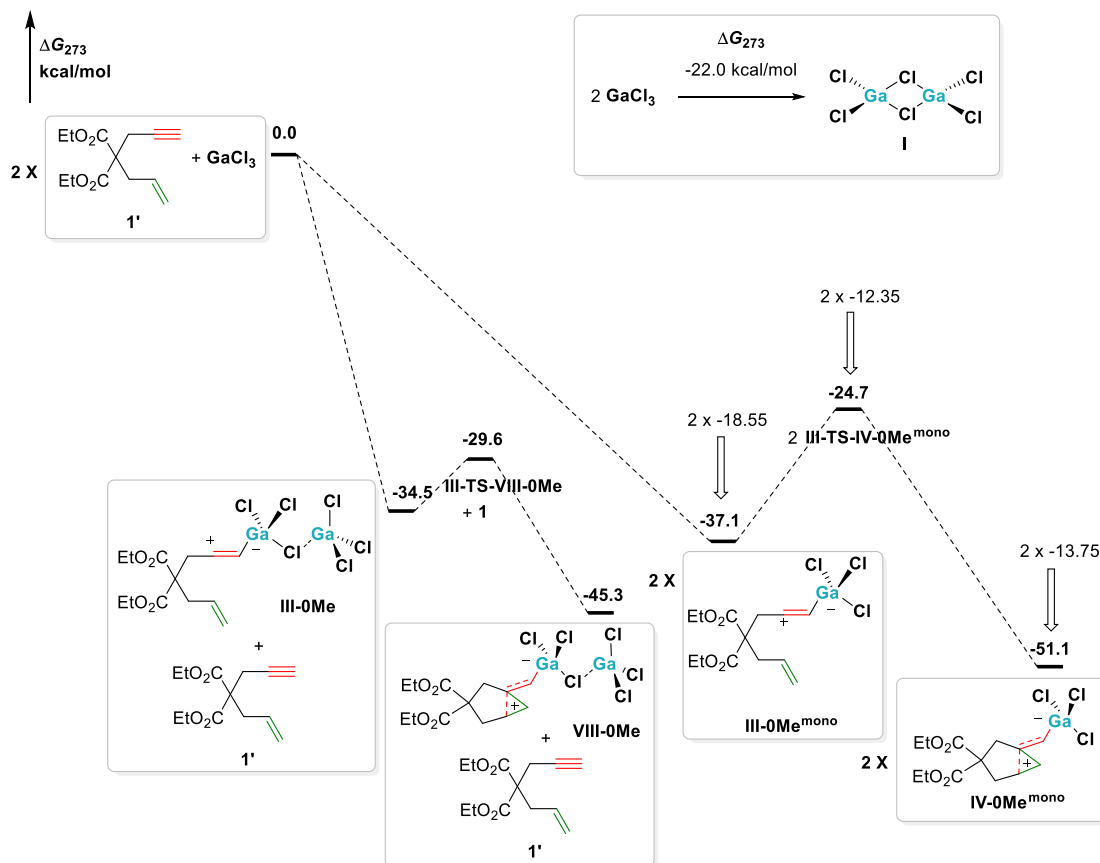
preference is of 3.7 kcal/mol. However, the gain in free energy of the coordination of the enyne triple bond to the gallium center is 4.3 kcal/mol higher than the coordination of chlorine (**Scheme 3.11**: -36.1 vs -40.4 kcal/mol). This clearly compensates the lower free energy of activation of 1.4 vs 2.5 kcal/mol of the RDS (**III-TS-IV** vs **III-TS-IV<sup>mono</sup>**).



**Scheme 3.11.** Selectivity between superelectrophilic and standard activation of enyne **1**.

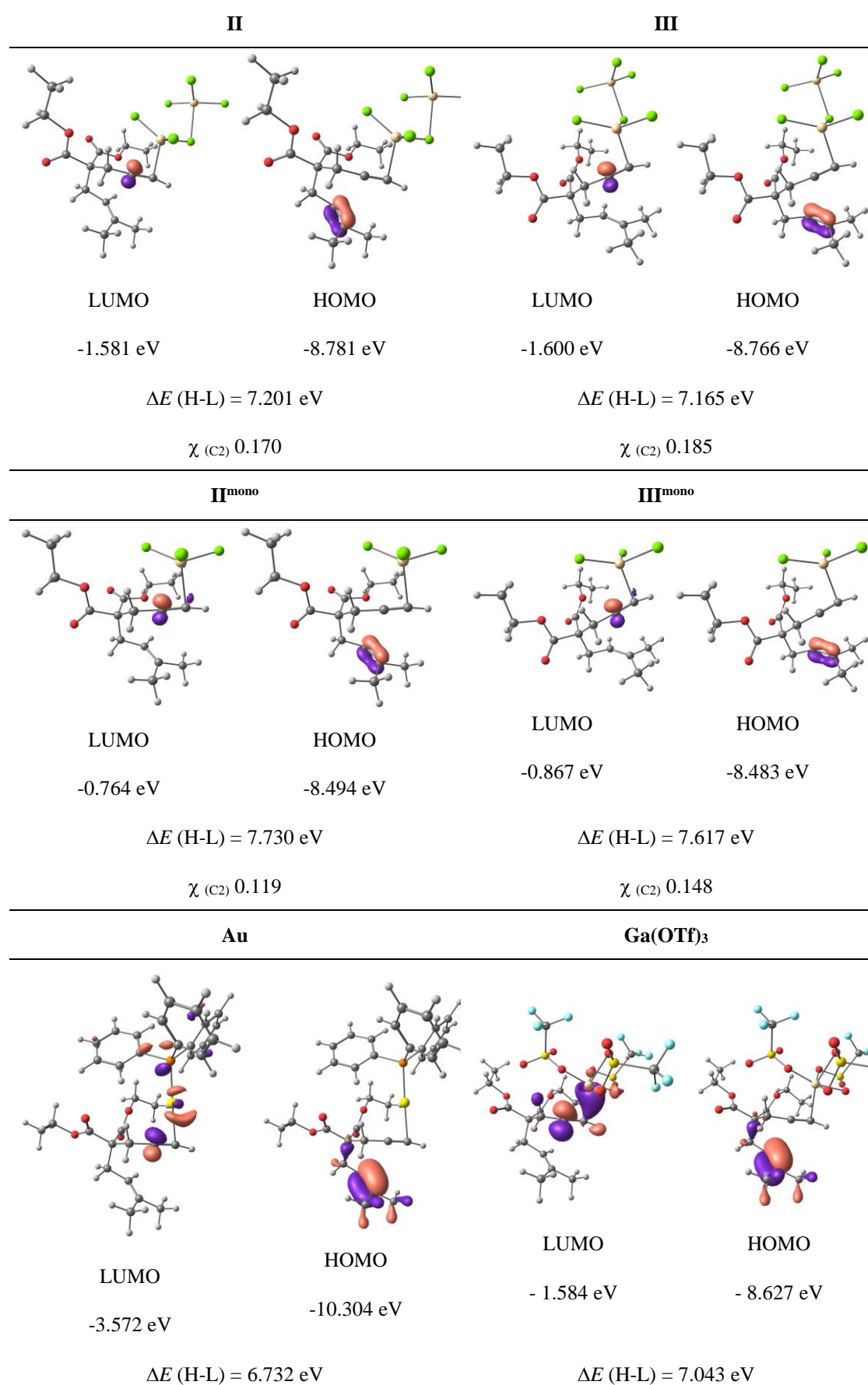
Therefore, unlike the  $\sigma$ -Lewis acid-catalyzed reactions shown in **Scheme 3.5**, the interest of superelectrophilic activation of enyne **1** is not supported by the computations. However, enyne **1** possesses a highly nucleophilic alkene moiety. With one less methyl group or no methyl group at the alkene terminus, the free energy of activation of the first C–C bond formation significantly increases (**Scheme 3.9**). In such case, even if the formation of mono-gallium alkyne species is more favorable than a digallium

alkyne species (**Scheme 3.12**: -37.1 vs -34.5 kcal/mol), it does not compensate the higher barrier of the mono-gallium series (**III-TS-IV-0Me<sup>mono</sup>**) and there is a positive effect of the superelectrophilic activation.



**Scheme 3.12.** Selectivity between superelectrophilic and standard activation of enyne **1'**.

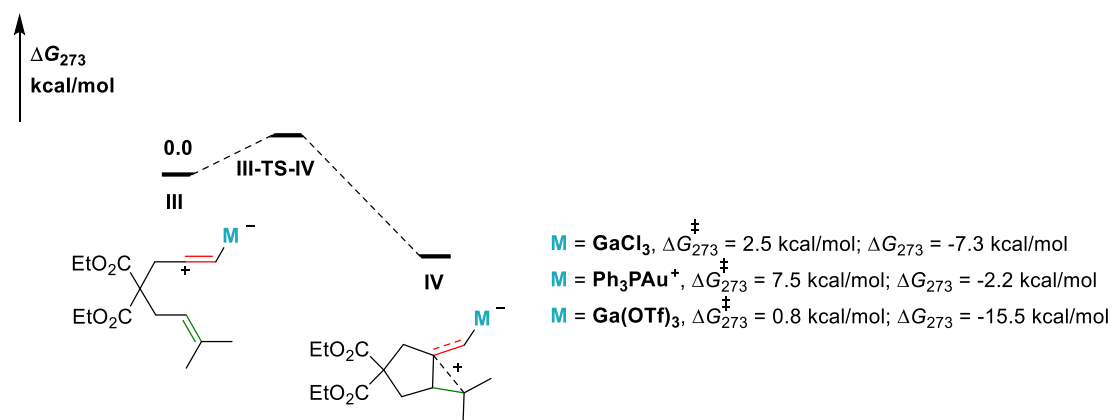
The electronic properties of the metal alkyne complexes were then analyzed.<sup>35</sup> The vinyl cation character of species **II**, **III**, **II<sup>mono</sup>**, and **III<sup>mono</sup>** is actually revealed by a significant positive charge and a large lowest unoccupied molecular orbital (LUMO) lobe at C2 (**Figure 3.2**). The highest occupied molecular orbital (HOMO) of these complexes is concentrated on the alkene moiety. Type **III** isomers have a lower HOMO–LUMO energy difference and a higher positive charge at C2 compared to **II**. The presence of a second  $\text{GaCl}_3$  molecule also reduces the HOMO–LUMO gap and increases the charge at C2.



$\chi_{(C2)} 0.057$  $\chi_{(C2)} 0.200$ 

**Figure 3.2.** Frontier orbitals of type **II** and **III** compounds (contour plot 0.1290) and of the corresponding AuPPh<sub>3</sub><sup>+</sup> and Ga(OTf)<sub>3</sub> complexes (contour plot 0.0622). Energy of the Frontier orbitals and NPA charge at C2.

There is no correlation between  $\Delta E$  (H – L) and the free energy of activation between **III** and **IV** in different metal complex series (**Figure 3.2** and **Scheme 3.13**). With the Ph<sub>3</sub>PAu<sup>+</sup> moiety,  $\Delta E$  (H – L) is the lowest of the series (6.732 eV) but the highest barrier was computed (7.5 kcal/mol).<sup>36</sup> With Ga(OTf)<sub>3</sub>, a complex which is not active experimentally, a very low barrier of 0.8 kcal/mol was computed in spite of a higher  $\Delta E$  (H – L) of 7.043 eV. It should also be noted that the formation of the gold-stabilized nonclassical carbocation is also the less exergonic process of the series (–2.2 vs –7.3 and –15.5 kcal/mol).



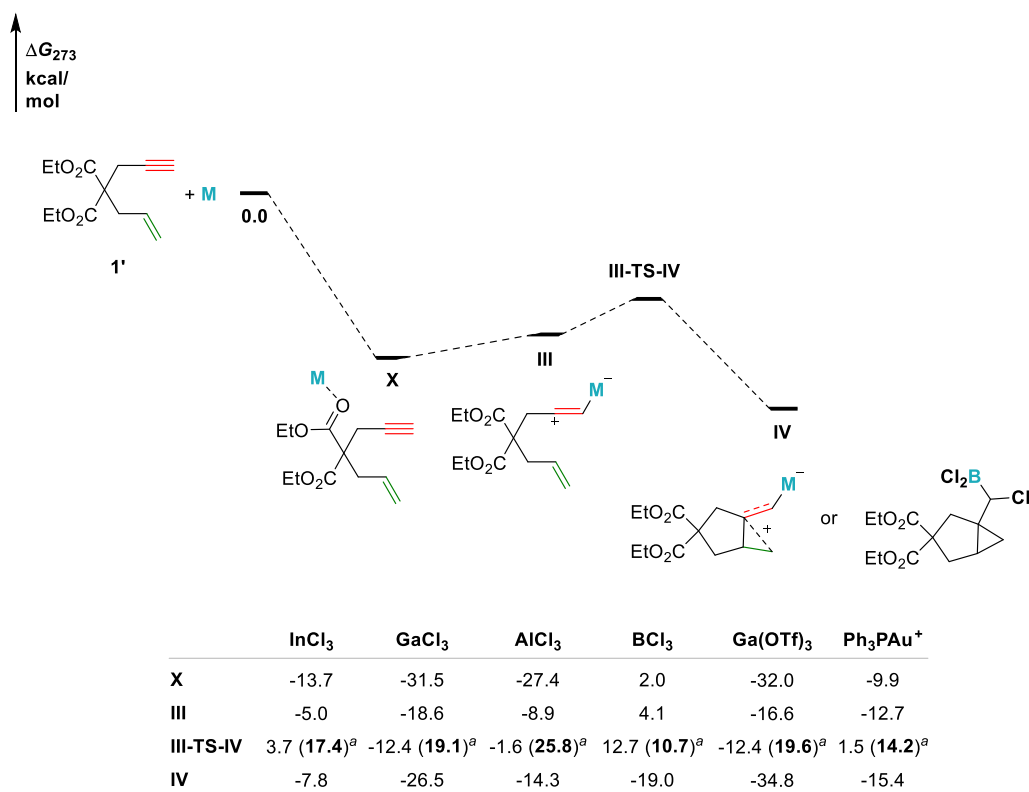
**Scheme 3.13.** Cyclization of some ( $\eta^1$ -Alkyne)metal complexes derived from enyne **1**.

Thus, although superelectrophilic activation has a positive impact on the reaction rate, this effect is not a prerequisite for alkynophilicity. The barrier of the formation of intermediate **III<sup>mono</sup>** is sufficiently low and the reaction sufficiently exergonic to qualify GaCl<sub>3</sub>, as a monomer, as an alkynophilic species. The case of Ga(OTf)<sub>3</sub>, an experimentally inactive catalyst which yet leads to the lowest activation energy, brings

further questions and stimulates the test of other group 13 species. In addition, to avoid a particular case effect of the *gem*-dimethyl at the alkene terminus or the *gem*-diester group in the tether of enyne **1**, over enynes were also studied.

### 3.4.2. $\sigma$ - vs $\pi$ -Lewis Acidity

As mentioned above, group 13 MX<sub>3</sub> salts are not only  $\pi$ -Lewis acids able to activate C–C  $\pi$ -bonds but also strong oxophilic  $\sigma$ -Lewis acids. Enyne **1'** was used to study the effect of the ester group coordination to the overall free energy required to reach the cyclization transition state (**Scheme 3.14**). As expected, the coordination of the ester moiety of the enyne is always more favorable than the coordination of the alkyne, except for the gold complex.<sup>23</sup> Of note, even InCl<sub>3</sub> does not form a chelate with the two carbonyl group. None of these species seem to be intrinsically poorly alkynophilic, but we can note that the free energy difference between **X** and **III-TS-IV** is quite too high for the reaction to occur at room or lower temperatures with AlCl<sub>3</sub> (25.8 kcal/mol).



**Scheme 3.14.** Cyclization of some ( $\eta^1$ -alkyne)metal complexes derived from enyne

**1<sup>a</sup>** (<sup>a</sup>Free energy difference between the most stable donor-acceptor adduct **X** or **III** and **III-TS-IV**.)

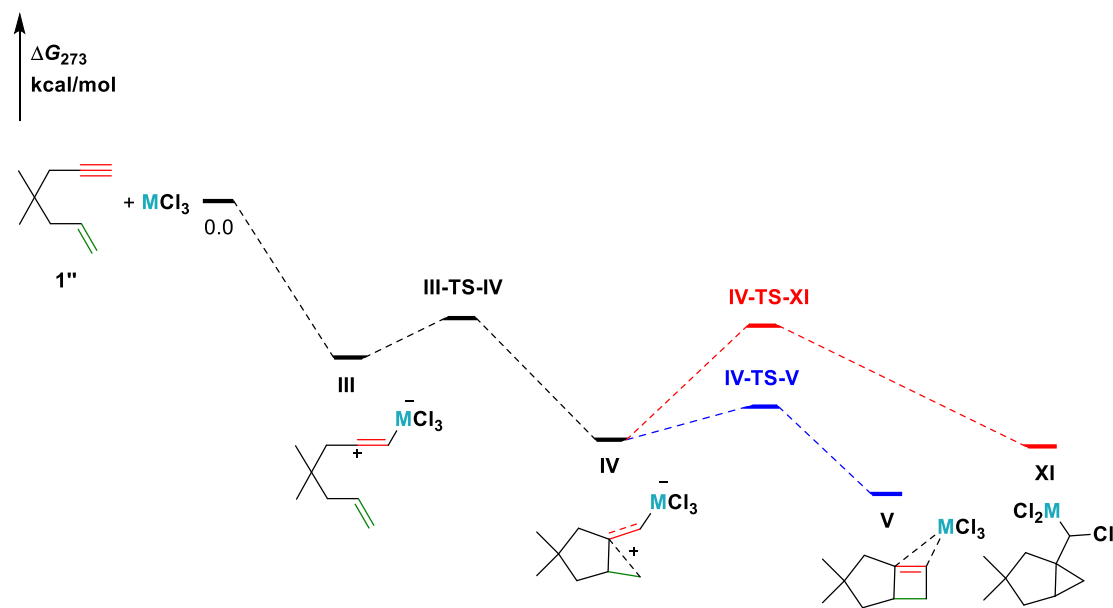
Although BCl<sub>3</sub> is a good Lewis acid, it is reluctant to pyramidalization.<sup>37</sup> The donor-acceptor adducts of BCl<sub>3</sub> with alkynes or ester groups are activated forms toward nucleophilic attack, but they can be made in an endergonic manner,<sup>38</sup> as it is the case here. The transition state remains easily accessible (12.7 kcal/mol), and the cyclization is appreciably exergonic by 19.0 kcal/mol. However, the cyclized product does not converge as a BCl<sub>3</sub> adduct. A spontaneous 1,2-chloride transfer to the carbocationic center leads to an alkyldichloroboron species. Such group transfer has been reported in the case of the B(C<sub>6</sub>F<sub>5</sub>)<sub>3</sub>-promoted cyclopropanation/carboboration of enynes.<sup>39,40</sup>

At this stage, we can conclude that all of these species are potentially alkynophilic, but oxophilicity<sup>41</sup> and chloride transfer can be an issue. Unlike all other MCl<sub>3</sub> salts, AlCl<sub>3</sub> is poorly soluble in apolar solvents such as toluene. The use of a more polar solvent such as acetone, nitrobenzene, or tetrahydrofuran (THF), in which AlCl<sub>3</sub> dissolves, means the formation of strongly bound O–Al donor–acceptor adducts that can be dormant species. The same is true for Ga(OTf)<sub>3</sub>, which in spite of a good intrinsic alkynophilicity in the gas phase, is soluble in strongly bonding solvents only (i.e., H<sub>2</sub>O, MeNO<sub>2</sub>, etc.).<sup>42</sup> As for BCl<sub>3</sub>, a catalytic use is compromised by the formation of an RBCl<sub>2</sub> species after chloroboration. This specific kind of deactivation led us to study the 1,2-chloride transfer with the other group 13 species. We also noted that in the absence of the esters in the tether, it became possible to optimize species **IV** with BCl<sub>3</sub> intact, offering a comparative analysis between the formation of the next species on the cycloisomerization pathway (i.e., the cyclobutene) and the formation of the chlorinated species.

### 3.4.3. Deactivation Pathways?

With a *gem*-dimethyl rather than a *gem*-diester group in the enyne tether, the 1,2-

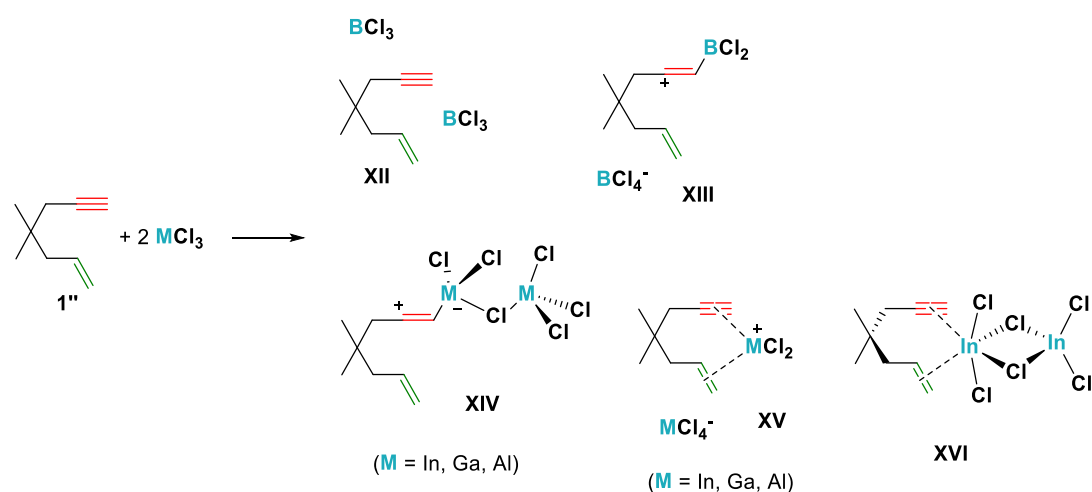
chloride transfer described above is no longer spontaneous (**Scheme 3.15**).<sup>43</sup> This process was thus compared with the formation of the cyclobutene intermediate. Again, all MX<sub>3</sub> species appear as good alkynophilic  $\pi$ -Lewis acids in the sense that the transition state **III-TS-IV** is readily accessible and the formation of **IV** is exergonic and followed by another low-lying transition state **IV-TS-V** leading to an even more stable species. The 1,2-chloride transfer could be modeled in the indium, gallium, and boron series, but not in the aluminum one. With aluminum, even trying to get **XI** led back to **IV**. With indium and gallium, the chloride transfer is strongly disfavored over the cyclobutene formation, both thermodynamically and kinetically. With boron, the difference between the transition states is only 0.3 kcal/mol in favor of the cyclobutene formation, but the chlorinated product **XI** is more stable by 2.2 kcal/mol than cyclobutene **V**. Thus, by reversibility, the formation of **XI** can be a trap.



	InCl <sub>3</sub>	GaCl <sub>3</sub>	AlCl <sub>3</sub>	BCl <sub>3</sub>
<b>III</b>	-11.2	-17.8	-11.9	6.1
<b>III-TS-IV</b>	-1.4	-11.1	-3.7	11.2
<b>IV</b>	-11.6	-25.2	-15.1	-10.9
<b>IV-TS-V</b>	<b>-9.2</b>	<b>-22.5</b>	<b>-12.8</b>	<b>-9.1</b>
<b>V</b>	-22.6	-30.7	-19.2	-13.3
<b>IV-TS-XI</b>	<b>0.5</b>	<b>-12.9</b>	-	<b>-8.8</b>
<b>XI</b>	-6.9	-18.5	-	-15.5

**Scheme 3.15.** Cyclobutene formation vs 1,2-chloride transfer.

Another deactivation pathway that could explain the inactivity of AlCl<sub>3</sub> and BCl<sub>3</sub> could be the formation of ion pairs. We have already reported in a precedent study that the [GaCl<sub>2</sub>]<sup>+</sup>[GaCl<sub>4</sub>]<sup>-</sup> ion pair is less active than GaCl<sub>3</sub> with enynes exhibiting a *gem*-diester group in their tether.<sup>8f</sup> Even in the absence of the *gem*-diester group, the alkyne and the alkene could trap the cationic MCl<sub>2</sub><sup>+</sup> ion by forming a chelate. All of this was studied within the entire MCl<sub>3</sub> series (**Scheme 3.16**).



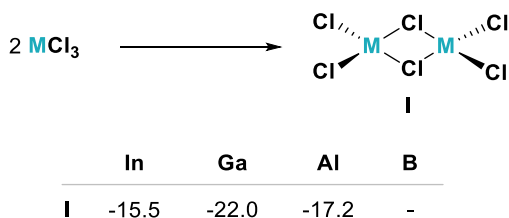
	InCl <sub>3</sub>	GaCl <sub>3</sub>	AlCl <sub>3</sub>	BCl <sub>3</sub>
<b>XII</b>	-	-	-	10.8
<b>XIII</b>	-	-	-	27.1
<b>XIV</b>	-21.0	-32.4	-18.5	-
<b>XV</b>	-6.7	-22.4	-6.5	-
<b>XVI</b>	-21.5	-	-	-

**Scheme 3.16.** Molecular adduct vs ion pair formation between enyne **1''** and MCl<sub>3</sub> (2 equiv,  $\Delta G_{273}$ , kcal/mol).

With BCl<sub>3</sub>, the molecular adduct **XII**, lying 10.8 kcal/mol above the reactants, was modeled. The corresponding ion pair **XIII** in which there is no interaction between the alkene and the boron center was obtained at a much higher free energy of 27.1 kcal/mol. For gallium and aluminum, the catalytically viable vinyl cation **XIV** was found to be markedly more stable than the corresponding chelate **XV** (Ga: -32.4 vs -22.4 kcal/mol;

Al: -18.5 vs -6.5 kcal/mol). In the indium series, the molecular chelated adduct **XVI** was computed in addition to the vinyl cation **XIV**. These two compounds have similar energies and are much more stable than the ion pair **XV** (-21.0/-21.5 vs -6.7 kcal/mol). Thus, the formation of ion pairs cannot be blamed for catalyst deactivation, at least in solvents of low polarity such as toluene.

Finally, the aforementioned Ga<sub>2</sub>Cl<sub>6</sub> dimer formation was reevaluated with the other group 13 elements (**Scheme 3.17**). It is well known that GaCl<sub>3</sub> forms Ga<sub>2</sub>Cl<sub>6</sub> dimers in the solid state and in weakly coordinating solvents.<sup>33,44</sup> As shown in **Scheme 3.16**, the formation of the vinyl cation **XIV** liberates 32.4 kcal/mol of free energy, while that of Ga<sub>2</sub>Cl<sub>6</sub> provides 22.0 kcal/mol. Even the formation of two monomeric alkyne adducts such as **III** in **Scheme 3.15** would release  $2 \times 17.8 = 35.6$  kcal/mol, meaning that Ga<sub>2</sub>Cl<sub>6</sub> is not a thermodynamic trap. The same conclusion can be reached with In<sub>2</sub>Cl<sub>6</sub> (-15.5 vs -21.0 or -22.4 kcal/mol) and Al<sub>2</sub>Cl<sub>6</sub> (-17.2 vs -18.5 or -23.8 kcal/mol). As for the boron case, there is no question asked since BCl<sub>3</sub> does not form dimers.<sup>15</sup>

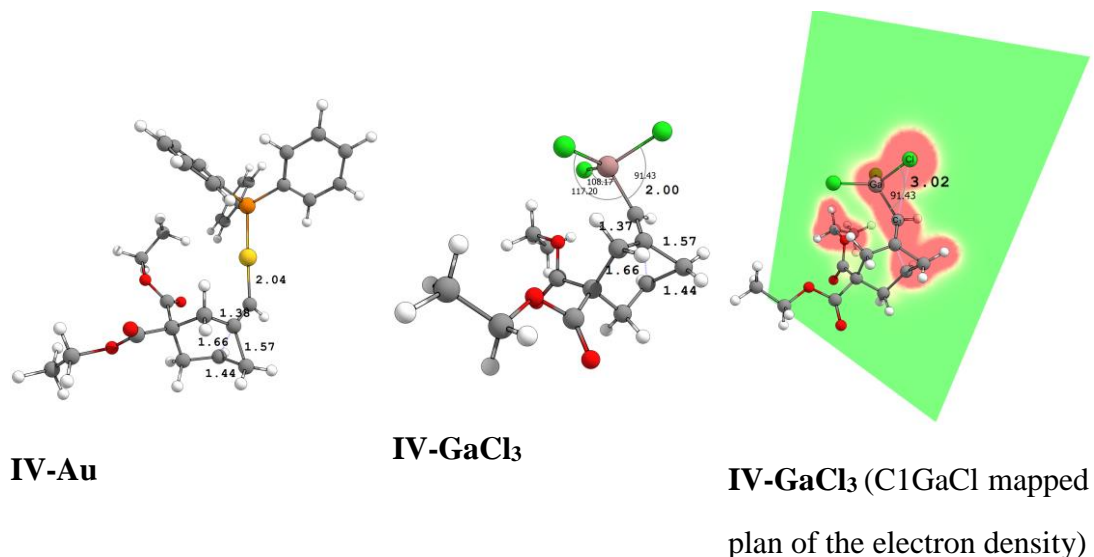


**Scheme 3.17.** Formation of M<sub>2</sub>Cl<sub>6</sub> dimers ( $\Delta G_{273}$ , kcal/mol).

### 3.4.4. Origin of the Alkynophilicity

As seen above, even though superelectrophilic activation is helpful with less reactive enynes, it is not a requirement for a successful reaction. The reason why MX<sub>3</sub> species are alkynophilic lies somewhere else, and the fact that they are all intrinsically alkynophilic in the gas phase rules out an explanation based on d-block contraction or hardness vs softness. Obviously, the exceptional stabilization of type **IV** intermediates cannot be related to d orbitals or M → L back-donation since d orbitals are either absent

(B, Al) or inaccessible (Ga, In).<sup>45</sup> We looked for an answer in the ligands themselves. As far as the organic fragment originating from the enyne is concerned in complexes **IV-Au** and **IV-GaCl<sub>3</sub>** (**Figure 3.3**), there is virtually no geometrical difference. In the gallium complex, one can note that one C1GaCl angle is smaller than the other (91.43 vs 108.17 and 117.20°). This suggests that one chlorine atom is well oriented to transfer electron density to the carbocationic part of the complex. A mapped plan of the electron density passing through C1, Ga, and Cl shows the flow of electron density in this area. The LUMO of **IV-GaCl<sub>3</sub>** shows the empty p orbital system with the largest contribution in the vicinity of one chlorine atom. Examination of the occupied orbitals reveals an overlap on the Cl–C1–C2–C6 system in HOMO-5. The same features were observed in the **IV-Ga<sub>2</sub>Cl<sub>6</sub>** series, the Cl–C1–C2–C6 overlap corresponding this time to HOMO-2. Of note, we found the same kind of interaction in **IV-Ga(OTf)<sub>3</sub>** in which one oxygen and one fluorine atom stabilize the carbocationic system. Thus, we attribute the stabilization of type **IV** intermediates to noncovalent or weakly covalent interactions between the heteroatoms of the metal ligands and the carbocationic system.



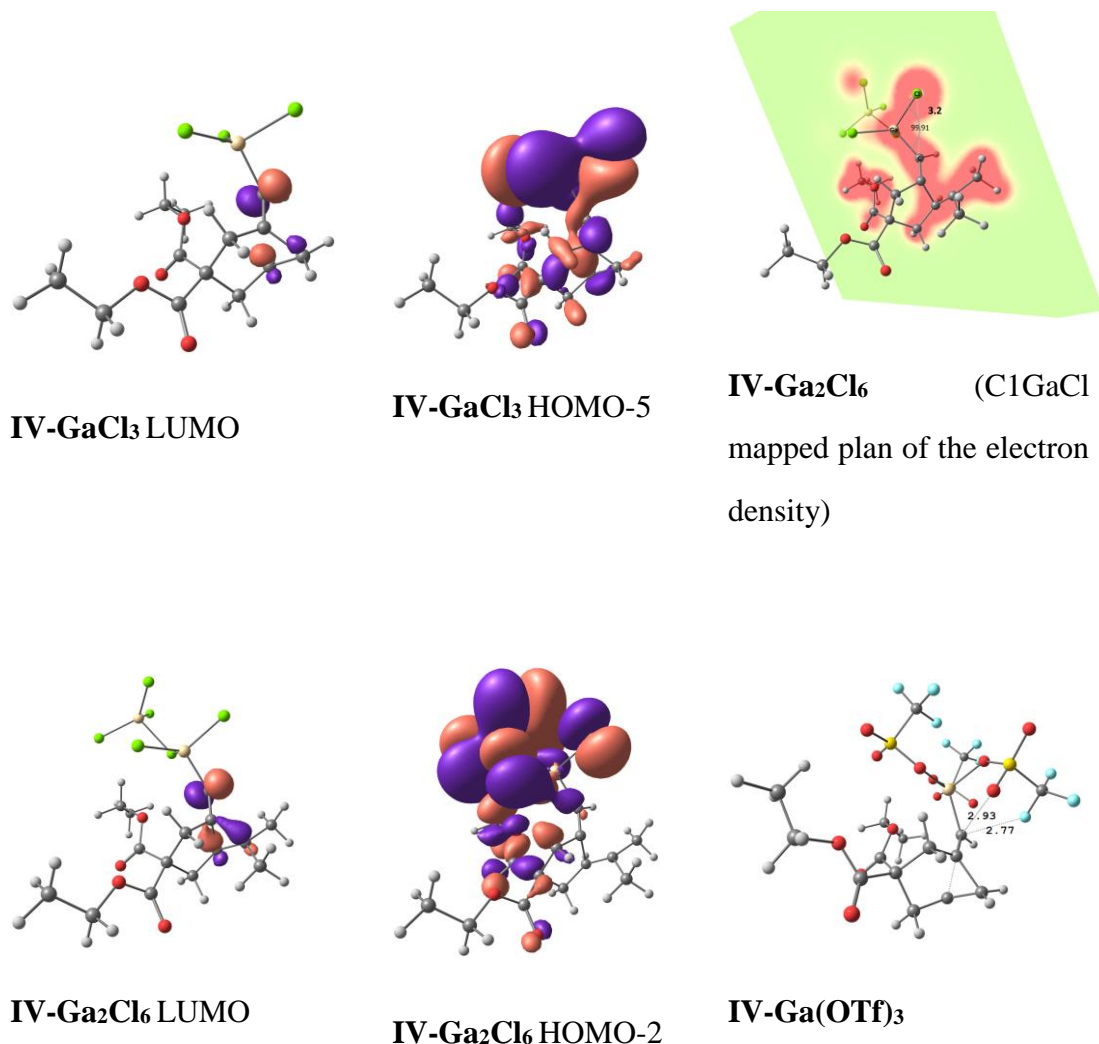


**Figure 3.3.** Selected type IV complexes from enyne **1'** (selected distances in Å and angles in degrees).

### 3.5. Conclusions

This study has shown that MX<sub>3</sub> salts are all alkynophilic in the gas phase, regardless of their hardness or softness. What makes a large difference between active catalysts such as GaCl<sub>3</sub> or InCl<sub>3</sub> and inactive ones such as AlCl<sub>3</sub> or Ga(OTf)<sub>3</sub> is their solubility in apolar solvents. While GaCl<sub>3</sub> is even soluble in pentane, dissolving AlCl<sub>3</sub> or Ga(OTf)<sub>3</sub> requires the use of heteroatom-containing polar solvents, which traps the catalyst. On the other hand, the highly soluble BCl<sub>3</sub> salt follows particular deactivation pathways due to a weaker M–Cl bond. No other factors such as the formation of dormant

oligomers or ion pairs could rationalize the inactivity of AlCl<sub>3</sub> or BCl<sub>3</sub>. Among the group 13 MX<sub>3</sub> salts studied, GaCl<sub>3</sub> showed a pronounced ability to activate enynes in spite of its strong oxophilicity. The lack of nucleophilic character of the enyne alkene moiety can be counterbalanced by increasing the electrophilicity of the alkyne moiety by superelectrophilic activation using the Ga<sub>2</sub>Cl<sub>6</sub> homodimer. The mechanism of the skeletal reorganization is similar to the gold-catalyzed one. What makes GaCl<sub>3</sub> such a good  $\pi$ -acid is a combination of: (i) its high solubility in apolar solvents, (ii) its strong Ga–Cl bonds, which do not easily break to give ion pairs or chlorogallation products, and (iii) its ability to stabilize the nonclassical carbocation **IV** by Cl p orbital back-donation to the empty p orbitals of the organic framework. A thorough knowledge of all of these subtle factors should stimulate the development of even more selective main-group-based Lewis acids able to compete with late-transition-metal complexes.

### 3.6. References

- 1 Nieto-Oberhuber, C.; Muñoz, M. P.; Buñuel, E.; Nevado, C.; Cárdenas, D. J.; Echavarren, A. M. Cationic Gold(I) Complexes: Highly Alkynophilic Catalysts for the *exo*- and *endo*-Cyclization of Enynes. *Angew. Chem., Int. Ed.* **2004**, *43*, 2402–2406.
- 2 See inter alia: (a) Zeng, X.; Liu, S.; Shi, Z.; Xu, B. Hydrogen Bonding Cluster-Enabled Addition of Sulfonic Acids to Haloalkynes: Access to Both (*E*)- and (*Z*)-Alkenyl Sulfonates. *Org. Lett.* **2016**, *18*, 4770–4773. (b) Shibuya, M.; Okamoto, M.; Fujita, S.; Abe, M.; Yamamoto, Y. Boron-Catalyzed Double Hydrofunctionalization Reactions of Unactivated Alkynes. *ACS Catal.* **2018**, *8*, 4189–4193. (c) Issaian, A.; Faizi, D. J.; Bailey, J. O.; Mayer, P.; Berionni, G.; Singleton, D. A.; Blum, S. A. Mechanistic Studies of Formal Thioboration Reactions of Alkynes. *J. Org. Chem.* **2017**, *82*, 8165–8178.
- 3 (a) Diver, S. T.; Giessert, A. J. Enyne Metathesis (Enyne Bond Reorganization). *Chem. Rev.* **2004**, *104*, 1317–1382. (b) Nicolaou, K. C.; Bulger, P. G.; Sarlah, D. Metathesis Reactions in Total Synthesis. *Angew. Chem., Int. Ed.* **2005**, *44*, 4490–4527. (c) Zhang, L.; Sun, J.; Kozmin, S. A. Gold and Platinum Catalysis of Enyne Cyclo-isomerization. *Adv. Synth. Catal.* **2006**, *348*, 2271–2296. (d) Mori, M. Synthesis of Natural Products and Related Compounds using Enyne Metathesis. *Adv. Synth. Catal.* **2007**, *349*,

121–135. (e) Mori, M.; Kitamura, T. Ene-Yne and Alkyne Metathesis. In *Comprehensive Organometallic Chemistry III*, Mingos, D. M. P.; Crabtree, R. H., Eds.; 2007; Vol. 11, pp 271–310. (f) Mori, M. Recent Progress on Enyne Metathesis: Its Application to Syntheses of Natural Products and Related Compounds. *Materials* **2010**, *3*, 2087–2140. (g) Echavarren, A. M.; Jiménez-Núñez, E. Complexity via Gold-Catalyzed Molecular Gymnastics. *Top. Catal.* **2010**, *53*, 924–930. (h) Dragutan, I.; Dragutan, V.; Demonceau, A.; Delaude, L. Enabling Access to Diverse Bioactive Molecules Through Enyne Metathesis Concepts. *Curr. Org. Chem.* **2013**, *17*, 2678–2720. (i) Michelet, V. Noble Metal-Catalyzed Enyne Cycloisomerizations and Related Reactions. In *Comprehensive Organic Synthesis*, 2nd ed.; Knochel, P.; Knochel, P.; Molander, G. A., Eds.; Elsevier: 2014; Vol. 5, pp 1483–1536. (j) Dorel, R.; Echavarren, A. M. Gold(I)-Catalyzed Activation of Alkynes for the Construction of Molecular Complexity. *Chem. Rev.* **2015**, *115*, 9028–9072. (k) Echavarren, A. M.; Muratore, M. E.; López-Carrillo, V.; Escribano-Cuesta, A.; Huguet, N.; Obradors, C. Gold-Catalyzed Cyclizations of Alkynes with Alkenes and Arenes. *Org. React.* **2017**, *92*, 1–288. (l) Hu, Y.; Bai, M.; Yang, Y.; Zhou, Q. Metal-Catalyzed Enyne Cycloisomerization in Natural Product Total Synthesis. *Org. Chem. Front.* **2017**, *4*, 2256–2275.

4 (a) Trost, B. M.; Krische, M. J. Transition Metal Catalyzed Cycloisomerizations. *Synlett* **1998**, *1998*, 1–16. (b) Aubert, C.; Buisine, O.; Malacria, M. The Behavior of 1,*n*-Enynes in the Presence of Transition Metals. *Chem. Rev.* **2002**, *102*, 813–834. (c) Lloyd-Jones, G. C. Mechanistic Aspects of Transition Metal Catalysed 1,6-Diene and 1,6-Enyne Cycloisomerisation Reactions. *Org. Biomol. Chem.* **2003**, *1*, 215–236. (d) Echavarren, A. M.; Nevado, C. Non-stabilized transition metal carbenes as intermediates in intramolecular reactions of alkynes with alkenes. *Chem. Soc. Rev.* **2004**, *33*, 431–436. (e) Bruneau, C. Electrophilic Activation and Cycloisomerization of Enynes: A New Route to Functional Cyclopropanes. *Angew. Chem., Int. Ed.* **2005**, *44*, 2328–2334. (f) Nieto-Oberhuberr, C.; López, S.; Jiménez-Núñez, E.; Echavarren, A. M. The Mechanistic Puzzle of Transition-Metal-Catalyzed Skeletal Rearrangements of Enynes. *Chem. - Eur. J.* **2006**, *12*, 5916–5923. (g) Zhang, L.; Sun, J.; Kozmin, S. A. Gold and Platinum Catalysis of Enyne Cyclo-isomerization. *Adv. Synth. Catal.* **2006**, *348*, 2271–2296. (h) Michelet, V.; Toullec, P. Y.; Genêt, J.-P. Cycloisomerization of 1,*n*-Enynes: Challenging Metal-Catalyzed Rearrangements and Mechanistic Insights. *Angew. Chem., Int. Ed.* **2008**, *47*, 4268–4315. (i) Jiménez-Núñez, E.; Echavarren, A. M. Gold-Catalyzed Cycloisomerizations of Enynes: A Mechanistic

- Perspective. *Chem. Rev.* **2008**, *108*, 3326–3350. (j) Lee, S. I.; Chatani, N. Catalytic Skeletal Reorganization of Enynes Through Electrophilic Activation of Alkynes: Double Cleavage of C–C Double and Triple Bonds. *Chem. Commun.* **2009**, 371–384. (k) Toullec, P. Y.; Michelet, V. Cycloisomerization of 1,*n*-Enynes Via Carbophilic Activation. In *Topics in Current Chemistry*, Soriano, E.; Marco-Contelles, J., Eds.; Springer: Berlin, Heidelberg, 2011; Vol. 302, pp 31–80. (l) Marinetti, A.; Jullien, H.; Voituriez, A. Enantioselective, transition metal catalyzed cycloisomerisations. *Chem. Soc. Rev.* **2012**, *41*, 4884–4908.
- 5 (a) Fürstner, A.; Stelzer, F.; Szillat, H. Platinum-Catalyzed Cycloisomerization Reactions of Enynes. *J. Am. Chem. Soc.* **2001**, *123*, 11863–11869. (b) Fürstner, A.; Davies, P. W. Catalytic Carbophilic Activation: Catalysis by Platinum and Gold  $\pi$  Acids. *Angew. Chem., Int. Ed.* **2007**, *46*, 3410–3449.
- 6 Escribano-Cuesta, A.; Pérez-Galán, P.; Herrero-Gómez, E.; Sekine, M.; Braga, A. A. C.; Maseras, F.; Echavarren, A. M. The Role of Cyclobutenes in Gold(I)-Catalysed Skeletal Rearrangement of 1,6-Enynes. *Org. Biomol. Chem.* **2012**, *10*, 6105–6110.
- 7 (a) Gupta, M. K.; O’Sullivan, T. P. Recent Applications of Gallium and Gallium Halides as Reagents in Organic Synthesis. *RSC Adv.* **2013**, *3*, 25498–25522. (b) Yamaguchi, M.; Matsunaga, S.; Shibasaki, M.; Michelet, B.; Bour, C.; Gandon, V. Gallium Trichloride. *e-EROS* **2014**, 1–8. (c) Bour, C.; Gandon, V. New Procedures for Catalytic Carbophilic Activation by Gold and Gallium  $\pi$ -Acids. *Synlett* **2015**, *26*, 1427–1436. (d) Sestelo, J. P.; Sarandeses, L. A.; Martínez, M. M.; Alonso- Marañón, L. Indium(III) as  $\pi$ -Acid Catalyst for the Electrophilic Activation of Carbon–Carbon Unsaturated Systems. *Org. Biomol. Chem.* **2018**, *16*, 5733–5747.
- 8 (a) Miyahana, Y.; Chatani, N. Skeletal Reorganization of Enynes Catalyzed by InCl<sub>3</sub>. *Org. Lett.* **2006**, *8*, 2155–2158. (b) Tang, S.; Monot, J.; El-Hellani, A.; Michelet, B.; Guillot, R.; Bour, C.; Gandon, V. Cationic Gallium(III) Halide Complexes: a New Generation of  $\pi$ -Lewis Acids. *Chem. - Eur. J.* **2012**, *18*, 10239–1024. (c) Zhuo, L.-G.; Zhang, J.-J.; Yu, Z.-X. DFT and Experimental Exploration of the Mechanism of InCl<sub>3</sub>-Catalyzed Type II Cyclo-isomerization of 1,6-Enynes: Identifying InCl<sub>2</sub><sup>+</sup> as the Catalytic Species and Answering Why Nonconjugated Dienes Are Generated. *J. Org. Chem.* **2012**, *77*, 8527–8540. (d) Zhuo, L.-G.; Zhang, J.-J.; Yu, Z.-X. Mechanisms of the InCl<sub>3</sub>-Catalyzed Type-I, II, and III Cycloisomerizations of 1,6-Enynes. *J. Org. Chem.* **2014**, *79*, 3809–3820. (e) Zhuo, L.-G.; Shi, Y.-C.;

Yu, Z.-X. Using the Type II Cycloisomerization Reaction of 1,6-Enynes as a Mechanistic Probe to Identify the Real Catalytic Species of GaX<sub>3</sub> and InX<sub>3</sub>. *Asian J. Org. Chem.* **2014**, *3*, 842–846. (f) Michelet, B.; Thiery, G.; Bour, C.; Gandon, V. On the Non-Innocent Behavior of Substrate Backbone Esters in Metal-Catalyzed Carbocyclizations and Friedel-Crafts Reactions of Enynes and Arenynes. *J. Org. Chem.* **2015**, *80*, 10925–10938. (g) Michelet, B.; Colard-Itté, J.-R.; Thiery, G.; Guillot, R.; Bour, C.; Gandon, V. Dibromoindium(III) Cation as  $\pi$ -Lewis Acid: Characterization of [IPr·InBr<sub>2</sub>][SbF<sub>6</sub>] and Catalytic Activity Towards Alkynes and Alkenes. *Chem. Commun.* **2015**, *51*, 7401–7404. (h) Michelet, B.; Tang, S.; Thiery, G.; Monot, J.; Li, H.; Guillot, R.; Bour, C.; Gandon, V. Catalytic Applications of [IPr·GaX<sub>2</sub>][SbF<sub>6</sub>] and Related Species. *Org. Chem. Front.* **2016**, *3*, 1603–1613. (i) Vayer, M.; Guillot, R.; Bour, C.; Gandon, V. Revealing the Activity of  $\pi$ -Acid Catalysts Using a 7-Alkynyl Cycloheptatriene. *Chem. - Eur. J.* **2017**, *23*, 13901–13905. (j) Li, Z.; Thiery, G.; Lichtenthaler, M. R.; Guillot, R.; Krossing, I.; Gandon, V.; Bour, C. Catalytic Use of Low-Valent Cationic Gallium(I) Complexes as  $\pi$ -Acids. *Adv. Synth. Catal.* **2018**, *360*, 544–549.

9 (a) Chatani, N.; Inoue, H.; Kotsuma, T.; Murai, S. Skeletal Reorganization of Enynes to 1-Vinylcycloalkenes Catalyzed by GaCl<sub>3</sub>. *J. Am. Chem. Soc.* **2002**, *124*, 10294–10295. (b) Kim, S. M.; Lee, S. I.; Chung, Y. K. GaCl<sub>3</sub>-Catalyzed Formation of Eight-Membered Rings from Enynes Bearing a Cyclic Olefin. *Org. Lett.* **2006**, *8*, 5425–5427. (c) Ben Hadj Hassen, K.; Gaubert, K.; Vaultier, M.; Pucheaule, M.; Antoniotti, S. Comparison of Homogeneous and Heterogeneous Ga(III) Catalysis in the Cycloisomerization of 1,6-Enynes. *Green Chem. Lett. Rev.* **2014**, *7*, 243–249.

10 Trost, B. M.; Yanai, M.; Hoogsteen, K. A Pd-Catalyzed [2 + 2] Cycloaddition. Mechanism of a Pd-Catalyzed Enyne Metathesis. *J. Am. Chem. Soc.* **1993**, *115*, 5294–5295.

11 (a) Simmons, E. M.; Sarpong, R. Ga(III)-Catalyzed Cyclo-isomerization Strategy for the Synthesis of Icetexane Diterpenoids: Total Synthesis of ( $\pm$ )-Salviasperanol. *Org. Lett.* **2006**, *8*, 2883–2886. (b) Cortez, F. J.; Sarpong, R. Ga(III)-Catalyzed Cycloisomerization Approach to ( $\pm$ )-Icetexone and ( $\pm$ )-epi-Icetexone. *Org. Lett.* **2010**, *12*, 1428–1431. (c) Cortez, F. J.; Lapointe, D.; Hamlin, A. H.; Simmons, E. M.; Sarpong, R. Synthetic Studies on the Icetexones: Enantioselective Formal Syntheses of Icetexone and epi-Icetexone. *Tetrahedron* **2013**, *69*, 5665–5676. (d) Hamlin, A. M.; Lapointe, D.; Owens, K.; Sarpong, R. Studies on C<sub>20</sub>-Diterpenoid Alkaloids: Synthesis of the Hetidine Framework and Its

Application to the Synthesis of Dihydronavirine and the Atisine Skeleton. *J. Org. Chem.* **2014**, *79*, 6783–6800.

12 Cabello, N.; Jiménez-Núñez, E.; Buñuel, E.; Cárdenas, D. J.; Echavarren, A. M. On the Mechanism of the Puzzling “Endocyclic” Skeletal Rearrangement of 1,6-Enynes. *Eur. J. Org. Chem.* **2007**, *2007*, 4217–4223.

13 Gorin, D. J.; Toste, F. D. Relativistic Effects in Homogeneous Gold Catalysis. *Nature* **2007**, *446*, 395–403.

14 (a) Pearson, R. G. Hard and Soft Acids and Bases. *J. Am. Chem. Soc.* **1963**, *85*, 3533–3539. (b) Pearson, R. G. Recent Advances in the Concept of Hard and Soft Acids and Bases. *J. Chem. Educ.* **1987**, *64*, 561–567. (c) Ho, T.-L. *Hard and Soft Acids and Bases Principle in Organic Chemistry*; Academic Press: New York, 1977. (d) Chattaraj, P. K.; Lee, H.; Parr, R. G. Principle of maximum hardness. *J. Am. Chem. Soc.* **1991**, *113*, 1855–1856.

15 Greenwood, N. N.; Earnshaw, A. *Chemistry of the Elements*, 2nd ed.; Elsevier, 1997.

16 Frisch, M. J.; Trucks, G. W.; Schlegel, H. B.; Scuseria, G. E.; Robb, M. A.; Cheeseman, J. R.; Scalmani, G.; Barone, V.; Petersson, G. A.; Nakatsuji, H.; Li, X.; Caricato, M.; Marenich, A. V.; Bloino, J.; Janesko, B. G.; Gomperts, R.; Mennucci, B.; Hratchian, H. P.; Ortiz, J. V.; Izmaylov, A. F.; Sonnenberg, J. L.; Williams-Young, D.; Ding, F.; Lipparini, F.; Egidi, F.; Goings, J.; Peng, B.; Petrone, A.; Henderson, T.; Ranasinghe, D.; Zakrzewski, V. G.; Gao, J.; Rega, N.; Zheng, G.; Liang, W.; Hada, M.; Ehara, M.; Toyota, K.; Fukuda, R.; Hasegawa, J.; Ishida, M.; Nakajima, T.; Honda, Y.; Kitao, O.; Nakai, H.; Vreven, T.; Throssell, K.; Montgomery, J. A., Jr.; Peralta, J. E.; Ogliaro, F.; Bearpark, M. J.; Heyd, J. J.; Brothers, E. N.; Kudin, K. N.; Staroverov, V. N.; Keith, T. A.; Kobayashi, R.; Normand, J.; Raghavachari, K.; Rendell, A. P.; Burant, J. C.; Iyengar, S. S.; Tomasi, J.; Cossi, M.; Millam, J. M.; Klene, M.; Adamo, C.; Cammi, R.; Ochterski, J. W.; Martin, R. L.; Morokuma, K.; Farkas, O.; Foresman, J. B.; Fox, D. J. *Gaussian 09*, Revision D.01; Gaussian, Inc.: Wallingford CT, 2016.

17 Zhao, Y.; Truhlar, D. G. The M06 Suite of Density Functionals for Main Group Thermochemistry, Thermochemical Kinetics, Noncovalent Interactions, Excited States, and Transition Elements. *Theor. Chem. Acc.* **2008**, *120*, 215–241.

- 18 (a) Hariharan, P. C.; Pople, J. A. The influence of Polarization Functions on Molecular Orbital Hydrogenation Energies. *Theor. Chim. Acta* **1973**, *28*, 213–222. (b) Franci, M. M.; Pietro, W. J.; Hehre, W. J.; et al. Self-Consistent Molecular Orbital Methods. XXIII. A Polarization-Type Basis Set for Second-Row Elements. *J. Chem. Phys.* **1982**, *77*, 3654–3665. (c) Rassolov, V. A.; Pople, J. A.; Ratner, M. A.; Windus, T. L. 6-31G\* Basis Set for Atoms K Through Zn. *J. Chem. Phys.* **1998**, *109*, 1223–1229.
- 19 Hay, P. J.; Wadt, W. R. Ab Initio Effective Core Potentials for Molecular Calculations. Potentials for K to Au Including the Outermost Core Orbitals. *J. Chem. Phys.* **1985**, *82*, 299–310.
- 20 (a) Barone, V.; Cossi, M. Quantum Calculation of Molecular Energies and Energy Gradients in Solution by a Conductor Solvent Model. *J. Phys. Chem. A* **1998**, *102*, 1995–2001. (b) Cossi, M.; Rega, N.; Scalmani, G.; Barone, V. Energies, Structures, and Electronic Properties of Molecules in Solution with the C-PCM Solvation Model. *J. Comput. Chem.* **2003**, *24*, 669–681.
- 21 (a) Fukui, K. The Path of Chemical Reactions—the IRC Approach. *Acc. Chem. Res.* **1981**, *14*, 363–368. (b) Hratchian, H. P.; Schlegel, H. B. Accurate Reaction Paths Using a Hessian Based Predictor–Corrector Integrator. *J. Chem. Phys.* **2004**, *120*, 9918–9924. (c) Hratchian, H. P.; Schlegel, H. B. Using Hessian Updating to Increase the Efficiency of a Hessian Based Predictor-Corrector Reaction Path Following Method. *J. Chem. Theory Comput.* **2005**, *1*, 61–69.
- 22 Reed, A. E.; Curtiss, L. A.; Weinhold, F. Intermolecular Interactions from a Natural Bond Orbital, Donor–Acceptor View-point. *Chem. Rev.* **1988**, *88*, 899–926.
- 23 Yamamoto, Y. From  $\sigma$ - to  $\pi$ -Electrophilic Lewis Acids. Application to Selective Organic Transformations. *J. Org. Chem.* **2007**, *72*, 7817–7831.
- 24 Djurovic, A.; Vayer, M.; Li, Z.; Guillot, R.; Baltaze, J.-P.; Gandon, V.; Bour, C. Synthesis of Medium-Sized Carbocycles by Gallium-Catalyzed Tandem Carbonyl-Olefin Metathesis/Transfer Hydrogenation. *Org. Lett.* **2019**, *21*, 8132–8137.
- 25 (a) DeHaan, f. P.; Brown, H. C. Catalytic Halides. XXXI. Directive Effect in Aromatic Substitutions. 59. Kinetic Gallium Chloride Catalyzed Methylation of Benzene in Excess of Methyl Chloride. *J. Am. Chem. Soc.* **1969**, *91*, 4844–4850. (b) Yang, S.; Bour, C.; Gandon, V. Superelectrophilic Gallium(III) Homodimers in Gallium Chloride Mediated Methylation of Benzene: a Theoretical Study. *ACS Catal.*

2020, 10, 3027–3033.

- 26 (a) Albright, H.; Richl, P. S.; McAtee, C. C.; Reid, J. P.; Ludwig, J. R.; Karp, L. A.; Zimmerman, P. M.; Sigman, M. S.; Schindler, C. S. Catalytic Carbonyl-Olefin Metathesis of Aliphatic Ketones: Iron (III) Homodimers as Lewis Acidic Superelectrophiles. *J. Am. Chem. Soc.* **2019**, *141*, 1690–1700. (b) Albright, H.; Vonesh, H. L.; Schindler, C. S. Superelectrophilic Fe(III)-Ion Pairs as Stronger Lewis Acid Catalysts for (*E*)-Selective Intermolecular Carbonyl-Olefin Metathesis. *Org. Lett.* **2020**, *22*, 3155–3160.
- 27 Negishi, E. Principle of Activation of Electrophiles by Electrophiles through Dimeric Association-Two Are Better than One. *Chem. - Eur. J.* **1999**, *5*, 411–420.
- 28 (a) Olah, G. A. Superelectrophiles. *Angew. Chem., Int. Ed.* **1993**, *32*, 767–788. (b) Olah, G. A.; Klumpp, D. A. *Superelectrophiles and Their Chemistry*; Wiley-VCH Verlag GmbH & Co. KGaA, 2007.
- 29 Borketey, J. B.; Opoku, E.; Tia, R.; Adei, E. The Mechanisms of Gallium-Catalysed Skeletal Rearrangement of 1,6-Enynes – Insights from Quantum Mechanical Computations. *J. Mol. Graphics Modell.* **2020**, *94*, No. 107476.
- 30 Zhu, Y.; Guo, Y.; Xie, D. Theoretical Investigation on the GaCl<sub>3</sub>-Catalyzed Ring-Closing Metathesis Reaction of N-2,3-Butadienyl-2-propynyl-1-amine: Three-Membered Ring versus Four-Membered Ring Mechanism. *J. Phys. Chem. A* **2007**, *111*, 9387–9392.
- 31 Li, H.-J.; Guillot, R.; Gandon, V. A Gallium-Catalyzed Cycloisomerization/Friedel–Crafts Tandem. *J. Org. Chem.* **2010**, *75*, 8435–8449.
- 32 Of note, the role of the [GaCl<sub>2</sub>]<sup>+</sup>[GaCl<sub>4</sub>]<sup>−</sup> ion pair has been ruled out, see ref 8f.
- 33 (a) Fischer, W.; Jübermann, O. Über Thermische Eigenschaften von Halogeniden. Dampfdrucke und Dampfdichten von Gallium III-Halogeniden. *Z. Anorg. Allg. Chem.* **1936**, *227*, 227–236. (b) Laubengayer, A. W.; Schirmer, F. B. The Chlorides of Gallium. *J. Am. Chem. Soc.* **1940**, *62*, 1578–1583.
- 34 Müller, T.; Juhasz, M.; Reed, C. A. The X-ray Structure of a Vinyl Cation. *Angew. Chem., Int. Ed.* **2004**, *43*, 1543–1546.
- 35 For stereoelectronic effects in Au(I)-alkyne complexes, see: dos Passos Gomes, G.; Alabugin, I. V. Drawing Catalytic Power from Charge Separation: Stereoelectronic and Zwitterionic Assistance in the

Au(I)-Catalyzed Bergman Cyclization. *J. Am. Chem. Soc.* **2017**, *139*, 3406–3416.

36 The Ph<sub>3</sub>PAu<sup>+</sup>-catalyzed cycloisomerization of enyne **1** also gives **2**, and the reported computed mechanism predicts the formation of **III** as RDS see ref 12.

37 (a) Jonas, V.; Frenking, G.; Reetz, M. T. Comparative Theoretical Study of Lewis Acid-Base Complexes of BH<sub>3</sub>, BF<sub>3</sub>, BCl<sub>3</sub>, AlCl<sub>3</sub>, and SO<sub>2</sub>. *J. Am. Chem. Soc.* **1994**, *116*, 8741–8753. (b) Brinck, T.; Murray, J. S.; Politzer, P. A Computational Analysis of the Bonding in Boron Trifluoride and Boron Trichloride and Their Complexes with Ammonia. *Inorg. Chem.* **1993**, *32*, 2622–2625. (c) Hirao, H.; Omoto, K.; Fujimoto, H. Lewis Acidity of Boron Trihalides. *J. Phys. Chem. A* **1999**, *103*, 5807–5811. (d) Ogawa, A.; Fujimoto, H. Lewis Acidity of Gallium Halides. *Inorg. Chem.* **2002**, *41*, 4888–4894. (e) Bessac, F.; Frenking, G. Why is BCl<sub>3</sub>a Stronger Lewis Acid with Respect to Strong Bases than BF<sub>3</sub>? *Inorg. Chem.* **2003**, *42*, 7990–7994.

38 (a) Wei, Y.; Liu, D.; Qing, X.; Xu, L. Mechanistic Insights on a Metal-Free Borylative Cyclization of Alkynes Using BCl<sub>3</sub>: A Theoretical Investigation. *Asian J. Org. Chem.* **2017**, *6*, 1575–1578. (b) Liu, W.; Zeng, R.; Han, Y.; Wang, Y.; Tao, H.; Chen, Y.; Liu, F.; Liang, Y. Computational and Experimental Investigation on the BCl<sub>3</sub> Promoted Intramolecular Amination of Alkenes and Alkynes. *Org. Biomol. Chem.* **2019**, *17*, 2776–2783. (c) Bagno, A.; Kantlehnerb, W.; Kreßb, R.; Saielli, G. Fries Rearrangement of Aryl Formates Promoted by BCl<sub>3</sub>. Mechanistic Evidence from <sup>11</sup>B NMR Spectra and DFT Calculations. *Z. Naturforsch., B* **2004**, *59*, 386–397.

39 Hansmann, M. M.; Melen, R. L.; Rudolph, M.; Rominger, F.; Wadeohl, H.; Stephan, D. W.; Hashmi, A. S. K. Cyclopropanation/Carboboration Reactions of Enynes with B(C<sub>6</sub>F<sub>5</sub>)<sub>3</sub>. *J. Am. Chem. Soc.* **2015**, *137*, 15469–15477.

40 For stoichiometric carboboration of arenynes, see: Warner, A. J.; Lawson, J. R.; Fasano, V.; Ingleson, M. J. Ingleson, Formation of C(sp<sup>2</sup>)-Boronate Esters by Borylative Cyclization of Alkynes Using BCl<sub>3</sub>. *Angew. Chem., Int. Ed.* **2015**, *54*, 11245–11249.

41 Of note, Au(I) complexes can be oxophilic too. See inter alia: Vidhani, D. V.; Cran, J. W.; Krafft, M. E.; Manoharan, M.; Alabugin, I. V. Gold(I)-Catalyzed Claisen Rearrangement of Allenyl Vinyl Ethers: Missing Transition States Revealed through Evolution of Aromaticity, Au(I) as an Oxophilic Lewis Acid,

- and Lower Energy Barriers from a High Energy Complex. *J. Org. Chem.* **2013**, *78*, 2059–2073.
- 42 Prakash, G. K. S.; Mathew, T.; Olah, G. A. Gallium(III) Triflate: An Efficient and a Sustainable Lewis Acid Catalyst for Organic Synthetic Transformations. *Acc. Chem. Res.* **2012**, *45*, 565–577.
- 43 Of note, the deactivation of BC<sub>13</sub> could also be due to a direct chloroboration of the alkyne moiety. Such processes have not been reported with other Group 13 MX<sub>3</sub> salts. See inter alia: (a) Lappert, M. F.; Prokai, B. Chloroboration and Allied Reactions of Unsaturated Compounds II. Haloboration and Phenylboration of Acetylenes; and the Preparation of Some Alkynylboranes. *J. Organomet. Chem.* **1964**, *1*, 384–400. (b) Kirschner, S.; Yuan, K.; Ingleson, M. J. Haloboration: Scope, Mechanism and Utility *New J. Chem.* **2021**, *45*, 14855–14868.
- 44 Černý, Z.; Macháčk, J.; Fusek, J.; Čásenský, B.; Kříž, O.; Tuck, D. G. Multinuclear NMR studies of mixtures of aluminium and gallium trihalides in benzene. *J. Chem. Soc., Dalton Trans.* **2001**, 2698–2703.
- 45 (a) Akiba, K.-Y. *Chemistry of Hypervalent Compounds*; Wiley-VCH, 1999. (b) Goesten, M. G.; Guerra, C. F.; Kapteijn, F.; Gascon, J.; Bickelhaupt, F. M. Six-Coordinate Group 13 Complexes: The Role of d Orbitals and Electron-Rich Multi-Center Bonding. *Angew. Chem., Int. Ed.* **2015**, *54*, 12034–12038.

# **Chapter 4. DFT Analysis into the Calcium(II)-Catalyzed Coupling of Alcohols with Vinylboronic Acids: Cooperativity of Two Different Lewis Acids and Counterion Effects**

Shengwen Yang, Christophe Bour, David Lebœuf, and Vincent Gandon

Publication Date: June 21, 2021

*J. Org. Chem.* 2021, 86, 13, 9134–9144

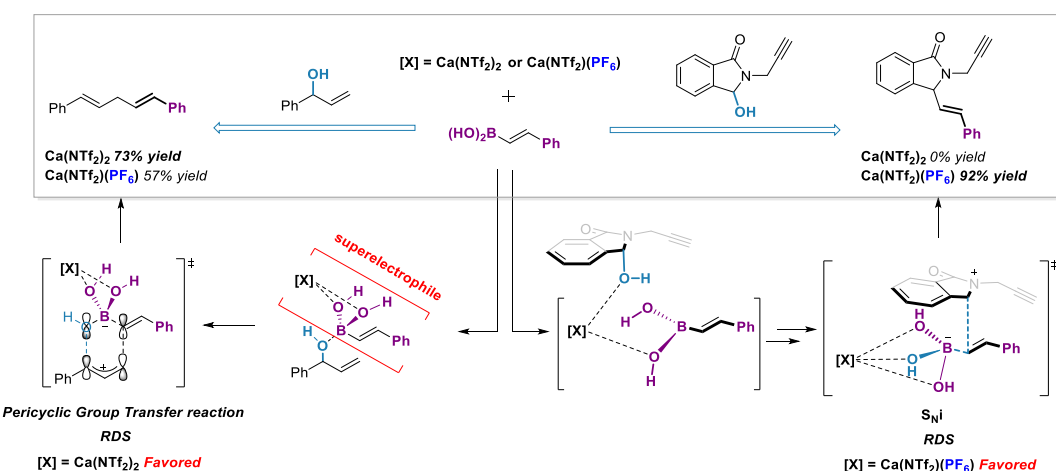
<https://doi.org/10.1021/acs.joc.1c01263>

Copyright © 2021 American Chemical Society



## 4.1. Abstract

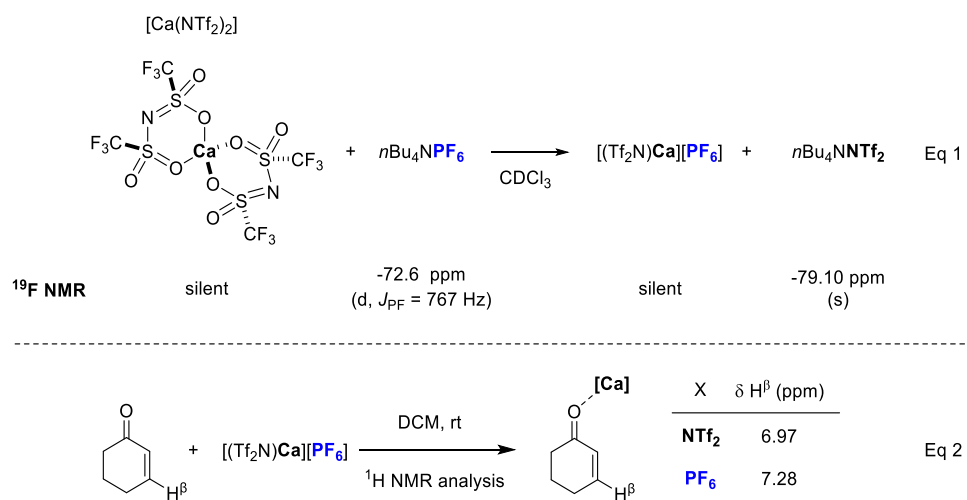
The mechanism of the calcium-catalyzed coupling of alcohols with vinylboronic acids has been analyzed by means of DFT computations. This study reveals that the calcium and the boron Lewis acids associate to form a superelectrophile able to trigger a pericyclic group transfer reaction with allyl alcohols. With other alcohols, the two Lewis acids act synergistically to activate the OH functionality and trigger a  $S_{N}I$  reaction pathway. These two mechanisms are affected by the nature of the counterion, which has been rationalized by electronic and steric factors.



## 4.2. Introduction

During the past decade, calcium-based Lewis acids have witnessed an upsurge in applications in homogeneous catalysis. This renaissance was mostly led by the group of Niggemann who reported that  $\text{Ca}(\text{NTf}_2)_2$  can be activated by an ammonium salt of a weakly coordinating anion such as  $n\text{Bu}_4\text{NPF}_6$  to give a highly oxophilic Lewis acid able to abstract hydroxy groups and promote cationic transformations.<sup>1,2</sup> This strategy is also efficient with  $\text{Ca}(\text{OTf})_2$ .<sup>3</sup> Other functional groups can also be activated, such as ketones or alkenes.<sup>4</sup> The structure of  $\text{Ca}(\text{NTf}_2)_2 \cdot 4\text{H}_2\text{O}$  was reported in 2005 and shows that the calcium ion is not bound to the nitrogen atom of the  $\text{NTf}_2^-$  counterion but to the oxygen atoms of the  $\text{SO}_2\text{CF}_3$  moiety adopting a *cis* configuration of the  $\text{CF}_3$  groups.

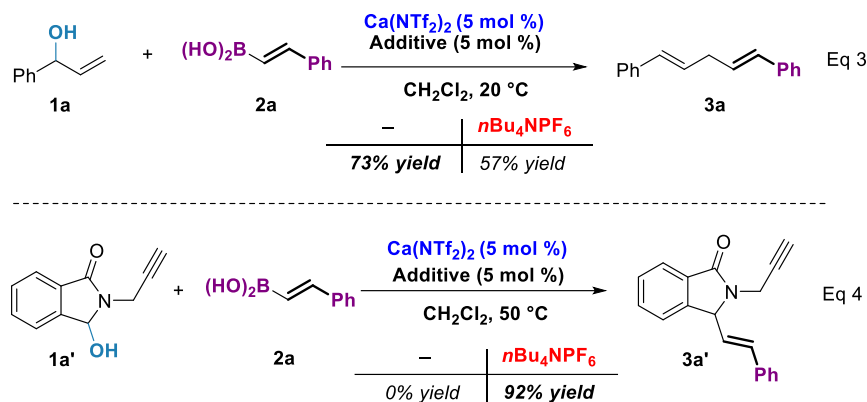
(**Scheme 4.1**, eq 1).<sup>5</sup> This relationship between the metal and its counterions is in sharp contrast with soft transition metals that are usually coordinated to the nitrogen atom, and it reveals the strong oxophilicity of calcium. Thus,  $\text{Ca}(\text{NTf}_2)_2$  is not a very strong Lewis acid since the counterions are strongly coordinated and occupy four coordination sites of the metal. On the other hand, a mixture of  $\text{Ca}(\text{NTf}_2)_2$  and  $n\text{Bu}_4\text{NPF}_6$  has a more pronounced Lewis acidity, as shown by the NMR Childs test (**Scheme 4.1**, eq 2).<sup>4b</sup> Indirect spectroscopic evidence based on the disappearance of the  $^{19}\text{F}$  NMR signals of the spinning counterions attached to the metal center suggested the formation of  $[\text{Ca}(\text{NTf}_2)]^+[\text{PF}_6]^-$  (**Scheme 4.1**, eq 1).<sup>4b,6</sup> The driving force of this anion metathesis, during which a strongly coordinated anion ( $\text{NTf}_2^-$  or  $\text{OTf}^-$ ) is replaced by a weakly coordinating one ( $\text{PF}_6^-$ ), might be due to a higher solubility of the heteroleptic species.



**Scheme 4.1.**  $\text{Ca}(\text{NTf}_2)_2$  and  $[\text{Ca}(\text{NTf}_2)][\text{PF}_6]$ .

The mixture composed of  $\text{Ca}(\text{NTf}_2)_2$  and  $n\text{Bu}_4\text{NPF}_6$  or other  $[\text{R}_4\text{N}]^+[\text{WCA}]^-$  species (WCA = weakly coordinating anion) proved particularly efficient for catalyzing the nucleophilic substitution of alcohols, a process that is believed to follow a  $\text{S}_{\text{N}}1$  pathway.<sup>1a</sup> As far as we are concerned, we have developed the calcium-catalyzed coupling of alcohols with vinylboronic acids (**Scheme 4.2**).<sup>7</sup> This alkenylation reaction is efficient toward allyl, benzyl, and propargyl alcohols (**Scheme 4.2** eq 3)<sup>7a</sup> and  $\text{N},\text{O}$ -acetals (**Scheme 4.2** eq 4).<sup>7b</sup> While the positive effect of the ammonium salt was

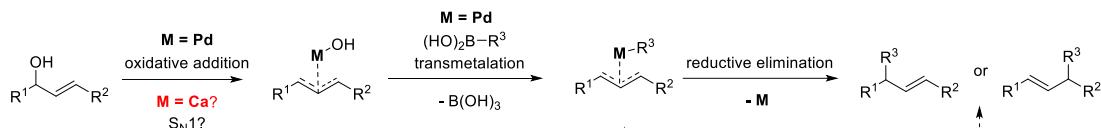
obvious with N,O-acetal **1a'**, a better yield was actually obtained in its absence with allyl alcohol **1a**. Besides, for alcohols such as **1a**, the structure of the product **3a** does not suggest a S<sub>N</sub>1 reaction but rather a S<sub>N</sub>2' process.



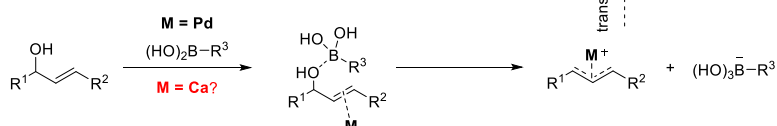
**Scheme 4.2.** Calcium-catalyzed alkenylation of alcohols.

To rationalize these experimental results, we decided to explore the mechanism of these two coupling reactions by density functional theory (DFT) calculations.<sup>8</sup> Of course, most data available on the cross-coupling of allyl alcohols with vinylboronic acids are related to palladium catalysis (**Scheme 4.3**). The reaction might start with the oxidative addition of palladium to produce a  $\pi$ -allylpalladium intermediate by direct activation of the hydroxy group (i).<sup>9</sup> Alternatively, the hydroxy group of the allyl alcohol can be activated by the boronic acid to facilitate the oxidative addition (ii).<sup>10</sup> With calcium, while these two activation modes can be envisaged, we also considered in this study the synergistic activation of the hydroxy group by the two Lewis acids (Ca and B) (iii).

i) the metal activates the hydroxy group



ii) Boronic acid activates the hydroxy group



iii) Calcium and boronic acid synergistically activate the hydroxy group



iv) Calcium activates boronic acid which activates the hydroxy group



**Scheme 4.3.** Mechanistic hypotheses.

A last possibility would be a Lewis acid activation of the boronic acid itself by coordination of the calcium salt to the oxygen atoms of the boronic acid (iv). We have shown in the past that the calcium(II) ion can strengthen the acidity of Brønsted acids such as hexafluoroisopropanol (HFIP),<sup>11</sup> which triggers reactions such as the hydroamidation<sup>4c</sup> or the hydroarylation of alkenes.<sup>4d</sup> Herein, the principle of activation of an electrophile (B) by another electrophile (Ca) through heterodimeric association, leading to a superelectrophile,<sup>12,13</sup> is revisited, and the role of the counterions is analyzed.

### 4.3. Computational Methods

We have used the Gaussian 09 set of programs<sup>14</sup> to perform density functional theory (DFT) computations. All structures were optimized and characterized as energy minima or transition states (TS) at the M06-2X<sup>15</sup>/6-31G(d) level. The energies were then refined by M06-2X/6-311+G(d,p) single-point calculations including solvation effects of

dichloromethane accounted for by the SMD<sup>16</sup> model. The M06-2X hybrid functional has been previously shown to achieve good accuracy for calcium-based systems.<sup>4c,e</sup> The refined single-point energies were then corrected to enthalpies and free energies at 1 atm and 293.15 K or 323.15 K using the gas phase M06-2X/6-31G(d) harmonic frequencies. We confirmed transition state structures by intrinsic reaction coordinate (IRC) calculations<sup>17</sup> to connect the correct reactant/product and intermediates on the potential energy surface (PES). The values presented are  $\Delta G_{293.15}$  (kcal mol<sup>-1</sup>) or  $\Delta G_{323.15}$  (kcal mol<sup>-1</sup>). The most significant three-dimensional structures are illustrated with CYLview.<sup>18</sup>

## 4.4. Results and Discussion

### 4.4.1. Mechanism of the Calcium(II)-Catalyzed Alkenylation of Allylbenzyl Alcohol 1a with (*E*)-Styrylboronic Acid 2a

#### 4.4.1.1. Activation of the Hydroxy Group by Calcium (*S<sub>N</sub>I*)

The feasibility of the above proposed mechanism (**Scheme 4.3**, (i)) was first examined (**Figure 4.1**). There are two reaction zero points considering that both Ca(NTf<sub>2</sub>)<sub>2</sub> and Ca(NTf<sub>2</sub>)(PF<sub>6</sub>) can be active catalysts depending on the use of *n*Bu<sub>4</sub>NPF<sub>6</sub> as additive.

The connection between these two profiles can be obtained from the free energy of the formation of Ca(NTf<sub>2</sub>)(PF<sub>6</sub>) from Ca(NTf<sub>2</sub>)<sub>2</sub> and *n*Bu<sub>4</sub>NPF<sub>6</sub>, which is 5.7 kcal mol<sup>-1</sup>.

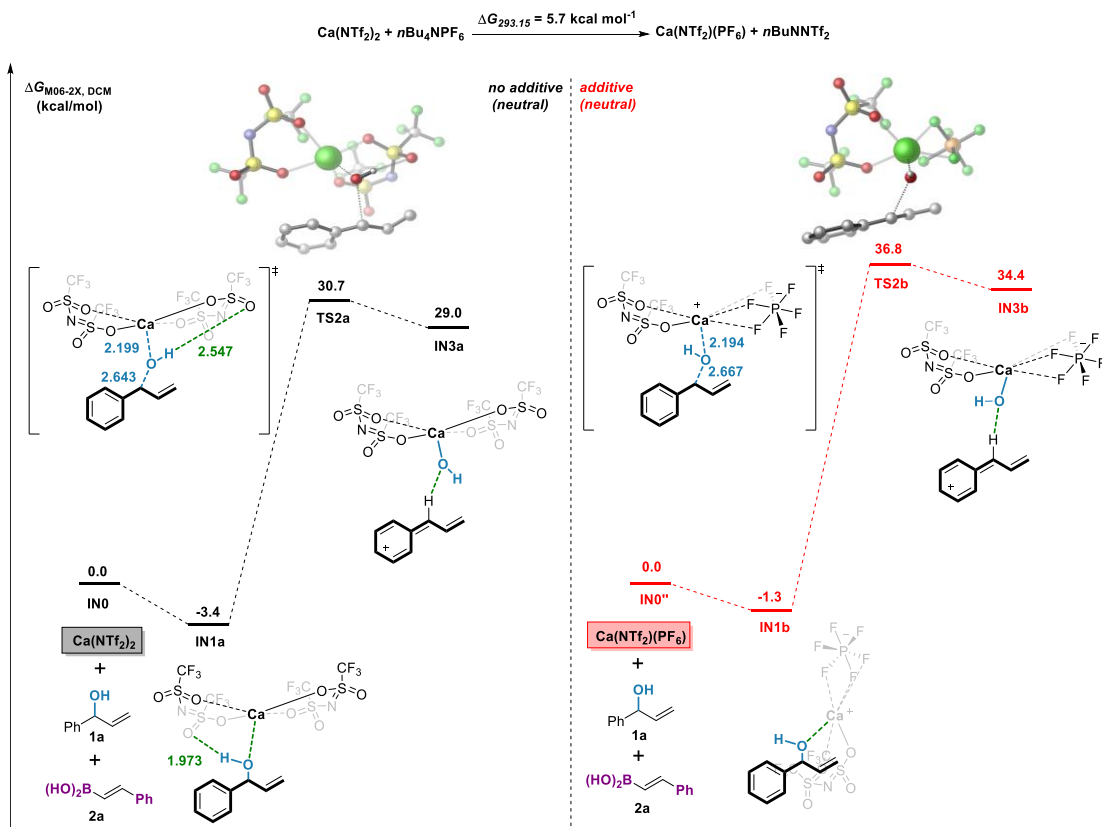


**Figure 4.1.** Free energy profile (kcal mol<sup>-1</sup>) for the calcium-mediated hydroxy group abstraction. Selected distances in Å.

The coordination of the hydroxy group of alcohol **1a** to Ca(NTf<sub>2</sub>)<sub>2</sub> to provide complex **IN1a** is exergonic by 3.4 kcal mol<sup>-1</sup>. There is a hydrogen bond between one sulfonyl oxygen and the OH group (S=O···H–O 1.973 Å) which disappears in the subsequent transition state (TS) and product. The cleavage of the C–O bond must overcome a barrier of 34.1 kcal mol<sup>-1</sup> through transition state **TS2a**. This process is markedly endergonic by 32.4 kcal mol<sup>-1</sup> (**IN3a**). In spite of its stronger Lewis acidity (**Scheme 4.1**, eq 2), Ca(NTf<sub>2</sub>)(PF<sub>6</sub>) leads to an even higher barrier of 38.1 kcal mol<sup>-1</sup> from **IN1b** to provide **IN3b** in a strongly endergonic fashion (34.4 kcal mol<sup>-1</sup>). With such high free energies of activation, this type of S<sub>N</sub>1 mechanism was not considered any further.

#### 4.4.1.2. Activation of the Hydroxy Group by (*E*)-Styrylboronic Acid (*S<sub>N</sub>1*)

Next, we evaluated a pathway corresponding to (ii) in **Scheme 4.3 (Figure 4.2)**. The activation free energies of the hydroxy abstraction are 61.5 kcal mol<sup>-1</sup> (TS2c) and 70.9 kcal mol<sup>-1</sup> (TS2d) with Ca(NTf<sub>2</sub>)<sub>2</sub> and Ca(NTf<sub>2</sub>)(PF<sub>6</sub>), respectively. This is, therefore, a very unlikely mechanism.

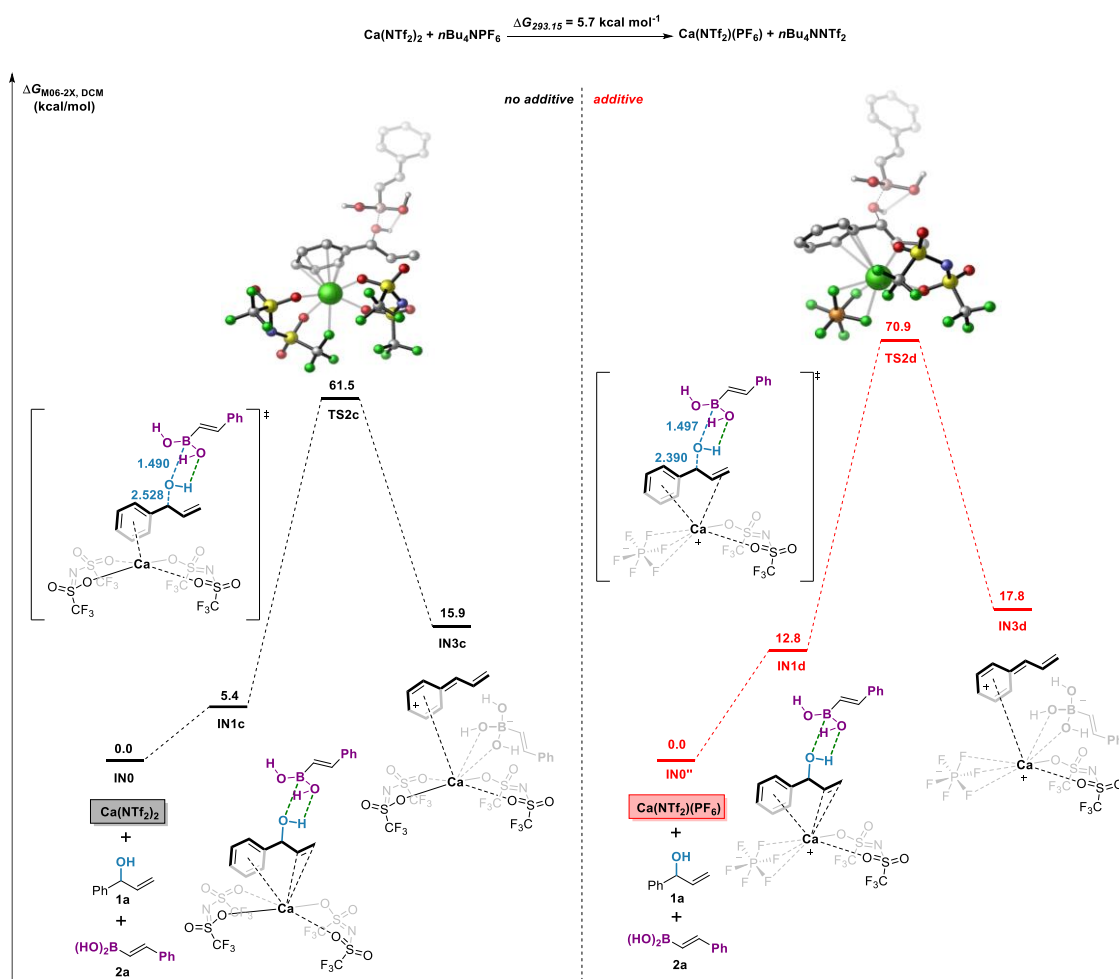


**Figure 4.2.** Free energy profile (kcal mol<sup>-1</sup>) for (*E*)-styrylboronic acid-mediated hydroxy group abstraction. Selected distances in Å.

#### 4.4.1.3. Attempted Hydroxy Group Activation by the Two Lewis Acids (Ca/B)

According to pathway (iii) proposed in **Scheme 4.3**, we studied the dual activation of the hydroxy group by the calcium complex and the vinylboronic acid. However, it was

not possible to accommodate the two Lewis acids on the same oxygen donor atom. The species converged as **IN1** (see **Figure 4.3**) in which calcium is coordinated to an OH group of the boronic acid, leading to the following discussion (Section 4.4.1.4).

#### 4.4.1.4. Lewis Acid Activation of the Boronic Acid (Ca/B; formal $S_N2'$ )

The formation of **IN1** from  $\text{Ca}(\text{NTf}_2)_2$ , **1a** and **2a** is exergonic by 1.0 kcal mol<sup>-1</sup> (**Figure 4.3**). Two oxygen atoms of **2a** are coordinated to the calcium center. The oxygen atom of **1a** is coordinated by the boron center and is bound to the calcium salt through a hydrogen bond involving the  $\text{NTf}_2^-$  counterion ( $\text{S}=\text{O}\cdots\text{H}-\text{O}$  1.889 Å). Trying to cleave the C–O bond of **1a** actually led to the concomitant formation of a C–C bond through the six-membered ring transition state **TS2**, which requires a reasonable activation energy of 20.2 kcal mol<sup>-1</sup> relatively to **IN1**.

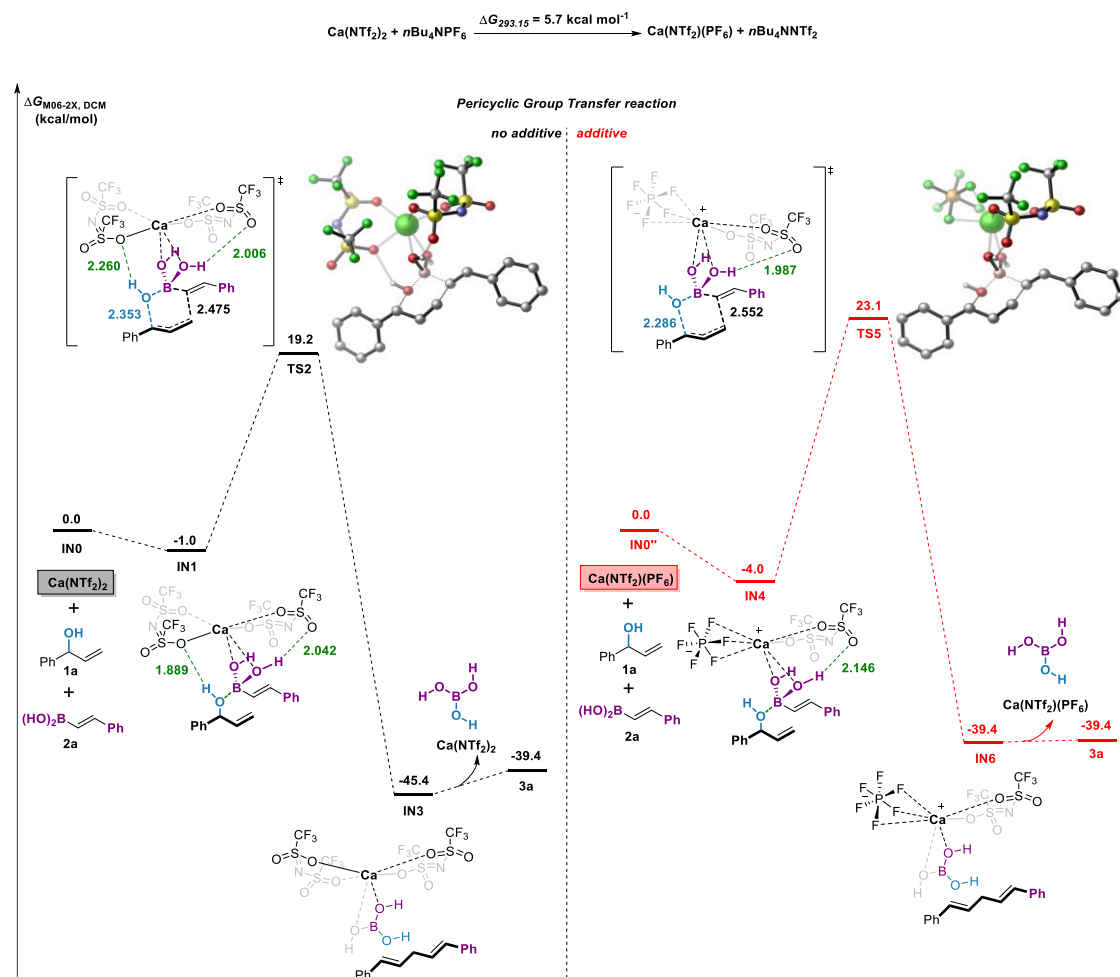


**Figure 4.3.** Free energy profile ( $\text{kcal mol}^{-1}$ ) for the concerted Ca/B-mediated hydroxy group abstraction/vinylation. Selected distances in Å.

This process is markedly exergonic by  $44.4 \text{ kcal mol}^{-1}$  and gives **IN3**. Elimination of  $\text{B(OH)}_3$  and  $\text{Ca(NTf}_2)_2$  finally leads to the final product **3a** lying at  $-39.4 \text{ kcal mol}^{-1}$ .

At this stage, two important features are worth emphasizing:

1– The geometry of **TS2** and the FMO analysis of its fragment clearly shows that it corresponds to a **pericyclic suprafacial/suprafacial group transfer reaction** (Figure 4.4).<sup>19</sup> To the best of our knowledge, such a group transfer reaction has not been described before.

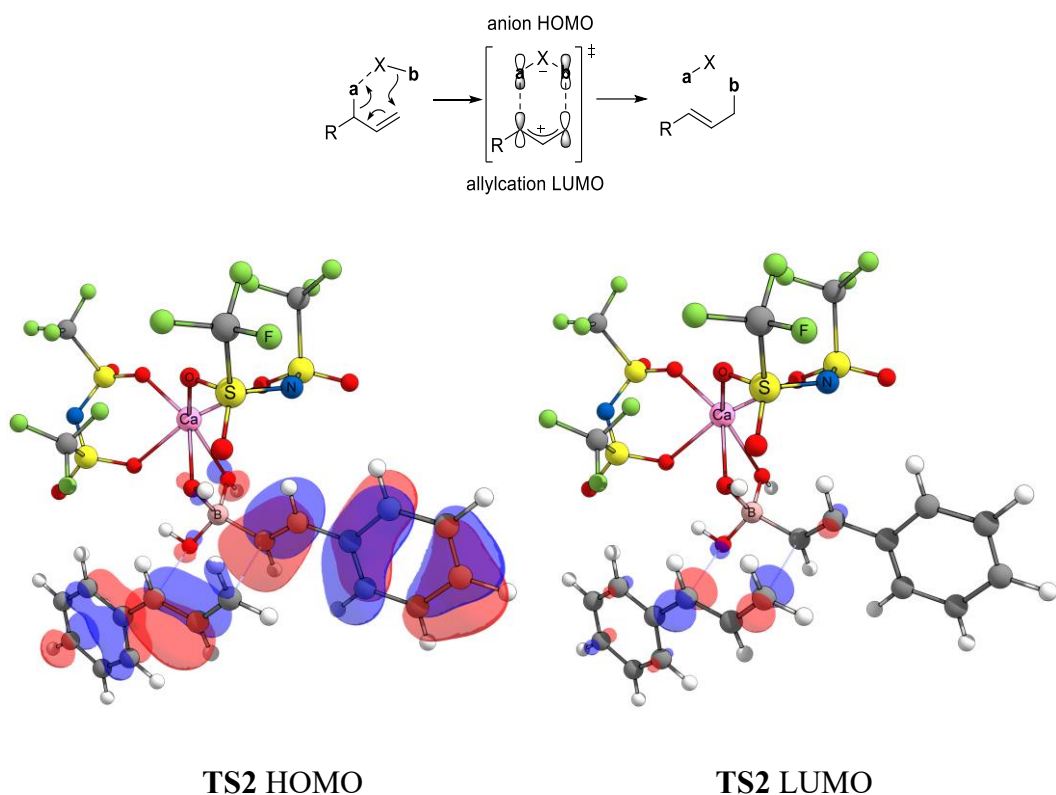
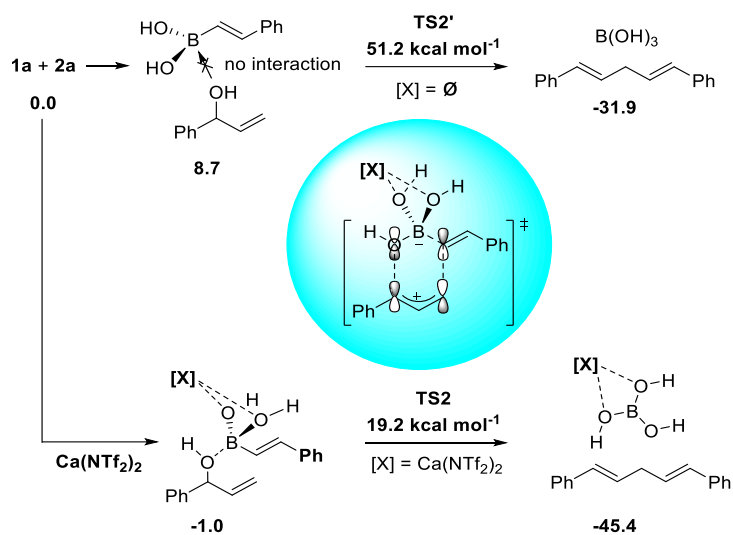


**Figure 4.4.** Prototype of the pericyclic group transfer reaction and FMO analysis of **TS2**.

2– In the absence of  $\text{Ca(NTf}_2)_2$ , the barrier to reach the same kind of six-membered ring

transition state becomes  $51.2 \text{ kcal mol}^{-1}$  (**Scheme 4.4**), which reveals the crucial role of the catalyst in activating the boron Lewis acid. The interaction between **1a** and **2a** cannot even be modeled if the calcium is not bound to the OH groups of the boronic acid (virtually planar  $\text{RB(OH)}_2$  moiety vs pyramidal boron center in **IN1**), showing that its role is to strengthen the electrophilicity of the boron reagent.



**Scheme 4.4.** Effect of calcium coordination to the boronic acid on the pericyclic group transfer reaction.

With the  $\text{Ca(NTf}_2)(\text{PF}_6)$  species, in agreement with the experimental results, the barrier to reach the same kind of six-membered ring transition state is markedly higher (**Figure 4.3**, right). The free energy difference between **IN4** and **TS5** is  $27.1 \text{ kcal mol}^{-1}$ , versus  $20.2 \text{ kcal mol}^{-1}$  with  $\text{Ca(NTf}_2)_2$ . Of note, inverting the position of the  $\text{PF}_6^-$  and the  $\text{NTf}_2^-$  ions led to an even higher-lying transition state ( $30.8 \text{ kcal mol}^{-1}$  instead of  $27.1 \text{ kcal mol}^{-1}$ , see **Figure 4.5**).

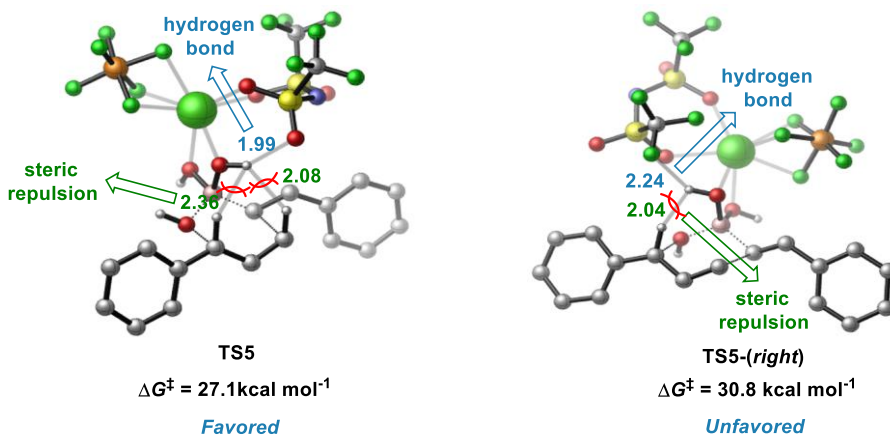


**Figure 4.5.** Optimized TSs for with  $\text{PF}_6^-$  pointing *left* or *right*- . Selected distances in Å.

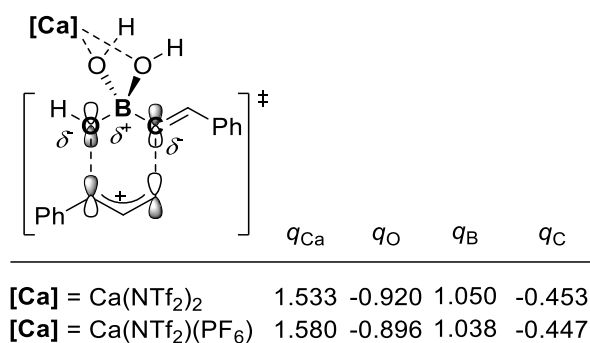


**Figure 4.6.** NPA charges of TS2 ( $[\text{Ca}] = \text{Ca}(\text{NTf}_2)_2$ ) and TS5 ( $[\text{Ca}] = \text{Ca}(\text{NTf}_2)(\text{PF}_6^-)$ ).

We have carefully analyzed the hydrogen bonds between the  $\text{NTf}_2^-$  oxygen atoms and the various OH groups of the two substrates (**1a** and **2a**). The strongest ones are indicated in **Figure 4.3**. Even though there are less possibilities of such noncovalent interactions with the  $\text{Ca}(\text{NTf}_2)(\text{PF}_6^-)$  fragment compared to  $\text{Ca}(\text{NTf}_2)_2$ , we could not explain the difference of efficiency between these two active species on the basis of hydrogen bonding. With the more electrophilic  $\text{Ca}(\text{NTf}_2)(\text{PF}_6^-)$  species, the coordinated boronic acid is also more electrophilic and this facilitates the OH abstraction, as shown by the shortest breaking C–O bond in **TS5** compared to **TS2** (2.286 vs 2.353 Å). However, the nucleophilicity of the vinyl group is also a crucial factor. With a more electrophilic calcium activator, the vinyl group will be less nucleophilic. This transpires

in the geometry of the transitions states as well, the forming C–C being longer in **TS5** than in **TS2** (2.552 vs 2.475 Å). The natural charges confirm this trend (**Figure 4.6**), with for instance the  $q_C$  charge which is more negative with  $\text{Ca}(\text{NTf}_2)_2$  than with  $\text{Ca}(\text{NTf}_2)(\text{PF}_6)$  (-0.453 vs -0.447 e). Thus, the right balance must be found to efficiently activate the boronic acid while maintaining its nucleophilicity. This is why the reaction of **1a** with **2a** is more efficient with  $\text{Ca}(\text{NTf}_2)_2$  than with  $\text{Ca}(\text{NTf}_2)(\text{PF}_6)$ . The fact that the reaction does not obey a  $S_{\text{N}}1$  mechanism but a concerted group transfer explains why a less electrophilic activator is a better option in this case.

#### **4.4.2. Mechanism of the Calcium(II)-Catalyzed Alkenylation of 3-Hydroxyisoindolinone **1a'** with (*E*)-Styrylboronic Acid **2a****

##### *4.4.2.1. Activation of the Hydroxy Group by Calcium ( $S_{\text{N}}1$ )*

The temperature of the reaction such as that shown in **Scheme 4.2** (Eq 4) is 50 °C. At that temperature, the anion metathesis requires a free energy of 5.5 kcal mol<sup>-1</sup> (**Figure 4.7**). Similarly to the results obtained in the first section, OH abstraction faces very high barriers: 34.8 kcal mol<sup>-1</sup> with  $\text{Ca}(\text{NTf}_2)_2$ ; 36.1 kcal mol<sup>-1</sup> with  $\text{Ca}(\text{NTf}_2)(\text{PF}_6)$ . The  $S_{\text{N}}1$  mechanism is therefore also ruled out for 3-hydroxyisoindolinone.

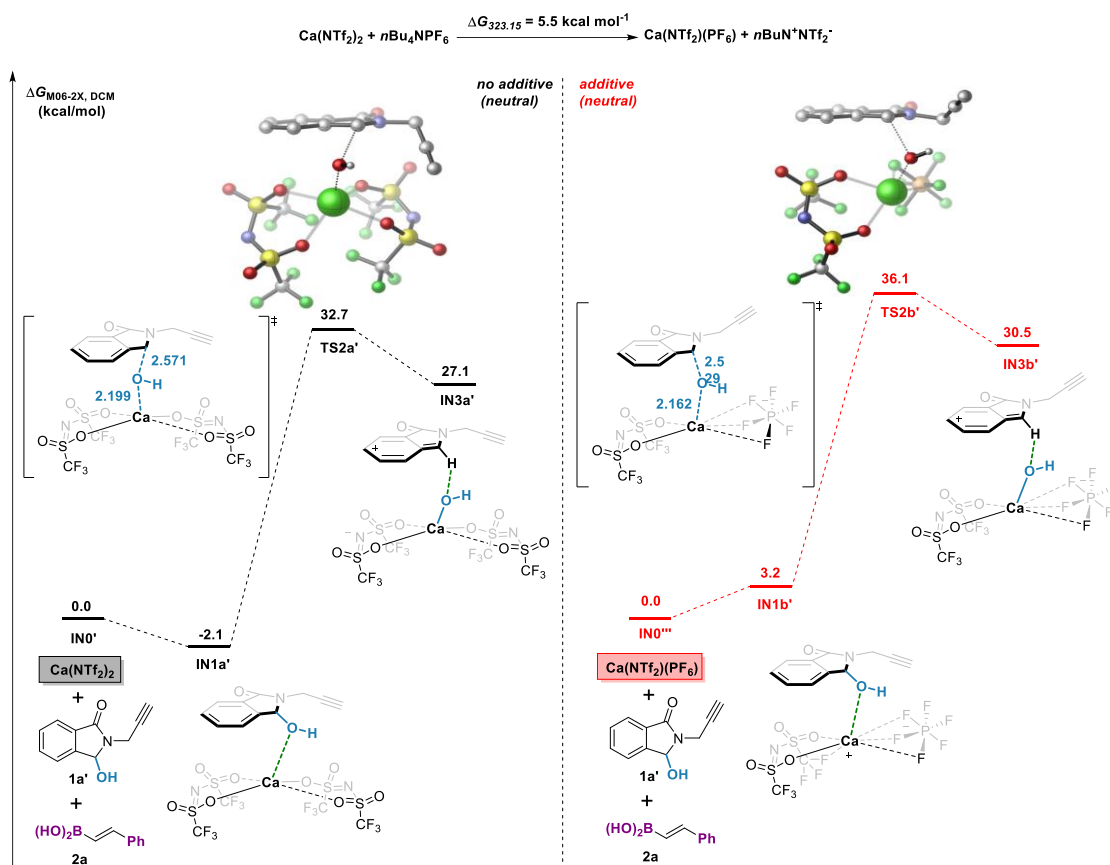


**Figure 4.7.** Free energy profile ( $\text{kcal mol}^{-1}$ ) for the calcium-mediated hydroxy group abstraction. Selected distances in Å.

#### 4.4.2.2. Activation of the Hydroxy Group by (*E*)-Styrylboronic Acid ( $S_N1$ )

Due to the very large barriers computed in Section 4.4.1.2, this type of activation was not studied.

#### 4.4.2.3. Hydroxy Group Activation by the Two Lewis Acids (Ca/B; $S_N1$ )

Again, it was not possible to accommodate the two metals on the OH group of the substrate.

#### 4.4.2.4. Lewis Acid Activation of the Boronic Acid (Ca/B; $S_N1$ )

Coordination of 3-hydroxyisoindolinone **1a'** and (*E*)-styrylboronic acid **2a** to calcium

center provides complex **IN1'**, lying 2.0 kcal mol<sup>-1</sup> below the reactants **IN0'** (**Figure 4.8**). There is not interaction between the OH group of **1a'** and the boron center at this stage, but while the C–O bond breaks, the OH group directly migrates to boron and not to calcium. This step through **TS2'** requires a free energy of activation of 21.1 kcal mol<sup>-1</sup> from **IN1'** and is endergonic by 14.6 kcal mol<sup>-1</sup>. The vinyl group is then delivered from the intimate ion pair **IN3'** to **IN5'** in a strongly exergonic fashion. The corresponding transition state **TS4'** culminates at 28.2 kcal mol<sup>-1</sup> on the free energy surface. Finally, the Ca(NTf<sub>2</sub>)<sub>2</sub> is regenerated with concomitant release of B(OH)<sub>3</sub> and product **3a'**, which is 31.0 kcal mol<sup>-1</sup> below the reactants. Overall, this process needs to overcome an energy barrier as high as 30.2 kcal mol<sup>-1</sup>, which is consistent with the experimental results in which no product was observed (**Scheme 4.2**, Eq 4). On the other hand, 92% yield was obtained with the use of *n*Bu<sub>4</sub>NPF<sub>6</sub>. The corresponding mechanism is shown by the red line in **Figure 4.8**. Coordination of 3-hydroxyisoindolinone **1a'** and (*E*)-styrylboronic acid **2a** to the calcium center is slightly endergonic, placing the resulting intermediate **IN6'** at 3.9 kcal mol<sup>-1</sup> on the free energy surface. Hydroxy group migration to boron to generate the ion pair **IN8'** is achieved through **TS7'**. This step needs to cross an energy barrier of 22.2 kcal mol<sup>-1</sup> relatively to **IN0''**. Then, the nucleophilic addition occurs through **TS9'**, located at 25.0 kcal mol<sup>-1</sup> on the free energy surface (vs 28.2 kcal mol<sup>-1</sup> for **TS4'**). We have also considered other possible hydroxy and counterions orientation, but the corresponding activation energies of these nucleophilic additions were significantly higher (see **Figure 4.9**). Finally, the Ca(NTf<sub>2</sub>)(PF<sub>6</sub>) is regenerated with concomitant release of the desired product **3a'** and B(OH)<sub>3</sub>. Thus, the best computed mechanism of the vinylation of 3-hydroxyisoindolinones is a **substitution nucleophilic intramolecular (Sni)** going through an ion pair. In such processes, the leaving group and the nucleophile are exchanged on the same side of the substrate.

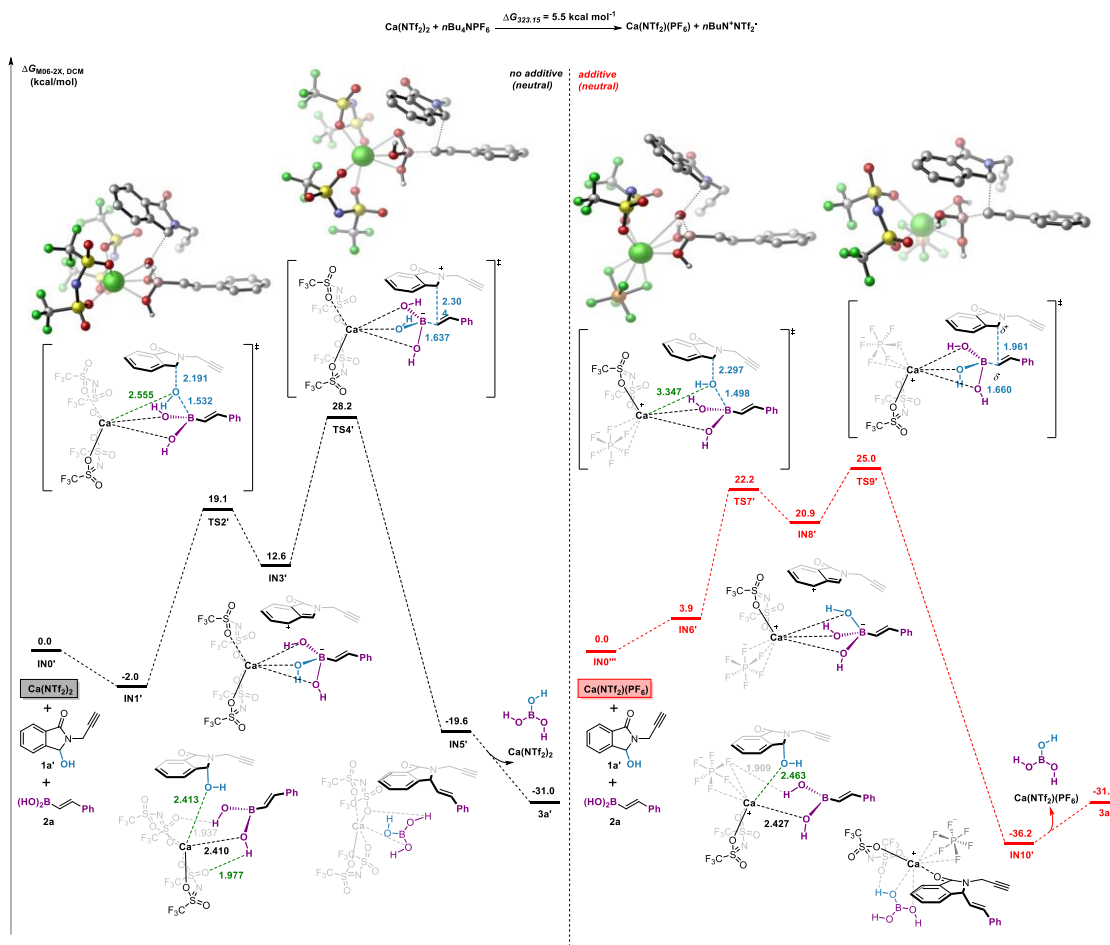


**Figure 4.8.** Free energy profile ( $\text{kcal mol}^{-1}$ ) for the Ca/B-mediated hydroxy group abstraction of **1a'**.

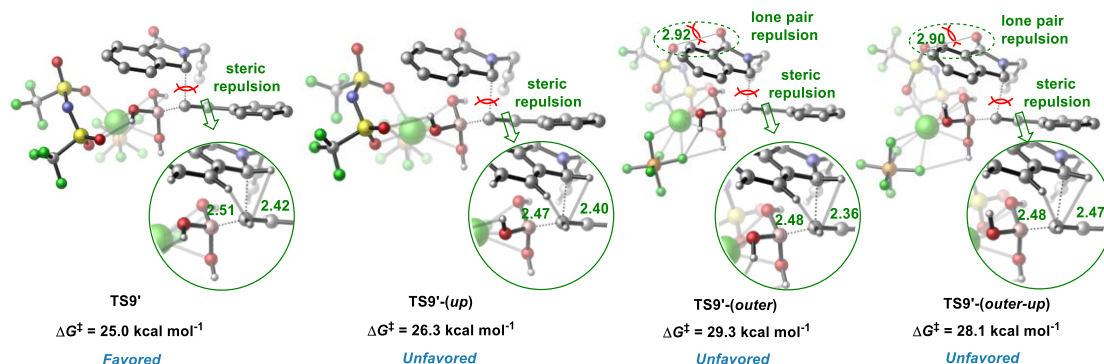


**Figure 4.9.** Optimized TSs for hydroxy pointing *down* or *up*- and with  $\text{PF}_6^-$  pointing *inward* or *outward*. Selected distances in Å.

To understand the better reactivity conferred by  $\text{Ca}(\text{NTf}_2)(\text{PF}_6)$  compared to  $\text{Ca}(\text{NTf}_2)_2$ ,

we have used the Global Nucleophilicity ( $N$ ) proposed by Domingo et al.<sup>20</sup> but no significant difference could be found (see **Figure 4.10**). On the other hand, noncovalent interactions analysis (NCIs)<sup>21</sup> of the nucleophilic addition transition states **TS4'** and **TS9'** proved relevant (**Figure 4.11**). There is a lone pair repulsion between the oxygen of  $\text{NTf}_2^-$  ion and the oxygen atom of the isoindolinone cation in transition state **TS4'**, which explains why this structure is more difficult to reach compared to **TS9'**. The proximity between the two oxygen atoms is imposed by the large size of the  $\text{NTf}_2^-$  ion. With the smaller  $\text{PF}_6^-$  counterion, the  $\text{NTf}_2^-$  is far from the carbonyl group.

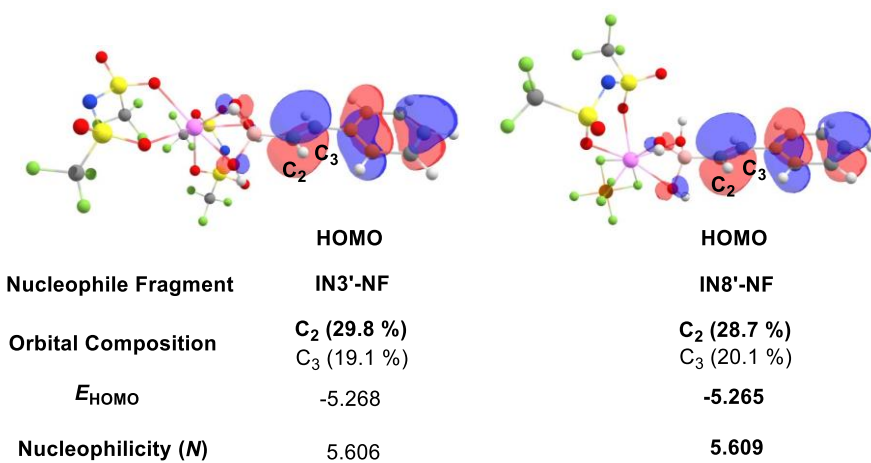


**Figure 4.10.** Frontier molecular orbitals (FMO) and Nucleophilicity ( $N$ , eV;  $N_{\text{Nu}} = E_{\text{HOMO(Nu)}} - E_{\text{HOMO(TCE)}}$ , TCE = Tetracyanoethylene) values for nucleophile fragment of key intermediates (contour value: 0.03)

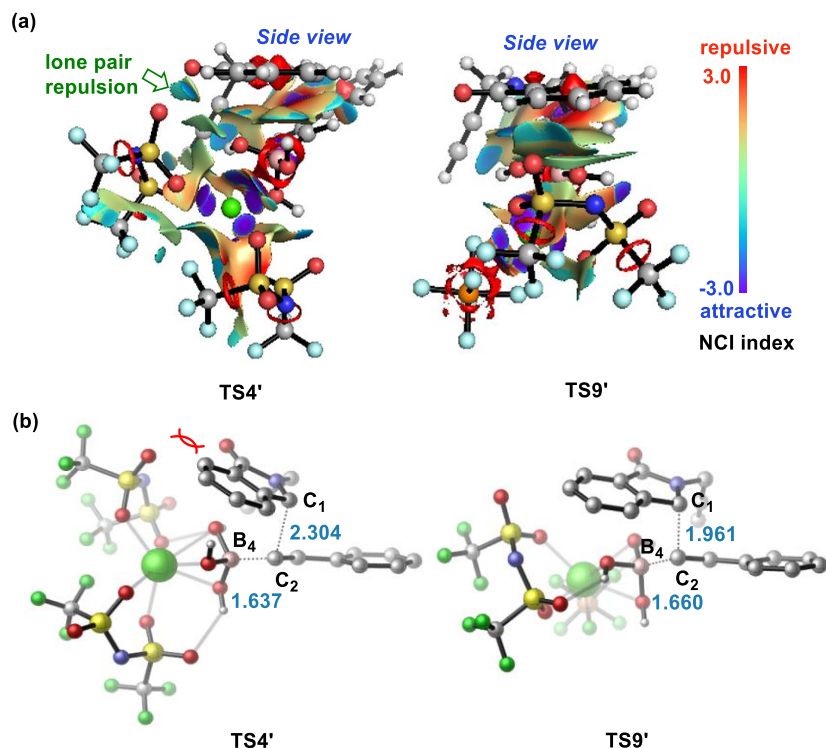
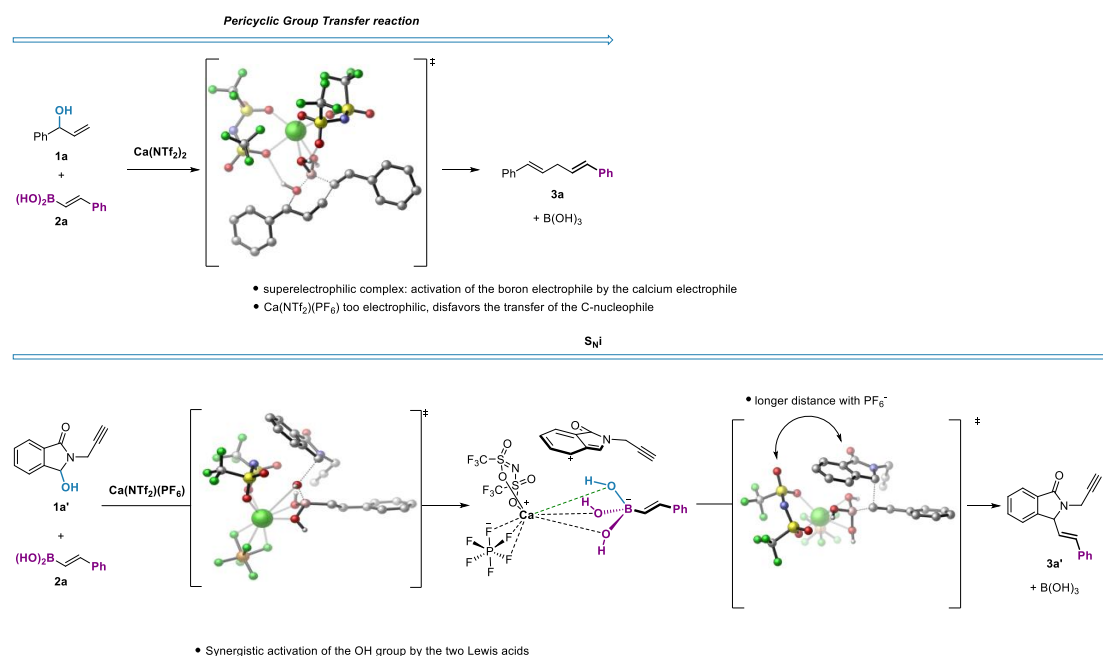


**Figure 4.11.** (a) Non-covalent interactions analysis of **TS4'** and **TS9'** (blue, strongly attractive; green, weakly attractive; red, strongly repulsive). (b) Optimized structure of the two transition states. Selected distances in Å.

## 4.5. Conclusions

The proposed mechanisms of the calcium(II)-catalyzed coupling of alcohols with vinylboronic acids are summarized in **Scheme 4.5**. For the reaction of allyl alcohols, the calculations favored a pericyclic group transfer reaction in which the calcium and the boron Lewis acids form a superelectrophilic complex. The reason why  $\text{Ca}(\text{NTf}_2)_2$  is better than  $\text{Ca}(\text{NTf}_2)(\text{PF}_6)$  is attributed to a better electronic balance. In the transition state, the activated boron is rendered electrophilic enough abstract the OH group of the alcohol but the nucleophilicity of the vinyl group should not be too much affected. Since  $\text{Ca}(\text{NTf}_2)_2$  is a weaker Lewis acid than  $\text{Ca}(\text{NTf}_2)(\text{PF}_6)$ , its counterion combination represents the best compromise. For alcohols for which a concerted mechanism is no longer possible, such as 3-hydroxyisoindolinones, the DFT study supported a  $\text{S}_{\text{Ni}}$ -type

reaction. The abstraction of the OH group is facilitated by a synergistic activation by the two Lewis acids. Rather than an electronic tuning provided by the counterion, we found that the better activity of the  $\text{Ca}(\text{NTf}_2)(\text{PF}_6)$  species was due to the smaller size of the  $\text{PF}_6^-$  ion compared to  $\text{NTf}_2^-$ , which allows to avoid a pair repulsion between one of the  $\text{NTf}_2^-$  oxygen and the carbonyl group of the substrate. Overall, this study sheds light on the cooperativity between two Lewis acids in catalysis and on the counterion effects in such coupling reactions.



**Scheme 4.5.** Proposed mechanisms of the calcium(II)-catalyzed coupling of alcohols with vinylboronic acids.

## 4.6. References

- For reviews on Ca(II) catalysis, see: (a) Begouin, J.-M.; Niggemann, M. Calcium-Based Lewis Acid Catalysts. *Chem. Eur. J.* **2013**, *19*, 8030–8041. (b) Lebœuf, D.; Gandon, V. Carbon-Carbon and Carbon-Heteroatom Bond-Forming Transformations Catalyzed by Calcium(II) Triflimide. *Synthesis* **2017**, *49*, 1500–1508. (c) Rauser, M.; Schröder, S.; Niggemann, M. In *Early Main Group Metal Lewis Acid Catalysis: Concepts and Reactions*; Harder, S., Ed.; Wiley-VCH, **2020**, pp 279–310. (d) Kobayashi, S.;

Yamashita, Y. Alkaline Earth Metal Catalysts for Asymmetric Reactions. *Acc. Chem. Res.* **2011**, *44*, 58–71. (e) Harder, S. From Limestone to Catalysis: Application of Calcium Compounds as Homogeneous Catalysts. *Chem. Rev.* **2010**, *110*, 3852–3876.

2 For selected examples of alcohol activation, see: (a) Niggemann, M.; Meel, M. J. Calcium-Catalyzed Friedel-Crafts Alkylation at Room Temperature. *Angew. Chem. Int. Ed.* **2010**, *49*, 3684–3687. (b) Haven, T.; Kubik, G.; Haubenreisser, S.; Niggemann, M. Calcium-Catalyzed Cyclopropanation. *Angew. Chem. Int. Ed.* **2013**, *52*, 4016–4019. (c) Wang, S.; Guillot, R.; Carpentier, J.-F.; Sarazin, Y.; Bour, C.; Gandon, V.; Leboeuf, D. Synthesis of Bridged Tetrahydrobenzo[b]azepines and Derivatives through an Aza-Piancatelli Cyclization/Michael Addition Sequence. *Angew. Chem. Int. Ed.* **2020**, *59*, 1134–1138.

3 See inter alia: (a) Yaragorla, S.; Rajesh, P; Pareek, A.; Kumar, A. Ca(II)-Mediated Regioselective One-Pot Sequential Annulation of Acyclic compounds to Polycyclic Fluorenopyrans. *Adv. Synth. Catal.* **2018**, *360*, 4422–4428. (b) Yaragorla, S.; Dada, R.; Rajesh, P.; Sharma, M. Highly Regioselective Synthesis of Oxindolyl-Pyrroles and Quinolines via a One-Pot, Sequential Meyer–Schuster Rearrangement, Anti-Michael Addition/C(sp<sup>3</sup>)–H Functionalization, and Azacyclization. *ACS Omega* **2018**, *3*, 2934–2946.

4 For selected examples: (a) Haubenreisser, S.; Hensenne, P.; Schröder, P. Niggemann, M. *Org. Lett.* **2013**, *15*, 2262–2265. (b) Davies, J.; Leonori, D. The First Calcium-Catalysed Nazarov Cyclisation. *Chem. Commun.* **2014**, *50*, 15171–15174. (c) Qi, C.; Hasenmaile, F.; Gandon, V.; Leboeuf, D. Calcium(II)-Catalyzed Intra- and Intermolecular Hydroamidation of Unactivated Alkenes in Hexafluoroisopropanol. *ACS Catal.* **2018**, *8*, 1734–1739. (d) Qi, C.; Gandon, V.; Leboeuf, D. Calcium(II)-Catalyzed Intermolecular Hydroarylation of Deactivated Styrenes in Hexafluoroisopropanol. *Angew. Chem. Int. Ed.* **2018**, *57*, 14245–14249. (e) Qi, C.; Yang, S.; Gandon, V.; Leboeuf, D. Calcium(II)- and Triflimide-Catalyzed Intramolecular Hydroacyloxylation of Unactivated Alkenes in Hexafluoroisopropanol. *Org. Lett.* **2019**, *21*, 7405–7409. (f) Wang, S.; Force, G.; Guillot, R.; Carpentier, J.-F.; Sarazin, Y.; Bour, C.; Gandon, V.; Leboeuf, D. Lewis Acid/Hexafluoroisopropanol: A Promoter System for Selective ortho-C-Alkylation of Anilines with Deactivated Styrene Derivatives and Unactivated Alkenes. *ACS Catal.* **2020**, *10*, 10794–10802.

5 Xue, L.; DesMarteaum, D. D.; Pennington, W. T. Synthesis and Structures of Alkaline Earth Metal Salts of bis[(Trifluoromethyl)sulfonyl]imide. *Solid State Sciences* **2005**, *7*, 311–318.

6 Haubenreisser, S.; Niggemann, M. Calcium-Catalyzed Direct Amination of  $\pi$ -Activated Alcohols. *Adv. Synth. Catal.* **2011**, *353*, 469–474.

7 (a) Lebœuf, D.; Presset, M.; Michelet, B.; Bour, C.; Bezzenine-Lafollée, S.; Gandon, V. Ca(II)-Catalyzed Alkenylation of Alcohols with Vinylboronic Acids. *Chem. Eur. J.* **2015**, *21*, 11001–11005. (b) Qi, C.; Gandon, V.; Leboeuf, D. Calcium(II)-Catalyzed Alkenylation of N-Acyliminiums and Related Ions with Vinylboronic Acids. *Adv. Synth. Catal.* **2017**, *359*, 2671–2675.

8. For previous computational studies on calcium-catalyzed reactions, see refs 4c–4d4e4f and: (a) Wu, X.; Zhao, L.; Jin, J.; Pan, S.; Li, W.; Jin, X.; Wang, G.; Zhou, M.; Frenking, G. Observation of Alkaline Earth Complexes  $M(CO)_8$  ( $M = Ca$ , Sr, or Ba) that Mimic Transition Metals. *Science* **2018**, *361*, 912–916. (b) Bauer, H.; Alonso, M.; Färber, C.; Elsen, H.; Pahl, J.; Causero, A.; Ballmann, G.; De Proft, F.; Harder, S. Imine hydrogenation with simple alkaline earth metal catalysts. *Nat. Catal.* **2018**, *1*, 40–47.

9 (a) Bandini, M.; Cera, G.; Chiarucci, M. Catalytic Enantioselective Alkylation with Allylic Alcohols. *Synthesis* **2012**, *44*, 504–512. (b) Pigge, F. C. Metal-Catalyzed Allylation of Organoboranes and Organoboronic acids. *Synthesis* **2010**, *11*, 1745–1762. (c) Norsikian, S.; Chang, C. W. Control of the Regioselectivity in Palladium(0)-Catalyzed Allylic Alkylation. *Curr. Org. Synth.*, **2009**, *6*, 264–289. (d) Trost, B. M.; Van Vranken, D. L. Asymmetric Transition Metal-Catalyzed Allylic Alkylation. *Chem. Rev.* **1996**, *96*, 395–422.

10 (a) Ye, J.; Zhao, J.; Xu, J.; Mao, Y.; Zhang, Y. J. Pd-Catalyzed Stereospecific Allyl–Aryl Coupling of Allylic Alcohols with Arylboronic Acids. *Chem. Commun.* **2013**, *49*, 9761–9763. (b) Wu, H. B.; Ma, X. T.; Tian, S. K. Palladium-Catalyzed Stereospecific Cross-Coupling of Enantioenriched Allylic Alcohols with Boronic Acids. *Chem. Commun.* **2014**, *50*, 219–221.

11 Pozhydaiev, V.; Power, M.; Gandon, V.; Moran, J.; Lebœuf, D. Exploiting Hexafluoroisopropanol (HFIP) in Lewis and Brønsted Acid-Catalyzed Reactions. *Chem. Commun.* **2020**, *56*, 11548–11564.

12 (a) Negishi, E. Principle of Activation of Electrophiles by Electrophiles through Dimeric Association—Two Are Better than One. *Chem. Eur. J.* **1999**, *5*, 411–420. (b) Olah, G. A. Superelectrophiles. *Angew. Chem. Int. Ed.* **1993**, *32*, 767–788. (c) Olah, G. A.; Klumpp, D. A. *Superelectrophiles and Their Chemistry*. Wiley-VCH Verlag GmbH & Co. KGaA 2007. (d) Klumpp, D.

A.; Anokhin, M. V. Superelectrophiles: Recent Advances. *Molecules* **2020**, *25*, 3281–3306.

13 For recent studies on the role of superelectrophiles in homogeneous catalysis, see: a) Albright, H.; Riehl, P. S.; McAtee, C. C. Reid, J. P.; Ludwig, J. R.; Karp, L. A.; Zimmerman, P. M.; Sigman, M. S.; Schindler, C. S. Catalytic Carbonyl-Olefin Metathesis of Aliphatic Ketones: Iron (III) Homodimers as Lewis Acidic Superelectrophiles. *J. Am. Chem. Soc.* **2019**, *141*, 1690–1700. b) Djurovic, A.; Vayer, M.; Li, Z.; Guillot, R.; Baltaze, J.-P.; Gandon, V.; Bour, C. Synthesis of Medium-Sized Carbocycles by Gallium-Catalyzed Tandem Carbonyl-Olefin Metathesis/Transfer Hydrogenation. *Org. Lett.* **2019**, *21*, 8132–8137. c) Albright, H.; Vonesh, H. L.; Schindler, C. S. Superelectrophilic Fe(III)-Ion Pairs as Stronger Lewis Acid Catalysts for (*E*)-Selective Intermolecular Carbonyl-Olefin Metathesis. *Org. Lett.* **2020**, *22*, 3155–3160. d) Yang, S.; Bour, C.; Gandon, V. Superelectrophilic Gallium(III) Homodimers in Gallium Chloride Mediated Methylation of Benzene: a Theoretical Study. *ACS Catal.* **2020**, *10*, 3027–3033. e) Davis, A. J.; Watson, R. B.; Nasrallah, D. J.; Gomez-Lopez, J. L.; Schindler, C. S. Superelectrophilic Aluminium(III)-Ion Pairs Promote a Distinct Reaction Path for Carbonyl-Olefin Ring-Closing Metathesis. *Nat. Catal.* **2020**, *3*, 787–796.

14 Frisch, M. J.; Trucks, G. W.; Schlegel, H. B.; Scuseria, G. E.; Robb, M. A.; Cheeseman, J. R.; Scalmani, G.; Barone, V.; Petersson, G. A.; Nakatsuji, H.; Li, X.; Caricato, M.; Marenich, A.; Bloino, J.; Janesko, B. G.; Gomperts, R.; Mennucci, B.; Hratchian, H. P.; Ortiz, J. V.; Izmaylov, A. F.; Sonnenberg, J. L.; Williams-Young, D.; Ding, F.; Lipparini, F.; Egidi, F.; Goings, J.; Peng, B.; Petrone, A.; Henderson, T.; Ranasinghe, D.; Zakrzewski, V. G.; Gao, J.; Rega, N.; Zheng, G.; Liang, W.; Hada, M.; Ehara, M.; Toyota, K.; Fukuda, R.; Hasegawa, J.; Ishida, M.; Nakajima, T.; Honda, Y.; Kitao, O.; Nakai, H.; Vreven, T.; Throssell, K.; Montgomery, J. A., Jr; Peralta, J. E.; Ogliaro, F.; Bearpark, M.; Heyd, J. J.; Brothers, E.; Kudin, K. N.; Staroverov, V. N.; Keith, T.; Kobayashi, R.; Normand, J.; Raghavachari, K.; Rendell, A.; Burant, J. C.; Iyengar, S. S.; Tomasi, J.; Cossi, M.; Millam, J. M.; Klene, M.; Adamo, C.; Cammi, R.; Ochterski, J. W.; Martin, R. L.; Morokuma, K.; Farkas, O.; Foresman, J. B.; Fox, D. J. *Gaussian 09*, Revision D.01, Gaussian, Inc.: Wallingford CT, 2016.

15 Zhao, Y.; Truhlar, D. G. The M06 Suite of Density Functionals for Main Group Thermochemistry, Thermochemical Kinetics, Noncovalent Interactions, Excited States, and Transition Elements. *Theor. Chem. Acc.* **2008**, *120*, 215–241.

- 16 Marenich, A. V.; Cramer, C. J.; Truhlar, D. G. Universal Solvation Model Based on Solute Electron Density and on a Continuum Model of the Solvent Defined by the Bulk Dielectric Constant and Atomic Surface Tensions. *J. Phys. Chem. B* **2009**, *113*, 6378–6396.
- 17 (a) Fukui, K. Formulation of the Reaction Coordinate. *J. Phys. Chem.* **1970**, *74*, 4161–4163. (b) Fukui, K. The Path of Chemical Reactions - the IRC Approach. *Acc. Chem. Res.* **1981**, *14*, 363–368.
- 18 Legault, C. Y. *CYLview, Version 1.0b*; Université de Sherbrooke, **2009** (available at: <http://www.cylview.org>).
- 19 Dinda, B. Group Transfer Reactions. *Essentials of Pericyclic and Photochemical Reactions. Lecture Notes in Chemistry*; Springer: Cham, 2017; Vol 93.
- 20 (a) Domingo, L. R.; Chamorro, E.; Perez, P. Understanding the Reactivity of Captodative Ethylenes in Polar Cycloaddition Reactions. A Theoretical Study. *J. Org. Chem.* **2008**, *73*, 4615–4624. (b) Domingo, L. R.; Perez, P. The Nucleophilicity N Index in Organic Chemistry. *Org. Biomol. Chem.* **2011**, *9*, 7168–7175. (c) Parr, R. G.; Szentpály, L. v.; Liu, S. Electrophilicity Index. *J. Am. Chem. Soc.* **1999**, *121*, 1922–1924. For a recent example of the use of the global nucleophilicity: (d) Liu, F.; Zhu, L.; Zhang, T.; Zhong, K.; Xiong, Q.; Shen, B.; Liu, S.; Lan, Y.; Bai, R. Nucleophilicity versus Brønsted Basicity Controlled Chemoselectivity: Mechanistic Insight into Silver- or Scandium-Catalyzed Diazo Functionalization. *ACS Catal.* **2020**, *10*, 1256–1263.
- 21 Johnson, E. R.; Keinan, S.; Mori-Sanchez, P.; Contreras-Garcia, J.; Cohen, A. J.; Yang, W. Revealing Noncovalent Interactions. *J. Am. Chem. Soc.* **2010**, *132*, 6498–6506.

## General Conclusion

This doctoral thesis has been meant to broaden our knowledge about the mechanisms involved in important main group metal-catalyzed organic transformations using computational chemistry. Many of the preceding theoretical studies reported in the literature have considered the active species as corresponding to its molecular formula, e.g.  $\text{MX}_3$  for simple salts such as  $\text{AlCl}_3$ . However, several  $\text{MX}_3$  units can associate to form in situ various unsuspected complexes, including singly bridged  $\text{M}_2\text{X}_6$  compounds, whose Lewis acidity is more pronounced than isolated  $\text{MX}_3$  molecules. Referred to as superelectrophiles, we have shown that they can play a crucial role in well-known reactions such as the Friedel-Crafts alkylation or the skeletal reorganization of enynes.

In addition, we have played our part in debates regarding the Friedel-Crafts reaction, including the fact that such transformations can be concerted, or that the Lewis acid does not activate the nucleophile.

Clearly, this work on the Friedel-Crafts reaction has taught us that the chlorine atoms are not innocent, as they participate in the formation of superelectrophilic species. Our work on the skeletal reorganization of enynes revealed that they also participate in the stabilization of important intermediates such as nonclassical carbocations. This finding was essential to understand why  $\text{GaCl}_3$  or  $\text{InCl}_3$ , which have no accessible empty d orbitals nor orbitals that can be engaged in back bonding, are yet able to catalyze enyne metathesis reactions just like late transition metal complexes do. This teamplay between the main group metal and the halogen ligand confers a similar reactivity to  $\text{MX}_3$  salts compared to gold or platinum complexes. This feature could be exploited in the future to develop new transition metal free reactions.

While the role of halide ligands has been shown to be fundamental in main group metal catalyzed Friedel-Crafts and cycloisomerization reactions, we have also carefully looked into the role of supposedly non-coordinating anions such as  $\text{NTf}_2^-$  or  $\text{PF}_6^-$ . Since

most of the literature available is about transition metal catalyzed reactions and not main group metal catalyzed ones, we may have a biased vision of the mechanisms and we must forget what we have learned. With main group *s* or *p* elements, oxidative additions or reductive eliminations are not viable routes. Likewise, the coordinating ability of a counterion is not the same for a transition metal or a main group one. In that respect, the study of a calcium-catalyzed cross coupling reaction was an edifying glimpse behind the scenes. Our calculations have delineated an unsuspected mechanism in which the counterions remain coordinated to the metal center and in which one Lewis acid activates another to ultimately allow the activation of the substrate. This journey was another source of inspiration for the development of other transition metal free reactions mimicked by the use of main group complexes as catalysts.

Due to the complexity of the studied systems, including the fact that the metals used are difficult to detect by NMR, or even quench the signals of the standard nuclei, all these precious pieces of mechanistic information could only be obtained through molecular modeling. This approach has proved to be very powerful, even if we have only used the implemented methods. To go further, it may become necessary to use non-standard methodologies that would provide a more dynamic picture of the reaction profiles, and I hope I will be able to participate in the development of such methods in the future.

## Publications List

*(Details are shown in Chapters 2, 3 and 4 of the thesis)*

1. **Shengwen Yang**, Christophe Bour, Vincent Gandon<sup>\*</sup> Superelectrophilic Gallium (III) Homodimers in Gallium Chloride-Mediated Methylation of Benzene: A Theoretical Study, *ACS Catal.* **2020**, *10*, 3027–3033.
2. **Shengwen Yang**, Aurélien Alix, Christophe Bour, Vincent Gandon<sup>\*</sup> Alkynophilicity of Group 13 MX<sub>3</sub> Salts: A Theoretical Study, *Inorg. Chem.* **2021**, *60*, 5507–5522.
3. **Shengwen Yang**, Christophe Bour, David Lebœuf, Vincent Gandon<sup>\*</sup> DFT Analysis into the Calcium(II)-Catalyzed Coupling of Alcohols With Vinylboronic Acids: Cooperativity of Two Different Lewis Acids and Counterion Effects. *J. Org. Chem.* **2021**, *86*, 9134–9144.

*(Collaborative work with experimentalists. Details are not shown in the thesis)*

4. Manash Protim Gogoi, Rajeshwer Vanjari, B. Prabagar, **Shengwen Yang**, Shubham Duttaa, Rajendra K. Mallicka, Vincent Gandon<sup>\*</sup> and Akhila K. Sahoo<sup>\*</sup> Yb(III)-catalysed syn-thioallylation of ynamides. *Chem. Commun.*, **2021**, *57*, 7521–7524
5. Zhilong Li, **Shengwen Yang**, Guillaume Thiery, Vincent Gandon<sup>\*</sup>, and Christophe Bour<sup>\*</sup> On the Superior Activity of In(I) versus In(III) Cations Toward ortho-C-Alkylation of Anilines and Intramolecular Hydroamination of Alkenes. *J. Org. Chem.* **2020**, *85*, 12947–12959.
6. Shubham Dutta, **Shengwen Yang**<sup>+</sup>, Rajeshwer Vanjari, Rajendra K. Mallick, Vincent Gandon<sup>\*</sup>, Akhila K. Sahoo<sup>\*</sup>, Keteniminium-Driven Umpolung Difunctionalization of Ynamides. *Angew. Chem. Int. Ed.* **2020**, *59*, 10785–10790.
7. Nicolas Glinsky-Olivier, **Shengwen Yang**, Pascal Retailleau, Vincent Gandon<sup>\*</sup>, and Xavier Guinchard<sup>\*</sup> Enantioselective Gold-Catalyzed Pictet–Spengler Reaction. *Org. Lett.* **2019**, *21*, 9446–9451.

8. Chenxiao Qi, **Shengwen Yang**, Vincent Gandon,<sup>\*</sup> and David Lebœuf<sup>\*</sup> Calcium(II)- and Triflimide-Catalyzed Intramolecular Hydroacyloxylation of Unactivated Alkenes in Hexafluoroisopropanol. *Org. Lett.* **2019**, *21*, 7405–7409.

## **Supplementary Information**



## Supplementary Information of Chapter 2

<b>GaCl<sub>3</sub></b>	Zero-point correction=	0.003921 (Hartree/Particle)
	Thermal correction to Energy=	0.009613
	Thermal correction to Enthalpy=	0.010558
	Thermal correction to Gibbs Free Energy=	-0.028114
	Sum of electronic and zero-point Energies=	-3303.823168
	Sum of electronic and thermal Energies=	-3303.817476
	Sum of electronic and thermal Enthalpies=	-3303.816531
	Sum of electronic and thermal Free Energies=	-3303.855203
	E(RM062X) =	-3303.82708899
<b>Ga<sub>2</sub>Cl<sub>6</sub></b>	Zero-point correction=	0.009206 (Hartree/Particle)
	Thermal correction to Energy=	0.022085
	Thermal correction to Enthalpy=	0.023030
	Thermal correction to Gibbs Free Energy=	-0.034822
	Sum of electronic and zero-point Energies=	-6607.699121
	Sum of electronic and thermal Energies=	-6607.686241
	Sum of electronic and thermal Enthalpies=	-6607.685297
	E(RM062X) =	-6607.70832679
<b>benzene</b>	Zero-point correction=	0.101377 (Hartree/Particle)
	Thermal correction to Energy=	0.105744
	Thermal correction to Enthalpy=	0.106689
	Thermal correction to Gibbs Free Energy=	0.073929
	Sum of electronic and zero-point Energies=	-232.056959
	Sum of electronic and thermal Energies=	-232.052592
	Sum of electronic and thermal Enthalpies=	-232.051648
	Sum of electronic and thermal Free Energies=	-232.084407
	E(RM062X) =	-232.158336489
<b>MeCl</b>	Zero-point correction=	0.038043 (Hartree/Particle)
	Thermal correction to Energy=	0.041050
	Thermal correction to Enthalpy=	0.041994
	Thermal correction to Gibbs Free Energy=	0.014392
	Sum of electronic and zero-point Energies=	-500.014710
	Sum of electronic and thermal Energies=	-500.011704
	Sum of electronic and thermal Enthalpies=	-500.010760
	Sum of electronic and thermal Free Energies=	-500.038362E
	E(RM062X) =	-500.052753637
<b>intA1</b>	Zero-point correction=	0.106997 (Hartree/Particle)
	Thermal correction to Energy=	0.118537
	Thermal correction to Enthalpy=	0.119481
	Thermal correction to Gibbs Free Energy=	0.067214
	Sum of electronic and zero-point Energies=	-3535.909720
	Sum of electronic and thermal Energies=	-3535.898180

	Sum of electronic and thermal Enthalpies=	-3535.897236
	Sum of electronic and thermal Free Energies=	-3535.949503
	E(RM062X) =	-3536.01671732
<b>intA2</b>	Zero-point correction=	0.146834 (Hartree/Particle)
	Thermal correction to Energy=	0.162834
	Thermal correction to Enthalpy=	0.163778
	Thermal correction to Gibbs Free Energy=	0.099960
	Sum of electronic and zero-point Energies=	-4035.931741
	Sum of electronic and thermal Energies=	-4035.915742
	Sum of electronic and thermal Enthalpies=	-4035.914797
	Sum of electronic and thermal Free Energies=	-4035.978615
	E(RM062X) =	-4036.07857513
	<i>Frequency</i> -398.6569	
<b>tsA3</b>	Zero-point correction=	0.145838 (Hartree/Particle)
	Thermal correction to Energy=	0.161138
	Thermal correction to Enthalpy=	0.162082
	Thermal correction to Gibbs Free Energy=	0.099312
	Sum of electronic and zero-point Energies=	-4035.886336
	Sum of electronic and thermal Energies=	-4035.871035
	Sum of electronic and thermal Enthalpies=	-4035.870091
	Sum of electronic and thermal Free Energies=	-4035.932861
	E(RM062X) =	-4036.03217335
	<i>Frequency</i> -398.6569	
<b>int4</b>	Zero-point correction=	0.142640 (Hartree/Particle)
	Thermal correction to Energy=	0.158846
	Thermal correction to Enthalpy=	0.159790
	Thermal correction to Gibbs Free Energy=	0.095376
	Sum of electronic and zero-point Energies=	-4035.945587
	Sum of electronic and thermal Energies=	-4035.929380
	Sum of electronic and thermal Enthalpies=	-4035.928436
	Sum of electronic and thermal Free Energies=	-4035.992851
	E(RM062X) =	-4036.08822654
	<i>Frequency</i> -398.6569	
<b>intB1</b>	Zero-point correction=	0.112223 (Hartree/Particle)
	Thermal correction to Energy=	0.131102
	Thermal correction to Enthalpy=	0.132046
	Thermal correction to Gibbs Free Energy=	0.061119
	Sum of electronic and zero-point Energies=	-6839.769224
	Sum of electronic and thermal Energies=	-6839.750345
	Sum of electronic and thermal Enthalpies=	-6839.749401
	Sum of electronic and thermal Free Energies=	-6839.820328
	E(RM062X) =	-6839.88144688
	<i>Frequency</i> -398.6569	
<b>intB2</b>	Zero-point correction=	0.151133 (Hartree/Particle)
	Thermal correction to Energy=	0.174837
	Thermal correction to Enthalpy=	0.175782
	Thermal correction to Gibbs Free Energy=	0.090160

	Sum of electronic and zero-point Energies=	-7339.787671
	Sum of electronic and thermal Energies=	-7339.763967
	Sum of electronic and thermal Enthalpies=	-7339.763023
	Sum of electronic and thermal Free Energies=	-7339.848645
	E(RM062X) = -7339.93880464	
<b>tsB3</b>	Frequency -439.2573	
	Zero-point correction=	0.150716 (Hartree/Particle)
	Thermal correction to Energy=	0.173448
	Thermal correction to Enthalpy=	0.174392
	Thermal correction to Gibbs Free Energy=	0.093300
	Sum of electronic and zero-point Energies=	-7339.755210
	Sum of electronic and thermal Energies=	-7339.732478
	Sum of electronic and thermal Enthalpies=	-7339.731534
	Sum of electronic and thermal Free Energies=	-7339.812626
	E(RM062X) =	-7339.90592615
<b>intB4</b>	Zero-point correction=	0.148526 (Hartree/Particle)
	Thermal correction to Energy=	0.171592
	Thermal correction to Enthalpy=	0.172536
	Thermal correction to Gibbs Free Energy=	0.091310
	Sum of electronic and zero-point Energies=	-7339.800212
	Sum of electronic and thermal Energies=	-7339.777145
	Sum of electronic and thermal Enthalpies=	-7339.776201
	Sum of electronic and thermal Free Energies=	-7339.857427
	E(RM062X) =	-7339.94873745
<b>intB1'</b>	Zero-point correction=	0.111901 (Hartree/Particle)
	Thermal correction to Energy=	0.131152
	Thermal correction to Enthalpy=	0.132096
	Thermal correction to Gibbs Free Energy=	0.058493
	Sum of electronic and zero-point Energies=	-6839.755123
	Sum of electronic and thermal Energies=	-6839.735873
	Sum of electronic and thermal Enthalpies=	-6839.734929
	Sum of electronic and thermal Free Energies=	-6839.808531
	E(RM062X) =	-6839.86702451
<b>intB2'</b>	Zero-point correction=	0.151262 (Hartree/Particle)
	Thermal correction to Energy=	0.174130
	Thermal correction to Enthalpy=	0.175074
	Thermal correction to Gibbs Free Energy=	0.092488
	Sum of electronic and zero-point Energies=	-7339.783872
	Sum of electronic and thermal Energies=	-7339.761003
	Sum of electronic and thermal Enthalpies=	-7339.760059
	Sum of electronic and thermal Free Energies=	-7339.842645
	E(RM062X) =	-7339.93513324
<b>tsB3'</b>	Frequency -352.6378	
	Zero-point correction=	0.150769 (Hartree/Particle)

	Thermal correction to Energy=	0.173763
	Thermal correction to Enthalpy=	0.174707
	Thermal correction to Gibbs Free Energy=	0.089867
	Sum of electronic and zero-point Energies=	-7339.725578
	Sum of electronic and thermal Energies=	-7339.702583
	Sum of electronic and thermal Enthalpies=	-7339.701639
	Sum of electronic and thermal Free Energies=	-7339.786480
	E(RM062X) =	-7339.87634650
<b>intB4'</b>	Zero-point correction=	0.148253 (Hartree/Particle)
	Thermal correction to Energy=	0.171256
	Thermal correction to Enthalpy=	0.172200
	Thermal correction to Gibbs Free Energy=	0.091372
	Sum of electronic and zero-point Energies=	-7339.805652
	Sum of electronic and thermal Energies=	-7339.782649
	Sum of electronic and thermal Enthalpies=	-7339.781705
	Sum of electronic and thermal Free Energies=	-7339.862534
	E(RM062X) =	-7339.95390557
<b>intC2</b>	Zero-point correction=	0.190396 (Hartree/Particle)
	Thermal correction to Energy=	0.218906
	Thermal correction to Enthalpy=	0.219850
	Thermal correction to Gibbs Free Energy=	0.122519
	Sum of electronic and zero-point Energies=	-7839.812766
	Sum of electronic and thermal Energies=	-7839.784256
	Sum of electronic and thermal Enthalpies=	-7839.783312
	Sum of electronic and thermal Free Energies=	-7839.880643
	E(RM062X) =	-7840.00316209
<b>tsC3</b>	Frequency -433.7783	
	Zero-point correction=	0.190843 (Hartree/Particle)
	Thermal correction to Energy=	0.218155
	Thermal correction to Enthalpy=	0.219100
	Thermal correction to Gibbs Free Energy=	0.126152
	Sum of electronic and zero-point Energies=	-7839.778104
	Sum of electronic and thermal Energies=	-7839.750792
	Sum of electronic and thermal Enthalpies=	-7839.749847
	Sum of electronic and thermal Free Energies=	-7839.842795
	E(RM062X) =	-7839.96894705
<b>intC4</b>	Zero-point correction=	0.187506 (Hartree/Particle)
	Thermal correction to Energy=	0.215492
	Thermal correction to Enthalpy=	0.216436
	Thermal correction to Gibbs Free Energy=	0.122599
	Sum of electronic and zero-point Energies=	-7839.825895
	Sum of electronic and thermal Energies=	-7839.797910
	Sum of electronic and thermal Enthalpies=	-7839.796966
	Sum of electronic and thermal Free Energies=	-7839.890803

	E(RM062X) =	-7840.01340186
<b>intC2'</b>	Zero-point correction=	0.190188 (Hartree/Particle)
	Thermal correction to Energy=	0.218667
	Thermal correction to Enthalpy=	0.219611
	Thermal correction to Gibbs Free Energy=	0.121831
	Sum of electronic and zero-point Energies=	-7839.814002
	Sum of electronic and thermal Energies=	-7839.785523
	Sum of electronic and thermal Enthalpies=	-7839.784579
	Sum of electronic and thermal Free Energies=	-7839.882360
	E(RM062X) =	-7840.00419019
<b>tsC3'</b>	Frequency -430.2946	
	Zero-point correction=	0.189920 (Hartree/Particle)
	Thermal correction to Energy=	0.217394
	Thermal correction to Enthalpy=	0.218338
	Thermal correction to Gibbs Free Energy=	0.125108
	Sum of electronic and zero-point Energies=	-7839.777745
	Sum of electronic and thermal Energies=	-7839.750271
	Sum of electronic and thermal Enthalpies=	-7839.749327
	Sum of electronic and thermal Free Energies=	-7839.842557
	E(RM062X) =	-7839.96766524
<b>intC4'</b>	Zero-point correction=	0.187576 (Hartree/Particle)
	Thermal correction to Energy=	0.215956
	Thermal correction to Enthalpy=	0.216900
	Thermal correction to Gibbs Free Energy=	0.120826
	Sum of electronic and zero-point Energies=	-7839.824687
	Sum of electronic and thermal Energies=	-7839.796307
	Sum of electronic and thermal Enthalpies=	-7839.795363
	Sum of electronic and thermal Free Energies=	-7839.891437
	E(RM062X) =	-7840.01226301
<b>HCl</b>	Zero-point correction=	0.006818 (Hartree/Particle)
	Thermal correction to Energy=	0.009178
	Thermal correction to Enthalpy=	0.010123
	Thermal correction to Gibbs Free Energy=	-0.011057
	Sum of electronic and zero-point Energies=	-460.758113
	Sum of electronic and thermal Energies=	-460.755752
	Sum of electronic and thermal Enthalpies=	-460.754808
	Sum of electronic and thermal Free Energies=	-460.775988
	E(RM062X) =	-460.764930788
<b>pro</b>	Zero-point correction=	0.128794 (Hartree/Particle)
	Thermal correction to Energy=	0.134951
	Thermal correction to Enthalpy=	0.135896
	Thermal correction to Gibbs Free Energy=	0.098397
	Sum of electronic and zero-point Energies=	-271.329468
	Sum of electronic and thermal Energies=	-271.323310

	Sum of electronic and thermal Enthalpies=	-271.322366
	Sum of electronic and thermal Free Energies=	-271.359865
	E(RM062X) =	-271.458261702

## Supplementary Information of Chapter 3

<b>GaCl<sub>3</sub></b>	Zero-point correction=	0.003910 (Hartree/Particle)
	Thermal correction to Energy=	0.008991
	Thermal correction to Enthalpy=	0.009856
	Thermal correction to Gibbs Free Energy=	-0.024948
	Sum of electronic and zero-point Energies=	-3303.649427
	Sum of electronic and thermal Energies=	-3303.644345
	Sum of electronic and thermal Enthalpies=	-3303.643480
	Sum of electronic and thermal Free Energies=	-3303.678284
	E(RM062X) =	-3303.65648096
<b>I (Ga<sub>2</sub>Cl<sub>6</sub>)</b>	Zero-point correction=	0.008815 (Hartree/Particle)
	Thermal correction to Energy=	0.019580
	Thermal correction to Enthalpy=	0.020445
	Thermal correction to Gibbs Free Energy=	-0.028596
	Sum of electronic and zero-point Energies=	-6607.356344
	Sum of electronic and thermal Energies=	-6607.345579
	Sum of electronic and thermal Enthalpies=	-6607.344714
	Sum of electronic and thermal Free Energies=	-6607.393755
	E(RM062X) =	-6607.36940486
<b>1</b>	Zero-point correction=	0.347882 (Hartree/Particle)
	Thermal correction to Energy=	0.367300
	Thermal correction to Enthalpy=	0.368165
	Thermal correction to Gibbs Free Energy=	0.301009
	Sum of electronic and zero-point Energies=	-884.994782
	Sum of electronic and thermal Energies=	-884.975364
	Sum of electronic and thermal Enthalpies=	-884.974499
	Sum of electronic and thermal Free Energies=	-885.041655
	E(RM062X) =	-885.349871187
<b>II</b>	Zero-point correction=	0.358673 (Hartree/Particle)
	Thermal correction to Energy=	0.390593
	Thermal correction to Enthalpy=	0.391458
	Thermal correction to Gibbs Free Energy=	0.294063
	Sum of electronic and zero-point Energies=	-7492.386218
	Sum of electronic and thermal Energies=	-7492.354298
	Sum of electronic and thermal Enthalpies=	-7492.353433
	Sum of electronic and thermal Free Energies=	-7492.450828
	E(RM062X) =	-7492.75748662
<b>II-TS-IX</b>	<i>Frequency -279.7939</i>	
	Zero-point correction=	0.358084 (Hartree/Particle)
	Thermal correction to Energy=	0.389635
	Thermal correction to Enthalpy=	0.390500
	Thermal correction to Gibbs Free Energy=	0.293302

	Sum of electronic and zero-point Energies=	-7492.377874
	Sum of electronic and thermal Energies=	-7492.346323
	Sum of electronic and thermal Enthalpies=	-7492.345458
	Sum of electronic and thermal Free Energies=	-7492.442656
	E(RM062X) =	-7492.75007256
<b>IX</b>	Zero-point correction=	0.363192 (Hartree/Particle)
	Thermal correction to Energy=	0.392652
	Thermal correction to Enthalpy=	0.393517
	Thermal correction to Gibbs Free Energy=	0.302492
	Sum of electronic and zero-point Energies=	-7492.424153
	Sum of electronic and thermal Energies=	-7492.394693
	Sum of electronic and thermal Enthalpies=	-7492.393828
	Sum of electronic and thermal Free Energies=	-7492.484853
	E(RM062X) =	-7492.80292804
<b>II-TS-III</b>	<i>Frequency -13.4718</i>	
	Zero-point correction=	0.357709 (Hartree/Particle)
	Thermal correction to Energy=	0.389265
	Thermal correction to Enthalpy=	0.390130
	Thermal correction to Gibbs Free Energy=	0.291702
	Sum of electronic and zero-point Energies=	-7492.387023
	Sum of electronic and thermal Energies=	-7492.355467
	Sum of electronic and thermal Enthalpies=	-7492.354602
	Sum of electronic and thermal Free Energies=	-7492.453031
	E(RM062X) =	-7492.75719944
<b>III</b>	Zero-point correction=	0.357989 (Hartree/Particle)
	Thermal correction to Energy=	0.390273
	Thermal correction to Enthalpy=	0.391138
	Thermal correction to Gibbs Free Energy=	0.292443
	Sum of electronic and zero-point Energies=	-7492.391417
	Sum of electronic and thermal Energies=	-7492.359134
	Sum of electronic and thermal Enthalpies=	-7492.358269
	Sum of electronic and thermal Free Energies=	-7492.456963
	E(RM062X) =	-7492.76173439
<b>III-TS-IV</b>	<i>Frequency -183.2266</i>	
	Zero-point correction=	0.358476 (Hartree/Particle)
	Thermal correction to Energy=	0.389576
	Thermal correction to Enthalpy=	0.390441
	Thermal correction to Gibbs Free Energy=	0.294683
	Sum of electronic and zero-point Energies=	-7492.387869
	Sum of electronic and thermal Energies=	-7492.356769
	Sum of electronic and thermal Enthalpies=	-7492.355904
	Sum of electronic and thermal Free Energies=	-7492.451662
	E(RM062X) =	-7492.76181584
<b>IV</b>	Zero-point correction=	0.362519 (Hartree/Particle)

	Thermal correction to Energy=	0.392854
	Thermal correction to Enthalpy=	0.393719
	Thermal correction to Gibbs Free Energy=	0.300206
	Sum of electronic and zero-point Energies=	-7492.401826
	Sum of electronic and thermal Energies=	-7492.371491
	Sum of electronic and thermal Enthalpies=	-7492.370626
	Sum of electronic and thermal Free Energies=	-7492.464139
	E(RM062X) =	-7492.78430256
<b>IV-TS-V</b>	<i>Frequency -183.9174</i>	
	Zero-point correction=	0.361806 (Hartree/Particle)
	Thermal correction to Energy=	0.391893
	Thermal correction to Enthalpy=	0.392758
	Thermal correction to Gibbs Free Energy=	0.298775
	Sum of electronic and zero-point Energies=	-7492.397211
	Sum of electronic and thermal Energies=	-7492.367125
	Sum of electronic and thermal Enthalpies=	-7492.366260
	Sum of electronic and thermal Free Energies=	-7492.460243
	E(RM062X) =	-7492.77735257
<b>V</b>	Zero-point correction=	0.362643 (Hartree/Particle)
	Thermal correction to Energy=	0.392922
	Thermal correction to Enthalpy=	0.393787
	Thermal correction to Gibbs Free Energy=	0.299872
	Sum of electronic and zero-point Energies=	-7492.420473
	Sum of electronic and thermal Energies=	-7492.390193
	Sum of electronic and thermal Enthalpies=	-7492.389328
	Sum of electronic and thermal Free Energies=	-7492.483243
	E(RM062X) =	-7492.79543041
<b>V-TS-VI'</b>	<i>Frequency -136.1908</i>	
	Zero-point correction=	0.361130 (Hartree/Particle)
	Thermal correction to Energy=	0.391335
	Thermal correction to Enthalpy=	0.392200
	Thermal correction to Gibbs Free Energy=	0.298577
	Sum of electronic and zero-point Energies=	-7492.406909
	Sum of electronic and thermal Energies=	-7492.376704
	Sum of electronic and thermal Enthalpies=	-7492.375839
	Sum of electronic and thermal Free Energies=	-7492.469462
	E(RM062X) =	-7492.78807883
<b>VI'</b>	Zero-point correction=	0.361055 (Hartree/Particle)
	Thermal correction to Energy=	0.391962
	Thermal correction to Enthalpy=	0.392827
	Thermal correction to Gibbs Free Energy=	0.297760
	Sum of electronic and zero-point Energies=	-7492.413128
	Sum of electronic and thermal Energies=	-7492.382221
	Sum of electronic and thermal Enthalpies=	-7492.381356

	Sum of electronic and thermal Free Energies=	-7492.476423
	E(RM062X) =	-7492.79480841
<b>VI-TS-VI</b>	Frequency -52.9056	
	Zero-point correction=	0.360738 (Hartree/Particle)
	Thermal correction to Energy=	0.390841
	Thermal correction to Enthalpy=	0.391707
	Thermal correction to Gibbs Free Energy=	0.298421
	Sum of electronic and zero-point Energies=	-7492.415275
	Sum of electronic and thermal Energies=	-7492.385171
	Sum of electronic and thermal Enthalpies=	-7492.384306
	Sum of electronic and thermal Free Energies=	-7492.477592
	E(RM062X) =	-7492.79569294
<b>VI</b>	Zero-point correction=	0.362526 (Hartree/Particle)
	Thermal correction to Energy=	0.393193
	Thermal correction to Enthalpy=	0.394059
	Thermal correction to Gibbs Free Energy=	0.300847
	Sum of electronic and zero-point Energies=	-7492.457194
	Sum of electronic and thermal Energies=	-7492.426526
	Sum of electronic and thermal Enthalpies=	-7492.425661
	Sum of electronic and thermal Free Energies=	-7492.518872
	E(RM062X) =	-7492.83224878
<b>VII</b>	Zero-point correction=	0.351836 (Hartree/Particle)
	Thermal correction to Energy=	0.368526
	Thermal correction to Enthalpy=	0.369391
	Thermal correction to Gibbs Free Energy=	0.309175
	Sum of electronic and zero-point Energies=	-885.018133
	Sum of electronic and thermal Energies=	-885.001443
	Sum of electronic and thermal Enthalpies=	-885.000578
	Sum of electronic and thermal Free Energies=	-885.060794
	E(RM062X) =	-885.375787479
<b>VII-TS-2</b>	Frequency -473.6494	
	Zero-point correction=	0.349199 (Hartree/Particle)
	Thermal correction to Energy=	0.366751
	Thermal correction to Enthalpy=	0.367616
	Thermal correction to Gibbs Free Energy=	0.304528
	Sum of electronic and zero-point Energies=	-884.972937
	Sum of electronic and thermal Energies=	-884.955385
	Sum of electronic and thermal Enthalpies=	-884.954520
	Sum of electronic and thermal Free Energies=	-885.017609
	E(RM062X) =	-885.327623813
<b>2</b>	Zero-point correction=	0.351141 (Hartree/Particle)
	Thermal correction to Energy=	0.369431
	Thermal correction to Enthalpy=	0.370296
	Thermal correction to Gibbs Free Energy=	0.304901

	Sum of electronic and zero-point Energies=	-885.052557
	Sum of electronic and thermal Energies=	-885.034267
	Sum of electronic and thermal Enthalpies=	-885.033402
	Sum of electronic and thermal Free Energies=	-885.098797
	E(RM062X) =	-885.409821067
<b>III-1Me</b>	Zero-point correction=	0.329887 (Hartree/Particle)
	Thermal correction to Energy=	0.360961
	Thermal correction to Enthalpy=	0.361826
	Thermal correction to Gibbs Free Energy=	0.265360
	Sum of electronic and zero-point Energies=	-7453.119638
	Sum of electronic and thermal Energies=	-7453.088565
	Sum of electronic and thermal Enthalpies=	-7453.087700
	Sum of electronic and thermal Free Energies=	-7453.184165
	E(RM062X) =	-7453.46180315
<b>III-TS-VIII-1Me</b>	<i>Frequency -196.1362</i>	
	Zero-point correction=	0.330427 (Hartree/Particle)
	Thermal correction to Energy=	0.360210
	Thermal correction to Enthalpy=	0.361075
	Thermal correction to Gibbs Free Energy=	0.268409
	Sum of electronic and zero-point Energies=	-7453.114191
	Sum of electronic and thermal Energies=	-7453.084409
	Sum of electronic and thermal Enthalpies=	-7453.083544
	Sum of electronic and thermal Free Energies=	-7453.176210
	E(RM062X) =	-7453.46081734
<b>VIII-1Me</b>	Zero-point correction=	0.334202 (Hartree/Particle)
	Thermal correction to Energy=	0.363573
	Thermal correction to Enthalpy=	0.364438
	Thermal correction to Gibbs Free Energy=	0.271852
	Sum of electronic and zero-point Energies=	-7453.132399
	Sum of electronic and thermal Energies=	-7453.103028
	Sum of electronic and thermal Enthalpies=	-7453.102163
	Sum of electronic and thermal Free Energies=	-7453.194749
	E(RM062X) =	-7453.48566871
<b>III-1Me<sup>mono</sup></b>	Zero-point correction=	0.325086 (Hartree/Particle)
	Thermal correction to Energy=	0.349405
	Thermal correction to Enthalpy=	0.350270
	Thermal correction to Gibbs Free Energy=	0.270433
	Sum of electronic and zero-point Energies=	-4149.425993
	Sum of electronic and thermal Energies=	-4149.401674
	Sum of electronic and thermal Enthalpies=	-4149.400809
	Sum of electronic and thermal Free Energies=	-4149.480646
	E(RM062X) =	-4149.76050503
<b>III-TS-VIII</b>	<i>Frequency -206.4806</i>	
	Zero-point correction=	0.326004 (Hartree/Particle)

<b>-1Me<sup>mono</sup></b>	Thermal correction to Energy=	0.348842
	Thermal correction to Enthalpy=	0.349707
	Thermal correction to Gibbs Free Energy=	0.274419
	Sum of electronic and zero-point Energies=	-4149.416172
	Sum of electronic and thermal Energies=	-4149.393334
	Sum of electronic and thermal Enthalpies=	-4149.392469
	Sum of electronic and thermal Free Energies=	-4149.467757
	E(RM062X) =	-4149.75657442
<b>VIII-1Me<sup>mono</sup></b>	Zero-point correction=	0.329357 (Hartree/Particle)
	Thermal correction to Energy=	0.351964
	Thermal correction to Enthalpy=	0.352829
	Thermal correction to Gibbs Free Energy=	0.276932
	Sum of electronic and zero-point Energies=	-4149.434148
	Sum of electronic and thermal Energies=	-4149.411541
	Sum of electronic and thermal Enthalpies=	-4149.410676
	Sum of electronic and thermal Free Energies=	-4149.486573
	E(RM062X) =	-4149.77886363
<b>III-0Me</b>	Zero-point correction=	0.301615 (Hartree/Particle)
	Thermal correction to Energy=	0.331342
	Thermal correction to Enthalpy=	0.332207
	Thermal correction to Gibbs Free Energy=	0.239081
	Sum of electronic and zero-point Energies=	-7413.846769
	Sum of electronic and thermal Energies=	-7413.817042
	Sum of electronic and thermal Enthalpies=	-7413.816177
	Sum of electronic and thermal Free Energies=	-7413.909303
	E(RM062X) =	-7414.16042669
<b>III-TS-VIII-0Me</b>	Frequency -241.3960	
	Zero-point correction=	0.302385 (Hartree/Particle)
	Thermal correction to Energy=	0.330877
	Thermal correction to Enthalpy=	0.331742
	Thermal correction to Gibbs Free Energy=	0.241643
	Sum of electronic and zero-point Energies=	-7413.836096
	Sum of electronic and thermal Energies=	-7413.807604
	Sum of electronic and thermal Enthalpies=	-7413.806739
	Sum of electronic and thermal Free Energies=	-7413.896838
	E(RM062X) =	-7414.15509678
<b>VIII-0Me</b>	Zero-point correction=	0.306490 (Hartree/Particle)
	Thermal correction to Energy=	0.334361
	Thermal correction to Enthalpy=	0.335226
	Thermal correction to Gibbs Free Energy=	0.246143
	Sum of electronic and zero-point Energies=	-7413.858905
	Sum of electronic and thermal Energies=	-7413.831034
	Sum of electronic and thermal Enthalpies=	-7413.830169
	Sum of electronic and thermal Free Energies=	-7413.919252

	E(RM062X) =	-7414.18472460
<b>III-</b> <b>0Me<sup>mono</sup></b>	Zero-point correction=	0.297003 (Hartree/Particle)
	Thermal correction to Energy=	0.319934
	Thermal correction to Enthalpy=	0.320799
	Thermal correction to Gibbs Free Energy=	0.244845
	Sum of electronic and zero-point Energies=	-4110.153127
	Sum of electronic and thermal Energies=	-4110.130196
	Sum of electronic and thermal Enthalpies=	-4110.129331
	Sum of electronic and thermal Free Energies=	-4110.205285
	E(RM062X) =	-4110.45940077
<b>III-TS-</b> <b>VIII</b> <b>-0Me<sup>mono</sup></b>	<i>Frequency</i> -254.6243	
	Zero-point correction=	0.297203 (Hartree/Particle)
	Thermal correction to Energy=	0.319023
	Thermal correction to Enthalpy=	0.319888
	Thermal correction to Gibbs Free Energy=	0.245815
	Sum of electronic and zero-point Energies=	-4110.138848
	Sum of electronic and thermal Energies=	-4110.117029
	Sum of electronic and thermal Enthalpies=	-4110.116164
	Sum of electronic and thermal Free Energies=	-4110.190236
	E(RM062X) =	-4110.45050046
<b>VIII-</b> <b>0Me<sup>mono</sup></b>	Zero-point correction=	0.301321 (Hartree/Particle)
	Thermal correction to Energy=	0.321706
	Thermal correction to Enthalpy=	0.322571
	Thermal correction to Gibbs Free Energy=	0.252300
	Sum of electronic and zero-point Energies=	-4110.161043
	Sum of electronic and thermal Energies=	-4110.140658
	Sum of electronic and thermal Enthalpies=	-4110.139793
	Sum of electronic and thermal Free Energies=	-4110.210063
	E(RM062X) =	-4110.47794208
<b>II<sup>mono</sup></b>	Zero-point correction=	0.352912 (Hartree/Particle)
	Thermal correction to Energy=	0.378517
	Thermal correction to Enthalpy=	0.379382
	Thermal correction to Gibbs Free Energy=	0.297274
	Sum of electronic and zero-point Energies=	-4188.695760
	Sum of electronic and thermal Energies=	-4188.670154
	Sum of electronic and thermal Enthalpies=	-4188.669289
	Sum of electronic and thermal Free Energies=	-4188.751398
	E(RM062X) =	-4189.05838162
<b>II-TS-</b> <b>III<sup>mono</sup></b>	<i>Frequency</i> -24.8704	
	Zero-point correction=	0.352440 (Hartree/Particle)
	Thermal correction to Energy=	0.377631
	Thermal correction to Enthalpy=	0.378496
	Thermal correction to Gibbs Free Energy=	0.297187
	Sum of electronic and zero-point Energies=	-4188.695704

	Sum of electronic and thermal Energies=	-4188.670513
	Sum of electronic and thermal Enthalpies=	-4188.669648
	Sum of electronic and thermal Free Energies=	-4188.750956
	E(RM062X) =	-4189.05774861
<b>III<sup>mono</sup></b>	Zero-point correction=	0.353530 (Hartree/Particle)
	Thermal correction to Energy=	0.379013
	Thermal correction to Enthalpy=	0.379878
	Thermal correction to Gibbs Free Energy=	0.297832
	Sum of electronic and zero-point Energies=	-4188.697323
	Sum of electronic and thermal Energies=	-4188.671841
	Sum of electronic and thermal Enthalpies=	-4188.670976
	Sum of electronic and thermal Free Energies=	-4188.753021
	E(RM062X) =	-4189.06028730
<b>III-TS-IV<sup>mono</sup></b>	<i>Frequency -185.3811</i>	
	Zero-point correction=	0.353617 (Hartree/Particle)
	Thermal correction to Energy=	0.378050
	Thermal correction to Enthalpy=	0.378915
	Thermal correction to Gibbs Free Energy=	0.299407
	Sum of electronic and zero-point Energies=	-4188.690639
	Sum of electronic and thermal Energies=	-4188.666206
	Sum of electronic and thermal Enthalpies=	-4188.665341
	Sum of electronic and thermal Free Energies=	-4188.744849
	E(RM062X) =	-4189.05789882
<b>IV<sup>mono</sup></b>	Zero-point correction=	0.357063 (Hartree/Particle)
	Thermal correction to Energy=	0.381019
	Thermal correction to Enthalpy=	0.381884
	Thermal correction to Gibbs Free Energy=	0.303440
	Sum of electronic and zero-point Energies=	-4188.704135
	Sum of electronic and thermal Energies=	-4188.680179
	Sum of electronic and thermal Enthalpies=	-4188.679314
	Sum of electronic and thermal Free Energies=	-4188.757757
	E(RM062X) =	-4189.07760760
<b>IV-TS-V<sup>mono</sup></b>	<i>Frequency -168.1890</i>	
	Zero-point correction=	0.356519 (Hartree/Particle)
	Thermal correction to Energy=	0.380108
	Thermal correction to Enthalpy=	0.380973
	Thermal correction to Gibbs Free Energy=	0.303175
	Sum of electronic and zero-point Energies=	-4188.698382
	Sum of electronic and thermal Energies=	-4188.674793
	Sum of electronic and thermal Enthalpies=	-4188.673928
	Sum of electronic and thermal Free Energies=	-4188.751726
	E(RM062X) =	-4189.07021109
<b>V<sup>mono</sup></b>	Zero-point correction=	0.357534 (Hartree/Particle)
	Thermal correction to Energy=	0.381312

	Thermal correction to Enthalpy=	0.382178
	Thermal correction to Gibbs Free Energy=	0.304360
	Sum of electronic and zero-point Energies=	-4188.725551
	Sum of electronic and thermal Energies=	-4188.701773
	Sum of electronic and thermal Enthalpies=	-4188.700908
	Sum of electronic and thermal Free Energies=	-4188.778725
	E(RM062X) =	-4189.09251010
<b>V-TS- VI<sup>mono</sup></b>	<i>Frequency</i> -152.4082	
	Zero-point correction=	0.355869 (Hartree/Particle)
	Thermal correction to Energy=	0.379475
	Thermal correction to Enthalpy=	0.380340
	Thermal correction to Gibbs Free Energy=	0.302367
	Sum of electronic and zero-point Energies=	-4188.708535
	Sum of electronic and thermal Energies=	-4188.684929
	Sum of electronic and thermal Enthalpies=	-4188.684064
	Sum of electronic and thermal Free Energies=	-4188.762037
	E(RM062X) =	-4189.08096533
<b>VI<sup>mono</sup></b>	Zero-point correction=	0.356004 (Hartree/Particle)
	Thermal correction to Energy=	0.380104
	Thermal correction to Enthalpy=	0.380969
	Thermal correction to Gibbs Free Energy=	0.302469
	Sum of electronic and zero-point Energies=	-4188.718548
	Sum of electronic and thermal Energies=	-4188.694448
	Sum of electronic and thermal Enthalpies=	-4188.693583
	Sum of electronic and thermal Free Energies=	-4188.772082
	E(RM062X) =	-4189.09042615
<b>VI'-TS- VI<sup>mono</sup></b>	<i>Frequency</i> -110.9463	
	Zero-point correction=	0.355578 (Hartree/Particle)
	Thermal correction to Energy=	0.379219
	Thermal correction to Enthalpy=	0.380084
	Thermal correction to Gibbs Free Energy=	0.302647
	Sum of electronic and zero-point Energies=	-4188.717217
	Sum of electronic and thermal Energies=	-4188.693576
	Sum of electronic and thermal Enthalpies=	-4188.692711
	Sum of electronic and thermal Free Energies=	-4188.770148
	E(RM062X) =	-4189.08889159
<b>VI<sup>mono</sup></b>	Zero-point correction=	0.357087 (Hartree/Particle)
	Thermal correction to Energy=	0.381355
	Thermal correction to Enthalpy=	0.382220
	Thermal correction to Gibbs Free Energy=	0.303277
	Sum of electronic and zero-point Energies=	-4188.755096
	Sum of electronic and thermal Energies=	-4188.730828
	Sum of electronic and thermal Enthalpies=	-4188.729963
	Sum of electronic and thermal Free Energies=	-4188.808906

	E(RM062X) =	-4189.12234570
[III]- <b>Ph<sub>3</sub>PAu<sup>+</sup></b>	Zero-point correction=	0.627861 (Hartree/Particle)
	Thermal correction to Energy=	0.663645
	Thermal correction to Enthalpy=	0.664510
	Thermal correction to Gibbs Free Energy=	0.557213
	Sum of electronic and zero-point Energies=	-2055.892651
	Sum of electronic and thermal Energies=	-2055.856867
	Sum of electronic and thermal Enthalpies=	-2055.856002
	Sum of electronic and thermal Free Energies=	-2055.963299
	E(RM062X) =	-2056.55517331
[III-TS-IV] <b>-Ph<sub>3</sub>PAu<sup>+</sup></b>	Frequency -220.8886	
	Zero-point correction=	0.627623 (Hartree/Particle)
	Thermal correction to Energy=	0.662595
	Thermal correction to Enthalpy=	0.663460
	Thermal correction to Gibbs Free Energy=	0.557673
	Sum of electronic and zero-point Energies=	-2055.882582
	Sum of electronic and thermal Energies=	-2055.847610
	Sum of electronic and thermal Enthalpies=	-2055.846745
	Sum of electronic and thermal Free Energies=	-2055.952532
	E(RM062X) =	-2056.54366806
[IV]- <b>Ph<sub>3</sub>PAu<sup>+</sup></b>	Zero-point correction=	0.631665 (Hartree/Particle)
	Thermal correction to Energy=	0.665184
	Thermal correction to Enthalpy=	0.666049
	Thermal correction to Gibbs Free Energy=	0.562453
	Sum of electronic and zero-point Energies=	-2055.898374
	Sum of electronic and thermal Energies=	-2055.864854
	Sum of electronic and thermal Enthalpies=	-2055.863989
	Sum of electronic and thermal Free Energies=	-2055.967585
	E(RM062X) =	-2056.56397301
[III]- <b>Ga(OTf)<sub>3</sub></b>	Zero-point correction=	0.441958 (Hartree/Particle)
	Thermal correction to Energy=	0.482925
	Thermal correction to Enthalpy=	0.483790
	Thermal correction to Gibbs Free Energy=	0.369746
	Sum of electronic and zero-point Energies=	-5691.749416
	Sum of electronic and thermal Energies=	-5691.708448
	Sum of electronic and thermal Enthalpies=	-5691.707583
	Sum of electronic and thermal Free Energies=	-5691.821628
	E(RM062X) =	-5692.20324642
[III-TS-IV] <b>-Ga(OTf)<sub>3</sub></b>	Frequency -187.7817	
	Zero-point correction=	0.441527 (Hartree/Particle)
	Thermal correction to Energy=	0.481809
	Thermal correction to Enthalpy=	0.482674
	Thermal correction to Gibbs Free Energy=	0.369295
	Sum of electronic and zero-point Energies=	-5691.746338

	Sum of electronic and thermal Energies=	-5691.706056
	Sum of electronic and thermal Enthalpies=	-5691.705191
	Sum of electronic and thermal Free Energies=	-5691.818571
	E(RM062X) =	-5692.20153338
[IV]- <b>Ga(OTf)<sub>3</sub></b>	Zero-point correction=	0.445193 (Hartree/Particle)
	Thermal correction to Energy=	0.485709
	Thermal correction to Enthalpy=	0.486574
	Thermal correction to Gibbs Free Energy=	0.370882
	Sum of electronic and zero-point Energies=	-5691.768357
	Sum of electronic and thermal Energies=	-5691.727841
	Sum of electronic and thermal Enthalpies=	-5691.726976
	Sum of electronic and thermal Free Energies=	-5691.842668
	E(RM062X) =	-5692.22906979
<b>InCl<sub>3</sub></b>	Zero-point correction=	0.003212 (Hartree/Particle)
	Thermal correction to Energy=	0.008618
	Thermal correction to Enthalpy=	0.009483
	Thermal correction to Gibbs Free Energy=	-0.026664
	Sum of electronic and zero-point Energies=	-1382.510085
	Sum of electronic and thermal Energies=	-1382.504679
	Sum of electronic and thermal Enthalpies=	-1382.503814
	Sum of electronic and thermal Free Energies=	-1382.539960
	E(RM062X) =	-1382.52085786
[X]-InCl <sub>3</sub>	Zero-point correction=	0.297748 (Hartree/Particle)
	Thermal correction to Energy=	0.321084
	Thermal correction to Enthalpy=	0.321949
	Thermal correction to Gibbs Free Energy=	0.243885
	Sum of electronic and zero-point Energies=	-2189.008762
	Sum of electronic and thermal Energies=	-2188.985426
	Sum of electronic and thermal Enthalpies=	-2188.984561
	Sum of electronic and thermal Free Energies=	-2189.062626
	E(RM062X) =	-2189.31675548
[III]-InCl <sub>3</sub>	Zero-point correction=	0.296785 (Hartree/Particle)
	Thermal correction to Energy=	0.320214
	Thermal correction to Enthalpy=	0.321079
	Thermal correction to Gibbs Free Energy=	0.242745
	Sum of electronic and zero-point Energies=	-2188.994453
	Sum of electronic and thermal Energies=	-2188.971024
	Sum of electronic and thermal Enthalpies=	-2188.970159
	Sum of electronic and thermal Free Energies=	-2189.048493
	E(RM062X) =	-2189.30182526
[III-TS-IV] - InCl <sub>3</sub>	Frequency -266.5505	
	Zero-point correction=	0.297059 (Hartree/Particle)
	Thermal correction to Energy=	0.319285
	Thermal correction to Enthalpy=	0.320150

	Thermal correction to Gibbs Free Energy=	0.243446
	Sum of electronic and zero-point Energies=	-2188.975696
	Sum of electronic and thermal Energies=	-2188.953471
	Sum of electronic and thermal Enthalpies=	-2188.952606
	Sum of electronic and thermal Free Energies=	-2189.029310
	E(RM062X) =	-2189.28859214
[IV]-InCl <sub>3</sub>	Zero-point correction=	0.300436 (Hartree/Particle)
	Thermal correction to Energy=	0.322187
	Thermal correction to Enthalpy=	0.323052
	Thermal correction to Gibbs Free Energy=	0.247263
	Sum of electronic and zero-point Energies=	-2188.992675
	Sum of electronic and thermal Energies=	-2188.970924
	Sum of electronic and thermal Enthalpies=	-2188.970059
	Sum of electronic and thermal Free Energies=	-2189.045848
	E(RM062X) =	-2189.31077274
[X]-GaCl <sub>3</sub>	Zero-point correction=	0.297695 (Hartree/Particle)
	Thermal correction to Energy=	0.320539
	Thermal correction to Enthalpy=	0.321404
	Thermal correction to Gibbs Free Energy=	0.246076
	Sum of electronic and zero-point Energies=	-4110.174195
	Sum of electronic and thermal Energies=	-4110.151351
	Sum of electronic and thermal Enthalpies=	-4110.150486
	Sum of electronic and thermal Free Energies=	-4110.225813
	E(RM062X) =	-4110.48127421
AlCl <sub>3</sub>	Zero-point correction=	0.004874 (Hartree/Particle)
	Thermal correction to Energy=	0.009592
	Thermal correction to Enthalpy=	0.010457
	Thermal correction to Gibbs Free Energy=	-0.023040
	Sum of electronic and zero-point Energies=	-1623.097737
	Sum of electronic and thermal Energies=	-1623.093020
	Sum of electronic and thermal Enthalpies=	-1623.092155
	Sum of electronic and thermal Free Energies=	-1623.125651
	E(RM062X) =	-1623.10585771
[X]-AlCl <sub>3</sub>	Zero-point correction=	0.298277 (Hartree/Particle)
	Thermal correction to Energy=	0.321025
	Thermal correction to Enthalpy=	0.321890
	Thermal correction to Gibbs Free Energy=	0.245296
	Sum of electronic and zero-point Energies=	-2429.612777
	Sum of electronic and thermal Energies=	-2429.590029
	Sum of electronic and thermal Enthalpies=	-2429.589164
	Sum of electronic and thermal Free Energies=	-2429.665758
	E(RM062X) =	-2429.92145618
[III]-AlCl <sub>3</sub>	Zero-point correction=	0.298031 (Hartree/Particle)
	Thermal correction to Energy=	0.320646

	Thermal correction to Enthalpy=	0.321511
	Thermal correction to Gibbs Free Energy=	0.246006
	Sum of electronic and zero-point Energies=	-2429.585644
	Sum of electronic and thermal Energies=	-2429.563029
	Sum of electronic and thermal Enthalpies=	-2429.562164
	Sum of electronic and thermal Free Energies=	-2429.637669
	E(RM062X) =	-2429.89267771
<b>[III-TS-IV]-AlCl<sub>3</sub></b>	<i>Frequency</i> -262.1079	
	Zero-point correction=	0.298307 (Hartree/Particle)
	Thermal correction to Energy=	0.319706
	Thermal correction to Enthalpy=	0.320571
	Thermal correction to Gibbs Free Energy=	0.247435
	Sum of electronic and zero-point Energies=	-2429.570388
	Sum of electronic and thermal Energies=	-2429.548989
	Sum of electronic and thermal Enthalpies=	-2429.548124
	Sum of electronic and thermal Free Energies=	-2429.621260
	E(RM062X) =	-2429.88248313
<b>[IV]-AlCl<sub>3</sub></b>	Zero-point correction=	0.302412 (Hartree/Particle)
	Thermal correction to Energy=	0.323097
	Thermal correction to Enthalpy=	0.323962
	Thermal correction to Gibbs Free Energy=	0.252702
	Sum of electronic and zero-point Energies=	-2429.590801
	Sum of electronic and thermal Energies=	-2429.570117
	Sum of electronic and thermal Enthalpies=	-2429.569252
	Sum of electronic and thermal Free Energies=	-2429.640511
	E(RM062X) =	-2429.90788124
<b>BCl<sub>3</sub></b>	Zero-point correction=	0.007716 (Hartree/Particle)
	Thermal correction to Energy=	0.011583
	Thermal correction to Enthalpy=	0.012448
	Thermal correction to Gibbs Free Energy=	-0.018622
	Sum of electronic and zero-point Energies=	-1405.452438
	Sum of electronic and thermal Energies=	-1405.448570
	Sum of electronic and thermal Enthalpies=	-1405.447705
	Sum of electronic and thermal Free Energies=	-1405.478776
	E(RM062X) =	-1405.46083394
<b>[X]-BCl<sub>3</sub></b>	Zero-point correction=	0.301681 (Hartree/Particle)
	Thermal correction to Energy=	0.323064
	Thermal correction to Enthalpy=	0.323929
	Thermal correction to Gibbs Free Energy=	0.252219
	Sum of electronic and zero-point Energies=	-2211.921121
	Sum of electronic and thermal Energies=	-2211.899738
	Sum of electronic and thermal Enthalpies=	-2211.898873
	Sum of electronic and thermal Free Energies=	-2211.970582
	E(RM062X) =	-2212.23198758

[III]-BCl <sub>3</sub>	Zero-point correction=	0.300078 (Hartree/Particle)
	Thermal correction to Energy=	0.322407
	Thermal correction to Enthalpy=	0.323272
	Thermal correction to Gibbs Free Energy=	0.247743
	Sum of electronic and zero-point Energies=	-2211.918048
	Sum of electronic and thermal Energies=	-2211.895719
	Sum of electronic and thermal Enthalpies=	-2211.894854
	Sum of electronic and thermal Free Energies=	-2211.970383
	E(RM062X) =	-2212.22423511
[III-TS-IV]-BCl <sub>3</sub>	Frequency -204.5510	
	Zero-point correction=	0.300781 (Hartree/Particle)
	Thermal correction to Energy=	0.321258
	Thermal correction to Enthalpy=	0.322123
	Thermal correction to Gibbs Free Energy=	0.252262
	Sum of electronic and zero-point Energies=	-2211.902074
	Sum of electronic and thermal Energies=	-2211.881596
	Sum of electronic and thermal Enthalpies=	-2211.880731
	Sum of electronic and thermal Free Energies=	-2211.950592
	E(RM062X) =	-2212.21502914
[IV]-BCl <sub>3</sub>	Zero-point correction=	0.306942 (Hartree/Particle)
	Thermal correction to Energy=	0.326530
	Thermal correction to Enthalpy=	0.327395
	Thermal correction to Gibbs Free Energy=	0.256256
	Sum of electronic and zero-point Energies=	-2211.955966
	Sum of electronic and thermal Energies=	-2211.936377
	Sum of electronic and thermal Enthalpies=	-2211.935512
	Sum of electronic and thermal Free Energies=	-2212.006651
	E(RM062X) =	-2212.26953486
Ga(OTf) <sub>3</sub>	Zero-point correction=	0.092193 (Hartree/Particle)
	Thermal correction to Energy=	0.112989
	Thermal correction to Enthalpy=	0.113854
	Thermal correction to Gibbs Free Energy=	0.043908
	Sum of electronic and zero-point Energies=	-4806.700872
	Sum of electronic and thermal Energies=	-4806.680076
	Sum of electronic and thermal Enthalpies=	-4806.679211
	Sum of electronic and thermal Free Energies=	-4806.749157
	E(RM062X) =	-4806.79978451
[X]-Ga(OTf) <sub>3</sub>	Zero-point correction=	0.385226 (Hartree/Particle)
	Thermal correction to Energy=	0.421917
	Thermal correction to Enthalpy=	0.422782
	Thermal correction to Gibbs Free Energy=	0.318413
	Sum of electronic and zero-point Energies=	-5613.231999
	Sum of electronic and thermal Energies=	-5613.195308
	Sum of electronic and thermal Enthalpies=	-5613.194443

	Sum of electronic and thermal Free Energies=	-5613.298812
	E(RM062X) =	-5613.62892216
<b>[III]- Ga(OTf)<sub>3</sub></b>	Zero-point correction=	0.385694 (Hartree/Particle)
	Thermal correction to Energy=	0.424055
	Thermal correction to Enthalpy=	0.424920
	Thermal correction to Gibbs Free Energy=	0.316902
	Sum of electronic and zero-point Energies=	-5613.205391
	Sum of electronic and thermal Energies=	-5613.167029
	Sum of electronic and thermal Enthalpies=	-5613.166164
	Sum of electronic and thermal Free Energies=	-5613.274183
	E(RM062X) =	-5613.60274752
<b>[III-TS-IV] -Ga(OTf)<sub>3</sub></b>	Frequency -244.0154	
	Zero-point correction=	0.385032 (Hartree/Particle)
	Thermal correction to Energy=	0.422646
	Thermal correction to Enthalpy=	0.423511
	Thermal correction to Gibbs Free Energy=	0.316265
	Sum of electronic and zero-point Energies=	-5613.196151
	Sum of electronic and thermal Energies=	-5613.158537
	Sum of electronic and thermal Enthalpies=	-5613.157672
	Sum of electronic and thermal Free Energies=	-5613.264917
<b>[IV]- Ga(OTf)<sub>3</sub></b>	E(RM062X) =	-5613.59552667
	Zero-point correction=	0.388990 (Hartree/Particle)
	Thermal correction to Energy=	0.426657
	Thermal correction to Enthalpy=	0.427522
	Thermal correction to Gibbs Free Energy=	0.318977
	Sum of electronic and zero-point Energies=	-5613.226997
	Sum of electronic and thermal Energies=	-5613.189329
	Sum of electronic and thermal Enthalpies=	-5613.188464
	Sum of electronic and thermal Free Energies=	-5613.297009
<b>Ph<sub>3</sub>PAu<sup>+</sup></b>	E(RM062X) =	-5613.63396667
	Zero-point correction=	0.278450 (Hartree/Particle)
	Thermal correction to Energy=	0.293660
	Thermal correction to Enthalpy=	0.294525
	Thermal correction to Gibbs Free Energy=	0.234000
	Sum of electronic and zero-point Energies=	-1170.838538
	Sum of electronic and thermal Energies=	-1170.823328
	Sum of electronic and thermal Enthalpies=	-1170.822463
	Sum of electronic and thermal Free Energies=	-1170.882988
<b>[X]- Ph<sub>3</sub>PAu<sup>+</sup></b>	E(RM062X) =	-1171.16033577
	Zero-point correction=	0.571471 (Hartree/Particle)
	Thermal correction to Energy=	0.604230
	Thermal correction to Enthalpy=	0.605095
	Thermal correction to Gibbs Free Energy=	0.503161
	Sum of electronic and zero-point Energies=	-1977.341719

	Sum of electronic and thermal Energies=	-1977.308960
	Sum of electronic and thermal Enthalpies=	-1977.308095
	Sum of electronic and thermal Free Energies=	-1977.410029
	E(RM062X) =	-1977.94884326
[III]- <b>Ph<sub>3</sub>PAu<sup>+</sup></b>	Zero-point correction=	0.570741 (Hartree/Particle)
	Thermal correction to Energy=	0.604345
	Thermal correction to Enthalpy=	0.605210
	Thermal correction to Gibbs Free Energy=	0.501075
	Sum of electronic and zero-point Energies=	-1977.342930
	Sum of electronic and thermal Energies=	-1977.309326
	Sum of electronic and thermal Enthalpies=	-1977.308461
	Sum of electronic and thermal Free Energies=	-1977.412596
	E(RM062X) =	-1977.95123015
[III-TS-IV] <b>-Ph<sub>3</sub>PAu<sup>+</sup></b>	Frequency -284.3400	
	Zero-point correction=	0.571607 (Hartree/Particle)
	Thermal correction to Energy=	0.602831
	Thermal correction to Enthalpy=	0.603696
	Thermal correction to Gibbs Free Energy=	0.508054
	Sum of electronic and zero-point Energies=	-1977.328799
	Sum of electronic and thermal Energies=	-1977.297576
	Sum of electronic and thermal Enthalpies=	-1977.296711
	Sum of electronic and thermal Free Energies=	-1977.392353
	E(RM062X) =	-1977.93556404
[IV]- <b>Ph<sub>3</sub>PAu<sup>+</sup></b>	Zero-point correction=	0.575532 (Hartree/Particle)
	Thermal correction to Energy=	0.606142
	Thermal correction to Enthalpy=	0.607007
	Thermal correction to Gibbs Free Energy=	0.512587
	Sum of electronic and zero-point Energies=	-1977.356390
	Sum of electronic and thermal Energies=	-1977.325779
	Sum of electronic and thermal Enthalpies=	-1977.324914
	Sum of electronic and thermal Free Energies=	-1977.419334
	E(RM062X) =	-1977.96704979
1''	Zero-point correction=	0.203658 (Hartree/Particle)
	Thermal correction to Energy=	0.212839
	Thermal correction to Enthalpy=	0.213704
	Thermal correction to Gibbs Free Energy=	0.172196
	Sum of electronic and zero-point Energies=	-350.939598
	Sum of electronic and thermal Energies=	-350.930417
	Sum of electronic and thermal Enthalpies=	-350.929552
	Sum of electronic and thermal Free Energies=	-350.971060
	E(RM062X) =	-351.145915189
[III]''- <b>InCl<sub>3</sub></b>	Zero-point correction=	0.208274 (Hartree/Particle)
	Thermal correction to Energy=	0.224503
	Thermal correction to Enthalpy=	0.225368

	Thermal correction to Gibbs Free Energy=	0.163452
	Sum of electronic and zero-point Energies=	-1733.486961
	Sum of electronic and thermal Energies=	-1733.470731
	Sum of electronic and thermal Enthalpies=	-1733.469866
	Sum of electronic and thermal Free Energies=	-1733.531783
	E(RM062X) =	-1733.70262073
[III-TS -IV]" <b>InCl<sub>3</sub></b>	<i>Frequency</i> -262.6869	
	Zero-point correction=	0.208904 (Hartree/Particle)
	Thermal correction to Energy=	0.223648
	Thermal correction to Enthalpy=	0.224513
	Thermal correction to Gibbs Free Energy=	0.167179
	Sum of electronic and zero-point Energies=	-1733.467982
	Sum of electronic and thermal Energies=	-1733.453238
	Sum of electronic and thermal Enthalpies=	-1733.452373
	Sum of electronic and thermal Free Energies=	-1733.509707
	E(RM062X) =	-1733.69067803
[IV]"- <b>InCl<sub>3</sub></b>	Zero-point correction=	0.212305 (Hartree/Particle)
	Thermal correction to Energy=	0.226602
	Thermal correction to Enthalpy=	0.227467
	Thermal correction to Gibbs Free Energy=	0.170684
	Sum of electronic and zero-point Energies=	-1733.482451
	Sum of electronic and thermal Energies=	-1733.468154
	Sum of electronic and thermal Enthalpies=	-1733.467289
	Sum of electronic and thermal Free Energies=	-1733.524072
	E(RM062X) =	-1733.71043624
[IV-TS -V]" <b>InCl<sub>3</sub></b>	<i>Frequency</i> -233.0284	
	Zero-point correction=	0.211563 (Hartree/Particle)
	Thermal correction to Energy=	0.225386
	Thermal correction to Enthalpy=	0.226251
	Thermal correction to Gibbs Free Energy=	0.170025
	Sum of electronic and zero-point Energies=	-1733.481810
	Sum of electronic and thermal Energies=	-1733.467987
	Sum of electronic and thermal Enthalpies=	-1733.467122
	Sum of electronic and thermal Free Energies=	-1733.523348
	E(RM062X) =	-1733.70592853
[V]"- <b>InCl<sub>3</sub></b>	Zero-point correction=	0.213049 (Hartree/Particle)
	Thermal correction to Energy=	0.227241
	Thermal correction to Enthalpy=	0.228106
	Thermal correction to Gibbs Free Energy=	0.171885
	Sum of electronic and zero-point Energies=	-1733.515579
	Sum of electronic and thermal Energies=	-1733.501386
	Sum of electronic and thermal Enthalpies=	-1733.500521
	Sum of electronic and thermal Free Energies=	-1733.556743
	E(RM062X) =	-1733.73551893

[IV-TS-XI]”-InCl <sub>3</sub>	<i>Frequency</i> -160.5101 Zero-point correction= 0.212159 (Hartree/Particle) Thermal correction to Energy= 0.225809 Thermal correction to Enthalpy= 0.226674 Thermal correction to Gibbs Free Energy= 0.171043 Sum of electronic and zero-point Energies= -1733.470436 Sum of electronic and thermal Energies= -1733.456786 Sum of electronic and thermal Enthalpies= -1733.455921 Sum of electronic and thermal Free Energies= -1733.511552 E(RM062X) = -1733.69143318
[XI]”-InCl <sub>3</sub>	Zero-point correction= 0.213790 (Hartree/Particle) Thermal correction to Energy= 0.227485 Thermal correction to Enthalpy= 0.228350 Thermal correction to Gibbs Free Energy= 0.172766 Sum of electronic and zero-point Energies= -1733.483335 Sum of electronic and thermal Energies= -1733.469641 Sum of electronic and thermal Enthalpies= -1733.468776 Sum of electronic and thermal Free Energies= -1733.524359 E(RM062X) = -1733.70500868
[III]”-GaCl <sub>3</sub>	Zero-point correction= 0.208684 (Hartree/Particle) Thermal correction to Energy= 0.224452 Thermal correction to Enthalpy= 0.225317 Thermal correction to Gibbs Free Energy= 0.165861 Sum of electronic and zero-point Energies= -3654.634835 Sum of electronic and thermal Energies= -3654.619068 Sum of electronic and thermal Enthalpies= -3654.618203 Sum of electronic and thermal Free Energies= -3654.677659 E(RM062X) = -3654.84943924
[III-TS-IV]”-GaCl <sub>3</sub>	<i>Frequency</i> -251.4633 Zero-point correction= 0.209251 (Hartree/Particle) Thermal correction to Energy= 0.223647 Thermal correction to Enthalpy= 0.224512 Thermal correction to Gibbs Free Energy= 0.168677 Sum of electronic and zero-point Energies= -3654.619982 Sum of electronic and thermal Energies= -3654.605586 Sum of electronic and thermal Enthalpies= -3654.604721 Sum of electronic and thermal Free Energies= -3654.660555 E(RM062X) = -3654.84147875
[IV]”-GaCl <sub>3</sub>	Zero-point correction= 0.213345 (Hartree/Particle) Thermal correction to Energy= 0.227070 Thermal correction to Enthalpy= 0.227935 Thermal correction to Gibbs Free Energy= 0.173425 Sum of electronic and zero-point Energies= -3654.642044 Sum of electronic and thermal Energies= -3654.628319

	Sum of electronic and thermal Enthalpies=	-3654.627454
	Sum of electronic and thermal Free Energies=	-3654.681964
	E(RM062X) =	-3654.86871239
<b>[IV-TS-V]”-GaCl<sub>3</sub></b>	Frequency -183.3314	
	Zero-point correction=	0.212294 (Hartree/Particle)
	Thermal correction to Energy=	0.225657
	Thermal correction to Enthalpy=	0.226523
	Thermal correction to Gibbs Free Energy=	0.172504
	Sum of electronic and zero-point Energies=	-3654.639637
	Sum of electronic and thermal Energies=	-3654.626274
	Sum of electronic and thermal Enthalpies=	-3654.625409
	Sum of electronic and thermal Free Energies=	-3654.679427
	E(RM062X) =	-3654.86358500
<b>[V]”-GaCl<sub>3</sub></b>	Zero-point correction=	0.212956 (Hartree/Particle)
	Thermal correction to Energy=	0.226534
	Thermal correction to Enthalpy=	0.227399
	Thermal correction to Gibbs Free Energy=	0.173262
	Sum of electronic and zero-point Energies=	-3654.651648
	Sum of electronic and thermal Energies=	-3654.638070
	Sum of electronic and thermal Enthalpies=	-3654.637205
	Sum of electronic and thermal Free Energies=	-3654.691341
	E(RM062X) =	-3654.87735781
<b>[IV-TS-XI]”-GaCl<sub>3</sub></b>	Frequency -135.1567	
	Zero-point correction=	0.213134 (Hartree/Particle)
	Thermal correction to Energy=	0.226320
	Thermal correction to Enthalpy=	0.227185
	Thermal correction to Gibbs Free Energy=	0.173501
	Sum of electronic and zero-point Energies=	-3654.628785
	Sum of electronic and thermal Energies=	-3654.615598
	Sum of electronic and thermal Enthalpies=	-3654.614733
	Sum of electronic and thermal Free Energies=	-3654.668418
	E(RM062X) =	-3654.84929081
<b>[XI]”-GaCl<sub>3</sub></b>	Zero-point correction=	0.214371 (Hartree/Particle)
	Thermal correction to Energy=	0.227746
	Thermal correction to Enthalpy=	0.228611
	Thermal correction to Gibbs Free Energy=	0.174539
	Sum of electronic and zero-point Energies=	-3654.640238
	Sum of electronic and thermal Energies=	-3654.626862
	Sum of electronic and thermal Enthalpies=	-3654.625997
	Sum of electronic and thermal Free Energies=	-3654.680069
	E(RM062X) =	-3654.85924665
<b>[III]”-AlCl<sub>3</sub></b>	Zero-point correction=	0.209754 (Hartree/Particle)
	Thermal correction to Energy=	0.225094
	Thermal correction to Enthalpy=	0.225959

	Thermal correction to Gibbs Free Energy=	0.167088
	Sum of electronic and zero-point Energies=	-1974.073044
	Sum of electronic and thermal Energies=	-1974.057703
	Sum of electronic and thermal Enthalpies=	-1974.056838
	Sum of electronic and thermal Free Energies=	-1974.115710
	E(RM062X) =	-1974.28865427
[III-TS-IV]"- $\text{AlCl}_3$	Frequency -261.6149	
	Zero-point correction=	0.210123 (Hartree/Particle)
	Thermal correction to Energy=	0.224147
	Thermal correction to Enthalpy=	0.225012
	Thermal correction to Gibbs Free Energy=	0.169985
	Sum of electronic and zero-point Energies=	-1974.056632
	Sum of electronic and thermal Energies=	-1974.042608
	Sum of electronic and thermal Enthalpies=	-1974.041743
	Sum of electronic and thermal Free Energies=	-1974.096770
	E(RM062X) =	-1974.27851985
[IV]"- $\text{AlCl}_3$	Zero-point correction=	0.213856 (Hartree/Particle)
	Thermal correction to Energy=	0.227295
	Thermal correction to Enthalpy=	0.228160
	Thermal correction to Gibbs Free Energy=	0.174255
	Sum of electronic and zero-point Energies=	-1974.074298
	Sum of electronic and thermal Energies=	-1974.060859
	Sum of electronic and thermal Enthalpies=	-1974.059994
	Sum of electronic and thermal Free Energies=	-1974.113899
	E(RM062X) =	-1974.30102797
[IV-TS-V]"- $\text{AlCl}_3$	Zero-point correction=	0.213140 (Hartree/Particle)
	Thermal correction to Energy=	0.226104
	Thermal correction to Enthalpy=	0.226969
	Thermal correction to Gibbs Free Energy=	0.174174
	Sum of electronic and zero-point Energies=	-1974.073773
	Sum of electronic and thermal Energies=	-1974.060809
	Sum of electronic and thermal Enthalpies=	-1974.059944
	Sum of electronic and thermal Free Energies=	-1974.112738
	E(RM062X) =	-1974.29727675
[V]"- $\text{AlCl}_3$	Zero-point correction=	0.213670 (Hartree/Particle)
	Thermal correction to Energy=	0.226986
	Thermal correction to Enthalpy=	0.227851
	Thermal correction to Gibbs Free Energy=	0.174244
	Sum of electronic and zero-point Energies=	-1974.081812
	Sum of electronic and thermal Energies=	-1974.068496
	Sum of electronic and thermal Enthalpies=	-1974.067631
	Sum of electronic and thermal Free Energies=	-1974.121237
	E(RM062X) =	-1974.30754435
[III]"-	Zero-point correction=	0.212355 (Hartree/Particle)

<b>B<sub>Cl</sub><sub>3</sub></b>	Thermal correction to Energy=	0.227174
	Thermal correction to Enthalpy=	0.228039
	Thermal correction to Gibbs Free Energy=	0.170410
	Sum of electronic and zero-point Energies=	-1756.398943
	Sum of electronic and thermal Energies=	-1756.384124
	Sum of electronic and thermal Enthalpies=	-1756.383259
	Sum of electronic and thermal Free Energies=	-1756.440888
	E(RM062X) =	-1756.61384697
<b>[III-TS-IV]"-B<sub>Cl</sub><sub>3</sub></b>	Frequency -220.1187	
	Zero-point correction=	0.212667 (Hartree/Particle)
	Thermal correction to Energy=	0.225629
	Thermal correction to Enthalpy=	0.226494
	Thermal correction to Gibbs Free Energy=	0.174287
	Sum of electronic and zero-point Energies=	-1756.386201
	Sum of electronic and thermal Energies=	-1756.373238
	Sum of electronic and thermal Enthalpies=	-1756.372373
	Sum of electronic and thermal Free Energies=	-1756.424581
	E(RM062X) =	-1756.60955311
<b>[IV]"-B<sub>Cl</sub><sub>3</sub></b>	Zero-point correction=	0.218325 (Hartree/Particle)
	Thermal correction to Energy=	0.230432
	Thermal correction to Enthalpy=	0.231297
	Thermal correction to Gibbs Free Energy=	0.181258
	Sum of electronic and zero-point Energies=	-1756.422719
	Sum of electronic and thermal Energies=	-1756.410612
	Sum of electronic and thermal Enthalpies=	-1756.409747
	Sum of electronic and thermal Free Energies=	-1756.459786
	E(RM062X) =	-1756.65182312
<b>[IV-TS-V]"-B<sub>Cl</sub><sub>3</sub></b>	Frequency -105.8858	
	Zero-point correction=	0.217202 (Hartree/Particle)
	Thermal correction to Energy=	0.228918
	Thermal correction to Enthalpy=	0.229783
	Thermal correction to Gibbs Free Energy=	0.180190
	Sum of electronic and zero-point Energies=	-1756.421158
	Sum of electronic and thermal Energies=	-1756.409441
	Sum of electronic and thermal Enthalpies=	-1756.408576
	Sum of electronic and thermal Free Energies=	-1756.458169
	E(RM062X) =	-1756.64794711
<b>[V]"-B<sub>Cl</sub><sub>3</sub></b>	Zero-point correction=	0.217390 (Hartree/Particle)
	Thermal correction to Energy=	0.229511
	Thermal correction to Enthalpy=	0.230376
	Thermal correction to Gibbs Free Energy=	0.180423
	Sum of electronic and zero-point Energies=	-1756.424787
	Sum of electronic and thermal Energies=	-1756.412666
	Sum of electronic and thermal Enthalpies=	-1756.411801

	Sum of electronic and thermal Free Energies=	-1756.461754
	E(RM062X) =	-1756.65488093
<b>[IV-TS-XI]”- BCl<sub>3</sub></b>	Frequency -29.9438	
	Zero-point correction=	0.217803 (Hartree/Particle)
	Thermal correction to Energy=	0.229332
	Thermal correction to Enthalpy=	0.230197
	Thermal correction to Gibbs Free Energy=	0.181734
	Sum of electronic and zero-point Energies=	-1756.421823
	Sum of electronic and thermal Energies=	-1756.410294
	Sum of electronic and thermal Enthalpies=	-1756.409429
	Sum of electronic and thermal Free Energies=	-1756.457892
	E(RM062X) =	-1756.64897492
<b>[XI]”- BCl<sub>3</sub></b>	Zero-point correction=	0.219081 (Hartree/Particle)
	Thermal correction to Energy=	0.231076
	Thermal correction to Enthalpy=	0.231941
	Thermal correction to Gibbs Free Energy=	0.181146
	Sum of electronic and zero-point Energies=	-1756.438080
	Sum of electronic and thermal Energies=	-1756.426084
	Sum of electronic and thermal Enthalpies=	-1756.425219
	Sum of electronic and thermal Free Energies=	-1756.476015
	E(RM062X) =	-1756.65907154
<b>[XIV]”- InCl<sub>3</sub></b>	Zero-point correction=	0.213045 (Hartree/Particle)
	Thermal correction to Energy=	0.235907
	Thermal correction to Enthalpy=	0.236772
	Thermal correction to Gibbs Free Energy=	0.159112
	Sum of electronic and zero-point Energies=	-3116.038111
	Sum of electronic and thermal Energies=	-3116.015249
	Sum of electronic and thermal Enthalpies=	-3116.014384
	Sum of electronic and thermal Free Energies=	-3116.092044
	E(RM062X) =	-3116.26131530
<b>[XV]”- InCl<sub>3</sub></b>	Zero-point correction=	0.212588 (Hartree/Particle)
	Thermal correction to Energy=	0.235201
	Thermal correction to Enthalpy=	0.236066
	Thermal correction to Gibbs Free Energy=	0.157874
	Sum of electronic and zero-point Energies=	-3116.000272
	Sum of electronic and thermal Energies=	-3115.977658
	Sum of electronic and thermal Enthalpies=	-3115.976793
	Sum of electronic and thermal Free Energies=	-3116.054986
	E(RM062X) =	-3116.23732276
<b>[XVI]”- InCl<sub>3</sub></b>	Zero-point correction=	0.213860 (Hartree/Particle)
	Thermal correction to Energy=	0.236280
	Thermal correction to Enthalpy=	0.237145
	Thermal correction to Gibbs Free Energy=	0.161535
	Sum of electronic and zero-point Energies=	-3116.039894

	Sum of electronic and thermal Energies=	-3116.017474
	Sum of electronic and thermal Enthalpies=	-3116.016609
	Sum of electronic and thermal Free Energies=	-3116.092220
	E(RM062X) =	-3116.26459974
[XIV]"- <b>GaCl<sub>3</sub></b>	Zero-point correction=	0.214180 (Hartree/Particle)
	Thermal correction to Energy=	0.236179
	Thermal correction to Enthalpy=	0.237044
	Thermal correction to Gibbs Free Energy=	0.162294
	Sum of electronic and zero-point Energies=	-6958.328403
	Sum of electronic and thermal Energies=	-6958.306404
	Sum of electronic and thermal Enthalpies=	-6958.305539
	Sum of electronic and thermal Free Energies=	-6958.380289
	E(RM062X) =	-6958.55062255
[XV]"- <b>GaCl<sub>3</sub></b>	Zero-point correction=	0.214096 (Hartree/Particle)
	Thermal correction to Energy=	0.235703
	Thermal correction to Enthalpy=	0.236568
	Thermal correction to Gibbs Free Energy=	0.162873
	Sum of electronic and zero-point Energies=	-6958.301725
	Sum of electronic and thermal Energies=	-6958.280119
	Sum of electronic and thermal Enthalpies=	-6958.279254
	Sum of electronic and thermal Free Energies=	-6958.352949
	E(RM062X) =	-6958.53511570
[XIV]'- <b>AlCl<sub>3</sub></b>	Zero-point correction=	0.216006 (Hartree/Particle)
	Thermal correction to Energy=	0.237282
	Thermal correction to Enthalpy=	0.238147
	Thermal correction to Gibbs Free Energy=	0.164267
	Sum of electronic and zero-point Energies=	-3597.202533
	Sum of electronic and thermal Energies=	-3597.181256
	Sum of electronic and thermal Enthalpies=	-3597.180391
	Sum of electronic and thermal Free Energies=	-3597.254272
	E(RM062X) =	-3597.42532440
[XV]"- <b>AlCl<sub>3</sub></b>	Zero-point correction=	0.216297 (Hartree/Particle)
	Thermal correction to Energy=	0.237084
	Thermal correction to Enthalpy=	0.237949
	Thermal correction to Gibbs Free Energy=	0.166994
	Sum of electronic and zero-point Energies=	-3597.172729
	Sum of electronic and thermal Energies=	-3597.151942
	Sum of electronic and thermal Enthalpies=	-3597.151076
	Sum of electronic and thermal Free Energies=	-3597.222031
	E(RM062X) =	-3597.40890035
[XII]"- <b>BCl<sub>3</sub></b>	Zero-point correction=	0.220092 (Hartree/Particle)
	Thermal correction to Energy=	0.240964
	Thermal correction to Enthalpy=	0.241829
	Thermal correction to Gibbs Free Energy=	0.165694

	Sum of electronic and zero-point Energies=	-3161.858211
	Sum of electronic and thermal Energies=	-3161.837340
	Sum of electronic and thermal Enthalpies=	-3161.836475
	Sum of electronic and thermal Free Energies=	-3161.912609
	E(RM062X) =	-3162.08104357
<b>[XIII]"-</b> <b>BCl<sub>3</sub></b>	Zero-point correction=	0.218572 (Hartree/Particle)
	Thermal correction to Energy=	0.238032
	Thermal correction to Enthalpy=	0.238897
	Thermal correction to Gibbs Free Energy=	0.169182
	Sum of electronic and zero-point Energies=	-3161.829123
	Sum of electronic and thermal Energies=	-3161.809663
	Sum of electronic and thermal Enthalpies=	-3161.808798
	Sum of electronic and thermal Free Energies=	-3161.878513
	E(RM062X) =	-3162.05863262
<b>In<sub>2</sub>Cl<sub>6</sub></b>	Zero-point correction=	0.007454 (Hartree/Particle)
	Thermal correction to Energy=	0.019841
	Thermal correction to Enthalpy=	0.020706
	Thermal correction to Gibbs Free Energy=	-0.034671
	Sum of electronic and zero-point Energies=	-2765.068058
	Sum of electronic and thermal Energies=	-2765.055671
	Sum of electronic and thermal Enthalpies=	-2765.054806
	Sum of electronic and thermal Free Energies=	-2765.110183
	E(RM062X) =	-2765.08505804
<b>Al<sub>2</sub>Cl<sub>6</sub></b>	Zero-point correction=	0.011226 (Hartree/Particle)
	Thermal correction to Energy=	0.021774
	Thermal correction to Enthalpy=	0.022639
	Thermal correction to Gibbs Free Energy=	-0.026026
	Sum of electronic and zero-point Energies=	-3246.243706
	Sum of electronic and thermal Energies=	-3246.233158
	Sum of electronic and thermal Enthalpies=	-3246.232293
	Sum of electronic and thermal Free Energies=	-3246.280958
	E(RM062X) =	-3246.25918603

## Supplementary Information of Chapter 4

<b>Ca(NTf<sub>2</sub>)<sub>2</sub></b> <b>(20°C)</b>	Zero-point correction=	0.116498 (Hartree/Particle)
	Thermal correction to Energy=	0.146304
	Thermal correction to Enthalpy=	0.147232
	Thermal correction to Gibbs Free Energy=	0.053640
	Sum of electronic and zero-point Energies=	-4331.015203
	Sum of electronic and thermal Energies=	-4330.985398
	Sum of electronic and thermal Enthalpies=	-4330.984469
	Sum of electronic and thermal Free Energies=	-4331.078062
	E(RM062X) =	-4332.04214445
<b>Ca(NTf<sub>2</sub>)(PF<sub>6</sub>)</b> <b>(20°C)</b>	Zero-point correction=	0.079813 (Hartree/Particle)
	Thermal correction to Energy=	0.102110
	Thermal correction to Enthalpy=	0.103039
	Thermal correction to Gibbs Free Energy=	0.025931
	Sum of electronic and zero-point Energies=	-3444.692201
	Sum of electronic and thermal Energies=	-3444.669903
	Sum of electronic and thermal Enthalpies=	-3444.668975
	Sum of electronic and thermal Free Energies=	-3444.746082
	E(RM062X) =	-3445.51268446
<b>1a</b>	Zero-point correction=	0.168355 (Hartree/Particle)
	Thermal correction to Energy=	0.177119
	Thermal correction to Enthalpy=	0.178047
	Thermal correction to Gibbs Free Energy=	0.134438
	Sum of electronic and zero-point Energies=	-423.800329
	Sum of electronic and thermal Energies=	-423.791564
	Sum of electronic and thermal Enthalpies=	-423.790636
	Sum of electronic and thermal Free Energies=	-423.834245
	E(RM062X) =	-424.117007877
<b>2a (20°C)</b>	Zero-point correction=	0.160399 (Hartree/Particle)
	Thermal correction to Energy=	0.170208
	Thermal correction to Enthalpy=	0.171136
	Thermal correction to Gibbs Free Energy=	0.123956
	Sum of electronic and zero-point Energies=	-485.290698
	Sum of electronic and thermal Energies=	-485.280889
	Sum of electronic and thermal Enthalpies=	-485.279961
	Sum of electronic and thermal Free Energies=	-485.327142
	E(RM062X) =	-485.628961189
<b>IN1a</b>	Zero-point correction=	0.287827 (Hartree/Particle)
	Thermal correction to Energy=	0.327552
	Thermal correction to Enthalpy=	0.328480
	Thermal correction to Gibbs Free Energy=	0.211571
	Sum of electronic and zero-point Energies=	-4754.876316

	Sum of electronic and thermal Energies=	-4754.836591
	Sum of electronic and thermal Enthalpies=	-4754.835662
	Sum of electronic and thermal Free Energies=	-4754.952571
	E(RM062X) =	-4756.18799534
<b>TS2a</b>	Frequency -85.5854	
	Zero-point correction=	0.283003 (Hartree/Particle)
	Thermal correction to Energy=	0.323391
	Thermal correction to Enthalpy=	0.324319
	Thermal correction to Gibbs Free Energy=	0.207080
	Sum of electronic and zero-point Energies=	-4754.796843
	Sum of electronic and thermal Energies=	-4754.756455
	Sum of electronic and thermal Enthalpies=	-4754.755527
	Sum of electronic and thermal Free Energies=	-4754.872766
	E(RM062X) =	-4756.12916047
<b>IN3a</b>	Zero-point correction=	0.283484 (Hartree/Particle)
	Thermal correction to Energy=	0.324515
	Thermal correction to Enthalpy=	0.325443
	Thermal correction to Gibbs Free Energy=	0.207198
	Sum of electronic and zero-point Energies=	-4754.799481
	Sum of electronic and thermal Energies=	-4754.758451
	Sum of electronic and thermal Enthalpies=	-4754.757522
	Sum of electronic and thermal Free Energies=	-4754.875768
	E(RM062X) =	-4756.13201406
<b>IN1b</b>	Zero-point correction=	0.250094 (Hartree/Particle)
	Thermal correction to Energy=	0.282583
	Thermal correction to Enthalpy=	0.283511
	Thermal correction to Gibbs Free Energy=	0.183551
	Sum of electronic and zero-point Energies=	-3868.548684
	Sum of electronic and thermal Energies=	-3868.516196
	Sum of electronic and thermal Enthalpies=	-3868.515268
	Sum of electronic and thermal Free Energies=	-3868.615228
	E(RM062X) =	-3869.65490916
<b>TS2b</b>	Frequency -57.7442	
	Zero-point correction=	0.246316 (Hartree/Particle)
	Thermal correction to Energy=	0.278907
	Thermal correction to Enthalpy=	0.279835
	Thermal correction to Gibbs Free Energy=	0.182499
	Sum of electronic and zero-point Energies=	-3868.470726
	Sum of electronic and thermal Energies=	-3868.438135
	Sum of electronic and thermal Enthalpies=	-3868.437207
	Sum of electronic and thermal Free Energies=	-3868.534543
	E(RM062X) =	-3869.59319093
<b>IN3b</b>	Zero-point correction=	0.246947 (Hartree/Particle)
	Thermal correction to Energy=	0.280232

	Thermal correction to Enthalpy=	0.281160
	Thermal correction to Gibbs Free Energy=	0.181433
	Sum of electronic and zero-point Energies=	-3868.471837
	Sum of electronic and thermal Energies=	-3868.438552
	Sum of electronic and thermal Enthalpies=	-3868.437623
	Sum of electronic and thermal Free Energies=	-3868.537351
	E(RM062X) =	-3869.59600467
<b>IN1c</b>	Zero-point correction=	0.448847 (Hartree/Particle)
	Thermal correction to Energy=	0.500534
	Thermal correction to Enthalpy=	0.501463
	Thermal correction to Gibbs Free Energy=	0.356744
	Sum of electronic and zero-point Energies=	-5240.168549
	Sum of electronic and thermal Energies=	-5240.116862
	Sum of electronic and thermal Enthalpies=	-5240.115934
	Sum of electronic and thermal Free Energies=	-5240.260652
	E(RM062X) =	-5241.82415451
<b>TS2c</b>	<i>Frequency</i> -232.6085	
	Zero-point correction=	0.445323 (Hartree/Particle)
	Thermal correction to Energy=	0.496246
	Thermal correction to Enthalpy=	0.497175
	Thermal correction to Gibbs Free Energy=	0.355229
	Sum of electronic and zero-point Energies=	-5240.072096
	Sum of electronic and thermal Energies=	-5240.021172
	Sum of electronic and thermal Enthalpies=	-5240.020244
	Sum of electronic and thermal Free Energies=	-5240.162190
	E(RM062X) =	-5241.73333679
<b>IN3c</b>	Zero-point correction=	0.446956 (Hartree/Particle)
	Thermal correction to Energy=	0.498153
	Thermal correction to Enthalpy=	0.499081
	Thermal correction to Gibbs Free Energy=	0.358971
	Sum of electronic and zero-point Energies=	-5240.153939
	Sum of electronic and thermal Energies=	-5240.102742
	Sum of electronic and thermal Enthalpies=	-5240.101814
	Sum of electronic and thermal Free Energies=	-5240.241924
	E(RM062X) =	-5241.80971689
<b>IN1d</b>	Zero-point correction=	0.411762 (Hartree/Particle)
	Thermal correction to Energy=	0.456045
	Thermal correction to Enthalpy=	0.456974
	Thermal correction to Gibbs Free Energy=	0.326959
	Sum of electronic and zero-point Energies=	-4353.840278
	Sum of electronic and thermal Energies=	-4353.795995
	Sum of electronic and thermal Enthalpies=	-4353.795067
	Sum of electronic and thermal Free Energies=	-4353.925081
	E(RM062X) =	-4355.28096689

<b>TS2d</b>	<i>Frequency</i> -332.1754 Zero-point correction= 0.407957 (Hartree/Particle) Thermal correction to Energy= 0.451368 Thermal correction to Enthalpy= 0.452296 Thermal correction to Gibbs Free Energy= 0.326169 Sum of electronic and zero-point Energies= -4353.736982 Sum of electronic and thermal Energies= -4353.693572 Sum of electronic and thermal Enthalpies= -4353.692643 Sum of electronic and thermal Free Energies= -4353.818770 E(RM062X) = -4355.18743310
<b>IN3d</b>	Zero-point correction= 0.410161 (Hartree/Particle) Thermal correction to Energy= 0.454077 Thermal correction to Enthalpy= 0.455006 Thermal correction to Gibbs Free Energy= 0.330418 Sum of electronic and zero-point Energies= -4353.834005 Sum of electronic and thermal Energies= -4353.790090 Sum of electronic and thermal Enthalpies= -4353.789161 Sum of electronic and thermal Free Energies= -4353.913748 E(RM062X) = -4355.27649504
<b>IN1</b>	Zero-point correction= 0.449997 (Hartree/Particle) Thermal correction to Energy= 0.500068 Thermal correction to Enthalpy= 0.500996 Thermal correction to Gibbs Free Energy= 0.362537 Sum of electronic and zero-point Energies= -5240.194495 Sum of electronic and thermal Energies= -5240.144424 Sum of electronic and thermal Enthalpies= -5240.143496 Sum of electronic and thermal Free Energies= -5240.281956 E(RM062X) = -5241.84013030
<b>TS2</b>	<i>Frequency</i> -192.7502 Zero-point correction= 0.447361 (Hartree/Particle) Thermal correction to Energy= 0.497630 Thermal correction to Enthalpy= 0.498558 Thermal correction to Gibbs Free Energy= 0.358368 Sum of electronic and zero-point Energies= -5240.150951 Sum of electronic and thermal Energies= -5240.100682 Sum of electronic and thermal Enthalpies= -5240.099754 Sum of electronic and thermal Free Energies= -5240.239944 E(RM062X) = -5241.80377883
<b>IN3</b>	Zero-point correction= 0.449713 (Hartree/Particle) Thermal correction to Energy= 0.500745 Thermal correction to Enthalpy= 0.501673 Thermal correction to Gibbs Free Energy= 0.359081 Sum of electronic and zero-point Energies= -5240.259805 Sum of electronic and thermal Energies= -5240.208774

	Sum of electronic and thermal Enthalpies=	-5240.207845
	Sum of electronic and thermal Free Energies=	-5240.350438
	E(RM062X) =	-5241.90744930
<b>IN4</b>	Zero-point correction=	0.413370 (Hartree/Particle)
	Thermal correction to Energy=	0.456196
	Thermal correction to Enthalpy=	0.457124
	Thermal correction to Gibbs Free Energy=	0.332993
	Sum of electronic and zero-point Energies=	-4353.872097
	Sum of electronic and thermal Energies=	-4353.829271
	Sum of electronic and thermal Enthalpies=	-4353.828343
	Sum of electronic and thermal Free Energies=	-4353.952474
	E(RM062X) =	-4355.31370434
<b>TS5</b>	<i>Frequency</i> -239.2964	
	Zero-point correction=	0.409976 (Hartree/Particle)
	Thermal correction to Energy=	0.452890
	Thermal correction to Enthalpy=	0.453819
	Thermal correction to Gibbs Free Energy=	0.328911
	Sum of electronic and zero-point Energies=	-4353.825362
	Sum of electronic and thermal Energies=	-4353.782447
	Sum of electronic and thermal Enthalpies=	-4353.781519
	Sum of electronic and thermal Free Energies=	-4353.906426
<b>TS5-(right)</b>	<i>Frequency</i> -198.8322	
	Zero-point correction=	0.410607 (Hartree/Particle)
	Thermal correction to Energy=	0.453312
	Thermal correction to Enthalpy=	0.454240
	Thermal correction to Gibbs Free Energy=	0.331404
	Sum of electronic and zero-point Energies=	-4353.816145
	Sum of electronic and thermal Energies=	-4353.773440
	Sum of electronic and thermal Enthalpies=	-4353.772511
	Sum of electronic and thermal Free Energies=	-4353.895348
<b>IN6</b>	E(RM062X) =	-4355.25661282
	Zero-point correction=	0.413118 (Hartree/Particle)
	Thermal correction to Energy=	0.456212
	Thermal correction to Enthalpy=	0.457140
	Thermal correction to Gibbs Free Energy=	0.334404
	Sum of electronic and zero-point Energies=	-4353.935874
	Sum of electronic and thermal Energies=	-4353.892780
	Sum of electronic and thermal Enthalpies=	-4353.891852
	Sum of electronic and thermal Free Energies=	-4354.014588
<b>3a</b>	E(RM062X) =	-4355.37153246
	Zero-point correction=	0.280653 (Hartree/Particle)
	Thermal correction to Energy=	0.294886
	Thermal correction to Enthalpy=	0.295815

	Thermal correction to Gibbs Free Energy=	0.236912
	Sum of electronic and zero-point Energies=	-656.825360
	Sum of electronic and thermal Energies=	-656.811126
	Sum of electronic and thermal Enthalpies=	-656.810198
	Sum of electronic and thermal Free Energies=	-656.869100
	E(RM062X) =	-657.311062287
<b>Ca(NTf<sub>2</sub>)<sub>2</sub></b> <b>(50°C)</b>	Zero-point correction=	0.116498 (Hartree/Particle)
	Thermal correction to Energy=	0.151530
	Thermal correction to Enthalpy=	0.152553
	Thermal correction to Gibbs Free Energy=	0.043800
	Sum of electronic and zero-point Energies=	-4331.015203
	Sum of electronic and thermal Energies=	-4330.980172
	Sum of electronic and thermal Enthalpies=	-4330.979148
	Sum of electronic and thermal Free Energies=	-4331.087901
	E(RM062X) =	-4332.04214447
<b>Ca(NTf<sub>2</sub>)(PF<sub>6</sub>)</b> <b>(50°C)</b>	Zero-point correction=	0.079813 (Hartree/Particle)
	Thermal correction to Energy=	0.106082
	Thermal correction to Enthalpy=	0.107105
	Thermal correction to Gibbs Free Energy=	0.017841
	Sum of electronic and zero-point Energies=	-3444.692201
	Sum of electronic and thermal Energies=	-3444.665931
	Sum of electronic and thermal Enthalpies=	-3444.664908
	Sum of electronic and thermal Free Energies=	-3444.754173
	E(RM062X) =	-3445.51268446
<b>1a'</b>	Zero-point correction=	0.179200 (Hartree/Particle)
	Thermal correction to Energy=	0.192941
	Thermal correction to Enthalpy=	0.193964
	Thermal correction to Gibbs Free Energy=	0.136067
	Sum of electronic and zero-point Energies=	-629.284905
	Sum of electronic and thermal Energies=	-629.271164
	Sum of electronic and thermal Enthalpies=	-629.270141
	Sum of electronic and thermal Free Energies=	-629.328038
	E(RM062X) =	-629.678688720
<b>2a (50°C)</b>	Zero-point correction=	0.160399 (Hartree/Particle)
	Thermal correction to Energy=	0.172080
	Thermal correction to Enthalpy=	0.173103
	Thermal correction to Gibbs Free Energy=	0.119031
	Sum of electronic and zero-point Energies=	-485.290698
	Sum of electronic and thermal Energies=	-485.279017
	Sum of electronic and thermal Enthalpies=	-485.277994
	Sum of electronic and thermal Free Energies=	-485.332066
	E(RM062X) =	-485.628961193
<b>IN1a'</b>	Zero-point correction=	0.298549 (Hartree/Particle)
	Thermal correction to Energy=	0.348254

	Thermal correction to Enthalpy=	0.349277
	Thermal correction to Gibbs Free Energy=	0.209558
	Sum of electronic and zero-point Energies=	-4960.355290
	Sum of electronic and thermal Energies=	-4960.305586
	Sum of electronic and thermal Enthalpies=	-4960.304562
	Sum of electronic and thermal Free Energies=	-4960.444282
	E(RM062X) =	-4961.75379546
<b>TS2a'</b>	<i>Frequency</i> -97.4976	
	Zero-point correction=	0.293394 (Hartree/Particle)
	Thermal correction to Energy=	0.343778
	Thermal correction to Enthalpy=	0.344802
	Thermal correction to Gibbs Free Energy=	0.206292
	Sum of electronic and zero-point Energies=	-4960.285036
	Sum of electronic and thermal Energies=	-4960.234652
	Sum of electronic and thermal Enthalpies=	-4960.233629
	Sum of electronic and thermal Free Energies=	-4960.372138
	E(RM062X) =	-4961.69509115
<b>IN3a'</b>	Zero-point correction=	0.292601 (Hartree/Particle)
	Thermal correction to Energy=	0.344068
	Thermal correction to Enthalpy=	0.345091
	Thermal correction to Gibbs Free Energy=	0.202319
	Sum of electronic and zero-point Energies=	-4960.290778
	Sum of electronic and thermal Energies=	-4960.239311
	Sum of electronic and thermal Enthalpies=	-4960.238288
	Sum of electronic and thermal Free Energies=	-4960.381060
	E(RM062X) =	-4961.70004558
<b>IN1b'</b>	Zero-point correction=	0.261249 (Hartree/Particle)
	Thermal correction to Energy=	0.302422
	Thermal correction to Enthalpy=	0.303445
	Thermal correction to Gibbs Free Energy=	0.182563
	Sum of electronic and zero-point Energies=	-4074.026563
	Sum of electronic and thermal Energies=	-4073.985390
	Sum of electronic and thermal Enthalpies=	-4073.984366
	Sum of electronic and thermal Free Energies=	-4074.105249
	E(RM062X) =	-4075.21485497
<b>TS2b'</b>	<i>Frequency</i> -95.8134	
	Zero-point correction=	0.256831 (Hartree/Particle)
	Thermal correction to Energy=	0.298729
	Thermal correction to Enthalpy=	0.299752
	Thermal correction to Gibbs Free Energy=	0.178219
	Sum of electronic and zero-point Energies=	-4073.962177
	Sum of electronic and thermal Energies=	-4073.920279
	Sum of electronic and thermal Enthalpies=	-4073.919255
	Sum of electronic and thermal Free Energies=	-4074.040789

	E(RM062X) =	-4075.15821163
<b>IN3b'</b>	Zero-point correction=	0.256641 (Hartree/Particle)
	Thermal correction to Energy=	0.299386
	Thermal correction to Enthalpy=	0.300409
	Thermal correction to Gibbs Free Energy=	0.174846
	Sum of electronic and zero-point Energies=	-4073.966532
	Sum of electronic and thermal Energies=	-4073.923787
	Sum of electronic and thermal Enthalpies=	-4073.922764
	Sum of electronic and thermal Free Energies=	-4074.048327
	E(RM062X) =	-4075.16409437
<b>IN1'</b>	Zero-point correction=	0.460517 (Hartree/Particle)
	Thermal correction to Energy=	0.523325
	Thermal correction to Enthalpy=	0.524349
	Thermal correction to Gibbs Free Energy=	0.354433
	Sum of electronic and zero-point Energies=	-5445.692753
	Sum of electronic and thermal Energies=	-5445.629945
	Sum of electronic and thermal Enthalpies=	-5445.628922
	Sum of electronic and thermal Free Energies=	-5445.798837
	E(RM062X) =	-5447.40849162
<b>TS2'</b>	<i>Frequency -119.0676</i>	
	Zero-point correction=	0.456911 (Hartree/Particle)
	Thermal correction to Energy=	0.519650
	Thermal correction to Enthalpy=	0.520673
	Thermal correction to Gibbs Free Energy=	0.351415
	Sum of electronic and zero-point Energies=	-5445.642331
	Sum of electronic and thermal Energies=	-5445.579592
	Sum of electronic and thermal Enthalpies=	-5445.578568
	Sum of electronic and thermal Free Energies=	-5445.747827
	E(RM062X) =	-5447.37186127
<b>IN3'</b>	Zero-point correction=	0.458118 (Hartree/Particle)
	Thermal correction to Energy=	0.521477
	Thermal correction to Enthalpy=	0.522501
	Thermal correction to Gibbs Free Energy=	0.351162
	Sum of electronic and zero-point Energies=	-5445.660066
	Sum of electronic and thermal Energies=	-5445.596707
	Sum of electronic and thermal Enthalpies=	-5445.595683
	Sum of electronic and thermal Free Energies=	-5445.767022
	E(RM062X) =	-5447.38203754
<b>TS4'</b>	<i>Frequency -31.6946</i>	
	Zero-point correction=	0.458046 (Hartree/Particle)
	Thermal correction to Energy=	0.520132
	Thermal correction to Enthalpy=	0.521155
	Thermal correction to Gibbs Free Energy=	0.354440
	Sum of electronic and zero-point Energies=	-5445.633238

	Sum of electronic and thermal Energies=	-5445.571152
	Sum of electronic and thermal Enthalpies=	-5445.570129
	Sum of electronic and thermal Free Energies=	-5445.736844
	E(RM062X) =	-5447.36042526
<b>IN5'</b>	Zero-point correction=	0.460099 (Hartree/Particle)
	Thermal correction to Energy=	0.523109
	Thermal correction to Enthalpy=	0.524132
	Thermal correction to Gibbs Free Energy=	0.353848
	Sum of electronic and zero-point Energies=	-5445.711147
	Sum of electronic and thermal Energies=	-5445.648137
	Sum of electronic and thermal Enthalpies=	-5445.647114
	Sum of electronic and thermal Free Energies=	-5445.817397
	E(RM062X) =	-5447.43604342
<b>IN6'</b>	Zero-point correction=	0.423634 (Hartree/Particle)
	Thermal correction to Energy=	0.478156
	Thermal correction to Enthalpy=	0.479179
	Thermal correction to Gibbs Free Energy=	0.325391
	Sum of electronic and zero-point Energies=	-4559.364741
	Sum of electronic and thermal Energies=	-4559.310219
	Sum of electronic and thermal Enthalpies=	-4559.309195
	Sum of electronic and thermal Free Energies=	-4559.462984
	E(RM062X) =	-4560.86654074
<b>TS7'</b>	Frequency -82.3448	
	Zero-point correction=	0.421222 (Hartree/Particle)
	Thermal correction to Energy=	0.474755
	Thermal correction to Enthalpy=	0.475778
	Thermal correction to Gibbs Free Energy=	0.327590
	Sum of electronic and zero-point Energies=	-4559.323562
	Sum of electronic and thermal Energies=	-4559.270029
	Sum of electronic and thermal Enthalpies=	-4559.269006
	Sum of electronic and thermal Free Energies=	-4559.417194
<b>IN8'</b>	E(RM062X) =	-4560.83953050
	Zero-point correction=	0.421697 (Hartree/Particle)
	Thermal correction to Energy=	0.476041
	Thermal correction to Enthalpy=	0.477064
	Thermal correction to Gibbs Free Energy=	0.327146
	Sum of electronic and zero-point Energies=	-4559.324532
	Sum of electronic and thermal Energies=	-4559.270188
	Sum of electronic and thermal Enthalpies=	-4559.269165
	Sum of electronic and thermal Free Energies=	-4559.419083
<b>TS9'</b>	E(RM062X) =	-4560.84123055
	Frequency -200.6255	
	Zero-point correction=	0.420830 (Hartree/Particle)
	Thermal correction to Energy=	0.474304

	Thermal correction to Enthalpy=	0.475327
	Thermal correction to Gibbs Free Energy=	0.326464
	Sum of electronic and zero-point Energies=	-4559.316475
	Sum of electronic and thermal Energies=	-4559.263001
	Sum of electronic and thermal Enthalpies=	-4559.261977
	Sum of electronic and thermal Free Energies=	-4559.410841
	E(RM062X) =	-4560.83405839
<b>IN10'</b>	Zero-point correction=	0.424004 (Hartree/Particle)
	Thermal correction to Energy=	0.478361
	Thermal correction to Enthalpy=	0.479385
	Thermal correction to Gibbs Free Energy=	0.327573
	Sum of electronic and zero-point Energies=	-4559.423575
	Sum of electronic and thermal Energies=	-4559.369218
	Sum of electronic and thermal Enthalpies=	-4559.368194
	Sum of electronic and thermal Free Energies=	-4559.520006
	E(RM062X) =	-4560.93258133
<b>3a'</b>	Zero-point correction=	0.290783 (Hartree/Particle)
	Thermal correction to Energy=	0.311024
	Thermal correction to Enthalpy=	0.312048
	Thermal correction to Gibbs Free Energy=	0.238318
	Sum of electronic and zero-point Energies=	-862.296966
	Sum of electronic and thermal Energies=	-862.276725
	Sum of electronic and thermal Enthalpies=	-862.275702
	Sum of electronic and thermal Free Energies=	-862.349431
	E(RM062X) =	-862.860950946

## French Summary

La catalyse par les métaux du groupe principal est une stratégie efficace pour obtenir de nouvelles réactivités et de nouvelles sélectivités en chimie organique, en particulier dans les réactions de formation de liaisons carbone-carbone. Après une centaine d'années de recherche, ce domaine est devenu un aspect essentiel de la synthèse organique moderne et présente un large éventail d'applications en chimie médicinale, agrochimie, matériaux et produits naturels. Parmi ces approches, les complexes de gallium et de calcium en tant que catalyseurs acides de Lewis sont bien connus pour leur grande réactivité vis-à-vis de l'activation des benzènes, des énynes, des groupes hydroxyle, etc.

Le développement des réactions catalytiques par des acides de Lewis repose sur une compréhension approfondie du modèle catalytique, du mécanisme de la réaction, de la réactivité, de la sélectivité et des facteurs contrôlant la vitesse. Les ligands et contre-ions, comme par exemple  $\text{NTf}_2^-$  ou  $\text{PF}_6^-$ , contribuent largement à contrôler la réactivité et la sélectivité des processus catalysés par les métaux du groupe principal, tels que le couplage catalysé par le calcium(II) d'alcools avec des acides vinylboroniques. En effet, les modifications de la structure du ligand peuvent souvent conduire à un impact significatif sur les propriétés stériques et électroniques, et par conséquent sur les résultats de la réaction. Cependant, il reste difficile de bien comprendre les modèles catalytiques uniquement à partir d'une intuition chimique, compte tenu de la complexité des effets des ligands. En effet, de multiples facteurs (attraction d'électrons, encombrement stérique, solubilité, etc.) peuvent intervenir au cours d'une réaction catalysée par un acide de Lewis. Les études expérimentales des mécanismes de réaction et des effets des ligands sont également souvent difficiles en à mettre en œuvre en raison de la difficulté à caractériser les intermédiaires organométalliques réactifs à courte durée de vie.

L'analyse par chimie théorique a été largement appliquée à presque tous les types de réactions de formation de liaisons carbone-carbone catalysées par des acides de Lewis pour prédire le chemin réactionnel le plus favorable, pour comprendre les effets des ligands et des substituants et pour fournir des justifications plausibles pour concevoir de nouveaux catalyseurs. Bien que les mécanismes de réaction de la plupart des réactions catalysées par des acides de Lewis, comme illustré par la classique alkylation de Friedel-Crafts du benzène médiée par  $\text{GaCl}_3$ , soient bien acceptés, certains détails comme le rôle des homodimères superélectrophiles ou l'existence d'intermédiaires tels que le complexe de Wheland restent peu clairs. Au cours des dernières décennies, les calculs à base de la théorie de la fonctionnelle de la densité (DFT) sont devenus un outil important pour étudier le mécanisme des réactions catalysées par les acides de Lewis. La procédure généralement acceptée pour explorer le mécanisme implique l'optimisation des substrats de réaction et le calcul des énergies des intermédiaires et des états de transition le long d'une coordonnée plausible de réaction pour construire un profil énergétique. Classiquement, le mécanisme réactionnel proposé est construit par des étapes élémentaires bien définies contenant diverses voies de réaction chimio-, régio- et énantio-isomériques concurrentes. Les étapes déterminant la vitesse et la sélectivité peuvent être déterminées en comparant les énergies libres de Gibbs calculées de chaque voie concurrente. Les intermédiaires clés identifiés et les états de transition sont ensuite analysés plus avant pour fournir une interprétation chimiquement significative de la réactivité et de la sélectivité contrôlées par le ligand dans des systèmes de réaction complexes et pour construire des modèles prédictifs pour la conception de catalyseurs bien raisonnés.

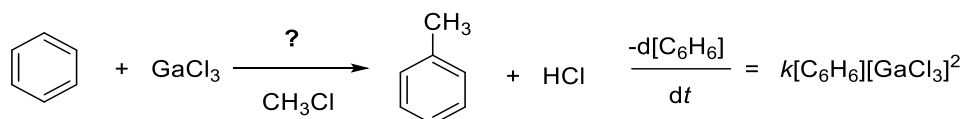
Dans cette thèse de doctorat, je présente des études de chimie computationnelles sur la méthylation du benzène catalysée par le gallium(III) (Chapitre 2), la réorganisation squelettique catalysée par le gallium(III) des enynes (Chapitre 3) et les réactions de couplage catalysées par le calcium(II) (Chapitre 4). Les objectifs généraux de mes études incluent l'étude des mécanismes de réaction, l'analyse des effets des ligands et la construction de modèles prédictifs.

**Extrait du Chapitre 2. Etude théorique portant sur les homodimères superélectrophiles de gallium(III) dans la méthylation du benzène médiée par le chlorure de gallium**

Bien que la réaction de Friedel-Crafts ait été découverte il y a plus de 140 ans, son mécanisme de réaction fait toujours débat. DeHaan, Brown et d'autres ont effectué un grand nombre d'études cinétiques dans ce domaine. Ils ont rapporté que la loi de vitesse de la méthylation catalysée par  $\text{GaCl}_3$  du benzène est  $-\frac{d[\text{C}_6\text{H}_6]}{dt} = k[\text{C}_6\text{H}_6][\text{GaCl}_3]^2$ . Concernant le second ordre de  $\text{GaCl}_3$ , le sujet du débat porte sur le rôle précis du catalyseur dans cette réaction : est-ce un simple électrophile ? aide-t-il à la déprotonation ? active-t-il le substrat sous des formes insoupçonnées (homodimère superélectrophile, paire d'ions ou double activation) ? C'est le genre de questions que nous avons essayé d'aborder en utilisant des techniques de calcul.

Un deuxième sujet de débat concerne la nature par étape ou concertée de la réaction de Friedel-Crafts. S'agit-il d'un processus par étapes à travers un complexe de type Wheland, comme indiqué dans n'importe quel manuel de chimie ? ou est-ce une réaction concertée ? C'est l'un des sujets qui ne cessent d'être discutés et auxquels nous avons essayé d'apporter une contribution.

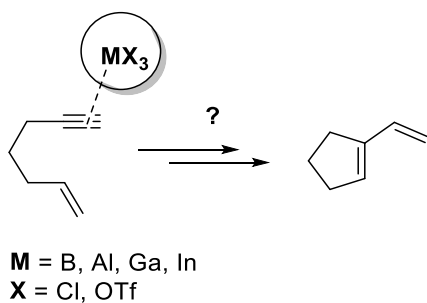
Toutes les questions ci-dessus sont de bonnes raisons d'utiliser les calculs DFT pour clarifier davantage les mécanismes de réaction.



**Extrait du chapitre 3. Etude théorique portant sur l'alcynophilie des sels  $\text{MX}_3$  du groupe 13.**

La cycloisomérisation des énynes 1,n est une stratégie bien établie pour augmenter rapidement la complexité moléculaire à partir de substrats simples et fournir des

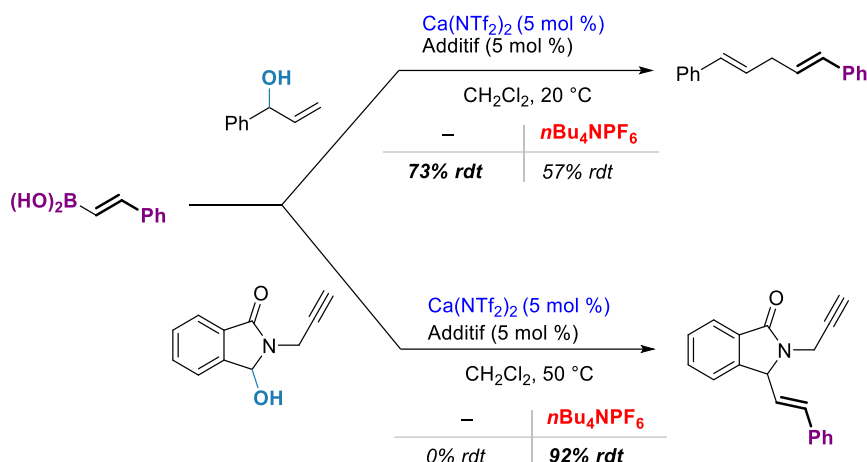
synthons utiles. Dès 2002, Chatani et al. ont rapporté la réorganisation squelettique catalysée par  $\text{GaCl}_3$  des enynes en 1-vinylcycloalcènes. Le mécanisme réactionnel qui a été proposé lorsque  $\text{GaCl}_3$  est utilisé comme catalyseur n'est en fait pas très différent de celui qui a été bien établi avec les complexes d' $\text{Au(I)}$ . Cependant, pour l'alcynophilie, les caractéristiques typiques du complexe d'or( $\text{I}$ ) métal de transition tardif, ne peuvent pas être utilisées pour expliquer les propriétés du sel  $\text{GaCl}_3$  dérivé d'un métal du groupe principal. Cela soulève la question de savoir ce qui fait d'une espèce simple telle que  $\text{GaCl}_3$  un bon acide de Lewis  $\pi$  alcynophile par rapport aux complexes de métaux de transition tardifs tels que les espèces  $\text{LAu(I)}^+$ , ou même par rapport à  $\text{BCl}_3$ ,  $\text{AlCl}_3$  ou  $\text{Ga(OTf)}_3$  qui ne fonctionnent pas comme catalyseur pour la cycloisomérisation d'enynes. En outre, le rôle possible des associations superélectrophiles nécessite également une étude théorique plus approfondie.



**Extrait du chapitre 4. Analyse DFT du couplage catalysé par le calcium(II) d'alcools avec des acides vinylboroniques : coopérativité de deux acides de Lewis différents et effets des contre-ions.**

Notre groupe a développé le couplage catalysé par le calcium d'alcools avec des acides vinylboroniques en 2015 et 2017. Les alcools allyliques, benzyliques et propargyliques, ainsi que les N,O-acétals ont été évalués comme substrats de réaction. Dans la réaction d'alkylation catalysée par le calcium avec l'alcool allylique comme substrat, le rendement diminue en présence du sel d'ammonium  $n\text{Bu}_4\text{NPF}_6$ . En revanche, aucun produit n'a été observé lorsque des N,O-acétals ont été utilisés comme substrats en l'absence de cet additif. Afin de comprendre en profondeur le mécanisme de ces deux

réactions et les caractéristiques contrôlant la réactivité, nous avons étudié quatre voies réactionnelles possibles : **a.** Le métal active le groupe hydroxyle du substrat. **b.** L'acide boronique active le groupe hydroxyle. **c.** Le calcium et l'acide de Lewis au bore activent en synergie le groupe hydroxyle. **d.** Le sel de calcium active l'acide boronique, qui à son tour active le groupe hydroxyle (activation superélectrophile). Sur la base des voies de réaction ci-dessus, nous avons effectué des calculs théoriques pour mieux comprendre un mécanisme impliquant deux métaux du groupe principal, tous deux agissant probablement comme des acides de Lewis, et parfois un sel d'ammonium comme activateur.







**Titre :** Rôle des superélectrophiles dans des réactions catalysées par le gallium(III) ou le calcium(II)

**Mots clés :** métaux du groupe principal, superélectrophiles, alkylation de Friedel-Crafts, réorganisations de squelettes, réactions de couplage, gallium, calcium.

**Résumé :** Des calculs DFT ont été réalisés afin d'étudier la méthylation du benzène, la réorganisation squelettique des énynes 1,6 et le couplage des alcools avec les acides vinylboroniques, catalysés respectivement par des sels métalliques du groupe principal dérivés du gallium et du calcium. En premier lieu, ce travail corrobore le rôle de l'homodimère superélectrophile  $\text{Ga}_2\text{Cl}_6$  en tant que catalyseur actif dans la méthylation du benzène catalysée par  $\text{GaCl}_3$ , conformément à l'étude cinétique de Brown. Il est également révélé que ce mécanisme d'alkylation est une substitution aromatique électrophile concertée (pas de complexe de type Wheland). En second lieu, cette étude explique pourquoi certains sels du type  $\text{MX}_3$  du groupe 13 se comportent comme des  $\pi$ -acides de Lewis mous vis-à-vis des énynes, tandis que d'autres restent inactifs. Le mécanisme de réorganisation squelettique catalysée par  $\text{GaCl}_3$  des énynes 1,6 a été calculé à cette fin. Enfin, le mécanisme du couplage catalysé par le Ca(II) des alcools avec les acides vinylboroniques a été analysé, révélant également comment la nature des contre-ions influence le résultat et comment deux acides de Lewis (Ca et B) fonctionnent en synergie pour former un superélectrophile.

**Title :** Superelectrophilic Activation in Ga(III)- and Ca(II)-Catalyzed Reactions

**Keywords :** main-group metals, superelectrophiles, Friedel-Crafts alkylation, skeletal reorganizations, coupling reactions, gallium, calcium.

**Abstract :** DFT calculations were used to study the methylation of benzene, the skeletal reorganization of 1,6-enynes, and the coupling of alcohols with vinylboronic acids, respectively catalyzed by main-group metal salts of the gallium and calcium series. Firstly, this work corroborates the role of the superelectrophilic  $\text{Ga}_2\text{Cl}_6$  homodimer as the active catalyst in the  $\text{GaCl}_3$ -catalyzed methylation of benzene, consistent Brown's kinetic study. It is also revealed that this alkylation mechanism is a concerted electrophilic aromatic substitution (no Wheland type  $\sigma$ -complex). Secondly, this study answers why some group 13  $\text{MX}_3$  salts behave as soft  $\pi$ -Lewis acids towards enynes, while others remain inactive. The mechanism of  $\text{GaCl}_3$ -catalyzed skeletal reorganization of 1,6-enynes was calculated towards this end. Finally, the mechanism of the Ca(II)-catalyzed coupling of alcohols with vinylboric acids was analyzed, also uncovering how the nature of the counterions influence the outcome and how two Lewis acids (Ca and B) work synergistically to form a superelectrophile.